

## INFORMATION TO USERS

This manuscript has been reproduced from the microfilm master. UMI films the text directly from the original or copy submitted. Thus, some thesis and dissertation copies are in typewriter face, while others may be from any type of computer printer.

**The quality of this reproduction is dependent upon the quality of the copy submitted.** Broken or indistinct print, colored or poor quality illustrations and photographs, print bleedthrough, substandard margins, and improper alignment can adversely affect reproduction.

In the unlikely event that the author did not send UMI a complete manuscript and there are missing pages, these will be noted. Also, if unauthorized copyright material had to be removed, a note will indicate the deletion.

Oversize materials (e.g., maps, drawings, charts) are reproduced by sectioning the original, beginning at the upper left-hand corner and continuing from left to right in equal sections with small overlaps. Each original is also photographed in one exposure and is included in reduced form at the back of the book.

Photographs included in the original manuscript have been reproduced xerographically in this copy. Higher quality 6" x 9" black and white photographic prints are available for any photographs or illustrations appearing in this copy for an additional charge. Contact UMI directly to order.

# UMI

A Bell & Howell Information Company  
300 North Zeeb Road, Ann Arbor MI 48106-1346 USA  
313/761-4700 800/521-0600



UNIVERSITY OF ALBERTA

MOBILITY CONTROL BY POLYMER UNDER  
BOTTOM-WATER CONDITIONS

BY

EZEDDIN SHIRIF ©

A THESIS

SUBMITTED TO THE FACULTY OF GRADUATE STUDIES AND RESEARCH IN  
PARTIAL FULFILLMENT OF THE REQUIREMENTS FOR THE DEGREE OF

DOCTOR OF PHILOSOPHY

IN

PETROLEUM ENGINEERING

DEPARTMENT OF CIVIL & ENVIRONMENTAL ENGINEERING

EDMONTON, ALBERTA

FALL 1998



National Library  
of Canada

Acquisitions and  
Bibliographic Services

395 Wellington Street  
Ottawa ON K1A 0N4  
Canada

Bibliothèque nationale  
du Canada

Acquisitions et  
services bibliographiques

395, rue Wellington  
Ottawa ON K1A 0N4  
Canada

*Your file Votre référence*

*Our file Notre référence*

The author has granted a non-exclusive licence allowing the National Library of Canada to reproduce, loan, distribute or sell copies of this thesis in microform, paper or electronic formats.

The author retains ownership of the copyright in this thesis. Neither the thesis nor substantial extracts from it may be printed or otherwise reproduced without the author's permission.

L'auteur a accordé une licence non exclusive permettant à la Bibliothèque nationale du Canada de reproduire, prêter, distribuer ou vendre des copies de cette thèse sous la forme de microfiche/film, de reproduction sur papier ou sur format électronique.

L'auteur conserve la propriété du droit d'auteur qui protège cette thèse. Ni la thèse ni des extraits substantiels de celle-ci ne doivent être imprimés ou autrement reproduits sans son autorisation.

0-612-34831-8

UNIVERSITY OF ALBERTA

**RELEASE FORM**

NAME OF AUTHOR: EZEDDIN SHIRIF

TITLE OF THESIS: MOBILITY CONTROL BY POLYMER UNDER  
BOTTOM-WATER CONDITIONS

DEGREE FOR WHICH THESIS WAS PRESENTED: DOCTOR OF PHILOSOPHY

YEAR THIS DEGREE GRANTED: 1998

Permission is hereby granted to THE UNIVERSITY OF ALBERTA LIBRARY to reproduce copies of this thesis and to lend or sell such copies for private, scholarly, or scientific research purposes only.

The author reserves all other publication and other rights in association with copyright rights in the thesis, and except as hereinbefore provided, neither the thesis nor any substantial portion thereof may be printed or otherwise reproduced in any material form whatever without the author's written permission.

( SIGNED )



PERMANENT ADDRESS:

12403 - 47 Ave  
Edmonton, Alberta  
Canada T6H 0B3

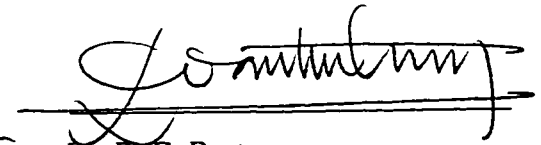
Dated: 26-08-1998

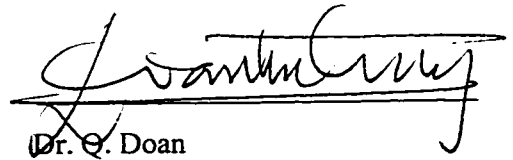
UNIVERSITY OF ALBERTA  
FACULTY OF GRADUATE STUDIES AND RESEARCH

The undersigned certify that they have read, and recommend to the Faculty of Graduate Studies and Research for acceptance, a thesis entitled "Mobility Control by Polymer Under Bottom-Water Conditions", submitted by Ezeddin Shirif in partial fulfillment of the requirements for the degree of Doctor of Philosophy in Petroleum Engineering.

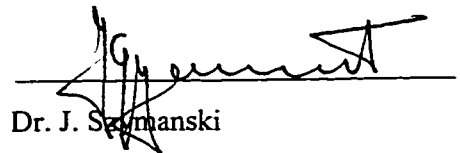


Dr. S. M. Farouq Ali (Supervisor)

for   
Dr. R. G. Bentsen



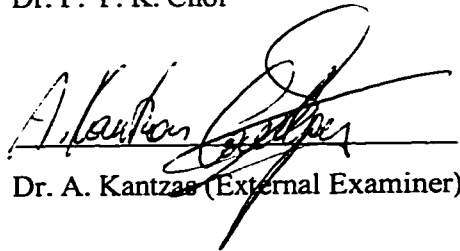
Dr. Q. Doan



Dr. J. Szamanski



Dr. P. Y. K. Choi



Dr. A. Kantzas (External Examiner)

Dated: Aug 14, 98

## ABSTRACT

In many light or moderately viscous oil reservoirs in Alberta and Saskatchewan, a high water saturation zone of varying thickness and extent ("bottom-water zone") occurs in communication with the oil zone above. As a result, the primary production period is short, and water coning occurs very early in the life of the reservoir. Later, during the secondary recovery stage, such a zone can have an adverse effect on the waterflood efficiency. This research addresses the problem of waterflooding such reservoirs.

The research was directed towards reducing water mobility in the bottom-water zone for more efficient oil displacement. Polymer in various concentrations was used as a blocking agent in the bottom-water zone and as a mobility control agent in the oil zone. Different strategies were investigated to reduce the water mobility in the bottom-water zone and improve the vertical sweep efficiency. The variables examined were: relative water-oil layer thickness, oil viscosity, polymer concentration, permeability contrast, injection rate and injection point, as well as the effect of vertical and horizontal injection and production wells.

An analytical model predicting fluid flow in a reservoir under bottom-water conditions considering the effects of viscous crossflow was developed. The model accounts only for crossflow due to potential gradients formed by the displacing and displaced fluids having unequal mobilities. All other forces responsible for initiating vertical and horizontal flow are considered negligible. The primary simplifying assumption requires the transfer of fluids between the oil zone and the bottom-water zone to be instantaneous; this assumption is usually referred to as vertical equilibrium. The model is restricted to two phases only and to any arbitrary initial and injection conditions. The model accounts for crossflow and predicts oil recovery, and the total volume of fluid injected.

A multiphase, three-dimensional, numerical model was developed to simulate water/polymer flooding experimental data. The model employs the implicit-pressure

explicit-saturation (IMPES) formulation for solving the system of finite-difference equations. Polymer characteristics such as rheology, adsorption, inaccessible pore volume and permeability reduction are included in the model.

The results showed that oil recovery can be increased by minimizing crossflow between layers by blocking the bottom-water zone completely. It was also found that for an unfavourable mobility ratio, as the injection rate increases the ultimate oil recovery increases.

The injection of a Polymer solution had a favourable impact on the waterflood performance. Moreover, the worse the conventional waterflood performance was, the more effective the polymer was as a mobility and blocking control agent. The use of horizontal wells showed slightly better oil recovery over vertical wells in a conventional waterflood of reservoirs under bottom-water conditions. In addition, some certain well combinations (horizontal production and vertical injection) gave better oil recovery due to the increase in the swept area.



**TO**

**MY PARENTS**

**WHOSE YEARS OF SUPPORT, GUIDANCE AND BLESSINGS  
MADE THIS WORK A REALITY**

**MY WIFE, Amal**

**WITHOUT WHOSE LOVE AND SACRIFICE THIS WORK  
COULD NOT HAVE BEEN POSSIBLE**

**AND**

**MY SONS, AHMED, MOHAMED, AND UMER  
WHOSE CURIOSITY KEPT ME GOING ON THIS PROJECT**

## **ACKNOWLEDGEMENTS**

I wish to express my sincere gratitude and thanks to Dr. S.M. Farouq Ali, not only for his valuable guidance, encouragement, and support during the thesis work but also for providing the academic freedom to pursue my scientific interests and for sharing frequently his wisdom. His continuous advice and invaluable suggestions all these years covered matters beyond the borders of petroleum engineering and therefore are sincerely appreciated.

I would like to thank Dr. Ramon G. Bentsen and Dr. Quang Doan for their continuous interest and the time and advice they provided with tremendous enthusiasm during the thesis work.

I am especially indebted to my wife, Amal and my sons, Ahmed, Mohamed, and Umer, for their love understanding and companionship during my Ph.D. years. They shared with me moments of joy and happiness, and also the moments of frustration, agony and stress which comes with the research work.

I would like to express my sincere gratitude to my parents, brothers, sisters and in-laws for their support and encouragement throughout these past years.

# TABLE OF CONTENTS

CHAPTER	PAGE
1. INTRODUCTION .....	1
2. LITERATURE REVIEW .....	2
2.1 Linear Flow in Discrete Layers with No Crossflow .....	2
2.2 Single-Phase, Two-Dimensional Flow with Crossflow .....	3
2.3 Reservoirs Under Bottom-Water Conditions .....	7
3. STATEMENT OF THE PROBLEM AND OBJECTIVES .....	11
4. EXPERIMENTAL APPARATUS AND PROCEDURE .....	13
4.1 Experimental Apparatus .....	13
4.1.1 Physical Model .....	13
4.1.2 Injection/Production and Pressure Monitoring Systems .....	14
4.1.3 Data Acquisition System .....	14
4.1.4 Porous Media and Fluids .....	14
4.2 Experimental Procedure .....	15
5. DEVELOPMENT OF THE ANALYTICAL MODEL .....	20
5.1 Derivation of the Crossflow Equations .....	21
5.1.1 Calculation of $q_{CF_{1 \rightarrow 2}}$ and $q_{CF_{2 \rightarrow 1}}$ .....	24
5.1.2 Calculation of $f_{wCF_{1 \rightarrow 2}}$ and $f_{wCF_{2 \rightarrow 1}}$ .....	25
5.1.3 Calculation of $q_E$ , $q_M$ and $q_R$ .....	26
5.1.4 Calculation of the unknown saturations $S_{M1}$ and $S_{M2}$ .....	27
5.2 Calculation of $x_{f1}$ and $x_{f2}$ .....	28
5.3 Calculation of Oil Recovery and Cumulative Fluid Injection .....	29
6. OIL DISPLACEMENT BY WATER AND POLYMERS .....	36

6.1	Mathematical Model of Water/Polymer Flood.....	37
6.1.1	Basic Assumptions.....	38
6.2	Physical Properties of Polymer Solutions.....	39
6.2.1	Non-Newtonian Viscosity and Shear Thinning.....	39
6.2.2	Permeability Reduction and Residual Resistance.....	43
6.2.3	Adsorption.....	44
6.2.4	Inaccessible Pore Volume.....	44
6.3	Numerical Formulation.....	45
6.3.1	Grid Selection.....	45
6.3.2	Finite Difference Formulation.....	45
6.3.3	Treatment of Boundary Conditions.....	46
6.3.4	Well Representation.....	46
6.4	Solution Procedure.....	47
6.4.1	Solution Method.....	48
6.4.2	Material Balance Calculation.....	48
6.5	General Solution Scheme.....	49
7.	EXPERIMENTAL AND THEORETICAL DATA PRESENTATION.....	51
7.1	Experimental Runs.....	51
7.2	Simulation Runs.....	61
7.3	Analytical Calculations.....	63
8.	DISCUSSION OF THE RESULTS.....	82
8.1	The Amount and Region of Crossflow.....	82
8.2	Polymer versus Waterflood.....	83
8.2.1	Effect of Varying Injection Rate on Recovery.....	83
8.2.2	Effect of Varying Thickness Ratio.....	84
8.2.3	Effect of Varying Oil Viscosity on Recovery.....	84
8.2.4	Effect of Varying Polymer Concentration.....	85
8.2.5	Effect of Barrier on Recovery.....	85
8.2.6	Effect of Permeability Contrast.....	86
8.2.7	Effect of Injection Strategies on Recovery.....	86
8.2.8	Effect of Using Horizontal Wells.....	87
8.3	Contribution of the Research.....	87

8.3 General Observations .....	88
9. CONCLUSIONS AND RECOMMENDATIONS.....	122
9.1 Conclusions.....	122
9.2 Recommendations.....	123
BIBLIOGRAPHY .....	124
APPENDICES .....	130
A Calculation of the Unknown Saturations.....	130
B Derivation of Differential Equations .....	133
C Finite Difference Approximation .....	139
D Flow Charts.....	154
E Production History of all Experimental Runs in Tabulated Form .....	157
F Production History of all Experimental Runs.....	187

## LIST OF TABLES

TABLE		PAGE
4-1	Properties of the Sand Pack and Fluids .....	16
6-1	User-Specified Parameters for Simulation Runs .....	41
7-1	Summary of the Experimental Results .....	52
7-2	Summary of the Theoretical Results .....	53
E-1	Production History for Run 1 .....	158
E-2	Production History for Run 2 .....	159
E-3	Production History for Run 3 .....	160
E-4	Production History for Run 4 .....	161
E-5	Production History for Run 5 .....	162
E-6	Production History for Run 6 .....	163
E-7	Production History for Run 7 .....	164
E-8	Production History for Run 8 .....	165
E-9	Production History for Run 9 .....	166
E-10	Production History for Run 10 .....	167
E-11	Production History for Run 11 .....	168
E-12	Production History for Run 12 .....	169
E-13	Production History for Run 13 .....	170
E-14	Production History for Run 14 .....	171
E-15	Production History for Run 15 .....	172
E-16	Production History for Run 16 .....	173
E-17	Production History for Run 17 .....	174
E-18	Production History for Run 18 .....	175
E-19	Production History for Run 19 .....	176
E-20	Production History for Run 20 .....	177
E-21	Production History for Run 21 .....	178
E-22	Production History for Run 22 .....	179
E-23	Production History for Run 23 .....	180
E-24	Production History for Run 24 .....	181
E-25	Production History for Run 25 .....	182
E-26	Production History for Run 26 .....	183

E-27	Production History for Run 27 .....	184
E-28	Production History for Run 28 .....	185
E-29	Production History for Run 29 .....	186

## LIST OF FIGURES

FIGURE	PAGE
4-1 Schematic of the Experimental Apparatus .....	18
4-2 Effect of Confining Pressure on Absolute Permeability of the Pack .....	19
5-1 Schematic Illustration for Viscous Crossflow .....	31
5-2 Illustration of Control Volume for the Trailing Flood Front.....	32
5-3 Illustration of Control Volume for the Advancing Flood Front .....	33
5-4 Schematic Illustration for Fluid Crossflow Around the Fronts .....	34
5-5 Schematic Illustration of the Reservoir Saturation Distribution .....	35
6-1 Node Representation of Three Dimensional Array of Reservoir Grid Blocks .	50
7-1 Summary Chart of all the Experiments .....	66
7-2 Summary Chart of all Simulation Runs.....	67
7-3 Production History for Run 4. Bottom-Water Pack Waterflood (Injection Rate = 450 ml/hr, $h_w/h_o = 1:3$ ).....	68
7-4 Production History for Run 5. Bottom-Water Pack Waterflood (Injection Rate = 300 ml/hr) .....	69
7-5 Production History for Run 15. Bottom-Water Pack Waterflood (No Crossflow Allowed in the Middle of the Pack).....	70
7-6 Production History for Run 16. Bottom-Water Pack Polymer Flood (Polymer Concentration = 500 ppm) .....	71
7-7 Production History for Run 21. Bottom-Water Pack Polymer Flood (Simultaneous Injection) .....	72
7-8 Production History for Run 28. Bottom-Water Pack Waterflood (Horizontal Wells) .....	73
7-9 Production History for Run 29. Bottom-Water Pack Waterflood (Vertical Injector / Horizontal Producer).....	74
7-10 Water/Oil Two Phase Relative Permeability.....	75
7-11 Water/Oil Capillary Pressure Curve.....	76
7-12 Production History for Simulation Run 51. Bottom-Water Pack Waterflood ( $k_1/k_2 = 1:10$ ).....	77
7-13 Production History for Simulation Run 52. Bottom-Water Pack Waterflood ( $k_z/k_x = 10:1$ ).....	78



7-14	Production History for Simulation Runs 53 Through 57. Bottom-Water Pack Waterflood ( $h_w/h_o = 0, 1:4, 1:3, 1:2, \text{ and } 1:1$ ) .....	79
7-15	Production History for Simulation Runs 58 and 59. Bottom-Water Pack Waterflood (Oil Viscosity = 11.0 mPa.s and 68.0 mPa.s).....	80
7-16	Production History for Simulation Runs 60 Through 62. Bottom-Water Pack Waterflood ( $k_1/k_2 = 1:1, 1:2, 1:3, \text{ and } 1:4$ ) .....	81
8-1	Driving Forces for Viscous Crossflow (no vertical communication) .....	89
8-2	Driving Forces for Viscous Crossflow (vertical communication).....	90
8-3	Comparison of Polymer and Waterflood under Bottom-Water Conditions .....	91
8-4	Comparison of Polymer and Waterflood under Bottom-Water Conditions (Simulation Model) .....	92
8-5	Effect of Water Injection Rate on Oil Recovery .....	93
8-6	Effect of Polymer Injection Rate on Oil Recovery.....	94
8-7	Effect of Water Injection Rate on Oil Recovery (Simulation Model).....	95
8-8	Effect of Thickness Ratio on Recovery (Waterflood-Experimental Model)....	96
8-9	Effect of Thickness Ratio on Recovery (Waterflood-Simulation Model).....	97
8-10	Effect of Thickness Ratio on Recovery (Waterflood-Analytical Model).....	98
8-11	Effect of Thickness Ratio on Recovery (Polymer- Experimental Model) .....	99
8-12	Effect of Thickness Ratio on Recovery (Polymer Flood-Simulation Model)	100
8-13	Effect of Thickness Ratio on Recovery for Waterflood (Recovery after 1 PV of Fluid injection).....	101
8-14	Effect of Thickness Ratio on Recovery for Polymer Flood (Recovery after 1 PV of Fluid injection) .....	102
8-15	Effect of Oil Viscosity on Recovery (Waterflood-Experimental Model) .....	103
8-16	Effect of Oil Viscosity on Recovery (Waterflood- Simulation Model) .....	104
8-17	Effect of Oil Viscosity on Recovery (Waterflood- Analytical Model) .....	105
8-18	Effect of Oil Viscosity on Recovery (Polymer Flood-Experimental Model).	106
8-19	Effect of Oil Viscosity on Recovery (Polymer Flood-Simulation Model).....	107
8-20	Effect of Oil Viscosity on Recovery for Waterflood (Recovery after 1 PV of Fluid injection) .....	108
8-21	Effect of Oil Viscosity on Recovery for Polymer Flood (Recovery after 1 PV of Fluid injection) .....	109
8-22	Dependence of Polymer Solution Viscosity on Polymer Concentrations .....	110
8-23	Effect of Polymer Concentration on Recovery (Experimental Model) .....	111
8-24	Effect of Polymer Concentration on Recovery (Simulation Model).....	112

8-25	Effect of Polymer Concentration on Recovery (Recovery after 1 PV of Fluid injection) .....	113
8-26	Effect of Barrier Recovery (Experimental Model).....	114
8-27	Effect of Barrier on Recovery (Simulation Model).....	115
8-28	Effect of Permeability Contrast on Recovery (Simulation Model) .....	116
8-29	Effect of Permeability Contrast on Recovery (Analytical Model) .....	117
8-30	Effect of Injection Strategy on Recovery for Polymer Flood.....	118
8-31	Comparison of Oil Recovery for Vertical and Horizontal Wells (Homogenous Pack Waterflood) .....	119
8-32	Comparison of Oil Recovery for Vertical and Horizontal Wells (Waterflood under a Bottom-Water Conditions).....	120
8-33	Effect of Horizontal/Vertical wells Combinations on Recovery.....	121
D-1	Main Program Flow Chart.....	155
D-2	Recurrent Data Flow Chart.....	156
F-1	Production History for Run 1. Homogeneous Pack Waterflood (Injection Rate = 450 ml/hr) .....	188
F-2	Production History for Run 2. Homogeneous Pack Waterflood (Injection Rate = 600 ml/hr) .....	189
F-3	Production History for Run 3. Homogeneous Pack Waterflood (Injection Rate = 750 ml/hr) .....	190
F-4	Production History for Run 4. Bottom-Water Pack Waterflood (Injection Rate = 450 ml/hr, $h_w/h_o = 1:3$ ).....	191
F-5	Production History for Run 5. Bottom-Water Pack Waterflood (Injection Rate = 300 ml/hr) .....	192
F-6	Production History for Run 6. Bottom-Water Pack Waterflood (Injection Rate = 600 ml/hr) .....	193
F-7	Production History for Run 7. Bottom-Water Pack Waterflood (Injection Rate = 750 ml/hr) .....	194
F-8	Production History for Run 8. Bottom-Water Pack Waterflood (Injection Rate = 1200 ml/hr) .....	195
F-9	Production History for Run 9. Bottom-Water Pack Waterflood ( $h_w/h_o = 1:4$ ) .....	196
F-10	Production History for Run 10. Bottom-Water Pack Waterflood ( $h_w/h_o = 1:2$ ) .....	197
F-11	Production History for Run 11. Homogeneous Pack Waterflood (Oil Viscosity = 68.0 mPa.s) .....	198

F-12	Production History for Run 12. Bottom-Water Pack Waterflood (Oil Viscosity = 68.0 mPa.s) .....	199
F-13	Production History for Run 13. Bottom-Water Pack Waterflood (Oil Viscosity = 11.0 mPa.s) .....	200
F-14	Production History for Run 14. Homogeneous Pack Waterflood (Oil Viscosity = 11.0 mPa.s) .....	201
F-15	Production History for Run 15. Bottom-Water Pack Waterflood (No Crossflow Allowed in the Middle of the Pack).....	202
F-16	Production History for Run 16. Bottom-Water Pack Polymer Flood (Polymer Concentration = 500 ppm).....	203
F-17	Production History for Run 17. Bottom-Water Pack Polymer Flood (Polymer Concentration = 1000 ppm).....	204
F-18	Production History for Run 18. Bottom-Water Pack Polymer Flood (Polymer Concentration = 1500 ppm).....	205
F-19	Production History for Run 19. Bottom-Water Pack Polymer Flood (Polymer Concentration = 2000 ppm).....	206
F-20	Production History for Run 20. Bottom-Water Pack Polymer Flood (Injection Rate = 750 ml/hr Polymer) .....	207
F-21	Production History for Run 21. Bottom-Water Pack Polymer Flood (Simultaneous Injection) .....	208
F-22	Production History for Run 22. Bottom-Water Pack Polymer Flood ( $h_w/h_o = 1:2$ ) .....	209
F-23	Production History for Run 23. Bottom-Water Pack Polymer Flood ( $h_w/h_o = 1:4$ ) .....	210
F-24	Production History for Run 24. Bottom-Water Pack Polymer Flood ( $h_w/h_o = 1:1$ ) .....	211
F-25	Production History for Run 25. Bottom-Water Pack Polymer Flood (Oil Viscosity = 68.0 mPa.s) .....	212
F-26	Production History for Run 26. Bottom-Water Pack Polymer Flood (Oil Viscosity = 11.0 mPa.s) .....	213
F-27	Production History for Run 27. Homogeneous Pack Waterflood (Horizontal Wells) .....	214
F-28	Production History for Run 28. Bottom-Water Pack Waterflood (Horizontal Wells) .....	215
F-29	Production History for Run 29. Bottom-Water Pack Waterflood (Vertical Injector / Horizontal Producer).....	216

F-30	Production History for Simulation Run 30. Homogeneous Pack Waterflood (Injection Rate = 450 ml/hr).....	217
F-31	Production History for Simulation Run 31. Bottom-Water Pack Waterflood (Injection Rate = 450 ml/hr, $h_w/h_o = 1:3$ ).....	218
F-32	Production History for Simulation Run 32. Bottom-Water Pack Waterflood (Injection Rate = 1200 ml/hr).....	219
F-33	Production History for Simulation Run 33. Bottom-Water Pack Waterflood ( $h_w/h_o = 1:4$ ).....	220
F-34	Production History for Simulation Run 34. Bottom-Water Pack Waterflood ( $h_w/h_o = 1:2$ ).....	221
F-35	Production History for Simulation Run 35. Bottom-Water Pack Waterflood ( $h_w/h_o = 1:1$ ).....	222
F-36	Production History for Simulation Run 36. Homogeneous Pack Waterflood (Oil Viscosity = 68.0 mPa.s).....	223
F-37	Production History for Simulation Run 37. Bottom-Water Pack Waterflood (Oil Viscosity = 68.0 mPa.s).....	224
F-38	Production History for Simulation Run 38. Bottom-Water Pack Waterflood (Oil Viscosity = 11.0 mPa.s).....	225
F-39	Production History for Simulation Run 39. Homogeneous Pack Waterflood (Oil Viscosity = 11.0 mPa.s).....	226
F-40	Production History for Simulation Run 40. Bottom-Water Pack Waterflood (No Crossflow Allowed in the Middle of the Pack).....	227
F-41	Production History for Simulation Run 41. Bottom-Water Pack Polymer Flood (Polymer Concentration = 500 ppm).....	228
F-42	Production History for Simulation Run 42. Bottom-Water Pack Polymer Flood (Polymer Concentration = 1000 ppm).....	229
F-43	Production History for Simulation Run 43. Bottom-Water Pack Polymer Flood (Polymer Concentration = 1500 ppm).....	230
F-44	Production History for Simulation Run 44. Bottom-Water Pack Polymer Flood (Polymer Concentration = 2000 ppm).....	231
F-45	Production History for Simulation Run 45. Homogeneous Pack Polymer Flood (Polymer Concentration = 500 ppm).....	232
F-46	Production History for Simulation Run 46. Bottom-Water Pack Polymer Flood ( $h_w/h_o = 1:2$ ).....	233
F-47	Production History for Simulation Run 47. Bottom-Water Pack Polymer Flood ( $h_w/h_o = 1:4$ ).....	234

F-48	Production History for Simulation Run 48. Bottom-Water Pack Polymer Flood ( $h_w/h_o = 1:1$ ) .....	235
F-49	Production History for Simulation Run 49. Bottom-Water Pack Polymer Flood (Oil Viscosity = 68.0 mPa.s) .....	236
F-50	Production History for Simulation Run 50. Bottom-Water Pack Polymer Flood (Oil Viscosity = 11.0 mPa.s) .....	237
F-51	Production History for Simulation Run 51. Bottom-Water Pack Waterflood ( $k_1/k_2 = 1:10$ ).....	238
F-52	Production History for Simulation Run 52. Bottom-Water Pack Waterflood ( $k_z/k_x = 10:1$ ).....	239
F-53	Production History for Simulation Runs 53 Through 57. Bottom-Water Pack Waterflood ( $h_w/h_o = 0, 1:4, 1:3, 1:2, \text{ and } 1:1$ ) .....	240
F-54	Production History for Simulation Runs 58 and 59. Bottom-Water Pack Waterflood (Oil Viscosity = 11.0 mPa.s and 68.0 mPa.s).....	241
F-55	Production History for Simulation Runs 60 Through 62. Bottom-Water Pack Waterflood ( $k_1/k_2 = 1:1, 1:2, 1:3, \text{ and } 1:4$ ) .....	242

## NOMENCLATURE

### Symbols

$A$	Cross-sectional area, $L^2$
$A_{ad}$	Adsorption parameters
$a_1$	Constant, $1/m/m$
$a_2$	Constant, $1/(m/m)^2$
$a_{m1}, a_{m2}, a_{m3}$	Unit constants
$B$	Formation volume factor, $L^3/L^3$
$B_{ad}$	Adsorption parameters, $1/m/m$
$C_p$	Mass concentration of polymer in water phase, $m/m$
$C_s$	Mass concentration of polymer on the rock (adsorption), $m/m$
$C_s^*$	Critical onset value for $C_s$ , $m/m$
$D_p$	Dispersion coefficient, $L^2/t$
$f_w$	Fractional flow of water,
$g$	Acceleration due to gravity, $L/t^2$
$H$	Height of the model, $L$
$h_1, h_o$	Height of the oil zone, $L$
$h_2, h_w$	Height of the bottom water zone, $L$
$k$	Absolute permeability, $L^2$
$k_{ro}$	Relative permeability to oil
$k_{rw}$	Relative permeability to water
$k_{owr}$	Effective permeability to oil at irreducible water saturation, $L^2$
$k_{wor}$	Effective permeability to water at residual oil saturation, $L^2$
$l$	Length of the model, $L$
$l_p$	User specified parameter
$M$	Mobility ratio
$\dot{m}_p$	Mass flux of polymer, $m/L^2t$

$p$	Pressure, m/Lt <sup>2</sup>
$p_b$	Block pressure, m/Lt <sup>2</sup>
$p_c$	Capillary pressure, m/Lt <sup>2</sup>
$p_{wf}$	Bottom hole flowing pressure, m/Lt <sup>2</sup>
$q_{L1}$	Volumetric flow rate in the oil zone at region $L$ , L <sup>3</sup> /t
$q_{L2}$	Volumetric flow rate in the bottom-water zone at region $L$ , L <sup>3</sup> /t
$q_{M1}$	Volumetric flow rate in the oil zone at region $M$ , L <sup>3</sup> /t
$q_{M2}$	Volumetric flow rate in the bottom-water zone at region $M$ , L <sup>3</sup> /t
$q_{R1}$	Volumetric flow rate in the oil zone at region $R$ , L <sup>3</sup> /t
$q_{R2}$	Volumetric flow rate in the bottom-water zone at region $R$ , L <sup>3</sup> /t
$q_{CF_{1\rightarrow 2}}$	Volumetric crossflow rate from the oil zone into the water zone, L <sup>3</sup> /t
$q_{CF_{2\rightarrow 1}}$	Volumetric crossflow rate from the bottom-water into the oil zone, L <sup>3</sup> /t
$q_T$	Total volumetric flow rate in the model, L <sup>3</sup> /t
$Q_i$	Cumulative fluid injected, L <sup>3</sup>
$Q_o$	Cumulative oil produced, L <sup>3</sup>
$R_{so}$	Solution gas-oil ratio, L <sup>3</sup> /L <sup>3</sup>
$R_{sw}$	Solution gas-water ratio, L <sup>3</sup> /L <sup>3</sup>
$r_{eq}$	Equivalent grid-block radius, L
$R_k$	Permeability reduction factor
$R_{rf}$	Residual resistance factor
$r_w$	Wellbore radius, L
$S_{L1}$	Water saturation in the oil zone at region $L$
$S_{L2}$	Water saturation in the bottom-water zone at region $L$
$S_{M1}$	Water saturation in the oil zone at region $M$
$S_{M2}$	Water saturation in the bottom-water zone at region $M$
$S_{R1}$	Water saturation in the oil zone at region $R$
$S_{R2}$	Water saturation in the bottom-water zone at region $R$

$S_{or}$	Residual oil saturation
$S_{wc}$	Irreducible water saturation
$S_{skin}$	Skin factor
$v_{xf1}$	Velocity of the trailing flood front in the oil zone, L/t
$v_{xf2}$	Velocity of the advancing flood front in the bottom-water zone, L/t
$T_\ell$	Phase transmissibility, L <sup>4</sup> /m
$u_\ell$	Darcy phase velocity, L/t
$W$	Width of the model, L
$x_{f1}$	Trailing flood front distance in the oil zone, L
$x_{f2}$	Advancing flood front distance in the bottom-water zone, L

### Greek Symbols

$\mu_\ell$	Phase viscosity, m/Lt
$\mu_{p_0}$	Polymer solution viscosity at zero shear rate, m/Lt
$\mu_{p_\infty}$	Polymer solution viscosity at infinite shear rate, m/Lt
$\dot{\gamma}$	Shear rate, 1/t
$\dot{\gamma}_{1/2}$	Shear rate at which the viscosity is half of $\mu_{p_0}$ , 1/t
$\gamma_0, \gamma_1, \gamma_2$	Shear rate parameters
$\beta_a, \beta_b$	Exponent parameters
$\eta$	Power law exponent
$\alpha_m$	Exponent parameter
$\phi$	Porosity
$\phi_p$	Effective porosity for polymer
$\rho_\ell$	Phase density, m/L <sup>3</sup>
$\rho_{rm}$	Density of rock matrix, m/L <sup>3</sup>
$\lambda_\ell$	Phase mobility, L <sup>3</sup> /m
$\varphi_\ell$	Phase potential, m/Lt <sup>2</sup>



$\omega_b$	Relaxation parameter
$\sigma_G$	Spectral radius

### **Subscripts and Superscripts**

1	Oil zone layer (layer 1)
2	Bottom-water zone layer (layer 2)
→	Flow direction
<i>CF</i>	Crossflow
<i>ℓ</i>	Phase
<i>o, w, g</i>	Oil, water, and gas phases
<i>n</i>	Time step indexing
<i>P</i>	Polymer
<i>L, M, R</i>	Regions
<i>x, y, z</i>	Cartesian coordinate system
<i>i, j, k</i>	Node indexing
$\Delta$	Difference operator

### **Abbreviations**

<i>D</i>	Dimensionless
<i>IMPES</i>	Implicit pressure/explicit saturation
<i>IOIP</i>	Initial oil-in-place
<i>HCPV</i>	Hydrocarbon pore volume
<i>L</i>	Length
<i>LSOR</i>	Line-successive over-relaxation solution technique
<i>m</i>	Mass
<i>PV</i>	Pore volume, fraction
<i>p</i>	Pressure
<i>V<sub>b</sub></i>	Bulk volume
<i>S</i>	Saturation
<i>SC</i>	Standard conditions

<i>t</i>	Time
<i>T</i>	Total
<i>WOR</i>	Water-oil ratio

## Chapter 1

### INTRODUCTION

Many reservoirs in Alberta and Saskatchewan contain some type of high water saturation zone (bottom-water) underlying the oil zone. Waterflooding under such conditions is typically ineffective because of channeling of water through the bottom-water zone. However, in some cases, waterflooding such reservoirs may still be feasible and economically viable. While there is no doubt that some of the injected water bypasses the oil zone through the bottom-water zone, most of the injected water may still displace the oil, depending on the reservoir conditions. Therefore, a mechanistic understanding of oil displacement by waterflooding in the presence of a bottom-water zone is the basis for predicting recovery performance, and there is a need for developing a mathematical model to describe water channeling under bottom-water conditions. Given the reservoir description, the mathematical model should be able to estimate oil recovery as well as the amount of water channeling into the bottom-water zone.

A few techniques have been proposed to improve waterflood performance in layered reservoirs and reservoirs under bottom-water conditions. Most of these are based upon the use of chemicals to block the bottom-water zone near the injection well. However, only a few of the previous bottom-water studies accounted for crossflow when planning a chemical flood. Thus, a systematic way of utilizing a chemical, in particular polymers, as blocking and mobility control agents under bottom-water conditions and accounting for crossflow is required for efficient displacement of oil.

## Chapter 2

### LITERATURE REVIEW

#### ***2.1 Linear Flow in Discrete Layers with No Crossflow***

A number of papers have appeared in which the reservoir is assumed to consist of discrete layers like a layer-cake. Each layer is uniform within itself and differs from the others only in its basic physical constants, viz., thickness, porosity and absolute permeability. The layers are non-communicating and no crossflow can occur. The performance within each layer is treated by linear flow theory, and the performance of the total reservoir is obtained by combining the performance of the individual layers. Capillary and gravity effects are not considered.

Many authors have considered flow in a layered formation, assuming no crossflow between layers. The method of Stiles<sup>1</sup> employed a field permeability distribution, and assumes that the flow through each layer always is proportional to its permeability-thickness product, i.e. the effective mobility ratio is unity. Dykstra and Parsons<sup>2</sup> demonstrated the important effect of mobility ratio on waterflood recovery efficiency and incorporated this feature into their discrete layer analysis. Correlations were presented to expedite calculations, which are based on the use of field “permeability variation”, mobility ratio and initial oil and water saturations. Johnson<sup>3</sup> presented a simplified graphical treatment of the Dykstra-Parsons method extended to any number of layers. However, his approach used the Dykstra-Parson’s coefficient of variation to characterize the reservoir. Therefore, reservoirs with equal Dykstra-Parson’s coefficients had the same recovery performance if all other initial conditions were the same. Finally, in an attempt to relax the assumption of piston-like displacement and allow for fractional flow effects in each layer of a stratified reservoir, Snyder and Ramey<sup>4</sup> combined the Buckley-Leverett solution<sup>5</sup> with the Dykstra-Parsons solution. This method is impractical since the reservoir must be divided into many blocks similar to a finite difference grid.

In the calculation of the performance of each discrete layer by linear flow theory, the effect of gravity and capillary forces usually is neglected. The effect of these forces on the performance of water-wet and oil-wet one-dimensional flow system has been studied numerically by Fayers and Sheldon<sup>6</sup> and it was concluded that gravity and capillary forces cause significant deviation only at low displacement rates.

## ***2.2 Single-Phase, Two-dimensional Flow with Crossflow***

Studies of single-phase two-dimensional flow in a layered reservoir with crossflow fall into two categories: a) steady-state flow of an incompressible fluid, and b) unsteady-state flow of slightly compressible fluid. The first category is the most relevant to the present study.

A number of papers dealing with analytical and numerical solutions of the unsteady state equations of flow for a slightly compressible fluid have appeared in the literature. These studies are not directly applicable to two-phase incompressible flow, since flow to the production well is caused by expansion of the reservoir fluid, instead of the pressure gradient between the injection and production wells.

Katz and Tek<sup>7</sup> presented an analytical solution for slightly-compressible fluid flow in two and three-layered linear and radial systems, concluding that the lower bound on performance for a stratified system corresponded to that for a system with non-communicating layers. Conversely, the upper performance bound corresponded to that for a uniform reservoir, using average values for permeability and porosity.

Russell and Prats<sup>8</sup> employed Hankel and Laplace transforms to obtain an analytical solution for flow in a two-layered cylindrical reservoir. Pendergrass and Berry<sup>9</sup> used a combination of analytical and numerical techniques to solve a similar problem. For a brief initial period, the production rate of a two-layer crossflow system behaves like a two-layer system with non-communicating layers. Thereafter, the transient performance is essentially the same as for a homogeneous reservoir having the same average

permeability. The early transient period is of too brief duration to attempt diagnosis of reservoir stratification from well drawdown data.

The concept of vertical equilibrium viscous crossflow was introduced in 1958 by Hiatt<sup>10</sup>, but the importance of these effects was qualitatively studied later by Russell and Prats<sup>11</sup>.

Following the work of Hiatt's vertical equilibrium viscous crossflow mathematical solution, Warren and Cosgrove<sup>12</sup> applied the assumption of log normally distributed permeability to Hiatt's solution. They approximated the effect of crossflow based on Dietz's theory<sup>13</sup> and claimed that the failure to use all available permeability data could lead to large errors in the prediction of the performance of a stratified reservoir. It was concluded that the effect of crossflow in a stratified system could be appreciable, particularly at very favourable or very unfavourable mobility ratios.

Use of the vertical equilibrium viscous crossflow solution was discussed by Hearn<sup>14</sup>. Hearn used the vertical equilibrium viscous crossflow solution to calculate the velocities of each flood front in each layer using pseudo-relative permeabilities.

Zapata and Lake<sup>15</sup> defined a crossflow index,  $I_{xf}$ , which varied between zero and one, with one being a measure of maximum crossflow. The parameter  $I_{xf}$  in turn was correlated with an effective length to thickness ratio,  $R_L$ , where a larger  $R_L$  corresponded to an increased ability of the reservoir to transmit fluids. They concluded that oil recovery was largely independent of  $R_L$  for  $R_L$  less than about 5.0 and this result was independent of mobility ratio.

Much of the understanding of crossflow has been through physical laboratory models. Kereluk and Crawford<sup>16</sup> presented their results for a two-layered model considering there were no obstructions to vertical flow. Lewis<sup>17</sup> did his experimental work by placing a plate of very low permeability between the two layers to limit the vertical flow of fluid. Gaucher and Lindley<sup>18</sup> used their five-spot laboratory model containing two equally-thick

layers of packed sand with different permeabilities to study the effects of capillary, gravitational and viscous forces on crossflow. It was concluded that a decrease in mobility ratio and a decrease in water rate could increase oil recovery.

Wright *et al.*<sup>19</sup> investigated the basic flow mechanisms and dispersion of an injected chemical in layered reservoirs. The variables controlled were layer permeability and dimensions, fluid viscosity and flow rate. Based on the study, they concluded that crossflow increased the dispersion effect. Surfactant slugs would be susceptible to breakdown in layered reservoirs.

Lambeth and Dawe<sup>20</sup> studied the effect of viscous crossflow experimentally and theoretically. Experiments in layered formations utilized viscous fluids, designed to examine the crossflow behaviour. The analytical solution of a two-layer case was developed, assuming a linear pressure distribution in one layer while allowing the pressure in the other layer to vary with crossflow. Although this over-simplification is self-contradictory, the solution gave an indication of the magnitude of crossflow when one fluid displaces another fluid. The authors attempted to solve the case of non-linear flow in both layers; however, the solutions obtained did not satisfy the original material balance equations. An experimental study suggested that the viscous crossflow effects were rate independent.

Wright *et al.*<sup>21</sup> studied slug size and mobility requirements for chemically enhanced oil recovery within heterogeneous reservoirs. Using a modification of the analytical solution obtained by Lambeth and Dawe<sup>20</sup>, the authors suggested that the criteria for the chemical slug disintegration caused by the effect of crossflow were more demanding than previously considered necessary for reservoirs with common heterogeneities. They claimed that a high-mobility slug would preferentially sweep the higher-conductivity layers, but a low-mobility slug would tend to be pushed by crossflow into the lower-conductivity layers. This mechanism must be considered when low-mobility slugs are used for waterflood conformance improvement.

Ahmed *et al.*<sup>22</sup> carried out an experimental study of waterflooding in a two-dimensional layered sand model. The effect of flow rate on oil recovery by waterflooding a three-layer sand visual model was also studied. The authors reported that intermediate oil recovery during a waterflood in a stratified reservoir with vertical communication was sensitive to flow rate, oil viscosity, and interfacial tension (IFT). During the displacement, oil recovery was observed to increase when flow rate was decreased. Ahmed *et al.* concluded that oil recovery increased significantly when mobility ratio was reduced.

In view of a lack of analytical solutions for multi-layer reservoirs, only numerical solutions have been attempted to examine the effect of crossflow. Root and Skiba<sup>23</sup> were among the first researchers to investigate the crossflow effects during a waterflood in a stratified reservoir. They employed numerical methods to solve Laplace's equation for two-dimensional steady-state, single-phase, incompressible flow in a layered reservoir. Their finding was that the completion of injection and production wells in the tight zone only improved sweep efficiency by hindering the tendency of water to bypass through the high conductivity zone.

Goddin *et al.*<sup>24</sup> reported a numerical study of waterflood performance in a stratified system with crossflow. Viscous and capillary crossflow were examined in a field-scale model of a two-layer, water-wet sandstone reservoir. The authors reported that maximum crossflow occurred in the vicinity of the flood front in the permeable layer, similar to the observation of Barnes<sup>25</sup> in his visual model. It was concluded that viscous crossflow was a function of mobility ratio.

Silva and Farouq Ali<sup>26</sup> developed a two-phase, three-dimensional reservoir simulator to study the effect of selective formation plugging in waterflooding a layered model. The authors concluded that partially plugging a high permeability layer was ineffective if the layers were in communication. They further concluded that reservoirs containing bottom-



water zone might be susceptible to efficient waterflooding.

El-Khatib<sup>27</sup> developed a mathematical model for waterflood simulation in linear stratified non-communicating layers, with no crossflow, and communicating layers with complete crossflow (i.e., lower and upper bounds in Katz and Tek's study<sup>7</sup>). The study showed that the effect of crossflow between layers increased oil recovery at favourable mobility ratios and decreased it at unfavourable mobility ratios. El-Khatib concluded that crossflow increased the influence of mobility ratio in waterflood performance prediction.

### ***2.3 Reservoirs Under Bottom-Water Conditions***

The efficient and economic recovery of oil from reservoirs under bottom-water conditions is recognized as a formidable task. High water cuts and rapidly decreasing oil rates early in the production life of such reservoirs have in many instances prompted their suspension or abandonment at very low levels of oil recovery. Reservoir characteristics and rock and fluid properties combine to yield the single most important parameter (mobility ratio) in a waterflood. A number of chemicals such as polymers, emulsion, biopolymer, foam and carbon dioxide-activated silica gel have been used to control the mobility ratio.

One of the oldest techniques to control mobility of water in waterflooding is the use of polymers. This control agent was shown to be effective in the early sixties by Pye<sup>28</sup>. He performed numerous field and laboratory studies of polymer flooding using polyacrylamide solutions. It was observed experimentally that the viscosity of the water-soluble polymer solutions measured in the formation sample departed markedly from that obtained using a viscometer. He quantified the unusual departure of the measured values from the expected response as the resistance factor. It was assumed that the permeability was constant. Pye pointed out that at constant flow the injection pressure rose, and this effect was not a core plugging problem because the system reached equilibrium after some time. It was also observed that the extent of departure from the measured viscosity

value was most pronounced at low concentrations but at higher concentrations the effect was approximately proportional to the solution viscosity. It was suggested that this unusual behaviour was a property of only selected water-soluble polymers, among which were the extensive family of acrylamide polymers and copolymers. It was recommended that rapid laboratory flood rates should be avoided in order to keep the resistance factor constant.

The problem in recovering oil under bottom-water conditions was first recognized in the early sixties when Barnes<sup>25</sup> suggested the use of a viscous water slug to improve waterflood efficiency in a reservoir partially invaded by bottom water. The viscous water in Barnes' study referred to water thickened by a chemical additive such that the viscosity of water was greater than 1.0 cp. He argued that injecting a viscous water slug in bottom-water reservoirs would 1) reduce the flood life, 2) reduce lifting costs, and 3) increase ultimate recovery. He also pointed out that the larger the quantity and the higher the viscosity of the viscous slug injected into such a system, the greater the crossflow of oil ahead of the displacing front, thus leading to a higher oil rate during displacement. His visual model studies showed that crossflow was most severe immediately ahead of the front and diminished to zero at the producing well. However, such a crossflow phenomenon was not described quantitatively in the study. Barnes' study was directed towards increasing the viscosity of water. Other chemical slugs that could reduce relative permeability to water were not considered.

Unlike the viscous water used by Barnes<sup>25</sup>, polymers have the ability to lower the mobility by reducing the relative permeability to water, as well as increasing its viscosity<sup>28</sup>, so that the mobility ratio is improved.

Over two decades after Barnes' work, Zaidel<sup>29</sup> looked at waterflooding bottom-water reservoirs with a polymer slug. His analytical model was based on the assumption of instantaneous gravitational phase separation in the vertical direction, i.e., the polymer

solution did not enter the region with the residual oil saturation in a given section until it had filled the zone containing zero oil saturation. He concluded that a polymer with a mobility lower than that of water ( $R = \text{Mobility of Water} / \text{Mobility of Polymer} > 1$ , where  $R$  is the resistance factor) improved oil recovery by increasing flow resistance in the bottom-water zone, so that improved displacement in the oil zone would result. However, as the polymer mobility is lowered to a certain point ( $R \geq 4$ ), the increase in resistance is primarily due to the oil bank formed in the bottom-water zone during the displacement. Thus, a polymer flood under bottom-water conditions can have both favourable and unfavourable manifestations: in the favourable sense, a high oil rate is obtained during the displacement; in the unfavourable sense, a certain amount of oil is lost to the bottom-water zone if the polymer mobility is too low. As a result, Zaidel suggested that a moderately low mobility polymer ( $R = 2$  to  $3$ ) would increase the oil rate during displacement while minimizing loss of oil to the water zone.

Shortly after Zaidel's theoretical work, Islam and Farouq Ali<sup>30-35</sup> carried out an intensive experimental study on the use of various chemical slugs in waterfloods conducted under bottom-water conditions. The chemical slugs included polymer, emulsion, biopolymer gel, air, foam and carbon dioxide-activated silica gel. The variables examined were: slug size, permeability contrast, water-oil layer thickness ratio, oil viscosity, and injection rate of the mobility control agent. The study showed that polymer and emulsion performed better (i.e., high oil recovery and low WOR) than the other chemicals used. By comparing a polymer slug to a glycerine slug having the same viscosity, they showed that the reduction in the effective permeability to water by the polymer greatly improved oil recovery over that from the use of a glycerine slug. They claimed that a recovery improvement of 27% IOIP was due to the reduction in the effective permeability by adsorption and mechanical entrapment of the polymer.

Yeung and Farouq Ali<sup>36-38</sup> introduced three different displacement techniques, the Emulsion Slug Process (ESP), the Alternating Water Emulsion Process (AWE) and the Dynamic Blocking Process (DBP) to improve the vertical sweep efficiency while water-

flooding bottom-water formations. For emulsion with low surfactant concentration, the DBP and AWE processes were found to give higher oil recoveries than the ESP process under bottom-water conditions. For emulsion with higher surfactant concentrations, the reverse was found to be true. According to Yeung and Farouq Ali, the crossflow was very prominent ahead of the flood front for high viscosity fluids. It was concluded that a high surfactant concentration did not necessarily give a higher oil recovery for both homogenous and bottom-water reservoirs.

Yeung<sup>38</sup> developed a mathematical model for a two layered reservoir, the lower layer being a water zone to account for crossflow, based on the major assumption that crossflow did not alter the mobility in either layer. It was concluded that crossflow occurred near the injection end and waterflood performance was independent of the point of injection and the injection rate.

Two years later, Hassan<sup>39</sup> modified Yeung's model but used the same assumption. He also developed a semi-analytical model to predict oil recovery performance and to calculate the frontal movement of the two flood fronts for bottom-water reservoirs.

In view of the foregoing, when a stratified reservoir is being studied for waterflooding, failure to account for crossflow can lead to large errors in oil recovery prediction; however, under bottom-water conditions, this effect is aggravated due to the presence of the mobile water phase.

## Chapter 3

### STATEMENT OF THE PROBLEM AND OBJECTIVES

Three major observations can be made from the literature survey. First, waterflooding under bottom-water conditions is ineffective due to water channelling through the bottom-water zone; however, a lack of suitable analytical expressions for fluid flow in layered formations may lead to conclusions that may not be valid. Second, injection of a blocking agent under bottom-water conditions has led to improved oil recovery;<sup>32-37</sup> however, the mechanism of this process is still not fully understood. Third, the previous analytical solutions<sup>38,39</sup> for layered reservoirs under bottom-water conditions are unrealistic, because one of the major assumptions used in deriving the solution was that the crossflow does not alter the mobility in either layer. As a result of this assumption, the concept of relative permeability was not introduced, and these solutions are, therefore, suitable only for the single-phase flow case.

The proposed research is to consist of experimental and theoretical work. The principal objective is to use and evaluate the effectiveness of horizontal-vertical well combinations for waterflooding formations where a contiguous water zone is present below the oil zone. A three-dimensional physical model is to be used for the experiments, with horizontal-vertical/production-injection well combinations. Chemicals, such as polymer solutions with different concentrations are to be used for mobility control and formation blocking.

The variables to be studied include: oil-to-water zone thickness ratio, permeability of each zone, injection rate, and oil viscosity. Oil recovery is to be examined as a function of the above variables. Certain injection strategies, where the injected fluid is injected at several points simultaneously, are to be studied also.

The experimental studies are to be carried out in a physical model, consisting of a three-dimensional flow system, packed with Ottawa sand, with two layers, one saturated with

oil and water, and the other by water only. The injection and production wells in the model are designed in such a way that either type of well can be used as an injector or producer, and the perforation interval of either one will be adjustable. The design of the model permits the placement of a water layer or gas layer of desired thickness. The sand pack is to be kept compressed by means of a diaphragm.

An analytical model for fluid flow in reservoirs under bottom-water conditions is to be developed for describing crossflow, together with a prediction of oil recovery.

A three-phase, three-dimensional water/polymer flooding simulator is to be developed to compare the theoretical calculated results with the experimental values and to determine under what conditions water/polymer are likely to improve waterflood performance under bottom-water conditions, for several situations. The simulator can be used to extend experimental results, once it is validated.

## Chapter 4

# EXPERIMENTAL APPARATUS AND PROCEDURE

This chapter provides a description of the experimental apparatus, procedure and materials used for the study.

### ***4.1 Experimental Apparatus***

The apparatus is comprised of the following components: a physical model, fluids, porous media, injection and production systems, a pressure monitoring system, a nitrogen cylinder for the application of an overburden pressure and a data acquisition system. Figure 4-1 (figures are at the end of the chapter) provides a schematic of the experimental apparatus.

#### ***4.1.1 Physical Model***

The model was designed to minimize the variations in the pack properties, for better control in the procedure used for well placement, and to set the exact ratio of the bottom-water-to-oil sand thickness. An additional feature of this model was the use of vertical/horizontal well combinations and the use of an overburden pressure which could be applied to the model by using a Neoprene diaphragm.

The model consisted of an aluminum block with a rectangular cavity, measuring 90 cm (35.43 in.) in length, 3.8 cm (1.5 in.) in width, and 9 cm (3.54 in.) in depth on a stand that allowed the desired orientation of the model in both the vertical and horizontal directions. Lids were provided on both sides and a packing port was provided at one of the ends through which the sand for the model could be packed. Two special horizontal wells and four vertical wells of different lengths and heights were constructed to simulate well completion intervals. These wells were made of brass and had a filter of 40 micrometers. The bottom lid had a cavity for applying the overburden pressure.

#### ***4.1.2 Injection/Production and Pressure Monitoring Systems***

Two constant-rate pumps, a Jefri pump controlled by a PC, and an ISSCO pump, were used for fluid injection. The ISSCO pump was used in conjunction with the Jefri pump. In some of the experiments which required simultaneous injection of two fluids, The Jefri pump was connected to two cylinders containing floating pistons. This permitted a maximum volume of 2000 ml of fluid to be injected at a maximum rate of 1200 ml/hr. The Jefri pump was monitored by an IBM PC with a precision of 0.1 ml/hr. The ISSCO pump had a capacity of 500 ml of fluid to be injected at a maximum rate of 400 ml/hr. The produced fluid was collected in 50 ml centrifuge tubes. A Heise gauge and a calibrated pressure transducer provided the pressure data for each run. A data acquisition system was incorporated to automate the pressure records.

#### ***4.1.3 Data Acquisition System***

The data acquisition system consisted of an IBM compatible computer, Labtech notebook Software, Das-8 board and an Exp-16 Multiplexer manufactured by MetraByte. The Labtech notebook is a package that is completely menu-driven which makes it easy to design a format for data acquisition-pressure and time. Data from the Labtech notebook can be interfaced with Lotus 1-2-3 for post acquisition analysis, file management and graphic presentation.

#### ***4.1.4 Porous Media and Fluids***

For all runs, the unconsolidated porous media were prepared by wet-packing<sup>30</sup> core-holders with fresh Ottawa silica sand (80-120 mesh) and vibrating them for 10 hours to make the sand-pack as uniformly packed as possible. For each run the sand-pack was dried, evacuated, and then resaturated with distilled water in order to be able to measure its porosity and absolute permeability.

Distilled water was used to determine both porosity and absolute permeability, as well as to create an irreducible water saturation. The displaced fluids used were refined oils, namely, MCT-5, MCT-10, and a Light Atmospheric Gas Oil (LAGO).



The polymer solutions used in all experiments were made with Dow Pusher 500, a polyacrylamide in powder form, supplied by Dow Chemical Company. Four polymer solutions were made at concentrations of 500, 1000, 1500, and 2000 ppm. The polymer was made up fresh and on a weight/volume basis. The powder was dispersed gradually into the vortex of distilled water while stirring with a caged stirrer and mixed for 5 hours. The relevant properties of all fluids are presented in Table 4-1.

#### **4.2 Experimental Procedure**

The model was packed by the wet-packing method by using 80-120 mesh Ottawa silica sand, having an average density of 2.5 g/ml. During the packing process, the model was vibrated for approximately 10 hours to obtain as uniform a sand-pack as possible. Once it was packed, air was driven through the sand pack for approximately 12 hours in order to remove the water used for packing. Then a vacuum was drawn overnight (approximately 24 hrs) to completely remove the air and any water vapour. The model was, then, connected to the pump and distilled water was pumped through. A material balance was performed to determine the pore volume of the sand pack. Subsequently, the absolute permeability of the sand pack was determined using Darcy's law for several flow rates.

In order to establish an irreducible water saturation, an oil flood was conducted by injecting about three to four pore volumes of refined oil, until no more mobile water was observed at the outlet. Subsequently, the permeability to oil at irreducible water saturation was determined for several flow rates. The model was then opened from the side for packing the bottom-water layer. In order to establish an accurate height of the bottom-water layer, a special scraper was used to remove part of the oil sand pack. When the desired height was scraped off, the bottom-water layer was packed manually using the Ottawa sand that was used for packing the oil zone. Applying the appropriate confining pressure (60 psi) will thus, restore the absolute permeability of the bottom-water layer to the same as that of the oil layer. Figure 4-2 illustrate how the optimum confining pressure was calculated.

Table 4-1: Properties of the Sand Pack and Fluids

Type of sand	80-120 mesh Ottawa silica sand
Core length	90.0 cm (35.43 in)
Cross-sectional area	34.2 cm <sup>2</sup> (5.3 in <sup>2</sup> )
Bulk volume	3078.0 cm <sup>3</sup> (178.83 in <sup>3</sup> )
Average porosity	36.21 %
Average absolute permeability	10.48 μm <sup>2</sup> (10.61 Darcies)
Viscosity of MCT-5	34.3 mPa.s (34.3 cp)
Viscosity of MCT-10	68.0 mPa.s (68.0 cp)
Viscosity of LAGO	11.0 mPa.s (11.0 cp)
Viscosity of distilled water	1.0 mPa.s (1.0 cp)
Density of distilled water	0.9982 g/cm <sup>3</sup> (62.287 lb/cf)
Density of MCT-5	0.8123 g/cm <sup>3</sup> (50.687 lb/cf)
Density of MCT-10	0.8576 g/cm <sup>3</sup> (53.514 lb/cf)
Density of LAGO	0.7963 g/cm <sup>3</sup> (49.689 lb/cf)
Polymer used	Polyacrylamide (Low Anionic/Medium Mol. Wt.)
Polymer molecular weight	3.0-4.5x10 <sup>6</sup>

The initial oil-in-place (IOIP) was calculated using the IOIP of the homogeneous pack before packing. The bottom-water layer was multiplied by the ratio of the height of the oil zone thickness to the model thickness. This method of obtaining the IOIP of the bottom-water layer was found to have less than 5% error when 4 checks were done by weighing the scraped-off oil layer to obtain the exact amount of the removed oil. All of the IOIP's of the bottom-water experiments were calculated using this method.

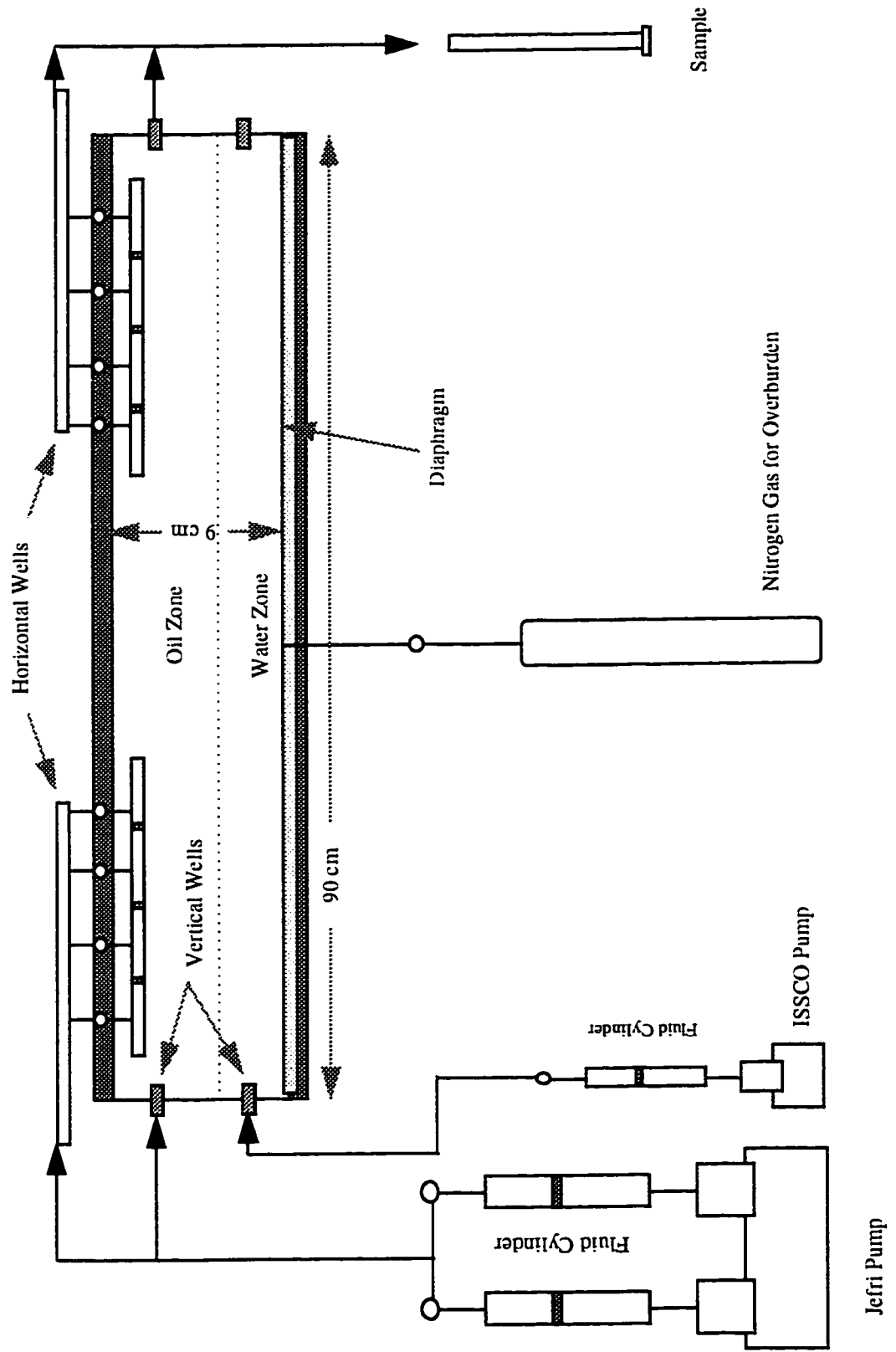


Figure 4-1: Schematic of the Experimental Apparatus

### Determination of the Optimum Confining Pressure

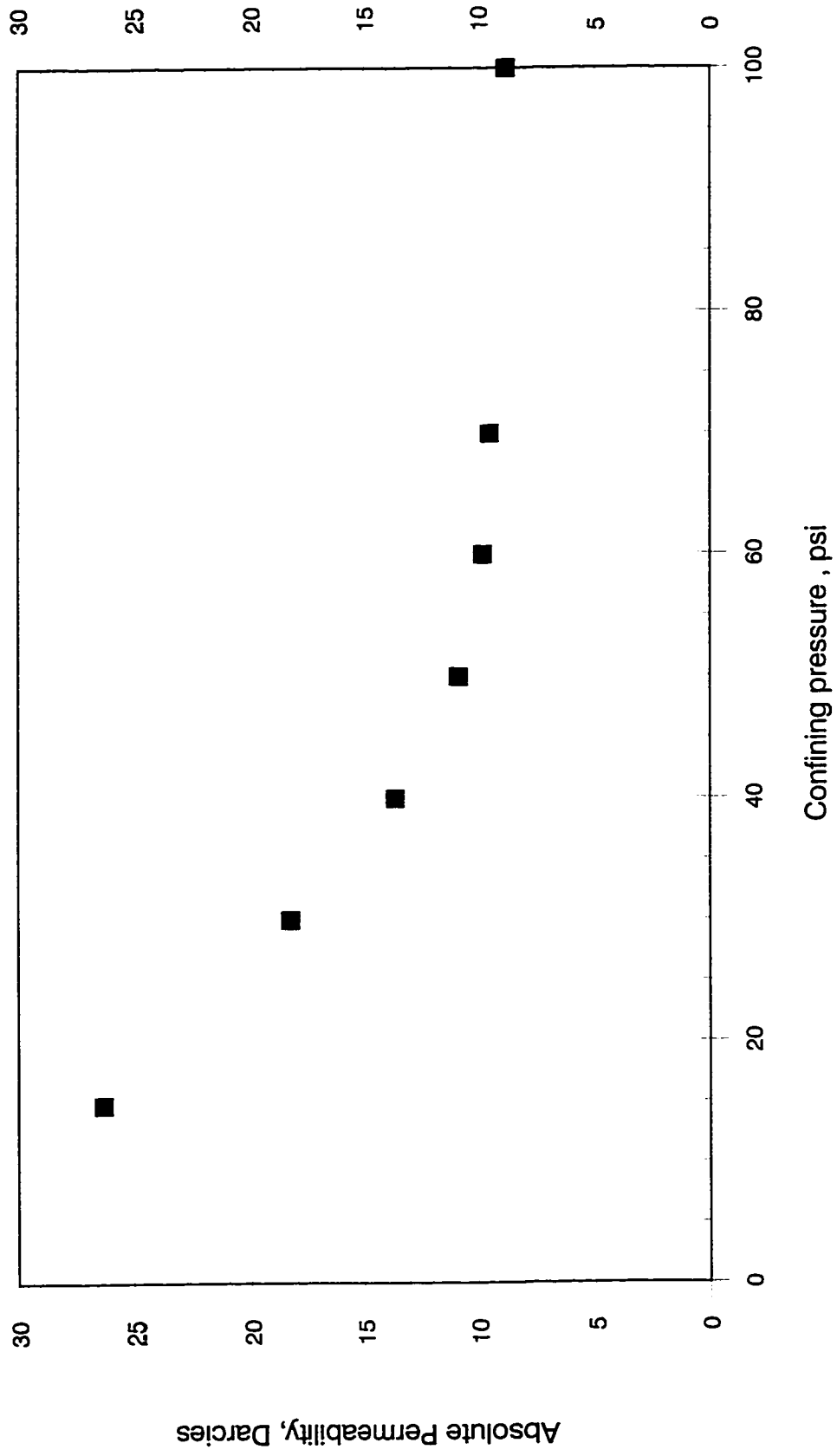


Figure 4-2: Effect of Confining Pressure on Absolute Permeability of the Pack

## Chapter 5

### DEVELOPMENT OF THE ANALYTICAL MODEL

Among the factors influencing fluid flow in layered permeable media is flow from one layer to another in a direction perpendicular to bulk flow. This crossflow may be the result of any or all of the four forces that cause fluid to flow in a permeable medium: viscous forces, capillarity, gravity and concentration. These driving forces interact with each other in experimental displacements,<sup>16-18</sup> making it difficult to credit the observed crossflow to the correct mechanism. This is true to a large extent in simulated displacements,<sup>24</sup> but it is possible to simulate displacements with only one effect present<sup>40,41</sup>.

The objective of this chapter is to describe theoretically the effects of the crossflow caused by viscous forces on displacements in a two-layer reservoir, the lower layer being a water zone. This can be accomplished in an unconventional way by solving the flow equations for maximum crossflow, which utilizes the idea of vertical equilibrium solution techniques.

The vertical equilibrium concept has been used extensively in the petroleum literature<sup>10,12,14,42,43</sup>, mainly as a way to collapse simulations to a lower dimension. Generally, vertical equilibrium means that the sum of the driving forces in the vertical direction is zero for all fluid components. Since only viscous crossflow is being dealt with, vertical equilibrium here means that the vertical pressure drop is zero at all times and positions in the reservoir. This means that the horizontal pressure gradients are equal at all vertical positions, though they can change with time and horizontal position. It is not generally recognized that assuming vertical equilibrium in a displacement implies perfect vertical communication<sup>14,42</sup>, and this is the basis for the claim that vertical equilibrium implies the maximum degree of crossflow possible.

### **5.1 Derivation of the Crossflow Equations**

In the following, an attempt is made to develop an expression for predicting cumulative oil recovery and cumulative fluid injection occurring while waterflooding a two-layer reservoir, the lower layer being a water zone.

Due to vertical pressure gradients caused by the displacing and displaced fluids having unequal mobilities, fluids would flow between layers if vertical communication is allowed to exist. As might be expected, fluid flows between the layers and, according to Darcy's law, the vertical pressure drop decreases. Just how much fluid flows and how much decrease in the pressure drop occurs depends on the vertical transmissibility.

Consider a two-layer porous medium as shown in Figure 5-1 (figures are at the end chapter), the upper layer being the oil zone with a permeability  $k_{owr}$ , and the lower layer being the water zone with a permeability of  $k_w$ . Water is being injected at a total rate  $q_T$ , of which  $q_1$  is entering the oil zone and  $q_2$  is entering the bottom-water zone. In order to isolate viscous crossflow from the other types of crossflow the following assumptions are made:

- 1) gravity forces and capillary pressure effects are negligible;
- 2) two-layered reservoir, the lower layer is the water zone;
- 3) homogenous properties exist throughout each layer;
- 4) rate constraint;
- 5) crossflow is vertical;
- 6) vertical equilibrium viscous crossflow;
- 7) fluids are incompressible and immiscible;
- 8) viscous fingering is negligible;
- 9) sharp fronts exist in each layer; and
- 10) only water flows behind the trailing flood front in both layers;

Consider a vertical section of thickness  $\Delta x_{f1}$  and width  $W$ , around the trailing flood front on Layer 1 as shown in Figure 5-2. Applying a mass balance over the water in the control volume in the section shown in Figure 5-2 across the trailing flood front ( $x_{f1}$ ) on Layer 1 yields:

$$\text{Rate in} - \text{Rate out} = \text{Rate of accumulation} \quad (5.1)$$

$$q_{L1}f_{wL1} - q_{CF1 \rightarrow 2}f_{wCF1 \rightarrow 2} - q_{M1}f_{wM1} = W\phi_1 h_1 \frac{\Delta x_{f1}}{\Delta t} (S_{L1} - S_{M1}) \quad (5.2)$$

Due to the assumption of vertical equilibrium viscous crossflow, a second front is set up in Layer 2 (bottom-water layer) traveling with the same velocity as the front in Layer 1 (oil layer). Therefore, a similar water balance across this front yields:

$$q_{L2}f_{wL2} + q_{CF1 \rightarrow 2}f_{wCF1 \rightarrow 2} - q_{M2}f_{wM2} = W\phi_2 h_2 \frac{\Delta x_{f1}}{\Delta t} (S_{L2} - S_{M2}) \quad (5.3)$$

where

$q_{L1}f_{wL1}$	= water flow rate in the oil zone in region $\mathcal{L}$ , $L^3/t$
$q_{L2}f_{wL2}$	= water flow rate in the bottom-water zone in region $\mathcal{L}$ , $L^3/t$
$q_{M1}f_{wM1}$	= water flow rate in the oil zone in region $\mathcal{M}$ , $L^3/t$
$q_{M2}f_{wM2}$	= water flow rate in the bottom-water zone in region $\mathcal{M}$ , $L^3/t$
$q_{CF1 \rightarrow 2}$	= flow rate of fluid flowing at the trailing flood front from the the oil zone into the water zone, $L^3/t$
$f_{wCF1 \rightarrow 2}$	= fractional flow of flowing fluid that is water, evaluated around the trailing flood front
$\Delta x_{f1}$	= distance the front position in oil zone travels in time $\Delta t$ , $L$
$S_{L1}$	= water saturation in the oil zone in region $\mathcal{L}$
$S_{L2}$	= water saturation in the bottom-water zone in region $\mathcal{L}$
$S_{M1}$	= water saturation in the oil zone in region $\mathcal{M}$
$S_{M2}$	= water saturation in the bottom-water zone in region $\mathcal{M}$



Applying another mass balance to the water in the control volume in the section shown in Figure 5-3, across the advancing flood front ( $x_{f2}$ ) on Layer 2 yields:

$$q_{M2}f_{wM2} - q_{CF2 \rightarrow 1}f_{wCF2 \rightarrow 1} - q_{R2}f_{wR2} = W\phi_2 h_2 \frac{\Delta x_{f2}}{\Delta t} (S_{M2} - S_{R2}) \quad (5.4)$$

Also a similar water balance can be made around the advancing front in Layer 1 which is caused by the crossflow from Layer 2

$$q_{M1}f_{wM1} + q_{CF2 \rightarrow 1}f_{wCF2 \rightarrow 1} - q_{R1}f_{wR1} = W\phi_1 h_1 \frac{\Delta x_{f2}}{\Delta t} (S_{M1} - S_{R1}) \quad (5.5)$$

where

- $q_{R1}f_{wR1}$  = water flow rate in the oil zone in region  $R$ ,  $L^3/t$
- $q_{R2}f_{wR2}$  = water flow rate in the bottom-water zone in region  $R$ ,  $L^3/t$
- $q_{CF2 \rightarrow 1}$  = flow rate of fluid flowing at the advancing flood front from the water zone into the oil zone,  $L^3/t$
- $f_{wCF2 \rightarrow 1}$  = fractional flow of flowing fluid that is water, evaluated around the advancing flood front
- $\Delta x_{f2}$  = distance the front position in the water zone travels in time  $\Delta t$ ,  $L$
- $S_{R1}$  = water saturation in the oil zone in region  $R$
- $S_{R2}$  = water saturation in the bottom-water zone in region  $R$

Eliminating  $W \frac{\Delta x_{f1}}{\Delta t}$  in Equations (5.2) and (5.3) and eliminating  $W \frac{\Delta x_{f2}}{\Delta t}$  in Equations (5.4) and (5.5) gives:

$$\begin{aligned} & (q_{L1}f_{wL1} - q_{CF1 \rightarrow 2}f_{wCF1 \rightarrow 2} - q_{M1}f_{wM1})(S_{L2} - S_{M2}) = \\ & (q_{L2}f_{wL2} + q_{CF1 \rightarrow 2}f_{wCF1 \rightarrow 2} - q_{M2}f_{wM2})(S_{L1} - S_{M1}) \frac{\phi_1 h_1}{\phi_2 h_2} \end{aligned} \quad (5.6)$$

and

$$\begin{aligned} & (q_{M1}f_{wM1} + q_{CF_{2 \rightarrow 1}}f_{wCF_{2 \rightarrow 1}} - q_{R1}f_{wR1})(S_{M2} - S_{R2}) = \\ & (q_{M2}f_{wM2} - q_{CF_{2 \rightarrow 1}}f_{wCF_{2 \rightarrow 1}} - q_{R2}f_{wR2})(S_{M1} - S_{R1}) \frac{\phi_1 h_1}{\phi_2 h_2} \end{aligned} \quad (5.7)$$

For the above equations, the saturations  $S_{M1}$  and  $S_{M2}$  are unknown as well as the crossflow flow rates, fractional flow terms, and the flow rates in each layer in regions  $\mathcal{E}$ ,  $\mathcal{M}$ , and  $\mathcal{R}$ .

### 5.1.1 Calculation of $q_{CF_{1 \rightarrow 2}}$ and $q_{CF_{2 \rightarrow 1}}$

In order to expand  $q_{CF_{1 \rightarrow 2}}$  and  $q_{CF_{2 \rightarrow 1}}$  in Equations (5.6) and (5.7), one should do an overall mass fluid balance (oil and water) for the trailing and advancing flood fronts in each layer.

$$q_{L1} = q_{CF_{1 \rightarrow 2}} + q_{M1} \quad (5.8)$$

$$q_{L2} + q_{CF_{1 \rightarrow 2}} = q_{M2} \quad (5.9)$$

$$q_{M2} = q_{CF_{2 \rightarrow 1}} + q_{R2} \quad (5.10)$$

$$q_{M1} + q_{CF_{2 \rightarrow 1}} = q_{R1} \quad (5.11)$$

where

$$q_{L1} = \text{flow rate in the oil zone in region } \mathcal{E}, L^3/t$$

$$q_{L2} = \text{flow rate in the bottom-water zone in region } \mathcal{E}, L^3/t$$

$$q_{M1} = \text{flow rate in the oil zone in region } \mathcal{M}, L^3/t$$

$$q_{M2} = \text{flow rate in the bottom-water zone in region } \mathcal{M}, L^3/t$$

$$q_{R1} = \text{flow rate in the oil zone in region } \mathcal{R}, L^3/t$$

$$q_{R2} = \text{flow rate in the bottom-water zone in region } \mathcal{R}, L^3/t$$

Combining Equations (5.8) and (5.9) to solve for  $q_{CF_{1 \rightarrow 2}}$

$$q_{CF_{1 \rightarrow 2}} = \frac{(q_{L1} - q_{M1}) + (q_{M2} - q_{L2})}{2} \quad (5.12)$$

Combining Equation (5.10) and (5.11) to solve for  $q_{CF_{2 \rightarrow 1}}$

$$q_{CF_2 \rightarrow 1} = \frac{(q_{M2} - q_{R2}) + (q_{R1} - q_{M1})}{2} \quad (5.13)$$

Eliminating  $q_{CF_1 \rightarrow 2}$  and  $q_{CF_2 \rightarrow 1}$  from Equations (5.6) and (5.7) using Equations (5.12) and (5.13) and dividing both sides of the resulting equations by total injection rate  $q_T$ , results in:

$$\left( \frac{q_{L1}}{q_T} f_{wL1} - \frac{(q_{L1} - q_{M1}) + (q_{M2} - q_{L2})}{2q_T} f_{wCF_1 \rightarrow 2} - \frac{q_{M1}}{q_T} f_{wM1} \right) (S_{L2} - S_{M2}) = \left( \frac{q_{L2}}{q_T} f_{wL2} + \frac{(q_{L1} - q_{M1}) + (q_{M2} - q_{L2})}{2q_T} f_{wCF_1 \rightarrow 2} - \frac{q_{M2}}{q_T} f_{wM2} \right) (S_{L1} - S_{M1}) \frac{\phi_1 h_1}{\phi_2 h_2} \quad (5.14)$$

and

$$\left( \frac{q_{M1}}{q_T} f_{wM1} + \frac{(q_{M2} - q_{R2}) + (q_{R1} - q_{M1})}{2q_T} f_{wCF_2 \rightarrow 1} - \frac{q_{R1}}{q_T} f_{wR1} \right) (S_{M2} - S_{R2}) = \left( \frac{q_{M2}}{q_T} f_{wM2} - \frac{(q_{M2} - q_{R2}) + (q_{R1} - q_{M1})}{2q_T} f_{wCF_2 \rightarrow 1} - \frac{q_{R2}}{q_T} f_{wR2} \right) (S_{M1} - S_{R1}) \frac{\phi_1 h_1}{\phi_2 h_2} \quad (5.15)$$

### 5.1.2 Calculation of $f_{wCF_1 \rightarrow 2}$ and $f_{wCF_2 \rightarrow 1}$

The fractional flow terms are usually evaluated at a single saturation value, but in this situation, water may flow from either side of the fronts as shown in Figure 5-4.

Therefore,  $f_{wCF_1 \rightarrow 2}$ , in this dissertation, is defined as:

$$f_{wCF_1 \rightarrow 2} = \frac{(q_{wCF_1 \rightarrow 2})_L + (q_{wCF_1 \rightarrow 2})_M}{(q_{wCF_1 \rightarrow 2} + q_{oCF_1 \rightarrow 2})_L + (q_{wCF_1 \rightarrow 2} + q_{oCF_1 \rightarrow 2})_M} \quad (5.16)$$

Substituting Darcy's equation for the flow rates in Equation (5.16) results in:

$$f_{wCF_1 \rightarrow 2} = \frac{k_{z1} \frac{k_{rw}}{\mu_w} W L_E \left( \frac{\Delta p}{\Delta h} \right)_{E1} + k_{z1} \frac{k_{rw}}{\mu_w} W L_M \left( \frac{\Delta p}{\Delta h} \right)_{M1}}{\left( \frac{k_{rw}}{\mu_w} + \frac{k_{ro}}{\mu_o} \right)_{E1} k_{z1} W L_E \left( \frac{\Delta p}{\Delta h} \right)_{E1} + \left( \frac{k_{rw}}{\mu_w} + \frac{k_{ro}}{\mu_o} \right)_{M1} k_{z1} W L_M \left( \frac{\Delta p}{\Delta h} \right)_{M1}} \quad (5.17)$$

By assuming that  $l_L$  is small and equal to  $l_M$  and that  $\left(\frac{\Delta p}{\Delta h}\right)_{L1}$  equals  $\left(\frac{\Delta p}{\Delta h}\right)_{M1}$  and cancelling all equivalent terms in Equation (5.17), the result is:

$$f_{wCF_{1 \rightarrow 2}} = \frac{\left(\frac{k_{rw}}{\mu_w}\right)_{L1} + \left(\frac{k_{rw}}{\mu_w}\right)_{M1}}{\left(\frac{k_{rw}}{\mu_w} + \frac{k_{ro}}{\mu_o}\right)_{L1} + \left(\frac{k_{rw}}{\mu_w} + \frac{k_{ro}}{\mu_o}\right)_{M1}} \quad (5.18)$$

Applying the same procedures, arguments and assumptions for the leading flood front on Layer 2 to calculate  $f_{wCF_{2 \rightarrow 1}}$  results in:

$$f_{wCF_{2 \rightarrow 1}} = \frac{\left(\frac{k_{rw}}{\mu_w}\right)_{M2} + \left(\frac{k_{rw}}{\mu_w}\right)_{R2}}{\left(\frac{k_{rw}}{\mu_w} + \frac{k_{ro}}{\mu_o}\right)_{M2} + \left(\frac{k_{rw}}{\mu_w} + \frac{k_{ro}}{\mu_o}\right)_{R2}} \quad (5.19)$$

### 5.1.3 Calculation of $q_L$ , $q_M$ and $q_R$

From Darcy's law,  $\left(\frac{q_{L1}}{q_T}\right)$  can be evaluated as:

$$\frac{q_{L1}}{q_T} = \frac{k_1 h_1 W \left(\frac{k_{rw}}{\mu_w}\right)_{L1} \left(\frac{dp}{dx}\right)_{L1}}{k_1 h_1 W \left(\frac{k_{rw}}{\mu_w}\right)_{L1} \left(\frac{dp}{dx}\right)_{L1} + k_2 h_2 W \left(\frac{k_{rw}}{\mu_w}\right)_{L2} \left(\frac{dp}{dx}\right)_{L2}} \quad (5.20)$$

The derivation to this point is completely general; however, invoking the vertical equilibrium assumption implies that the horizontal pressure drops for every layer are equal. This allows the pressure gradients in Equation (5.20) to be canceled out. Thus:

$$\frac{q_{L1}}{q_T} = \frac{k_1 h_1}{k_1 h_1 + k_2 h_2} \quad (5.21)$$

As stated earlier, the assumption of vertical equilibrium viscous crossflow is synonymous with zero vertical pressure drop. A zero vertical pressure drop implies that the horizontal pressure drop across any cross-section is the same for all layers. Thus:

$$\left(\frac{dp}{dx}\right)_{L1} = \left(\frac{dp}{dx}\right)_{L2}$$

which allows the pressure drop in Equation (5.20) to divide out.

A similar procedure can be carried out to calculate the flow rates for the other regions

$$\frac{q_{L2}}{q_T} = \frac{k_2 h_2}{k_1 h_1 + k_2 h_2} \quad (5.22)$$

$$\frac{q_{M1}}{q_T} = \frac{k_1 h_1 \left( \frac{k_{rw}}{\mu_w} + \frac{k_{ro}}{\mu_o} \right)_{M1}}{k_1 h_1 \left( \frac{k_{rw}}{\mu_w} + \frac{k_{ro}}{\mu_o} \right)_{M1} + k_2 h_2 \left( \frac{k_{rw}}{\mu_w} + \frac{k_{ro}}{\mu_o} \right)_{M2}} \quad (5.23)$$

$$\frac{q_{M2}}{q_T} = \frac{k_2 h_2 \left( \frac{k_{rw}}{\mu_w} + \frac{k_{ro}}{\mu_o} \right)_{M2}}{k_1 h_1 \left( \frac{k_{rw}}{\mu_w} + \frac{k_{ro}}{\mu_o} \right)_{M1} + k_2 h_2 \left( \frac{k_{rw}}{\mu_w} + \frac{k_{ro}}{\mu_o} \right)_{M2}} \quad (5.24)$$

$$\frac{q_{R1}}{q_T} = \frac{k_1 h_1 \left( \frac{k_{rw}}{\mu_w} + \frac{k_{ro}}{\mu_o} \right)_{R1}}{k_1 h_1 \left( \frac{k_{rw}}{\mu_w} + \frac{k_{ro}}{\mu_o} \right)_{R1} + k_2 h_2 \left( \frac{k_{rw}}{\mu_w} + \frac{k_{ro}}{\mu_o} \right)_{R2}} \quad (5.25)$$

and

$$\frac{q_{R2}}{q_T} = \frac{k_2 h_2 \left( \frac{k_{rw}}{\mu_w} + \frac{k_{ro}}{\mu_o} \right)_{R2}}{k_1 h_1 \left( \frac{k_{rw}}{\mu_w} + \frac{k_{ro}}{\mu_o} \right)_{R1} + k_2 h_2 \left( \frac{k_{rw}}{\mu_w} + \frac{k_{ro}}{\mu_o} \right)_{R2}} \quad (5.26)$$

#### 5.1.4 Calculation of the unknown saturations $S_{M1}$ and $S_{M2}$

All the terms in Equations (5.6) and (5.7) are known qualities of system and fluid properties or functions of the unknown saturations  $S_{M1}$  and  $S_{M2}$ . Therefore, Equations (5.6) and (5.7) are functions of saturation and reservoir parameters. They are non-linear equations in terms of  $S_{M1}$  and  $S_{M2}$ , and the solution to the set of equations can be

obtained using Newton's method for two-dependent variable,  $S_{M1}$  and  $S_{M2}$ . Appendix A illustrates the procedure for obtaining the unknown saturations  $S_{M1}$  and  $S_{M2}$ .

Once the mixing zone saturations ( $S_{M1}, S_{M2}$ ) are known, the front's position and hence cumulative fluid injection and oil recovery can be calculated as discussed in the following sections.

## 5.2 Calculation of $x_{f1}$ and $x_{f2}$

The front position in each layer can be determined by making an overall water balance for the trailing and advancing flood fronts in each layer.

$$\text{Rate in} - \text{Rate out} = \text{Rate of accumulation} \quad (5.27)$$

$$(q_{wL1} + q_{wL2}) - (q_{wM1} + q_{wM2}) = Wv_{x_{f1}} [\phi_1 h_1 (S_{L1} - S_{M1}) + \phi_2 h_2 (S_{L2} - S_{M2})] \quad (5.28)$$

Solving for  $v_{x_{f1}}$

$$v_{x_{f1}} = \frac{dx_{f1}}{dt} = \frac{(q_{wL1} + q_{wL2}) - (q_{wM1} + q_{wM2})}{W[\phi_1 h_1 (S_{L1} - S_{M1}) + \phi_2 h_2 (S_{L2} - S_{M2})]} \quad (5.29)$$

For the advancing front, calculation of  $v_{x_{f2}}$  is similar to that for  $v_{x_{f1}}$ , thus:

$$v_{x_{f2}} = \frac{dx_{f2}}{dt} = \frac{(q_{wM1} + q_{wM2}) - (q_{wR1} + q_{wR2})}{W[\phi_1 h_1 (S_{M1} - S_{R1}) + \phi_2 h_2 (S_{M2} - S_{R2})]} \quad (5.30)$$

Taking the velocities ratio  $\left(\frac{dx_{f1}}{dt} / \frac{dx_{f2}}{dt}\right)$  by dividing Equation (5.29) by Equation

(5.30) will eliminate the time and results in:

$$\frac{dx_{f1}}{dx_{f2}} = \frac{[(q_{wL1} + q_{wL2}) - (q_{wM1} + q_{wM2})][\phi_1 h_1 (S_{L1} - S_{M1}) + \phi_2 h_2 (S_{L2} - S_{M2})]}{[(q_{wM1} + q_{wM2}) - (q_{wR1} + q_{wR2})][\phi_1 h_1 (S_{M1} - S_{R1}) + \phi_2 h_2 (S_{M2} - S_{R2})]} \quad (5.31)$$

Integrating equation (5.31) results in the position ratio of the two fronts

$$\frac{x_{f1}}{x_{f2}} = \frac{[(q_{wL1} + q_{wL2}) - (q_{wM1} + q_{wM2})][\phi_1 h_1 (S_{L1} - S_{M1}) + \phi_2 h_2 (S_{L2} - S_{M2})]}{[(q_{wM1} + q_{wM2}) - (q_{wR1} + q_{wR2})][\phi_1 h_1 (S_{M1} - S_{R1}) + \phi_2 h_2 (S_{M2} - S_{R2})]} \quad (5.32)$$

Equation (5.32) allows one to obtain the front position in Layer 1 with respect to the front position in Layer 2. This enables one to calculate oil recovery and cumulative fluid injection by determining the front position in one layer if one chooses the position of the other front, provided that the saturations in the mixing zone are known.

### 5.3 Calculation of oil Recovery and Cumulative Fluid Injection

In order to calculate oil recovery and cumulative fluid injection, it is necessary to derive a simple analytical expression that allows for the use of the individual front positions which can be calculated by Equation (5.32).

Taking an oil balance over the entire system as shown in Figure 5-5 results in:

$$\text{Cumulative Oil Produced} = \text{Initial Oil In Place} - \text{Oil Remaining} \quad (5.33)$$

$$\begin{aligned} Q_o = & \phi_1 h_1 W x_{f1} (1 - S_{wc} - S_{or}) + \phi_1 h_1 W (x_{f2} - x_{f1}) (S_{M1} - S_{wc}) + \\ & \phi_1 h_1 W (l_x - x_{f2}) (S_{R1} - S_{wc}) - \phi_2 h_2 W x_{f1} S_{or} - \\ & \phi_2 h_2 W (x_{f2} - x_{f1}) (1 - S_{M2}) - \phi_2 h_2 W (l_x - x_{f2}) (1 - S_{R2}) \end{aligned} \quad (5.34)$$

Dividing Equation (5.34) by the total pore volume of the system results in:

$$\begin{aligned} Q_{Do} = & R_{\phi_1 h_1} x_{Df1} (1 - S_{wc} - S_{or}) + R_{\phi_1 h_1} (x_{Df2} - x_{Df1}) (S_{M1} - S_{wc}) + \\ & R_{\phi_1 h_1} (1 - x_{Df2}) (S_{R1} - S_{wc}) - R_{\phi_2 h_2} x_{Df1} S_{or} - \\ & R_{\phi_2 h_2} (x_{Df2} - x_{Df1}) (1 - S_{M2}) - R_{\phi_2 h_2} (1 - x_{Df2}) (1 - S_{R2}) \end{aligned} \quad (5.35)$$

where

$Q_{Do}$  = Cumulative oil production in pore volume

$$R_{\phi_1 h_1} = \frac{\phi_1 h_1}{\phi_1 h_1 + \phi_2 h_2} \quad (5.36)$$

$$R_{\phi_2 h_2} = \frac{\phi_2 h_2}{\phi_1 h_1 + \phi_2 h_2} \quad (5.37)$$

$$x_{Df1} = \frac{x_{f1}}{l_x} \quad (5.38)$$

$$x_{Df2} = \frac{x_{f2}}{l_x} \quad (5.39)$$

To calculate cumulative fluid injection, the total fluid balance is taken over the entire system as shown in Figure 5-5.

$$\text{Total water injection} = \text{Total oil production} + \text{Total water production} \quad (5.40)$$

Applying the same arguments and procedure as used above, results in:

$$Q_{Di} = R_{\phi_1 h_1} x_{Df1} (1 - S_{or} - S_{wc}) + R_{\phi_1 h_1} (x_{Df2} - x_{Df1}) (S_{M1} - S_{wc}) + R_{\phi_2 h_2} x_{Df1} (1 - S_{or} - S_{wc}) + R_{\phi_2 h_2} (x_{Df2} - x_{Df1}) (S_{M2} - S_{wc}) \quad (5.41)$$

where

$$Q_{Di} = \text{Cumulative water injection in pore volume}$$

In order to calculate the cumulative water injection after the breakthrough of the advancing flood front  $x_{f2}$ , the same procedure is repeated for calculating new unknown saturations ( $S_{M1}^n, S_{M2}^n$ ) for a new system with new flood fronts which will have a length of  $l_x - x_{f1}$ , and new saturations ahead of the advancing flood front. The new saturations of this zone will be set equal to the previous saturations ( $S_{M1}, S_{M2}$ ) of the old mixing zone. A schematic of the above procedure is illustrated in Figure 5-5.

To calculate the cumulative fluid injection after breakthrough, one takes a water balance over the entire system as shown in Figure 5-5. Applying the same procedure as before results in:

$$Q_{Di}^n = R_{\phi_1 h_1} x_{Df1}^n (1 - S_{M1} - S_{or}) + R_{\phi_1 h_1} (x_{Df2}^n - x_{Df1}^n) (S_{M1}^n - S_{M1}) + R_{\phi_2 h_2} x_{Df1}^n (1 - S_{M2} - S_{or}) + R_{\phi_2 h_2} (x_{Df2}^n - x_{Df1}^n) (S_{M2}^n - S_{M2}) \quad (5.42)$$

where

$$Q_{Di} = \text{Cumulative water injection in pore volume after breakthrough.}$$



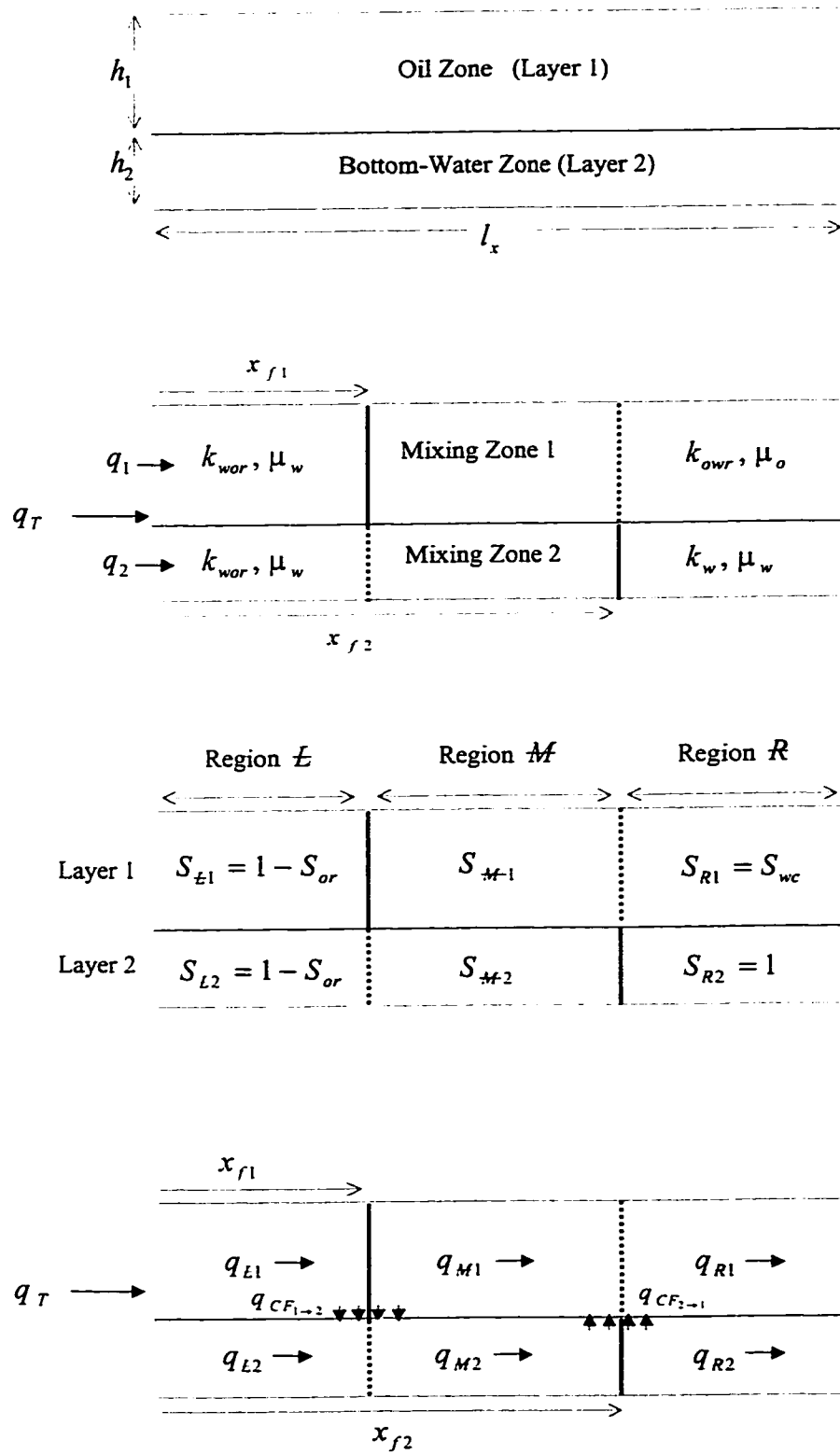


Figure 5-1: Schematic Illustration for Viscous Crossflow

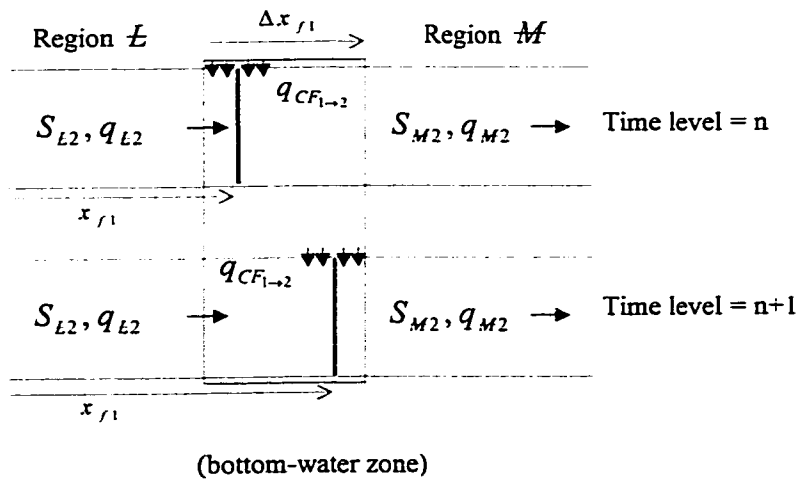
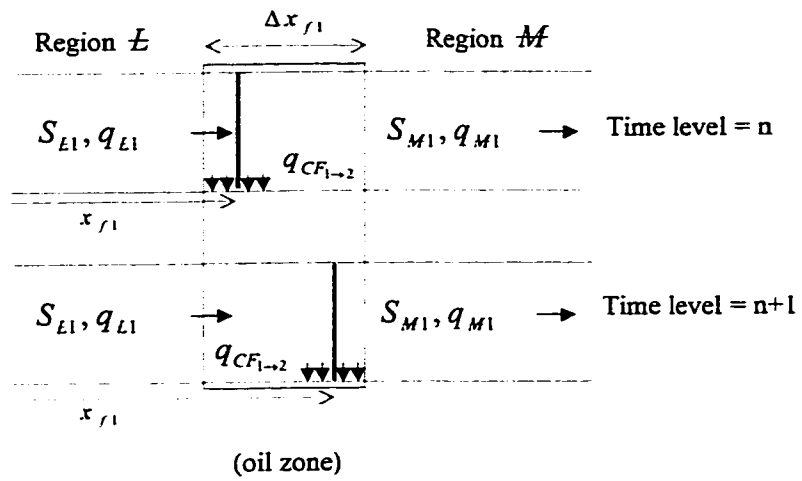


Figure 5-2: Illustration of Control Volume for the Trailing Flood Front

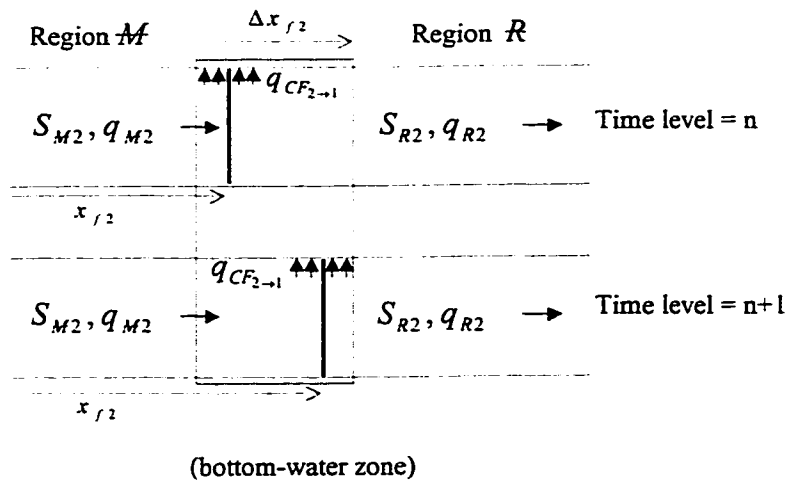
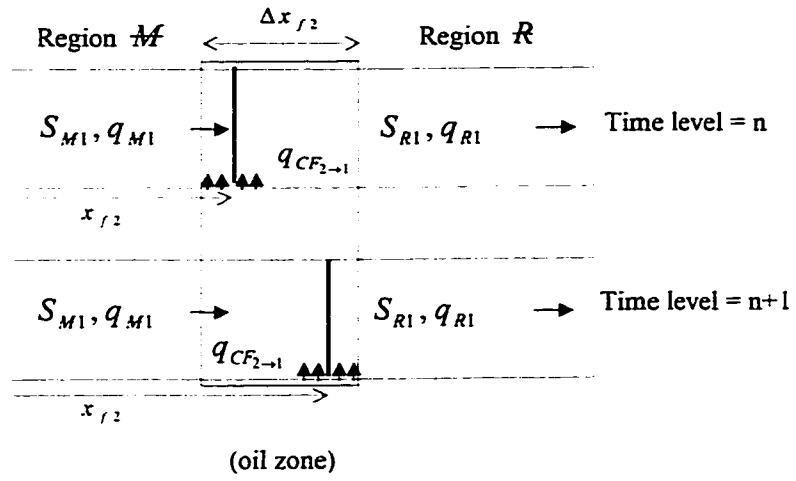


Figure 5-3: Illustration of Control Volume for the Advancing Flood Front

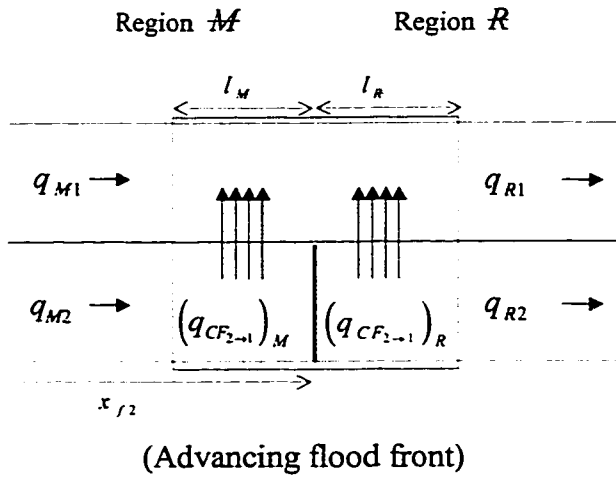
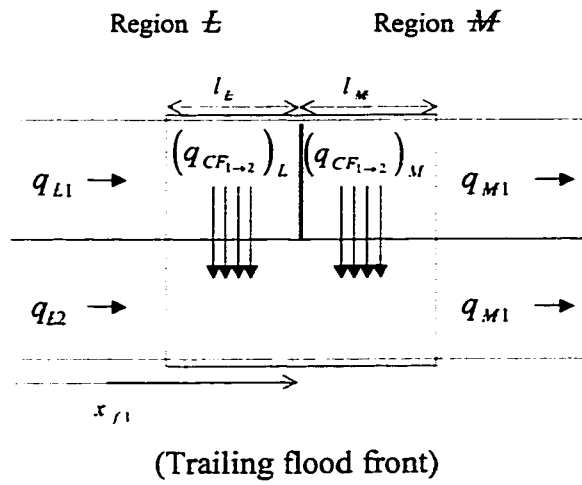
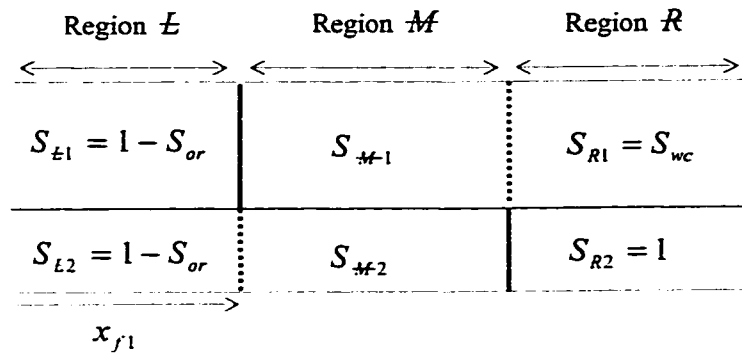
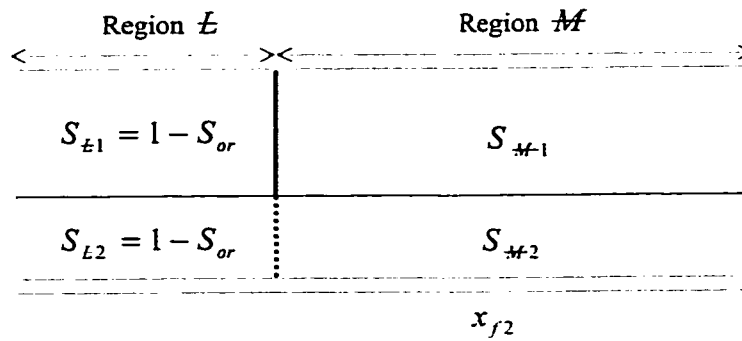


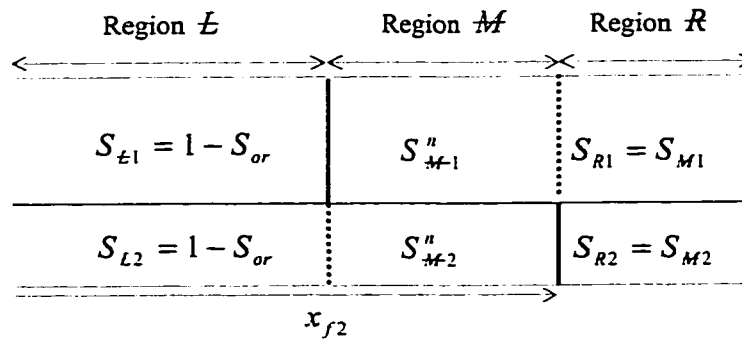
Figure 5-4: Schematic Illustration of Fluid Crossflow Around the Fronts



(Before breakthrough)



(At breakthrough)



(After breakthrough)

Figure 5-5: Schematic Illustration of the Reservoir Saturation Distribution

## Chapter 6

### OIL DISPLACEMENT BY WATER AND POLYMERS

When waterflooding a reservoir proves to be inefficient, in the sense that there is early water production and low oil recovery at breakthrough, polymer flooding may be considered as a possible remedy. However, exactly how the polymer flooding process is applied and how the design of the flood is determined depends on the nature of the recovery mechanism.

Central to all polymer oil recovery mechanisms<sup>44-47</sup>, however, is the idea of mobility ratio,  $M$ , defined as:

$$M = \frac{\lambda_w}{\lambda_o} = \frac{k_w \mu_o}{\mu_w k_o} \quad (6.1)$$

where  $\lambda_o$  and  $\lambda_w$  are the oil and water mobilities and  $k_o$  and  $k_w$  refer to the effective permeabilities of oil and water phases. Effective permeabilities are referred to since that quantity also allows for the selective reduction of (usually aqueous) phase permeability by pore-blocking mechanisms. There are essentially two situations where the application of polymers may be considered as follows:

- Unfavourable mobility ratio waterflood.
- Excessive reservoir heterogeneity.

In the first case, polymer improves the areal and vertical sweep efficiencies by remedying the mobility ratio problem. The polymer increases the aqueous-phase viscosity and may, in addition, decrease the permeability to the aqueous phase for certain polymers (usually synthetic).

In the second case, even in a reservoir where the water-oil mobility ratio is close to unity,

there may be a very inefficient sweep by waterflooding because of reservoir heterogeneity. Polymer improves the vertical sweep efficiency in this case. The mechanism of oil recovery in polymer flooding cases of this type is rather more complex due to fluid crossflow between layers which often plays a significant role in this type of flood. There are further complications that may come into play when considering water and polymer flooding in layered systems; other forces such as gravity and capillary pressure may also interact with the overall viscous effects of the polymer.

### ***6.1 Mathematical Model of Water/Polymer Flooding***

A simulator is very useful for facilitating the design of pilots and to assess potential reservoirs for mobility modification treatments using polymers. Such a simulator must be able to describe the transport of polymer in stratified reservoirs. It must be able to account for phenomena such as inaccessible pore volume to macromolecules, adsorption of polymer on rock surfaces and polymer rheology.

Since the commercial simulator (BOAST) available for this research is designed strictly for water flooding, a three-dimensional, multiphase water/polymer simulator was developed in this study by incorporating the above-mentioned features into it. This simulator is capable of modeling a three-dimensional reservoir of heterogeneous distribution of porosity, permeability, saturations and depths to the formation top. This multiple layer model allows investigations of crossflow of fluid in porous media at various vertical transmissibility values . Using the simulator the effect of selected parameters on additional oil recovery over that by waterflood and polymer flood can also be investigated. This simulator also can be modified as desired to suit specific operational conditions and well configurations.

The formulation of a reservoir simulator follows a straightforward but sometimes tedious process. First, mass balance equations are written for each component present. These are combined with momentum balance equations to develop general equations of momentum conservation<sup>48-50</sup>. Next, equations of state describing the pressure, volume, and

concentration behaviour of the fluids are introduced to reduce the number of primary variables. Simplifying assumptions are introduced where appropriate.

### 6.1.1 Basic Assumptions

The following assumption were made in developing the mathematical model for the water/polymer flooding process:

1. Isothermal conditions.
2. No chemical reactions occur except polymer adsorption.
3. Darcy's law applies (for non-Newtonian flow, the calculated apparent viscosity is used in Darcy's equation).
4. Immiscible displacement between oil and water phases is considered.
5. The porosity of the reservoir rock is assumed independent of reservoir pressure.
6. Ideal mixing holds (i.e. volume effects due to a change in the concentration of polymer are neglected).
7. Dispersion follows a generalization of Fick's law to multiphase flow in porous media.
8. Various assumptions about functional dependencies of the properties are made.

Exactly four partial differential equations are available. In Appendix B, the details of the derivation of these differential equations are discussed.

#### Oil Equation

$$\nabla(\lambda_o \nabla \phi_o) + q_o^* = \frac{\partial}{\partial t} \left( \frac{\phi S_o}{B_o} \right) \quad (6.2)$$

#### Water Equation

$$\nabla(\lambda_w \nabla \phi_w) + q_w^* = \frac{\partial}{\partial t} \left( \frac{\phi S_w}{B_w} \right) \quad (6.3)$$



## Gas Equation

$$\begin{aligned} \nabla(R_{sw}\lambda_w \nabla\phi_w) + \nabla(R_{so}\lambda_o \nabla\phi_o) + \nabla(\lambda_g \nabla\phi_g) + R_{sw}q_w^* + R_{so}q_o^* + q_g^* = \\ \frac{\partial}{\partial t} \left( R_{sw} \frac{\phi S_w}{B_w} + R_{so} \frac{\phi S_o}{B_o} + \frac{\phi S_g}{B_g} \right) \end{aligned} \quad (6.4)$$

## Polymer Transport Equation

$$-\nabla\left(\frac{C_p u_w}{B_w}\right) + \nabla\left(\frac{D_p}{B_w} \nabla C_p\right) = \frac{\partial}{\partial t} \left( \frac{\phi_p S_w C_p}{B_w} \right) + \frac{\partial}{\partial t} \left( \frac{\rho_{rm}}{\rho_{wsc}} (1-\phi) C_s \right) \quad (6.5)$$

## **6.2 Physical Properties of Polymer Solutions**

The displacement of oil by polymer solutions has several unique characteristics that are not present in normal waterflooding. These include the non-Newtonian behaviour of polymer solutions, permeability reduction, inaccessible pore volume for the polymer, adsorption of polymer on the rock surface, and dispersion of the polymer. In the following section, the details of the evaluation of these effects are presented.

### **6.2.1 Non-Newtonian Viscosity and Shear Thinning**

The water phase contains two components; pure water and polymer. Because of the non-Newtonian behaviour of a polymer solution, the water phase viscosity is not only a function of polymer concentration, pressure and temperature, but also a function of the flow rate<sup>51</sup>. Fortunately, this system is isothermal, so the effect of temperature is ignored.

The behaviour of a polymer solution can be divided into three regions. In the limits of very low shear rate and very high shear rate, the viscosity will approach its maximum and minimum values, respectively. Over a large range of intermediate shear rates, the polymer solutions often behave as a power-law fluid.

The shear rate dependence of the polymer viscosity in the three regions was modeled by Meter's Equation<sup>52</sup>. The polymer viscosity can be expressed as:

$$\mu_p = \mu_{p_\infty} + \frac{\mu_{p_0} - \mu_{p_\infty}}{1 + \left( \frac{\dot{\gamma}}{\dot{\gamma}_{1/2}} \right)^{\alpha_m}} \quad (6.6)$$

where

$\mu_{p_0}$  = polymer solution viscosity at zero shear rate, m/Lt

$\mu_{p_\infty}$  = polymer solution viscosity at infinite shear rate, m/Lt

$\alpha_m$  = exponent parameter,

$\dot{\gamma}$  = shear rate, 1/t

$\dot{\gamma}_{1/2}$  = shear rate at which the viscosity is half of  $\mu_{p_0}$ , 1/t, and is defined as:

$$\dot{\gamma}_{1/2} = \beta_a C_p^{\beta_b} \quad (6.7)$$

where  $\beta_a$  and  $\beta_b$  are user parameters given in Table 6-1.

The exponent parameter ( $\alpha_m$ ) in Meter's Equation is defined as:

$$\alpha_m = \gamma_0 + \gamma_1 C_p + \gamma_2 C_p^2 + \gamma_3 C_p^3 - 1 \quad (6.8)$$

where  $\gamma_0$ ,  $\gamma_1$ ,  $\gamma_2$  and  $\gamma_3$  are constants dependent on the polymer type; they are given in Table 6-1.

The viscosity of a polymer solution at zero shear rate was considered as a function of polymer concentration only, and the effect of polymer concentration on the solution viscosity was modeled by a quadratic polynomial<sup>53-55</sup> as follows:

$$\mu_{p_0} = \mu_w + a_1 C_p + a_2 C_p^2 \quad (6.9)$$

where

$C_p$  = polymer solution concentration, m/m

$\mu_w$  = water viscosity, m/Lt, and

$a_1$  and  $a_2$  are constants given in Table 6-1.

Table 6-1: User-Specified Parameters for Simulation Runs

$A_{ad}^*$	0.04273
$a_1^*$	$6.375 \times 10^{-3} \text{ ppm}^{-1}$
$a_2^*$	$7.969 \times 10^{-6} \text{ ppm}^{-2}$
$a_{m1}$	$7.6 \times 10^5$
$a_{m2}$	$2\pi$
$a_{m3}$	0.28
$B_{ad}$	0.0 $\text{ppm}^{-1}$
$D_p^*$	0.075 $\text{cm}^2/\text{hr}$
$\phi$	36.2 %
$\phi_p$	32.0 %
$\gamma_0$	1.471
$\gamma_1$	$1.96 \times 10^{-4} \text{ ppm}^{-1}$
$\gamma_2$	$-2.882 \times 10^{-8} \text{ ppm}^{-2}$
$\gamma_3$	0.00 $\text{ppm}^{-3}$
$\beta_a$	$3.923 \times 10^8 \text{ sec}^{-1} \text{ ppm}^{-1}$
$\beta_b$	-2.116
$cl_p^*$	0.185 $\text{ppm}^{-1}$
$C_s^*$	0.0 ppm

\* Reproduced from the literature<sup>46-63</sup>

The polymer viscosity at infinite shear rate is approximated by setting it equal to the solvent (water) viscosity ( $\mu_{p_\infty} = \mu_w$ ).

To obtain the viscosity of the polymer solution in a porous medium, the equivalent shear rate was calculated by the following equation<sup>53</sup>:

$$\dot{\gamma} = \left( \frac{1 + 3\eta}{4\eta} \right)^{\frac{\eta}{\eta-1}} \left( \frac{4|\bar{u}_w|}{\sqrt{\frac{8\bar{k}k_{rw}}{\phi S_w}}} \right) \quad (6.10)$$

where

$|\bar{u}_w|$  = magnitude of the Darcy velocity vector for the aqueous phase, L/t

$\bar{k}$  = absolute permeability in the flow direction, L<sup>2</sup>, and

$k_{rw}$  = aqueous phase relative permeability.

The exponent  $\eta$  can be changed from unity to zero and it indicates the degree of deviation from Newtonian behaviour. In the limit of  $\eta = 1$ , the first term of the right hand side of Equation (6.10) approaches 0.779. It approaches 1.0 as  $\eta$  goes to zero. This indicates that this term is bounded between 0.779 and 1.0. For this reason Equation (6.10) is used for the calculation of the shear rate to be used in Meter's model by setting this term equal to 0.8 as an approximation. Thus:

$$\dot{\gamma} = a_{mi} \frac{|\bar{u}_w|}{\sqrt{\frac{\bar{k}k_{rw}}{\phi S_w}}} \quad (6.11)$$

where

$a_{mi}$  = units constant

The absolute permeability in the flow direction  $\bar{k}$  has the form<sup>55,56</sup>:

$$\bar{k} = \left[ \frac{1}{k_x} \left( \frac{u_{xw}}{|\bar{u}_w|} \right)^2 + \frac{1}{k_y} \left( \frac{u_{yw}}{|\bar{u}_w|} \right)^2 + \frac{1}{k_z} \left( \frac{u_{zw}}{|\bar{u}_w|} \right)^2 \right]^{-1} \quad (6.12)$$

### 6.2.2 Permeability Reduction and Residual Resistance

Permeability Reduction and Residual Resistance refer to a reduction in water mobility resulting from adsorption of polymer on the rock surface. This phenomenon is observed with polymers such as partially hydrolyzed polyacrylamides. The permeability reduction factor ( $R_k$ ) and the residual resistance factor ( $R_{rf}$ ) are defined<sup>57</sup> as follows:

$$R_k = \frac{\text{Effective permeability of water}}{\text{Effective permeability of polymer solution}} \quad (6.13)$$

$$R_{rf} = \frac{\text{Water mobility before polymer flood}}{\text{Water mobility after polymer flood}} \quad (6.14)$$

The permeability reduction and residual resistance are postulated to be due to an adsorbed layer of polymer molecular coils that reduces the effective size of the pores.

The local modification to permeability of the model due to pore blocking associated with the adsorption of polymer is modeled<sup>58</sup> as:

$$k_p = \frac{k}{R_{rf}} \quad (6.15)$$

where

$k$  = absolute permeability of the sand pack, L<sup>2</sup>

$R_{rf}$  = residual resistance factor, defined<sup>59</sup> by:

$$R_{rf} = 1 + l_p \mathfrak{R}_p(C_s) \quad (6.16)$$

The quantity  $\mathfrak{R}_p(C_s)$  is the level of polymer adsorption. In some cases,  $\mathfrak{R}_p$  is corrected to allow for a critical onset value for  $C_s$ ; i.e., the polymer does not block pores below a certain value of adsorption. This is represented in the following way:

$$\mathfrak{R}_p = 0 \quad ; \quad (C_s^{n+1} \leq C_s^n) \quad (6.17)$$

$$\mathfrak{R}_p = C_s^{n+1} - C_s^n \quad ; \quad (C_s^{n+1} > C_s^n) \quad (6.18)$$

where

$C_s$  = the amount of polymer adsorbed, m/m, and

$C_s^*$  = a critical onset value for  $C_s$

The permeability reduction caused by adsorbed polymer is modeled as irreversible in the simulator. Thus  $R_k$  represents the residual resistance factor after the polymer concentration goes to zero. The effect of permeability reduction or residual resistance is to reduce the mobility of the polymer phase. This is accounted for in the simulator by decreasing the absolute permeability by the factor  $R_{rf}$ .

### 6.2.3 Adsorption

The adsorption isotherm for polymer is considered irreversible and assumed to follow the Langmuir Equation<sup>60</sup>

$$C_s = \frac{A_{ad} C_p}{1 + B_{ad} C_p} \quad (6.19)$$

where  $A_{ad}$  and  $B_{ad}$  are adsorption parameters and should be determined from experimental data.

This Langmuir isotherm is an equilibrium relationship and represents polymer adsorption when equilibrium is reached instantaneously.

### 6.2.4 Inaccessible Pore Volume

The inaccessible pore volume effect is accounted<sup>58,61</sup> for by dividing the polymer velocity by an effective porosity of polymer as shown below:

$$\phi_{p_{eff}} = \frac{\phi_p}{\phi} \quad \left( \frac{\phi_p}{\phi} < 1 \right) \quad (6.20)$$

where

$\phi_p$  = the apparent porosity for polymer determined from laboratory data, and

$\phi$  = actual porosity.

### **6.3 Numerical Formulation**

The governing equations, derived in the previous section, are a set of coupled, non-linear, partial differential equations. Solution of the equations is achieved in two stages for each time step by separate, successive solution of the two principal aspects of the problem: fluid flow, and polymer balance. In the first stage oil, water, and gas balance equations are solved simultaneously over the three dimensional model grid. In solving these equations, the polymer concentrations are considered constant over a given time step. At the end of the first stage, new pressure and saturation distributions are obtained. In the second stage, the polymer concentration balance is solved over the same grid. The pressure and saturation obtained from the first stage are considered constant in this calculation. At the end of the second stage, then, one has obtained new polymer concentration distributions. The resulting new values provide beginning information for entering the first stage for the subsequent time step. Thus the polymer properties are decoupled in time. The relatively small changes in these properties justify the approach used.

#### **6.3.1 Grid Selection**

A block-centered grid has been used in this formulation. The node representation of the three-dimensional array of grid blocks is shown in Figure 6-1 (figures are at the end of the chapter).

#### **6.3.2 Finite Difference Formulation**

The pressure and the polymer transport equations were discretised using a central finite difference scheme. The detailed derivation is given in Appendix C. As mentioned before, the oil phase pressure, saturation and concentration are chosen as the primitive unknowns. The solution follows a two-step procedure. First, the pressure equation is

solved implicitly using explicit saturations and concentrations and then the new saturations and polymer concentrations are updated explicitly. This scheme is basically the IMPES approach (implicit in pressure explicit in saturation). In the IMPES method, the oil, water, gas, capillary pressures, and saturation equations are used to eliminate all variables except the oil phase pressure. The resulting equation is written for all blocks and the equations thus obtained are solved for  $p_o^{n+1}$  for all blocks. The oil Equation (6.2) is then rearranged to yield the values of oil saturations  $S_o^{n+1}$  for all blocks. The water and gas pressures are obtained from the capillary pressure equations. The water Equation (6.3) is then rearranged to yield the values of water saturations  $S_w^{n+1}$  for all blocks and the gas saturations are calculated from the saturation constraint. Finally, the polymer transport Equation (6.5) is rearranged to obtain the value of polymer concentration  $C_p^{n+1}$  for all blocks.

The relative permeabilities and viscosities in the mobility term are computed using upstream weighting and an arithmetic average, respectively. Permeabilities at the block interfaces were computed using harmonic averaging. In order to determine the upstream direction, the difference in flow potentials between adjacent blocks is calculated. Stone's method<sup>62</sup> was used in the simulator to synthesize three-phase relative permeabilities from two-phase experimental data.

### ***6.3.3 Treatment of Boundary Conditions***

Because the wells have been treated as source and sink terms in the pressure equation, the only boundary condition that is pertinent here is the no-flow boundary condition. This is implemented by setting phase transmissibilities to zero at the boundaries.

### ***6.3.4 Well Representation***

There are essentially two methods<sup>48</sup> for represent a well in a simulator: by rate constraint, or by pressure constraint. Both methods are used in the simulator. Peaceman<sup>63</sup> has shown that for a block containing a well, the block pressure is the same as the pressure,



$p_e$  at an equivalent radius  $r_{eq}$ . Application of Darcy's law to a well-block in the k-th layer gives:

$$q_{t,i,j,k} = a_{m2} \left[ \frac{\sqrt{k_x k_y} k_{rf} \Delta z (p_b - p_{wf})}{B, \mu, \ln\left(\frac{r_{eq}}{r_w}\right) + S_{skin}} \right]_{i,j,k} \quad (6.21)$$

where

$p_b$  = block pressure, m/L<sup>2</sup>t

$p_{wf}$  = bottom hole flowing pressure, m/L<sup>2</sup>t

$a_{m2}$  = units constant,

$r_w$  = wellbore radius, L

$\sqrt{k_x k_y}$  = mean x-y permeability, L<sup>2</sup>

$\Delta z$  = layer thickness, L

$S_{skin}$  = layer skin factor, and

$r_{eq}$  = equivalent grid-block radius which may be calculated from Peaceman's formula:

$$r_{eq} = \frac{a_{m3} \sqrt{\left(\frac{k_y}{k_x}\right)^{\frac{1}{2}} \Delta x^2 + \left(\frac{k_x}{k_y}\right)^{\frac{1}{2}} \Delta y^2}}{\left(\frac{k_y}{k_x}\right)^{\frac{1}{4}} + \left(\frac{k_x}{k_y}\right)^{\frac{1}{4}}} \quad (6.22)$$

where

$a_{m3}$  = units constant

#### 6.4 Solution Procedure

The solution follows a two-step procedure. First, the pressure equation is solved implicitly using explicit saturations and concentrations and then the new saturations and polymer concentrations are updated explicitly. A flow chart of the main program describing is shown in Appendix D.

### 6.4.1 Solution Method

Various methods exist for solving such a system of linear equations, but generally these methods fall into one of two groups - direct methods, or iterative methods. The line successive overrelaxation (LSOR), iterative method, is used in the simulator which is particularly suited for a large, sparse system of equations. The relaxation parameter '  $\omega$  ' is automatically optimized as the solution proceeds, once a sub-optimal value has been supplied. The optimal value  $\omega$  , denoted by  $\omega_b$  , is given by<sup>64</sup>:

$$\omega_b = \frac{2}{1 + \sqrt{1 - \sigma_G^2}} \quad (6.23)$$

where  $\sigma_G$  is the 'spectral radius' of the Gauss-Seidel matrix which is assumed to have real eigenvalues. In the simulator, the spectral radius can be approximated as follows:

$$\sigma_G = \lim_{n \rightarrow \infty} \frac{\|\underline{p}^{n+1} - \underline{p}^n\|_{\max}^{m+1}}{\|\underline{p}^{n+1} - \underline{p}^n\|_{\max}^m} \quad (6.24)$$

where

$m$  = iteration number:

### 6.4.2 Material Balance Calculation

A simple material balance calculation is performed in the simulator as a check of the accuracy of the finite difference solution. The relative error for each component is calculated as:

$$\left( \begin{array}{c} \text{relative} \\ \text{error} \end{array} \right) = \frac{\left( \begin{array}{c} \text{cumulative} \\ \text{injection} \end{array} \right) + \left( \begin{array}{c} \text{originally} \\ \text{in place} \end{array} \right) - \left( \begin{array}{c} \text{cumulative} \\ \text{production} \end{array} \right) - \left( \begin{array}{c} \text{remaining} \\ \text{in place} \end{array} \right)}{\left( \begin{array}{c} \text{cumulative} \\ \text{injection} \end{array} \right) + \left( \begin{array}{c} \text{originally} \\ \text{in place} \end{array} \right)} \quad (6.25)$$

If the material balance errors are 1.0 percent or less, the program accuracy may be considered acceptable for most problems. By contrast, a large material balance error indicates that the IMPES formulation is having problems with the input data. As a rule of thumb, the first thing to do when faced with large material balance error is to reduce the

time step size.

### **6.5 General Solution Scheme**

The step by step computational procedure adopted in the simulator is summarized as follows:

1. Input initialization data and set initial conditions.
2. Solve pressure equation at the new time level by solving Equation (C.32).
3. Calculate Darcy's velocity of the phases using Equation (B.4).
4. Calculate polymer concentration at the new time level by solving Equation (C.39).
5. Check overall material balance.
6. Calculate polymer adsorption  $C_s$  from Equation (6.19).
7. Calculate mobile phase concentration after excluding the pore volume occupied by adsorbed polymer.
8. Calculate phase viscosities from Equations (6.6) through (6.18).
9. Calculate relative permeabilities and capillary pressures.
10. Increment time level and go to step 2.

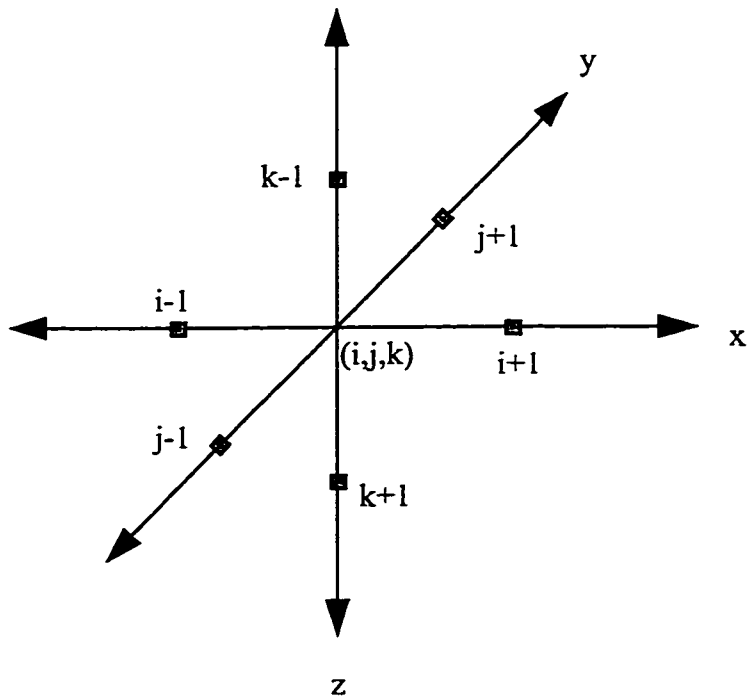
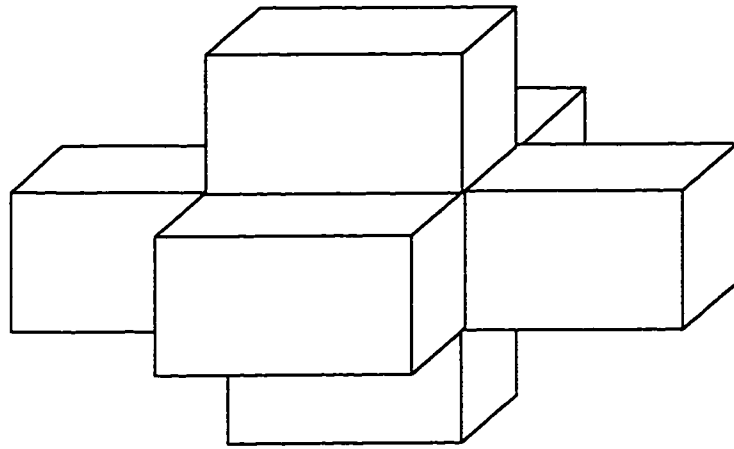


Figure 6-1. Node Representation of Three-Dimensional Array of Reservoir Grid Blocks

## Chapter 7

### EXPERIMENTAL AND THEORETICAL DATA PRESENTATION

This chapter provides a description of the sixty-two runs that were performed in this study. Figures 7-1 and 7-2 (figures are at the end of the chapter) depict the different types of experimental, numerical and analytical runs conducted. The results of all the runs are summarized in Tables 7-1 and 7-2. The production histories (figures) for all runs are presented in Appendix F.

#### 7.1 Experimental Runs

A total of 29 experiments was conducted to study waterflooding and various injection strategies with the use of polymer under bottom-water conditions. The experiments are presented in chronological order. A summary chart of the runs is given in Figure 7-1 for classification of the types of runs conducted. Results of all the experiments are summarized in Table 7-1. Data for each experiment is also presented in tabular form in Appendix E.

##### Runs 1, 2 and 3: Waterflood, Homogeneous Pack at Different Injection Rates

Runs 1, 2 and 3 were carried out at different water injection rates in a homogeneous pack saturated completely with oil with a viscosity ( $\mu_o$ ) of 34.3 mPa.s. (viz. no bottom-water). This was done to study the waterflood performance in the absence of the bottom-water layer, to estimate the effective permeability to water at residual oil saturation,  $k_{wor}$ , for later analysis and to investigate the effect of injection rate on waterflood performance. These runs served as base runs since the effect would be comparable to completely blocking the bottom-water layer, if present. In Run 1, an injection rate of 450 ml/hr was used, in Run 2, an injection rate of 600 ml/hr was used, and in Run 3, an injection rate of 750 ml/hr was used. The production histories for Runs 1, 2 and 3 are very similar. Thus, it is concluded that the injection rate does not play a significant role over the range of injection rates considered.

Table 7-1: Summary of the Experimental Results

Run No.	Fluid Injected	Thickness Ratio hw/ho	Oil Viscos. mPa.s	Polymer Con. ppm	Injection Rate ml/hr	Ultimate Recovery %	IOIP CC	$k_{abs}$ $\mu m^2$	$S_{wc}$
1	Water	Homo	34.3	N/A	450	59.3	908	11.554	12.9
2	Water	Homo	34.3	N/A	600	58.9	977	11.152	12.0
3	Water	Homo	34.3	N/A	750	58.6	898	10.066	11.7
4	Water	0.33	34.3	N/A	450	37.1	710	9.953	14.7
5	Water	0.33	34.3	N/A	300	24.5	729	10.388	12.4
6	Water	0.33	34.3	N/A	600	38.3	751	11.503	10.2
7	Water	0.33	34.3	N/A	750	42.1	735	13.268	12.1
8	Water	0.33	34.3	N/A	1200	46.0	737	11.815	11.8
9	Water	0.25	34.3	N/A	450	51.1	765	10.221	13.8
10	Water	0.5	34.3	N/A	450	34.7	647	9.953	14.7
11	Water	Homo	68	N/A	450	51.8	922	10.306	11.9
12	Water	0.33	68	N/A	450	30.4	746	10.362	10.4
13	Water	0.33	11	N/A	450	58.0	724	10.127	12.6
14	Water	Homo	11	N/A	450	66.0	954	10.703	14.0
15 <sup>+</sup>	Water	0.33	34.3	N/A	450	30.0	700	9.975	15.9
16	Polymer	0.33	34.3	500	450	66.3	733	10.227	11.6
17	Polymer	0.33	34.3	1000	450	69.1	746	12.533	10.5
18	Polymer	0.33	34.3	1500	450	74.2	734	10.994	10.8
19	Polymer	0.33	34.3	2000	450	72.7	730	10.758	11.8
20	Polymer	0.33	34.3	500	750	68.2	725	10.257	12.9
21 <sup>++</sup>	Polymer	0.33	34.3	500	450	64.0	737	10.115	11.4
22	Polymer	0.5	34.3	500	450	64.2	653	10.153	12.3
23	Polymer	0.25	34.3	500	450	68.8	773	9.674	12.4
24	Polymer	1	34.3	500	450	61.0	491	10.890	11.2
25	Polymer	0.33	68	500	450	59.4	741	9.994	11.2
26	Polymer	0.33	11	500	450	65.8	726	8.975	12.9
27 <sup>*</sup>	Water	Homo	34.3	N/A	450	50.0	920	9.220	14.0
28 <sup>*</sup>	Water	0.33	34.3	N/A	450	47.0	753	9.983	15.1
29 <sup>**</sup>	Water	0.33	34.3	N/A	450	52.0	751	9.847	13.9

Homo Homogeneous Run

N/A Not Applicable

\* No Crossflow Allowed in the Middle of the Pack (Barrier)

\*\* Simultaneous Injection into Oil and Bottom-water Zone Respectively

+ Horizontal Wells

++ Vertical Injector / Horizontal Producer Wells

Table 7-2: Summary of the Simulation and Analytical Results

Run No.	Fluid Injected	Thickness Ratio hw/ho	Oil Viscosity mPa.s	Polymer Con. ppm	Injection Rate ml/hr	Ultimate Recovery %	k <sub>1</sub> /k <sub>2</sub> Ratio	Process
30	Water	Homo	34.3	N/A	450	58.0	1:1	BR
31	Water	0.33	34.3	N/A	450	47.1	1:1	BWR
32	Water	0.33	34.3	N/A	1200	46.9	1:1	BWR
33	Water	0.25	34.3	N/A	450	50.0	1:1	BWR
34	Water	0.50	34.3	N/A	450	40.4	1:1	BWR
35	Water	1.00	34.3	N/A	450	25.1	1:1	BWR
36	Water	Homo	68.0	N/A	450	51.3	N/A	N/A
37	Water	0.33	68.0	N/A	450	38.5	1:1	BWR
38	Water	0.33	11.0	N/A	450	66.5	1:1	BWR
39	Water	Homo	11.0	N/A	450	74.1	N/A	N/A
40	Water	0.33	34.3	N/A	450	45.7	1:1	Barrier
41	Polymer	0.33	34.3	500	450	76.1	1:1	BWR
42	Polymer	0.33	34.3	1000	450	76.9	1:1	BWR
43	Polymer	0.33	34.3	1500	450	77.0	1:1	BWR
44	Polymer	0.33	34.3	2000	450	76.9	1:1	BWR
45	Polymer	Homo	34.3	500	450	72.0	N/A	N/A
46	Polymer	0.50	34.3	500	450	74.1	1:1	BWR
47	Polymer	0.25	34.3	500	450	77.1	1:1	BWR
48	Polymer	1.00	34.3	500	450	67.5	1:1	BWR
49	Polymer	0.33	68	500	450	71.2	1:1	BWR
50	Polymer	0.33	11	500	450	77.1	1:1	BWR
51	Water	0.33	34.3	N/A	450	40	1:10	BWR
52	Water	0.33	34.3	N/A	450	44.1	1:10	BWRZ
53	Water	Homo	34.3	N/A	N/A	N/A	N/A	N/A
54	Water	0.33	34.3	N/A	N/A	40.1	1:1	BWR
55	Water	0.25	34.3	N/A	N/A	45.6	1:1	BWR
56	Water	0.50	34.3	N/A	N/A	32.0	1:1	BWR
57	Water	1.00	34.3	N/A	N/A	16.4	1:1	BWR
58	Water	0.33	11	N/A	N/A	45.5	1:1	BWR
59	Water	0.33	68	N/A	N/A	36.9	1:1	BWR
60	Water	0.33	34.3	N/A	N/A	34.0	1:2	BWR
61	Water	0.33	34.3	N/A	N/A	24.8	1:3	BWR
62	Water	0.33	34.3	N/A	N/A	29.0	1:4	BWR

BR Base Run

BWR Bottom-Water Run

BWRZ Bottom-Water Run, vertical to horizontal permeability ratio was ten to one

Homo Homogeneous Run

N/A Not Applicable

Barrier No Crossflow Allowed in the Middle of the Pack

Note: Runs 53 through 62, the Ultimate Oil recovery Calculated at One PV of Fluid Injection

Due to the long duration of the experimental set-up and procedure, on average 10 days for each run, Runs 2 and 3 were considered also as replicate runs of Run 1 to examine the reproducibility of the experiments. Comparing Runs 2 and 3 with Run 1, it was found that Runs 2 and 3 exhibited almost identical production histories. The ultimate oil recovery was 59.3% for Run 1, 58.9% for Run 2 and 58.5% for Run 3, respectively (Note: ultimate oil recovery is defined as that obtained at a producing WOR equal to or greater than 15). Thus, it is concluded that the experiments in this study were reproducible with an error of less than 1% recovery of IOIP.

#### Run 4: Waterflood, Bottom-Water Run

This Run was conducted to study the performance of a waterflood under bottom-water conditions. An oil-to-bottom-water layer thickness ratio ( $h_o / h_w$ ) of 3:1 was used in all experiments. Absolute permeabilities of both zones were equal and the oil viscosity was ( $\mu_o$ ) equal to 34.3 mPa.s. The perforated intervals of the injection and production wells were over the top 25.0% of the oil zone (well penetration equal to 25.0%). Water was injected through a single injection well into the oil zone. In Run 4, an injection rate of 450 ml/hr was used, and this run served as a base run. The ultimate oil recovery was 37.1%. Figure 7-3 shows the production history of this run. Notice that the oil cut dropped very rapidly to 11.6%. This value of oil cut was sustained for a period of 0.20 PV of fluid injection before it started to increase to a value of 31.1%. Thus, it appears that there is a pseudostable region where the oil cut is approximately constant for a Newtonian fluid flooding a bottom-water formation. A similar pseudostable region was observed in all bottom-water Runs.

#### Runs 5, 6, 7 and 8: Waterflood, Bottom-Water Pack at Different Injection Rates

Runs 5 through 8 were conducted to study the effect of the injection rate on the performance of a waterflood under bottom-water conditions. These runs had the same parameters and experimental set-up as Run 4. In Run 5, an injection rate of 300 ml/hr was used, and the ultimate oil recovery was 24.5%. Figure 7-4 shows the production history for this run. Notice that the pressure declined to a minimum permissible value



and the oil cut dropped very rapidly to 10.0%, and was sustained at close to the minimum value for a period of 1.1 PV of injection fluid. This rapid drop in oil cut indicates that the water was going into the bottom-water zone. In Run 6, an injection rate of 600 ml/hr was used, in Run 7, an injection rate of 750 ml/hr was used and in Run 8, an injection rate of 1200 ml/hr was used. It appears that the pseudostable region was observed in all runs. The production histories for Runs 4 through 8 are very different. Thus, it is concluded that the injection rate does play a significant role when waterflooding under bottom-water conditions.

#### Runs 9 and 10: Waterflood, Bottom-Water Pack at Different Thickness Ratios

These runs had the same parameters as Run 4, the only difference being that the oil-to-bottom-water layer thickness ratio ( $h_o / h_w$ ) was changed. In Run 9, an oil-to-bottom-water layer thickness ratio ( $h_o / h_w$ ) of 4:1 was used. The ultimate oil recovery is 51.1%. Notice that a higher oil cut was observed for this run. In Run 10, an oil-to-bottom-water layer thickness ratio ( $h_o / h_w$ ) of 2:1 was used. The ultimate oil recovery was 34.7%. Again, notice that the oil cut dropped very sharply to 10.0%, and then increased rapidly to 19.0%. Again, this rapid drop in oil cut indicates that the water was going into the bottom-water zone. Notice that this run has the lowest oil cut among all previous runs.

#### Runs 11, 12, 13 and 14: Waterflood, Bottom-Water Pack at Different Oil Viscosities

Runs 11 through 14 were carried out to examine the effect of oil viscosity on oil recovery under bottom-water conditions. These runs had the same parameters as Run 4 and Run 1 respectively, the only difference being that the oil viscosity was changed. In Run 11 and Run 12, an oil viscosity of 68.0 mPa.s was used, and in Run 13 and Run 14 an oil viscosity of 11.0 mPa.s was used. Runs 11 and 14 were carried out in a homogeneous pack.

Runs 12 was carried out in a bottom-water pack. The ultimate oil recovery was 30.4%. Notice that the oil cut dropped very rapidly to 8.8%, and sustained this value for a period of 0.3 PV of fluid injection before increasing slowly to 19.1%. The drop in the oil cut

for this run is an indication of more water going into the water zone than in Run 4.

Run 13 was carried out in a bottom-water pack, as well. The ultimate oil recovery was 58.0%. Notice that the oil cut dropped very rapidly to 27.0%, and then increased rapidly to 83.2%. The 27.0% oil cut was sustained for a period of 0.15 PV of injection fluid. This pseudostable region is a good indication that the water indeed was going into the bottom-water zone.

#### Run 15: Waterflood, Bottom-Water Pack with no Crossflow in the Middle of the Pack.

Run 15 was conducted to examine the effect of preventing crossflow between layers in the middle of the pack on oil recovery performance and to determine the crossflow location under bottom-water conditions. This run employed the same experimental set-up as that used in Run 4. A barrier length equal to 80.0% of the total length was used to prevent crossflow in the middle of the pack. The oil layer and the bottom-water layer were communicating only at the injection and producing wells. Figure 7-5 shows the production history for this run. The ultimate oil recovery was 30.0%. The oil cut dropped very rapidly to 11.6%, and then was sustained at an average value of 10.0% as the flood progressed. Notice that, this run has the lowest oil cut among all previous runs due to the reduction of crossflow between layers.

#### Runs 16 through 26: Polymer Flood, Bottom-Water Pack

These Runs (16 through 26) had the same parameters and employed the same experimental set-up as all previous runs with bottom-water, the only difference being that polymer was used. In all polymer flood runs, a slug size<sup>39</sup> of 0.8 PV of polymer was injected at the beginning of the each run, followed by water injection at the same rate.

Run 16 was conducted to study the performance of a polymer flood on oil recovery under bottom-water conditions. Both the polymer and the water were injected through a single injection well in the oil zone. In Run 16, 0.8 PV of 500 ppm polymer was injected at the beginning of the Run at a rate of 450 ml/hr, followed by water injection at the same rate. An ultimate oil recovery of 66.3% was attained. Figure 7-6 shows the production history

for this Run. Notice that the oil cut decreased rapidly to less than 15.4%, while the pressure increased to the maximum value. This rapid drop in oil cut indicates that the polymer was going into bottom-water zone. After 0.3 PV polymer injection, an oil cut of 73.6% was sustained. However, despite the fact that the mobility ratios were favourable in both the oil and the bottom-water zones, the oil cut decreased to 15.4% for a period of 0.15 PV of fluid injection before it started to increase. Thus, it seems that the low oil rate during initial production of a bottom-water run is unavoidable, and also, it appears that there is a pseudostable region where the oil cut is approximately constant for a non-Newtonian fluid flooding a bottom-water formation. A similar pseudostable region was observed in Run 4.

Runs 17 through 19 were carried out to examine the effect of increasing polymer concentration on oil recovery performance. Once again, all parameters except the polymer concentration were kept constant. A 1000 ppm polymer concentration was used in Run 17. The production history for run 17 shows that all curves exhibit trends similar to those in Run 16. The ultimate oil recovery was 69.1%.

Runs 18 and Run 19 were conducted to investigate further the effect of polymer concentration on oil recovery. A 1500 ppm polymer concentration was used in Run 18 and 2000 ppm polymer concentration was used in Run 19. Like Runs 16 and 17, the initial oil cut dropped to a low value of 15.0%. A rising pressure during the initial period indicated that the polymer was starting to block off the bottom-water layer. After 0.22 PV of polymer injection, the oil cut started to increase and peaked at 0.41 PV of fluid injection. This value was higher than that for the previous run, but was sustained for a long period.

Since a larger polymer concentration was used in Run 19, it was expected that a higher ultimate recovery would be obtained. Contrary to expectations, the ultimate recovery (74.2% IOIP for Run 18 and 72.7% IOIP for Run 19) was less than that for Run 18. This decrease in oil recovery was credited to the inaccessible pore volume to polymer solution

as a result of the increase in polymer concentrations. The ultimate oil recovery for the four runs was very close. It was assumed that the optimal polymer concentration is 500 ppm (i.e., a larger polymer concentration would not recover any additional oil).

#### Run 20: Bottom-Water Run, Effect of Polymer Injection Rate

Run 20 was designed to investigate the effect of polymer injection rate on oil recovery. The polymer slug was injected through the injection well at a rate of 750 ml/hr, followed by a waterflood at the same rate. This run followed a trend similar to that of Run 16. Because of the similar nature of the production history of the two runs, it is concluded that the polymer injection rate does not play a significant role over the range of rates considered.

#### Run 21: Effect of Injection Strategy on Bottom-Water Run

Run 21 was conducted to examine the effect of injection strategy on oil recovery under bottom-water conditions. In this run, the experimental set-up and the polymer used in Run 16 were left unchanged. Unlike the previous runs with a single injection point, in this run, polymer and/or water were injected simultaneously into the oil and bottom-water zones, respectively. The injection rates were proportional to the cross-sectional areas to simulate a vertical front displacement. The 0.8 PV polymer slug was divided into two batches in order to achieve simultaneous injection in both layers. Similarly, the drive water was divided into two batches also, each of which had a different size. This run was conducted with special wells that allowed simultaneous injection of polymer and/or water into the water and the oil zone. The production history for this run is shown in Figure 7-7. The production history shows that the oil cut curve had a trend similar to that of Run 16, which employed the single injection strategy process. Notice how the oil cut peaked at 31.0%, and then dropped sharply to 14.8%, while the pressure increased to a maximum. This rapid drop indicates that the polymer was blocking the bottom-water zone. There was a noticeable difference between this run and Run 16. Because of the small decrease in the oil cut obtained in this run during oil production, the ultimate oil recovery was slightly decreased by 2.3% (64.0% compared to 66.3%). Thus, it was

concluded that the oil recovery was not strongly affected by the injection strategy used.

Runs 22, 23 and 24: Polymer Flood, Bottom-Water Pack with Different Thickness Ratios

These Runs had the same parameters as the previous runs (Run 16), the only difference being that the oil-to-bottom-water layer thickness ratio ( $h_o / h_w$ ) was changed. In Run 22, an oil-to-bottom-water layer thickness ratio of 2:1 was used. Unlike that of Run 16, the initial oil cut dropped to a very low value; that is, it declined to 9.0%. The rising pressure during the initial period indicated that the polymer was starting to block off the bottom-water layer. After 0.26 PV of polymer injection, the oil cut started to increase and peaked at 0.34 PV of fluid injection. This maximum value was less than that for the previous runs, and was not sustained for a longer period. In Run 23, an oil-to-bottom-water layer thickness ratio of 4:1 was used. Unlike the previous runs, the initial oil cut did not drop to a very low value; that is, it declined to 24.8%. The rapid rising pressure during the initial period of injection indicated that the polymer blocked off the bottom-water layer. After 0.13 PV of polymer injection, the oil cut started to increase and peaked at 0.23 PV of fluid injection. This maximum value was sustained for a longer period before it started to decrease. The ultimate oil recovery was higher than that for the previous runs. In Run 24, an oil-to-bottom-water layer thickness ratio of 1:1 was used. The initial oil cut dropped to 6.4%, which indicated that the injected fluid was going into the bottom-water zone. The slow increase in the injection pressure and the longer period of the pseudostable region indicated that the polymer was partially blocking the bottom-water layer. After the injection of 0.13 PV of polymer, the oil cut remained low for a while, before increasing to a maximum value of 60.8%. Unlike Run 23, this time the oil cut dropped sharply to a low value, which was sustained for a period of 0.34 PV of fluid injection before the oil cut started to increase, which resulted in a lower ultimate oil recovery of 61.0% IOIP.

Runs 25 and 26: Polymer Flood, Bottom-Water Pack with Different Oil Viscosities

Run 25 was designed to pinpoint the effect of changing the oil viscosity on polymer flooding. As before, all parameters except for the oil viscosity, which was changed to 68.0 mPa.s, were kept constant. This run followed a trend similar to that of Run 16,

except at the maximum oil cut, the oil cut was not sustained for a longer time. Because of that, the ultimate oil recovery (59.4% IOIP) was less than that of Run 16.

Run 26, in essence, duplicated the conditions of Run 25, except that the oil viscosity was changed to 11.0 mPa.s. The production history for this run shows that all curves exhibit trends similar to those in Run 25, except that the oil cut was sustained at a high value of 83.1% for a period of 0.3 PV of fluid injection, giving an increase of over 6.4% IOIP recovery. Also, the oil cut did not drop as rapidly as in Run 25; as a result, an ultimate oil recovery of 65.8% was obtained when the WOR reached 15. However, the difference is too small for it to be conclusive.

#### Run 27: Waterflood, Homogenous Pack with Horizontal wells

To investigate the oil recovery using horizontal wells, two horizontal wells (injector/producer) were designed, each made up of a 0.5 cm tubing with a length of 24 cm. In order to control well perforations, each horizontal well was divided into four sections. This run had the same parameters as all previous runs (Runs 1,2 and 3), the only difference being that horizontal wells were used instead of vertical wells. This was done in order to see the performance of a waterflood using horizontal wells in a homogeneous pack. With the previous runs in view, it was expected that the waterflood performance with the horizontal wells would be very good. However, an ultimate oil recovery of 50.0% of IOIP was obtained, which is far less than expected. The production history for this run shows that the pressure did not rise as high as in the previous runs, but it was sustained relatively close to the maximum value for a longer time. The oil cut dropped very rapidly to less than 10.0%.

#### Run 28: Waterflood, Bottom-Water Pack with Horizontal Wells

Run 27 employed the same parameters as all previous runs with bottom-water. It was conducted to further examine waterflooding performance under bottom-water conditions. This run had the same parameters as Run 4, the only difference being that horizontal wells were used instead of vertical wells. Figure 7-8 shows the production history of this run. Comparing Run 28 (Figure 7-8) with Run 4 (Figure 7-3), there are two major

differences to be noted in this run. First, it took about 0.1 PV of injected water before the oil cut started to decrease from the maximum value (100.0%). This value was the highest among the other runs. Second, the oil cut decreased to 43.0% (11.6% in Run 4), then increased rapidly to 60.4% (31.1% in Run 4) which was again the highest among the other runs. With these two changes, the ultimate oil recovery was 47.0% of IOIP, which is 10.0% percent higher than the recovery for Run 4, which is credited to the use of horizontal wells. Thus, it can be seen that the use of horizontal wells has a positive effect on oil recovery under bottom-water conditions.

#### Run 29: Waterflood, Bottom-Water Pack with Vertical/Horizontal Wells

Run 29, in essence, duplicated the conditions of Run 28, the only difference being that a vertical injector well and a horizontal producer well were used in this run. It was conducted to examine waterflooding performance under bottom-water conditions using a combination of wells. Figure 7-9 shows the production history of this run; it can be seen that all curves exhibit trends similar to those of Run 28. As in Run 28, the oil cut was sustained at a high average value over the same fluid injection period, giving an increase of over 6.0% IOIP recovery. Also, the oil cut did not drop as rapidly as in Run 28; as a result, an oil recovery of 52.0% was obtained when the WOR reached 13. Thus, by using a vertical injector and a horizontal producer, the ultimate oil recovery was improved by 5.0% over Run 28.

## **7.2 Simulation Runs**

The laboratory model used in the previous section was simulated using the three-dimensional three-phase simulator developed in Chapter 6. The rock and fluid properties used in this studies are listed in Table 4-1. The relative permeability and the capillary pressure are shown graphically as functions of water phase saturation in Figures 7-10 and 7-11, respectively<sup>65</sup> (These two graphs are reproduced from Sarma's thesis). The two fluid phases consisted of a water and an oil phase, considered incompressible in this study.

A total of 24 simulation runs was conducted to study waterflooding and various injection strategies with the use of polymer under bottom-water conditions. These runs were made primarily to illustrate the capability of the simulator and to predict water and polymer flooding. In essence, these runs duplicated the same conditions of all experimental runs in the previous section with the exception of Runs 27 through 29. The presentation of these runs is in chronological order. A summary chart of the runs is given in Figure 7-2 for classification of the types of runs conducted. Results of all the simulation runs are summarized in Table 7-2. The production history (figures) for each run is presented in Appendix F.

#### Run 30: Waterflood, Homogeneous Pack

This run was made primarily to illustrate the capability of the simulator. Run 30 was carried out to simulate waterflood in a homogeneous pack (viz. no bottom-water). This was done also for the purpose of history matching with experimental Run 1.

#### Runs 31 through 50: Polymer /Waterflood, Bottom-Water Pack

Runs 31 through 50 are duplicates of Runs 4 through 26. These runs had the same parameters and employed the same input data as all previous experimental runs under bottom-water conditions. Figures F-31 through F-50 show the production history for these runs. With all the results of the previous Runs in view, it is concluded that the same observations and conclusions made for the experimental results can also be applied to the simulation model.

#### Runs 51 and 52: Bottom-Water Runs, Effect of Permeability contrast on Waterflood

Two Runs were made to investigate the effect of the permeability contrast between the oil layer and the bottom-water layer. Both runs were conducted with the same input data and the same parameters as the previous bottom-water runs, the only difference being that the permeability was changed. The permeability contrast of Run 51 was ten to one, and the bottom-water layer was the most permeable layer. Figure 7-12 shows the production history of this run. The ultimate oil recovery of Run 51 (35.0%) was 13.0% less than that



of Run 31 (47.1%). This was because of the large crossflow of the injected fluid into the bottom-water layer, which effectively reduced the oil recovery.

Run 52 was made to investigate the effect of the permeability contrast between the horizontal and vertical (x and z) directions. The vertical to horizontal permeability ratio was 10 for Run 52 (and one for Run 31). The ultimate oil recovery for this run was only 3.0% less than that for Run 31 (47.1%). This shows that oil recovery is sensitive to vertical permeability in this range. Figure 7-13 shows the production history of this run.

### ***7.3 Analytical Calculations***

A series of a runs (10 runs) was made using the analytical model to study the sensitivity of oil recovery to various parameters under bottom-water conditions. The study for this model includes varying the following items: (1) permeability contrast, (2) oil viscosity and (3) different oil-to-bottom-water layer thickness ratios ( $h_o / h_w$ ). The input data used for the analytical model were the same as in the previous sections.

#### **Run 53: Waterflood, Homogeneous Pack**

This run was made primarily to test and illustrate the capability of the analytical model. Run 53 (duplicate of Run 1) was done to study waterflood performance in the absence of a bottom-water layer. This run served as a base run since the effect would be comparable to completely blocking the bottom-water layer, if present. Figure 7-14 shows the production history for this Run. Notice that, the number of PV of oil produced is equal to the number of PV of water injected. This is because of the assumption of a sharp front assumed in developing the analytical model.

#### **Run 54: Waterflood, Bottom-Water Pack**

This run was conducted to study the performance of a waterflood under bottom-water conditions using the analytical model. This run is a duplicate of Run 4 and served as base run. The cumulative oil recovery after one PV of fluid injection was 40.1%. Figure 7-14 shows the production history of this run. Again, notice that the oil recovery was

sustained at a low value for a period of 0.3 PV of fluid injection before it started to increase rapidly. Thus, it appears that there is a pseudostable region where the oil cut is approximately constant for a Newtonian fluid flooding a bottom-water formation. This is an indication of the injected water going into the water zone. Notice that the pseudostable region period lasted almost for the same period that will be required to flood the bottom-water layer.

#### Runs 55, 56 and 57: Waterflood, Bottom-Water Pack at Different Thickness Ratios

These runs had the same parameters as Run 54, the only difference being that the oil-to-bottom-water layer thickness ratio was changed. In Run 55, an oil-to-bottom-water layer thickness ratio of 4:1 was used, in Run 65, an oil-to-bottom-water layer thickness ratio of 2:1 was used and in Run 57, an oil-to-bottom-water layer thickness ratio of 1:1 was used. Figure 7-14 shows the production history for these Runs. Notice that the ultimate oil recoveries for these runs were very different. This shows that the oil recovery is sensitive to the oil-to-bottom-water layer thickness ratio.

#### Runs 58 and 59: Waterflood, Bottom-Water Pack at Different Oil Viscosities

Runs 58 and 59 were carried out to examine the effect of oil viscosity on oil recovery under bottom-water conditions. These runs had the same parameters as Run 54, the only difference being that the oil viscosity was changed. In Run 58, an oil viscosity of 11.0 mPa.s was used, and in Run 59 an oil viscosity of 68.0 mPa.s was used. Figure 7-15 shows the production history for these Runs. Notice that the pseudostable period for the higher oil viscosity resulted in a lower oil recovery than that for lower oil viscosity.

#### Runs 60, 61 and 62: Bottom-Water Pack, Effect of Permeability Contrast on Waterflood

Three runs were made to investigate the effect of the permeability contrast between the oil layer and the bottom-water layer. All runs were conducted with the same input data and the same parameters as the previous bottom-water runs, the only difference being that the permeability was changed. The permeability contrasts were two to one, three to one and four to one for Runs 60, 61 and 62, respectively. The bottom-water layer was the

most permeable layer in all runs. Figure 7-16 shows the production history of these runs. Notice that as the permeability contrast increases, the oil recovery decreases. This was a result of the large crossflow of the injected fluid into the bottom-water layer, which effectively reduced the oil recovery. This shows that oil recovery is very sensitive to the permeability contrast in this range.

**Homogenous Runs**

**Waterflood**

Run 1: Flow Rate = 450 ml/hr, Oil Viscosity = 34.3 mPa.s, VW
Run 2: Flow Rate = 600 ml/hr, Oil Viscosity = 34.3 mPa.s, VW
Run 3: Flow Rate = 750 ml/hr, Oil Viscosity = 34.3 mPa.s, VW
Run 11: Flow Rate = 600 ml/hr, Oil Viscosity = 68.0 mPa.s, VW
Run 14: Flow Rate = 450 ml/hr, Oil Viscosity = 11.0 mPa.s, VW
Run 27: Flow Rate = 450 ml/hr, Oil Viscosity = 34.3 mPa.s, HW

**Waterflood**

Run 4: Flow Rate = 300 ml/hr, Vis. = 34.3 mPa.s, hw/ho = 1/3, VW
Run 5: Flow Rate = 450 ml/hr, Vis. = 34.3 mPa.s, hw/ho = 1/3, VW
Run 6: Flow Rate = 600 ml/hr, Vis. = 34.3 mPa.s, hw/ho = 1/3, VW
Run 7: Flow Rate = 750 ml/hr, Vis. = 34.3 mPa.s, hw/ho = 1/3, VW
Run 8: Flow Rate = 1200 ml/hr, Vis. = 34.3 mPa.s, hw/ho = 1/3, VW
Run 9: Flow Rate = 450 ml/hr, Vis. = 34.3 mPa.s, hw/ho = 1/4, VW
Run 10: Flow Rate = 450 ml/hr, Vis. = 68.0 mPa.s, hw/ho = 1/2, VW
Run 12: Flow Rate = 450 ml/hr, Vis. = 34.3 mPa.s, hw/ho = 1/3, VW
Run 13: Flow Rate = 450 ml/hr, Vis. = 11.0 mPa.s, hw/ho = 1/3, VW
Run 28: Flow Rate = 450 ml/hr, Vis. = 34.3 mPa.s, hw/ho = 1/3, HW

**Bottom-Water Runs**

**Polymer Flood**

Run 15: q = 450 ml/hr, Oil Vis. = 34.3 mPa.s, hw/ho = 1/3, VW, Barrier

Run 29: q = 450 ml/hr, Oil Vis. = 34.3 mPa.s, hw/ho = 1/3, VW / HW

Run 16: q = 450 ml/hr, Vis. = 34.3 mPa.s, hw/ho = 1/3, C = 500 ppm, VW
Run 17: q = 450 ml/hr, Vis. = 34.3 mPa.s, hw/ho = 1/3, C = 1000 ppm, VW
Run 18: q = 450 ml/hr, Vis. = 34.3 mPa.s, hw/ho = 1/3, C = 1500 ppm, VW
Run 19: q = 450 ml/hr, Vis. = 34.3 mPa.s, hw/ho = 1/3, C = 2000 ppm, VW
Run 20: q = 750 ml/hr, Vis. = 34.3 mPa.s, hw/ho = 1/3, C = 500 ppm, VW
Run 21: 2q = 450 ml/hr, Vis. = 34.3 mPa.s, hw/ho = 1/3, C = 500 ppm, VW
Run 22: q = 450 ml/hr, Vis. = 34.3 mPa.s, hw/ho = 1/2, C = 500 ppm, VW
Run 23: q = 450 ml/hr, Vis. = 34.3 mPa.s, hw/ho = 1/4, C = 500 ppm, VW
Run 24: q = 450 ml/hr, Vis. = 34.3 mPa.s, hw/ho = 1/1, C = 500 ppm, VW
Run 25: q = 450 ml/hr, Vis. = 68.0 mPa.s, hw/ho = 1/3, C = 500 ppm, VW
Run 26: q = 450 ml/hr, Vis. = 11.0 mPa.s, hw/ho = 1/3, C = 500 ppm, VW

Figure 7-1: Summary Chart of all the Experiments

Homogenous Runs

Waterflood

Run 30: Flow Rate = 450 ml/hr, Oil Vis. = 34.3 mPa.s, hw/ho = 0
Run 36: Flow Rate = 450 ml/hr, Oil Vis. = 68.0 mPa.s, hw/ho = 0
Run 39: Flow Rate = 450 ml/hr, Oil Vis. = 11.0 mPa.s, hw/ho = 0

Waterflood

Run 31: Flow Rate = 450 ml/hr, Oil Vis. = 34.3 mPa.s, hw/ho = 1/3
Run 32: Flow Rate = 1200 ml/hr, Oil Vis. = 34.3 mPa.s, hw/ho = 1/3
Run 33: Flow Rate = 450 ml/hr, Oil Vis. = 34.3 mPa.s, hw/ho = 1/4
Run 34: Flow Rate = 450 ml/hr, Oil Vis. = 34.3 mPa.s, hw/ho = 1/2
Run 35: Flow Rate = 450 ml/hr, Oil Vis. = 34.3 mPa.s, hw/ho = 1/1
Run 37: Flow Rate = 450 ml/hr, Oil Vis. = 68.0 mPa.s, hw/ho = 1/3
Run 38: Flow Rate = 450 ml/hr, Oil Vis. = 11.0 mPa.s, hw/ho = 1/2

Run 40: Flow Rate = 450 ml/hr, Oil Vis. = 34.3 mPa.s, hw/ho = 1/3, Barrier

Run 51: q = 450 ml/hr, Oil Vis. = 34.3 mPa.s, hw/ho = 1/3, k1/k2 = 1:10

Run 52: q = 450 ml/hr, Oil Vis. = 34.3 mPa.s, hw/ho = 1/3, k1/k2 = 1:10

Bottom-Water Runs

Polymer Flood

Run 41: q = 450 ml/hr, Oil Vis. = 34.3 mPa.s, hw/ho = 1/3, C = 500 ppm
Run 42: q = 450 ml/hr, Oil Vis. = 34.3 mPa.s, hw/ho = 1/3, C = 1000 ppm
Run 43: q = 450 ml/hr, Oil Vis. = 34.3 mPa.s, hw/ho = 1/3, C = 1500 ppm
Run 44: q = 450 ml/hr, Oil Vis. = 34.3 mPa.s, hw/ho = 1/3, C = 2000 ppm
Run 45: q = 450 ml/hr, Oil Vis. = 34.3 mPa.s, hw/ho = 0, C = 500 ppm
Run 46: 2q = 450 ml/hr, Oil Vis. = 34.3 mPa.s, hw/ho = 1/2, C = 500 ppm
Run 47: q = 450 ml/hr, Oil Vis. = 34.3 mPa.s, hw/ho = 1/4, C = 500 ppm
Run 48: q = 450 ml/hr, Oil Vis. = 34.3 mPa.s, hw/ho = 1/1, C = 500 ppm
Run 49: q = 450 ml/hr, Oil Vis. = 68.0 mPa.s, hw/ho = 1/1, C = 500 ppm
Run 50: q = 450 ml/hr, Oil Vis. = 11.0 mPa.s, hw/ho = 1/3, C = 500 ppm

Figure 7-2: Summary Chart of all Simulation Runs

# Production History for Experimental Run 4

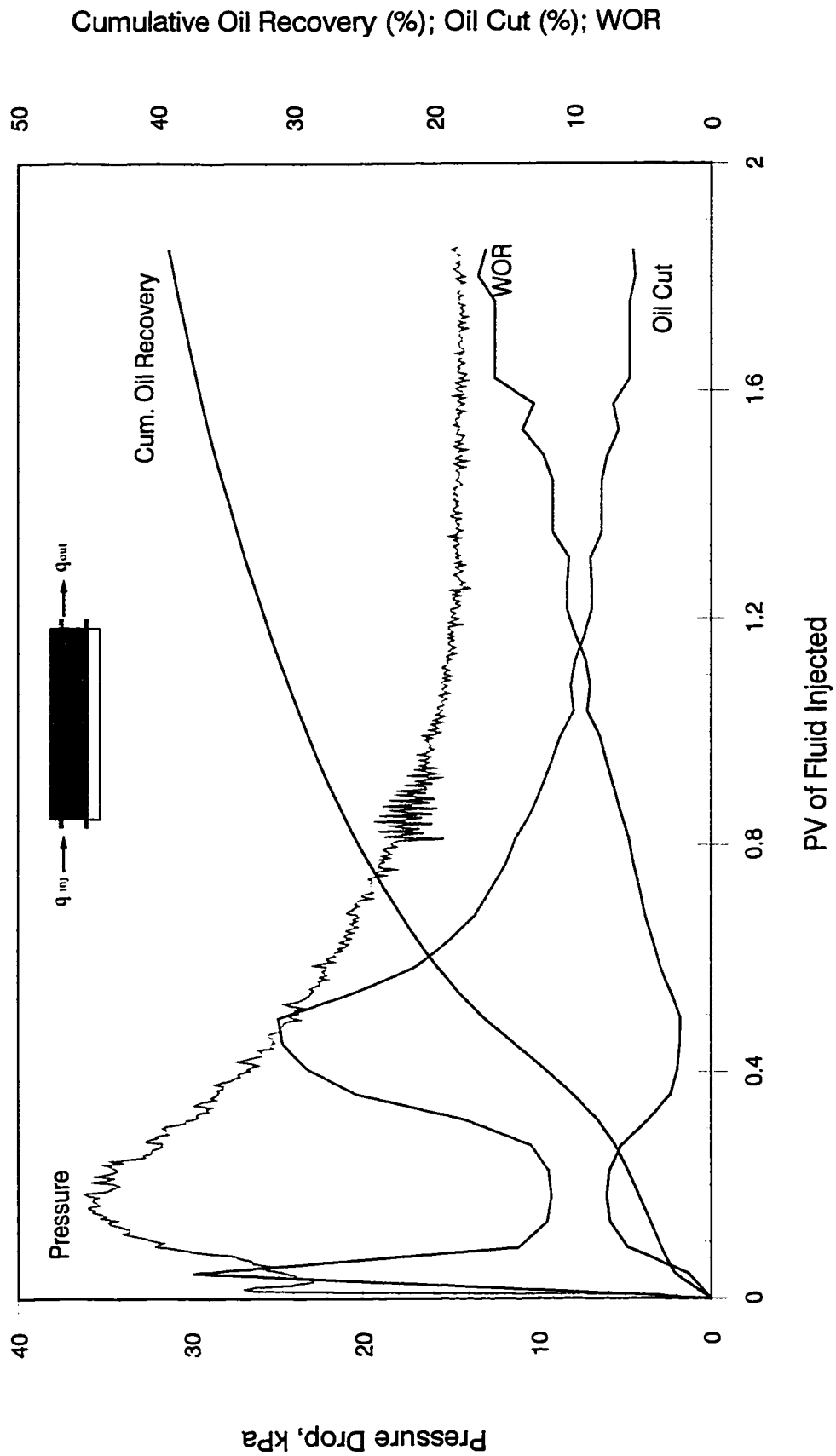


Figure 7-3: Bottom-Water Pack Waterflood ( $q = 450$  cc/hr,  $h_w/h_o = 1/3$ , Oil Viscosity =  $34.3$  mPa.s)

# Production History for Experimental Run 5

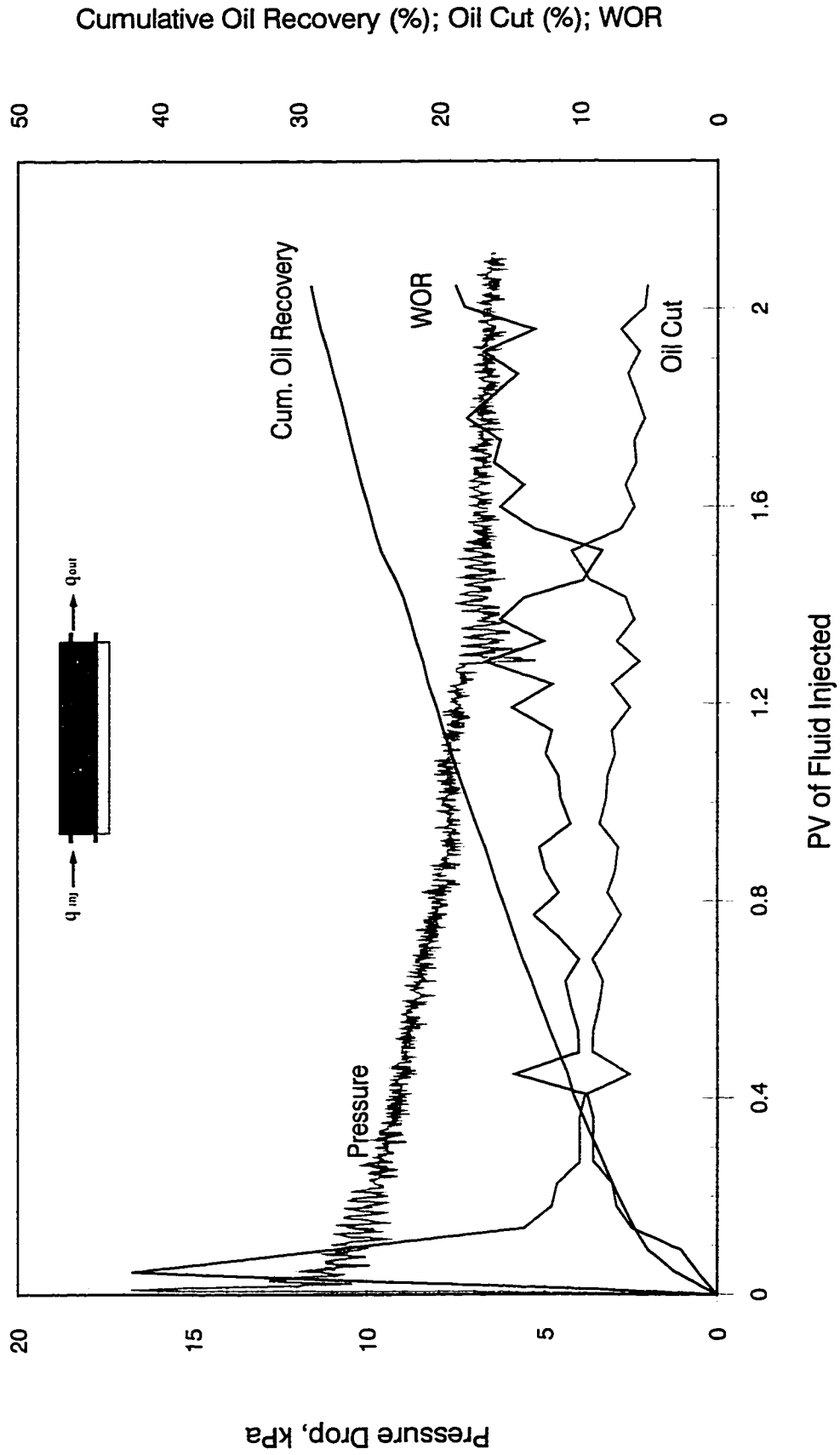


Figure 7-4: Bottom-Water Pack Waterflood ( $q = 300$  cc/hr,  $hw/h_o = 1/3$ , Oil Viscosity =  $34.3$  mPa.s)

# Production History for Experimental Run 15

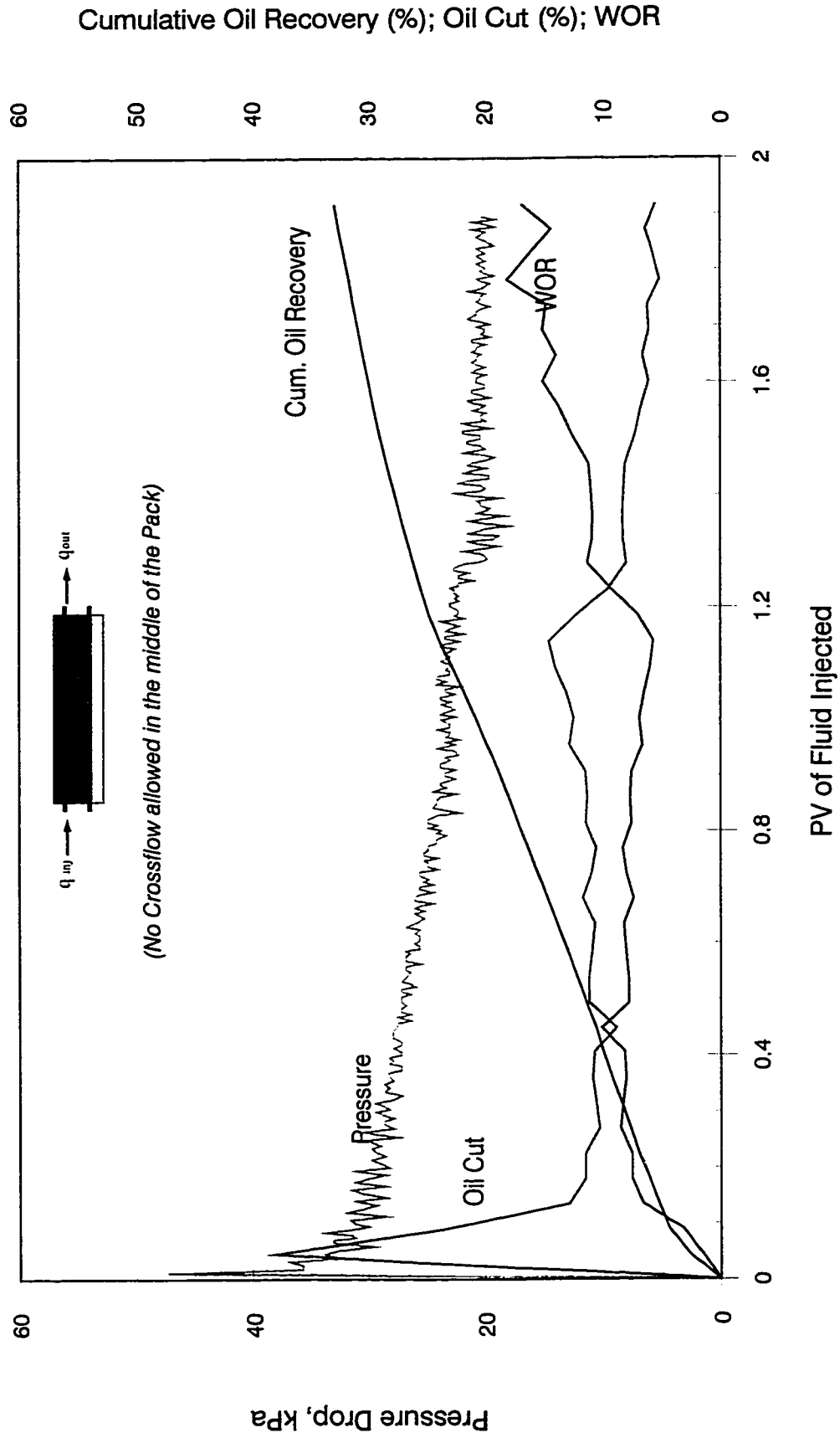


Figure 7-5: Bottom-Water Pack Waterflood (Injection Rate = 450 cc/hr,  $hw/ho = 1/3$ , Oil Viscosity = 34.3 mPa.s)



# Production History for Experimental Run 16

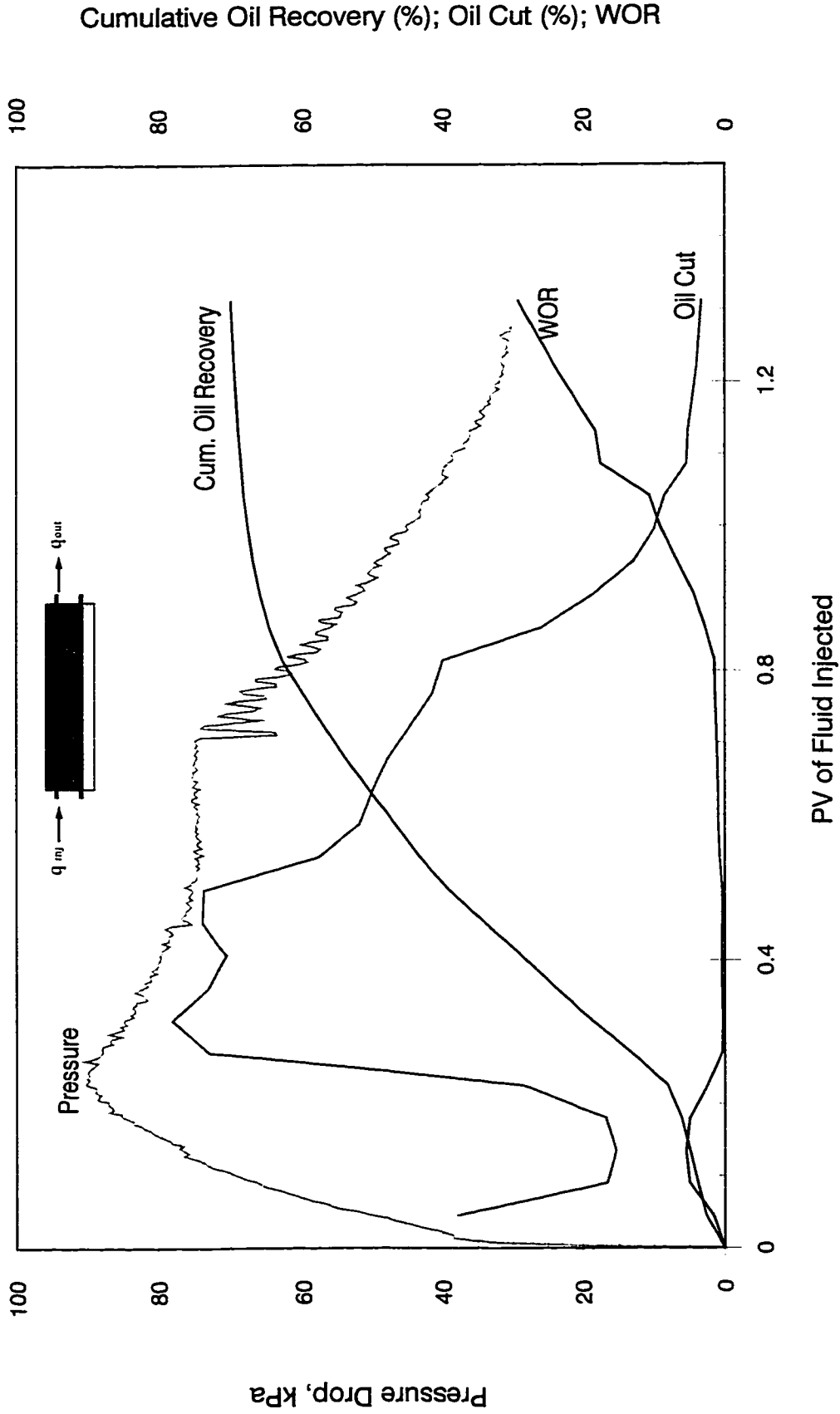


Figure 7-6: Bottom-Water Pack Polymer Flood ( $q = 450$  cc/hr, Con. = 500 ppm,  $hw/ho = 1/3$ ,  $U_o = 34.3$  mPa.s)

# Production History for Experimental Run 21

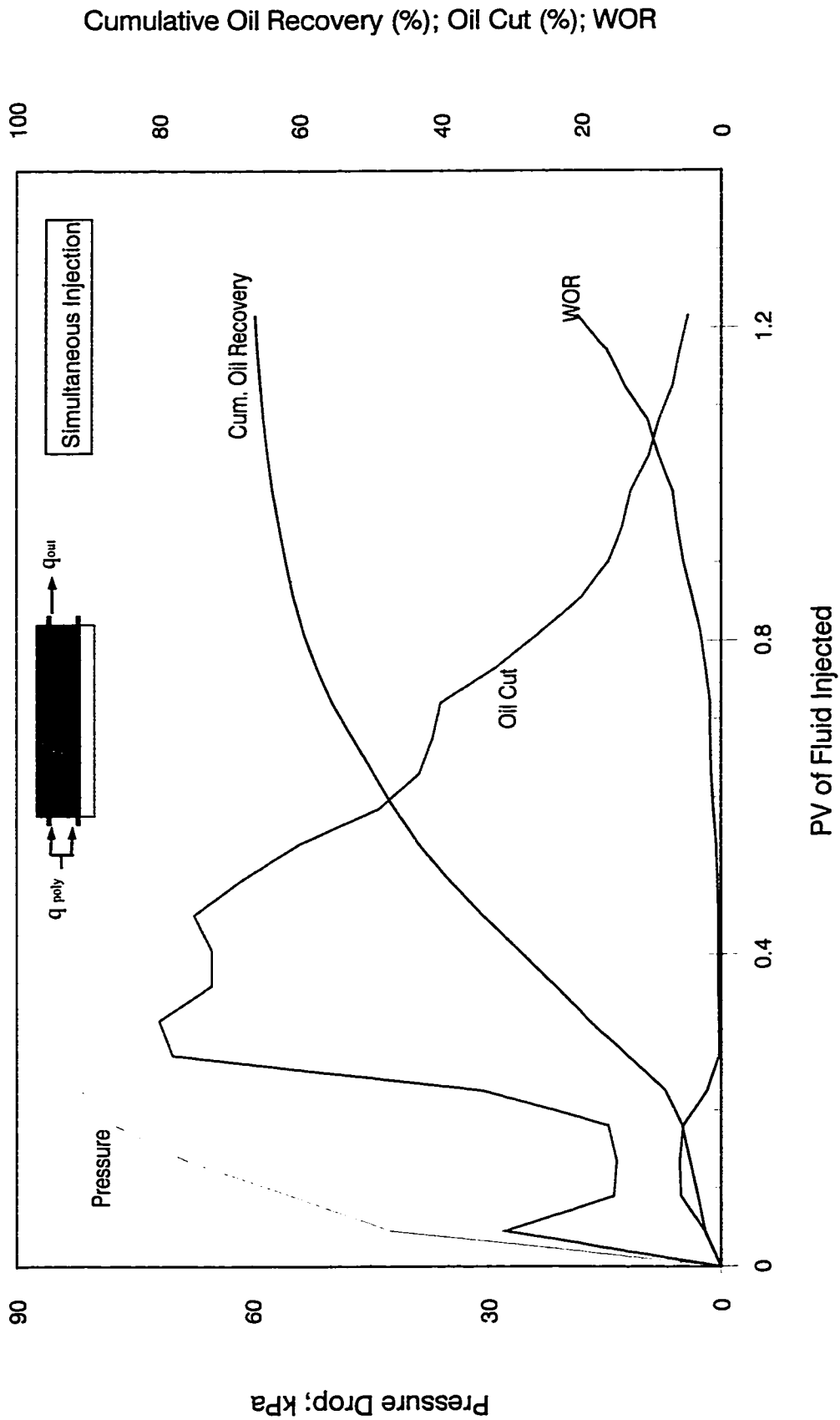
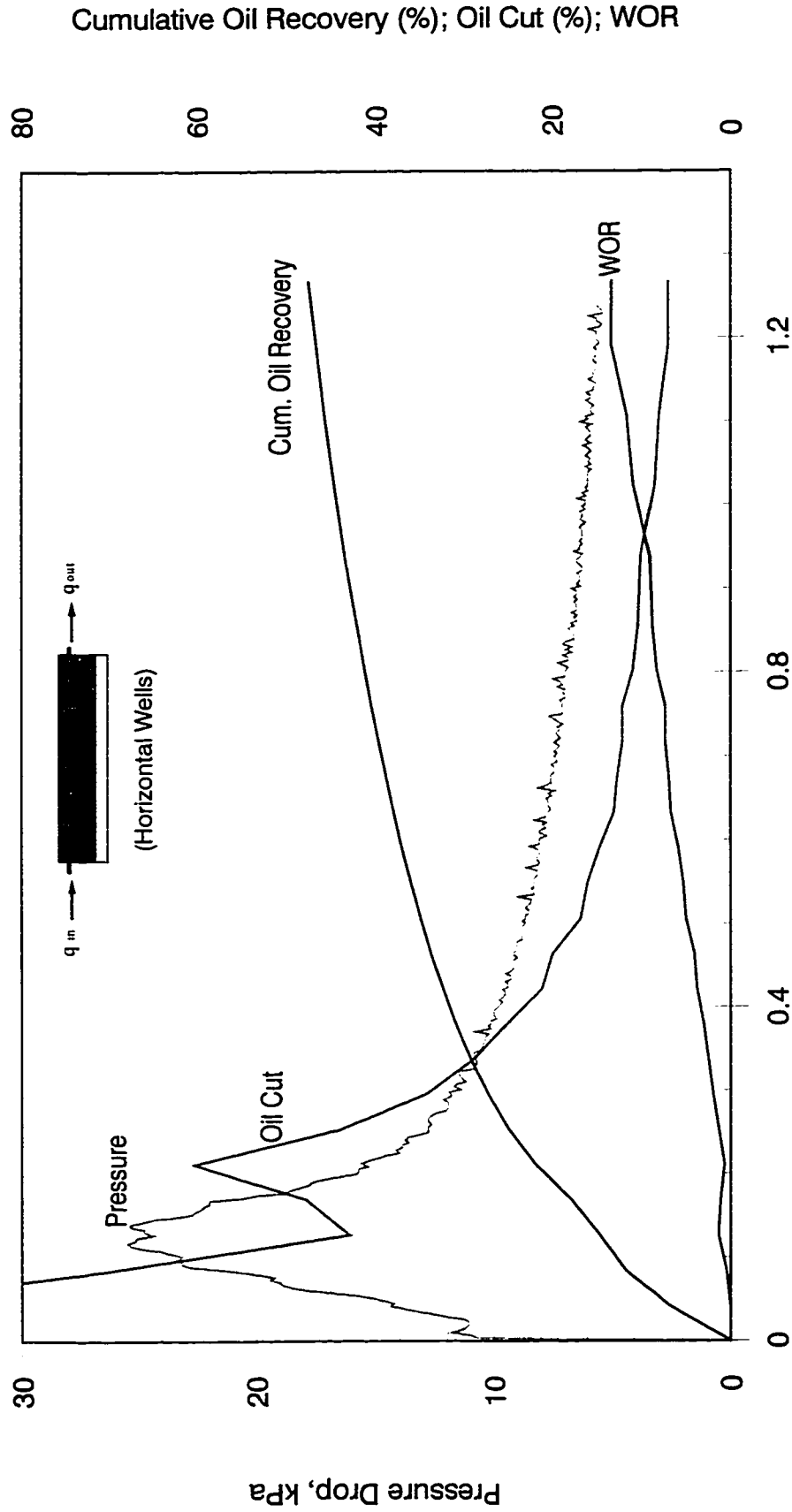


Figure 7-7: Bottom-Water Pack Polymer Flood ( $q = 450$  cc/hr, Con. = 500 ppm,  $hw/ho = 1/3$ ,  $U_o = 34.3$  mPa.s)

# Production History for Experimental Run 28



PV of Fluid Injected

Figure 7-8: Bottom-Water Pack Polymer Flood (  $q = 450$  cc/hr,  $hw/ho = 1/3$ , Oil Viscosity =  $34.3$  mPa.s )

# Production History for Experimental Run 29

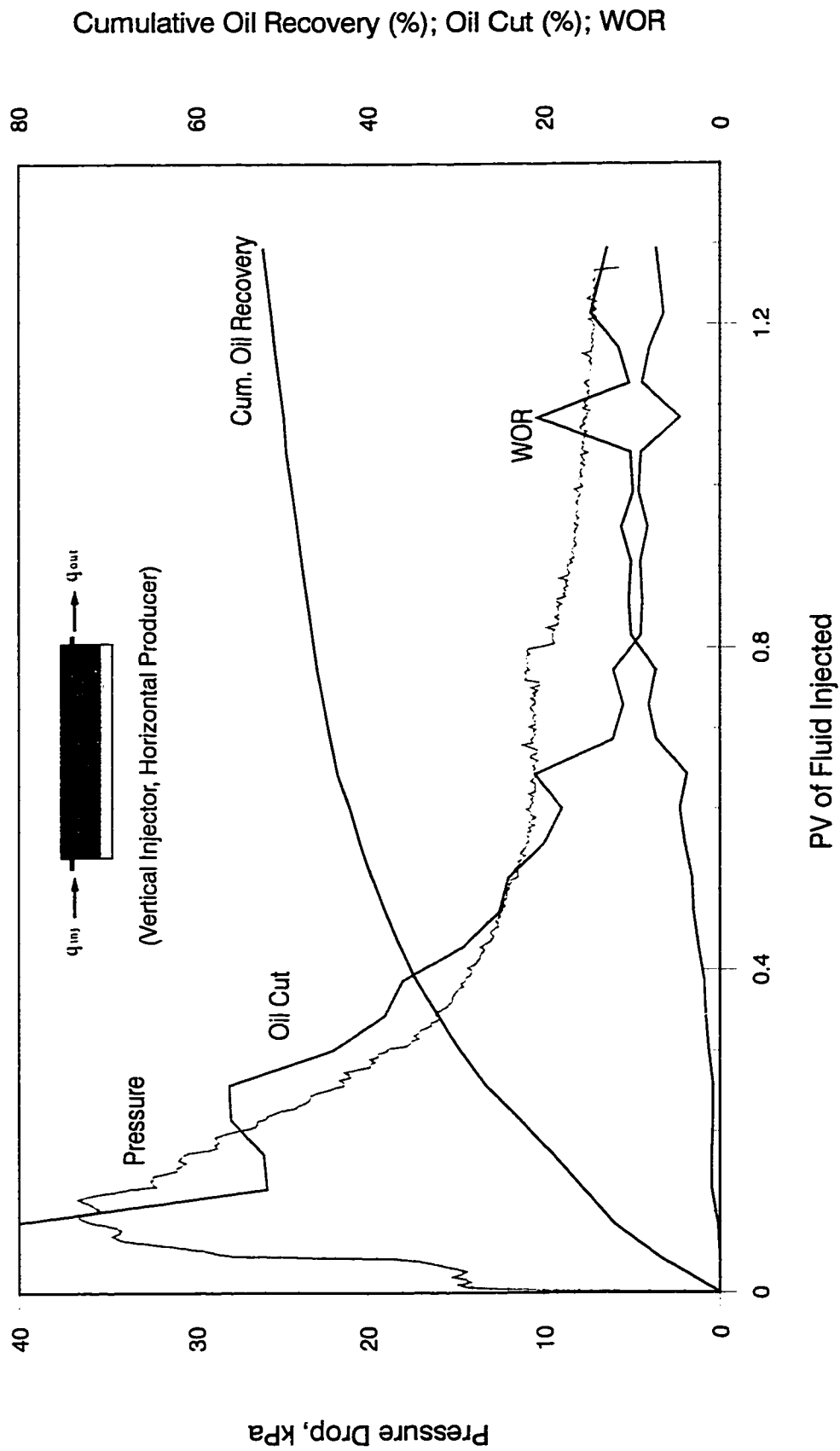


Figure 7-9: Bottom-Water Pack Polymer Flood ( $q = 450$  cc/hr,  $hw/ho = 1/3$ , Oil Viscosity =  $34.3$  mPa.s)

# Two Phase Relative Permeability

(Reproduced After Sarma, 1988)

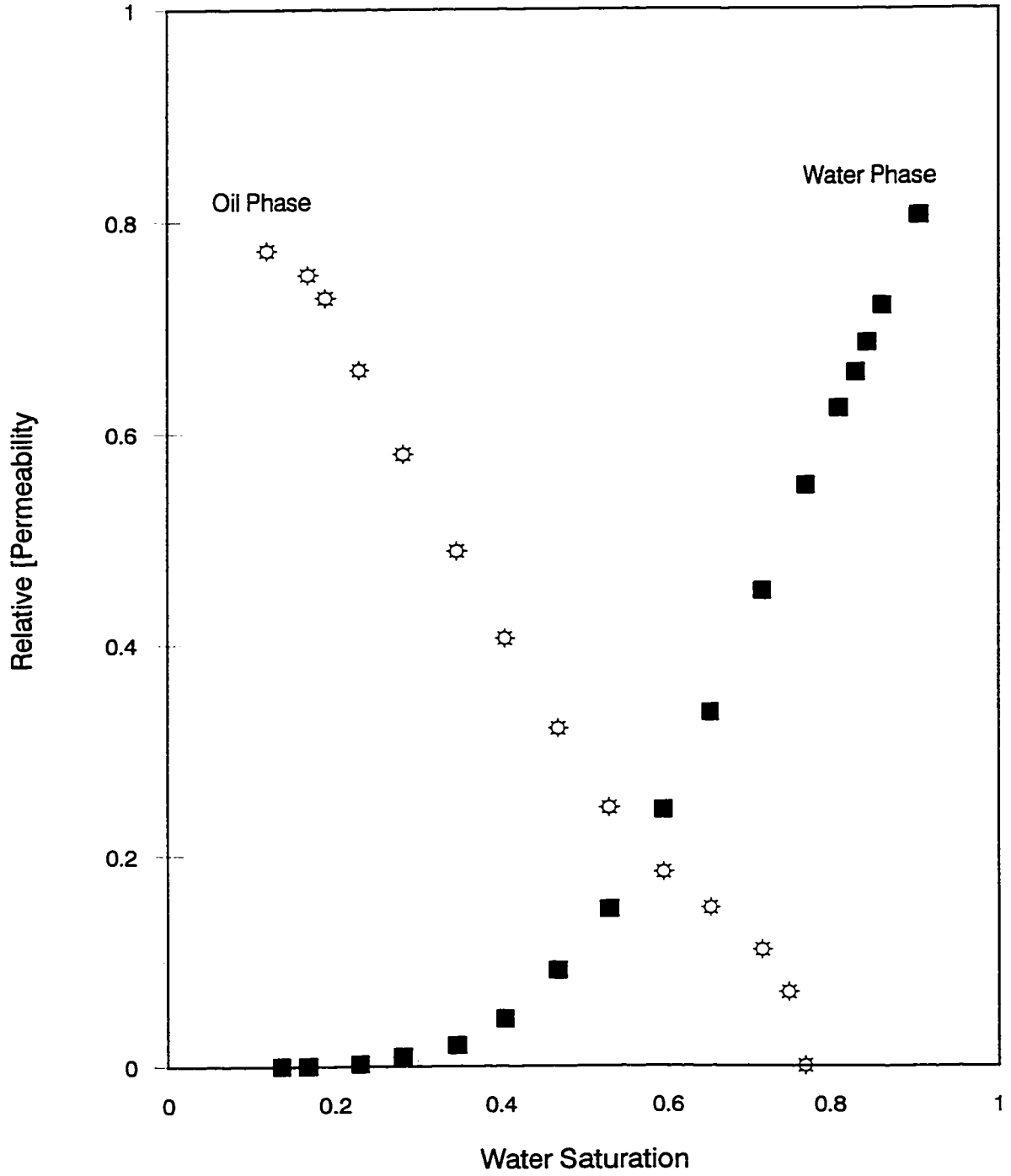


Figure 7-10: Water/Oil Two Phase Relative Permeability

### Capillary Pressure Curve (Reproduced After Sarma, 1988)

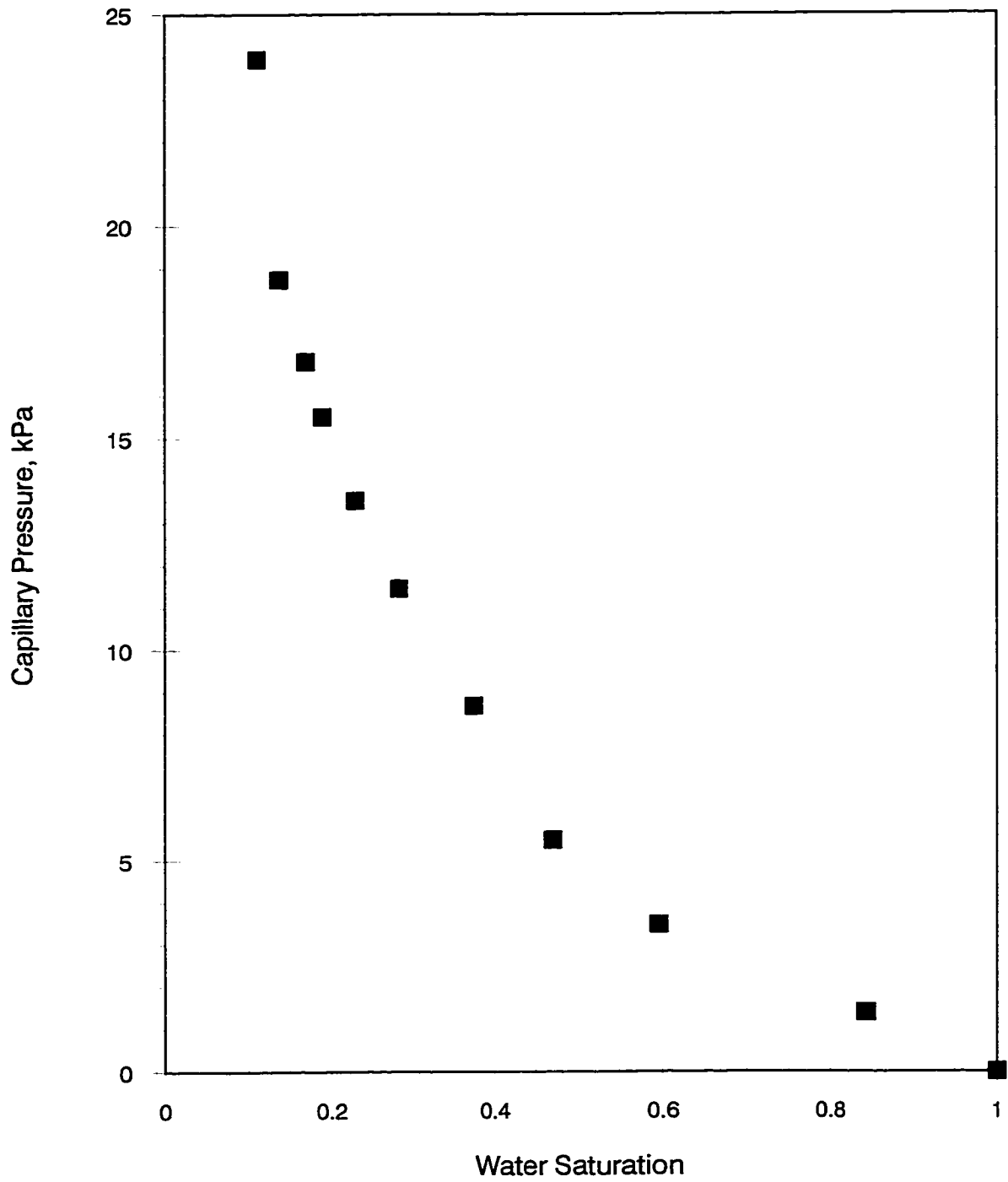


Figure 7-11: Water/Oil Two Phase Capillary Pressure Curve

# Production History for Simulation Run 51

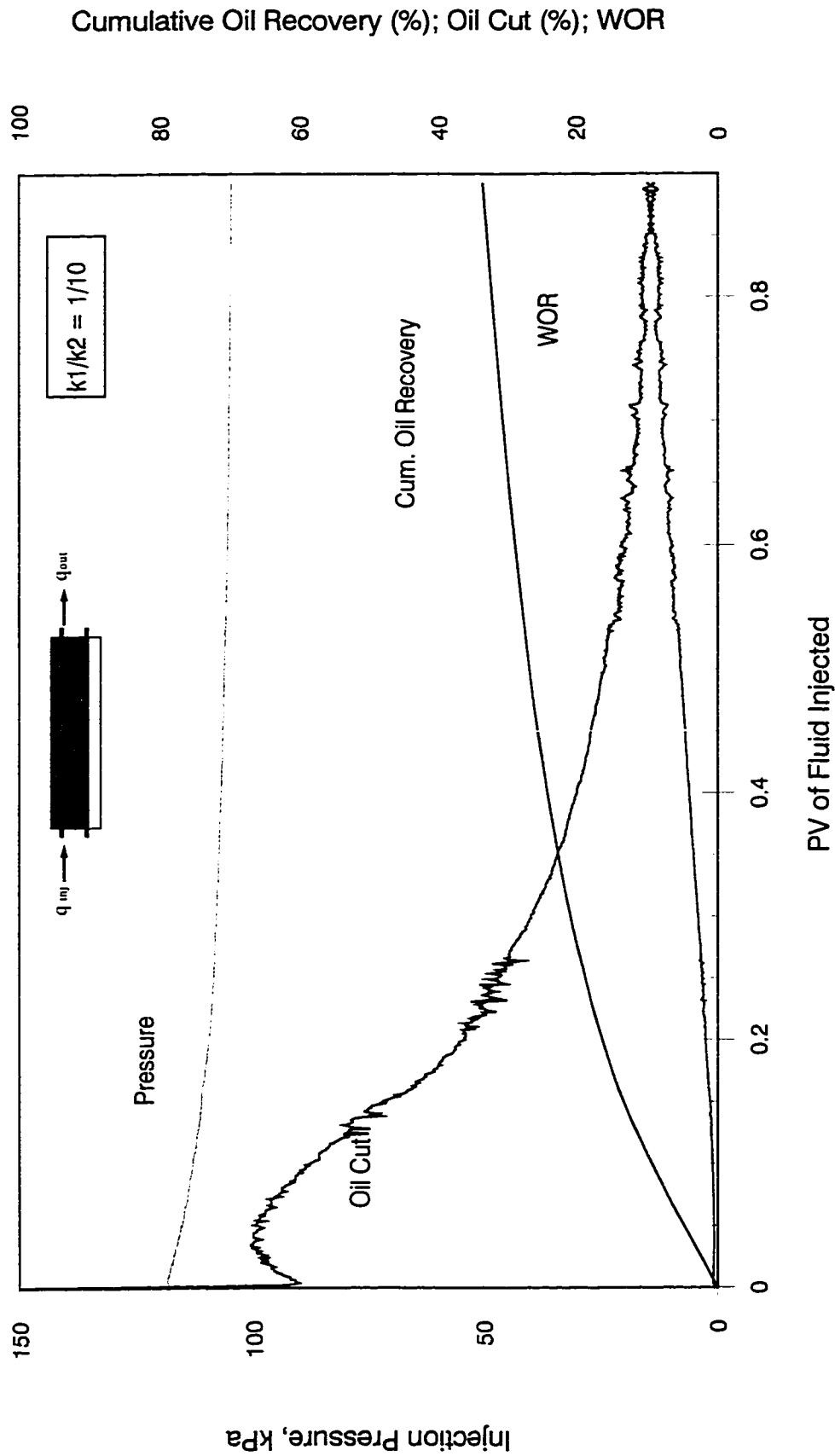


Figure 7-12: Bottom-Water Pack Polymer Flood ( $q = 450$  cc/hr,  $hw/ho = 1/3$ , Oil Viscosity =  $34.3$  mPa.s)

# Production History for Simulation Run 52

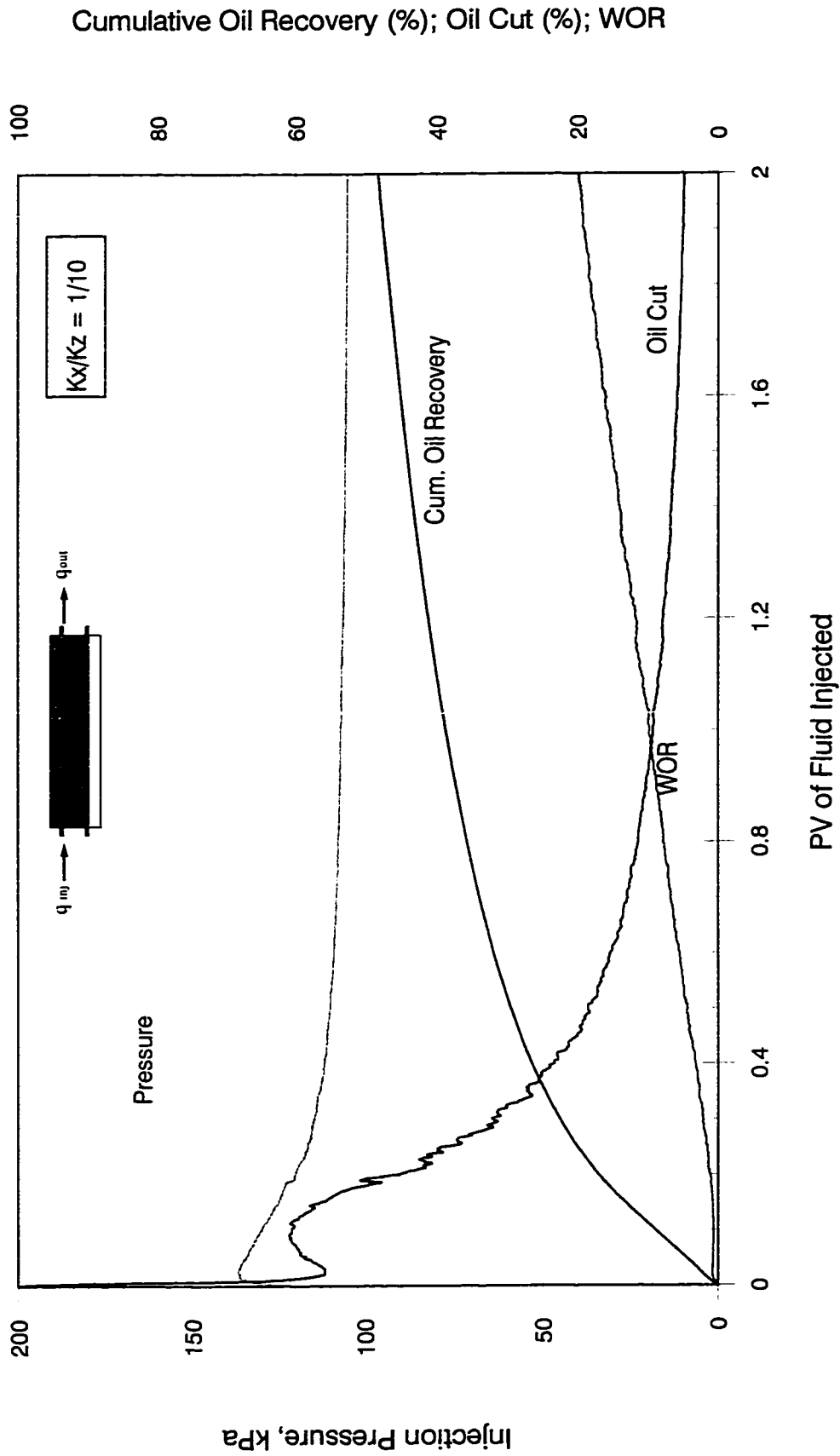


Figure 7-13: Bottom-Water Pack Polymer Flood (  $q = 450$  cc/hr,  $hw/ho = 1/3$ , Oil Viscosity =  $34.3$  mPa.s )



# Production History for Analytical Runs 53 Through 57

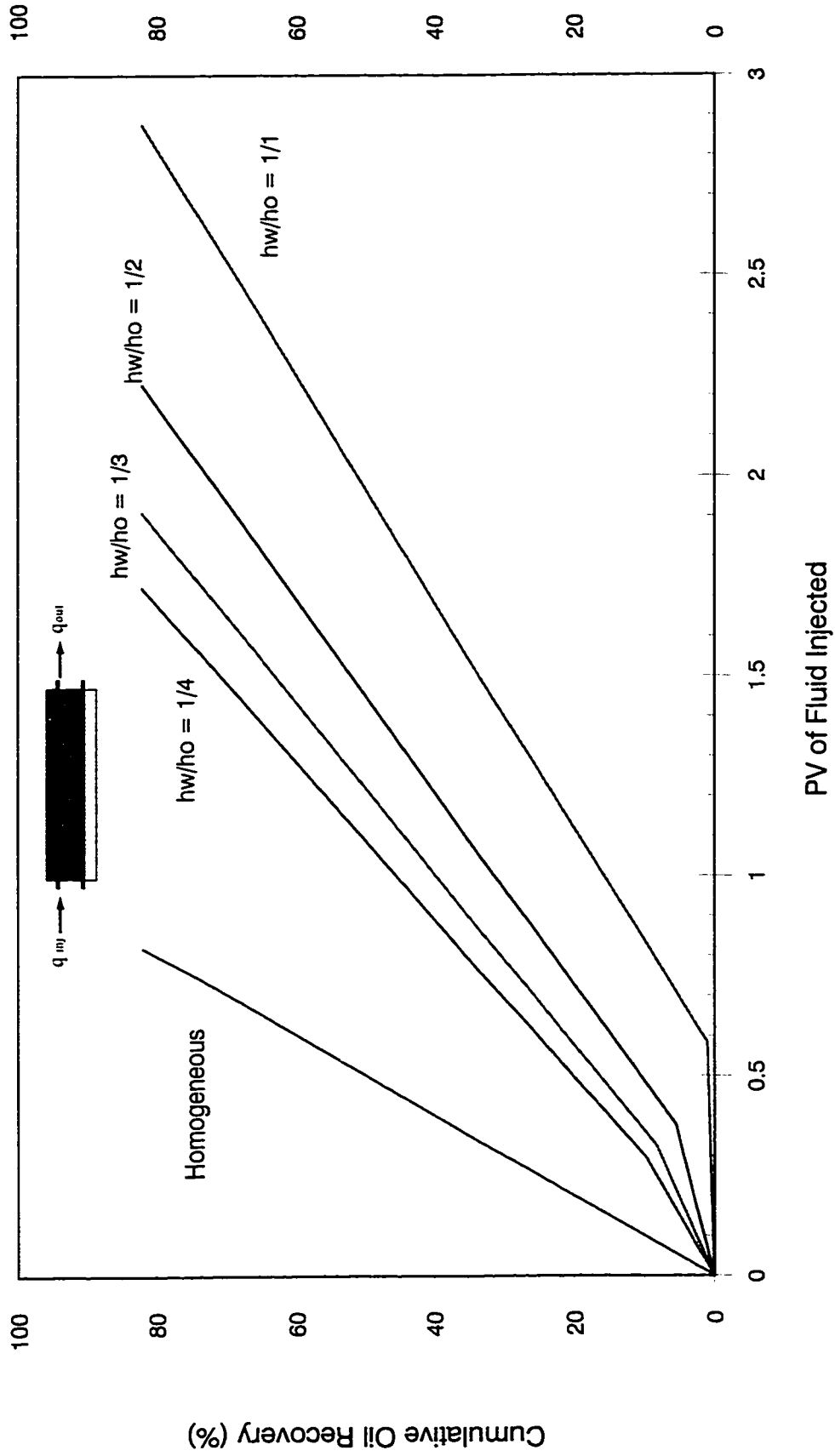


Figure 7-14: Bottom-Water Pack Waterflood (  $k_1/k_2 = 1:1$ , Oil Viscosity = 34.3 mPa.s )

# Production History for Analytical Runs 58 and 59

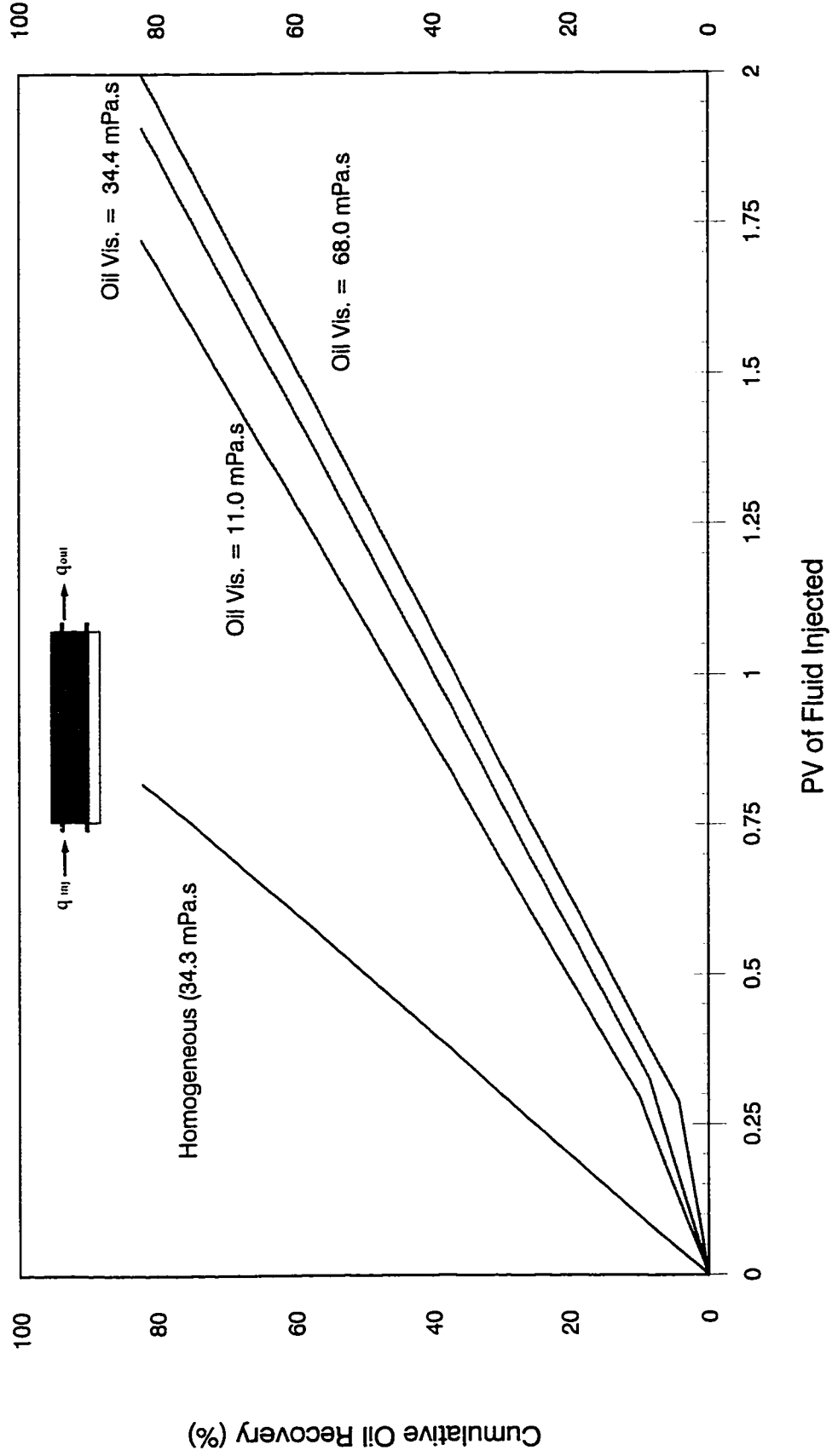


Figure 7-15: Bottom-Water Pack Waterflood (  $k_1/k_2 = 1:1$ ,  $h_w/h_o = 1/3$  )

# Production History for Analytical Runs 60 Through 62

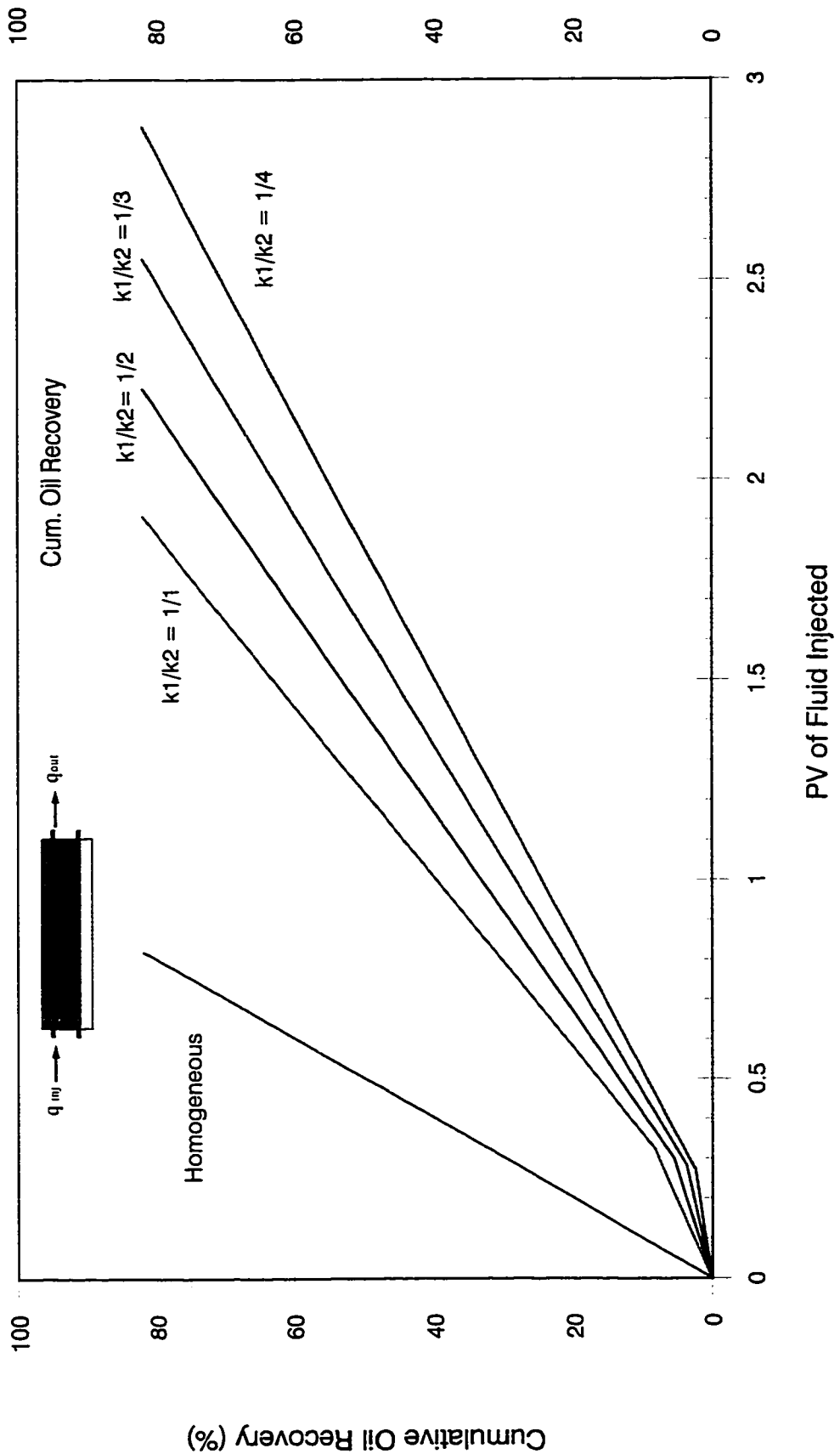


Figure 7-16: Bottom-Water Pack Waterflood (  $h_w/h_o = 1/3$ , Oil Viscosity = 34.3 mPa.s )

## Chapter 8

# DISCUSSION OF THE RESULTS

In this research, 62 Runs (29 experiments, 23 simulations and 10 analytical runs) were conducted to study water and polymer flooding under bottom-water conditions. The principal objectives were to study the crossflow effect and examine the use of polymer as a mobility control and blocking agent under bottom-water conditions. This chapter is divided into two main sections. First, different aspects of crossflow are discussed, based upon the theoretical observations in this study as well as the experimental results of previous studies<sup>38,39</sup>. Second, results obtained from the three models are discussed, and compared where appropriate. Finally, the usefulness of the approaches developed is considered.

### ***8.1 The Amount and Region of Crossflow***

Whenever vertical permeability exists between adjacent layers, viscous crossflow may occur if a vertical potential gradient is present. Figures 8-1 and 8-2 (figures are at the end of chapter) illustrate how a vertical pressure gradient (pressure difference between layers) can occur for a two-layered reservoir with no crossflow, the lower layer being a water zone. The unequal mobilities of the water and oil cause the horizontal pressure in each layer to take on different profiles.

What happens in Figure 8-1 (no vertical communication) if vertical communication is allowed to exist? As might be expected (see Figure 8-2), fluid would flow between the layers and, according to Darcy's law, the vertical pressure drop would decrease. The viscous crossflow is not uniform along the interface but it is maximum in the vicinity of the flood front. Just how much fluid flows and how much decrease in the pressure drop occurs depends on the vertical transmissibility. But the amount of fluid available to flow is physically limited, if nothing else, by the amount of fluid entering into the oil layer at

the injector. Although it is unrealistic to think that all the fluid entering a layer flows into another, it does point out the fact that the amount of crossflow must reach some maximum value. When this maximum crossflow value is reached, a further increase in vertical transmissibility only results in a decrease in vertical pressure drop. At some value of vertical transmissibility, the vertical pressure drop is nearly zero (it can never be exactly equal to zero) and crossflow is a maximum. In short, it can be concluded that crossflow under bottom-water conditions takes place at the flood front.

## ***8.2 Polymer versus Waterflood***

Polymer flooding<sup>1-23</sup> has been recognized as one of the most promising means of enhanced oil recovery. It can increase oil recovery by reducing the mobility ratio by two major mechanisms: (1) increase the water viscosity, (2) decrease the relative permeability to water. Figures 8-3 and 8-4 combine the histories of polymer and waterfloods under bottom-water conditions for the two base runs. Based on the results presented in these two figures, thus, it is concluded that plugging the bottom-water zone completely is the key to successful oil recovery. Despite the fact that the mobility ratios were favourable (polymer flood) in both the oil and the bottom-water zones, it took 0.25 PV of fluid injection before the oil rate started to increase. Thus, it seems that the low oil rate during the initial production stage of a bottom-water reservoir is unavoidable due to the crossflow.

### ***8.2.1 Effect of Varying Injection Rate on Recovery***

As mentioned in the previous section, crossflow takes place mainly around the flood fronts. A graphical view of the crossflow region is presented in Figures 8-1 and 8-2. The results for an unfavourable mobility ratio (waterflood) are given in Figure 8-5, showing that recovery increases considerably with a increase in injection rate. This shows that recovery under bottom-water conditions is sensitive to injection rate over the range investigated in this study. The increase in recovery for unfavourable mobility ratio with increasing flow rate is credited to the significant increase in crossflow. Thus, increasing the injection rate will affect crossflow which results in an increased recovery (higher

injection rates produce higher oil recovery, but may not be feasible in the field for practical reasons). In other words, crossflow is a function of injection rate as was concluded by Lambeth and Dawe<sup>33</sup>.

It should be noted that Yeung<sup>38</sup> and Hassan<sup>39</sup> concluded in their studies that crossflow is independent of flow rate and they also concluded that crossflow under bottom-water conditions takes place near the injection end.

Figure 8-6 shows that for a favourable mobility ratio, the oil recovery is insensitive to injection rate. Similarly, the simulation results shown in Figure 8-7 are insensitive to injection rate.

### ***8.2.2 Effect of Varying Thickness Ratio***

In general, the effect of oil-to bottom-water thickness ratio is predictable in the sense that the higher the oil-to-bottom-water thickness ratio, the more oil will be recovered. Figures 8-8 through 8-12 show the results of the three models used in this research. Figures 8-13 and 8-14 show a plot of cumulative oil recovery versus thickness ratio at one PV of fluid injection. Figure 8-13 compares the recovery of the three models for an unfavourable mobility ratio and Figure 8-14 shows the recovery comparison for a favourable mobility ratio. Because the three models are in good agreement, it is concluded that the thickness ratio does play a significant role on waterflood performance under bottom-water conditions over the range considered. For a polymer flood, the recovery is less sensitive to the thickness ratio provided that the polymer slug size is optimum.

### ***8.2.3 Effect of Varying Oil Viscosity on Recovery***

The effect of oil viscosity is also predictable in the same sense as the thickness ratio. Figures 8-15 through 8-19 show a comparison of oil recovery for 11.0 mPa.s, 34.3 mPa.s, and 68.0 mPa.s oil viscosity, respectively. The dependence of recovery on oil viscosity is predictable in the sense that low oil viscosity gives higher oil recovery. This behaviour is caused by the reduced resistance to oil flow in the transverse direction as well as in the

flow direction. This increases the crossflow of oil into the bottom-water layer, from where it can be produced more quickly. Figures 8-20 and 8-21 compare the results of the three models used in this research at one PV of fluid injection for favourable and unfavourable mobility ratios. Since the three models are in good agreement, it is concluded that the recovery is very sensitive to oil viscosity.

#### ***8.2.4 Effect of Varying Polymer Concentration***

The effect of polymer concentration is also predictable in the same sense as the thickness ratio. In this study, four different polymer concentrations were used as mobility control and blocking agents. It was found that polymer concentration plays an important role in oil recovery. The effect of polymer solution concentration is more understandable because the higher concentration polymer solution has a larger apparent viscosity as shown in Figure 8-22.

Figures 8-23 and 8-24 show the plot of injected pore volumes versus oil recovery of 500 ppm, 1000 ppm, 1500 ppm, and 2000 ppm polymer, respectively for experiments and simulations. Cumulative oil recovery at one pore volume of fluid injection for the simulation and for the experimental model is shown in Figure 8-25 for several polymer concentrations. The increase in polymer concentration is more effective on the incremental oil recovery, because polymer concentration directly reduces the mobility ratio by increasing the water phase viscosity and the reducing effective water permeability as well.

#### ***8.2.5 Effect of Barrier on Recovery***

Run 15 was conducted to investigate the effect of a barrier (no crossflow allowed in the middle of the pack) on oil recovery under bottom-water conditions, and to determine the region of crossflow. Figures 8-26 and 8-27 show the experimental and simulation results of this investigation. It is concluded that crossflow is very beneficial for waterflooding reservoirs under bottom-water conditions because the oil will be produced from both zones (oil zone and water zone). The results also support the conclusion made in the

previous sections that crossflow takes place at the flood front.

### ***8.2.6 Effect of Permeability Contrast***

To investigate the effect of permeability contrast between the oil and the bottom-water layers, analytical and simulation models were used. Figures 8-28 and 8-29 show the results of this investigation. As the permeability contrast in the x-direction increases between the layers (bottom-water layer being the most permeable), recovery decreases. This phenomena is a result of increasing the conductivity of the bottom-water layer. Figures 8-28 and 8-29 also show that as the permeability contrast in the z-direction increases, there will be an increase in oil recovery. This increase in recovery is due to the increase of crossflow between the oil and bottom-water layers.

### ***8.2.7 Effect of Injection Strategies on Recovery***

To elaborate on the differences between the two injection strategies used in a conventional waterflood (with or without the help of a blocking agent), the term "single" and "simultaneous" fluids injection are used, respectively. The two strategies are described individually in the following:

The single-fluid injection process consists of injecting the displacing and/or blocking fluids into the model through a single perforation interval, usually located in the oil zone. In an ideal situation, it is desired for the blocking mode to take place in the bottom-water zone, and the displacing mode to take place in the oil zone.

The simultaneous fluid injection process developed by Yeung<sup>38</sup> consists of injecting displacing and blocking fluids into the corresponding layers simultaneously. Yeung claims that better control of the displacement process is obtained using this process. That is, when displacing the oil zone, the blocking process in the water zone is externally controllable.

In Run 21, polymer was used as a blocking agent to lower the water mobility in the



bottom-water zone. Figure 8-30 shows the effect of injection strategies on cumulative oil recovery. The cumulative oil recovery for the single injection method resulted in higher recovery than the simultaneous injection process. This result contradicts Yeung's finding, because the flow of fluids in porous media cannot be controlled externally, because the direction of the flow is affected by flow rate, mobility ratio, mobility of the existing fluids in the porous media, density difference of fluids, permeability and thickness ratio, capillary pressure behavior, crossflow, and the geometric factors.

### ***8.2.8 Effect of Using Horizontal Wells***

Figures 8-31 through 8-33 show the effect of horizontal wells on oil recovery with and without the bottom-water zone. Using horizontal wells indicates that the performance of the waterflood without the bottom-water zone is reduced as the horizontal wells are used for injection and production. This phenomenon is caused by reducing the swept area. However, waterflooding with horizontal wells shows higher recovery than vertical wells in the presence of a bottom-water zone. This higher recovery is credited to fact that horizontal wells are suitable for thin reservoirs with high vertical permeability and the tendency of horizontal wells to reduce water-coning. Conventional waterflooding under bottom-water conditions, using a combination of vertical injectors and horizontal producers (Run 29), shows better oil recovery than horizontal wells (injector/producer).

## ***8.3 Contribution of the Research***

In Alberta and Saskatchewan, many reservoirs have a bottom-water zone, in communication with the oil zone. Examples are: Suffield, David, Hughenden, S. Jenner, and many other reservoirs. These, and even more viscous oil reservoirs, such as those in the Lindbergh and Lloydminster areas, are on primary production. Some of these are good candidates for waterflooding, but flooding is not likely to be very effective because of the water zone. This research addresses this problem. The experimental results, analytical model and numerical simulator developed in this research will be of value to operators in these area in planning waterfloods.

The other major aspect of the research concerns the extensive use of vertical/horizontal wells in some of these reservoirs. The results obtained in this research will provide useful information on how to implement waterfloods in the presence of vertical/horizontal wells and a bottom-water zone.

#### ***8.4 General Observations***

Polymer flooding is the most common enhanced oil recovery technique in existence. The reasons for this are that, short of waterflooding, polymer flooding is the simplest technique to apply in the field and requires a relatively small capital investment. Most of the field projects have been small, however, as has the amount of oil recovered, a fact that should be expected from the treatment given in this thesis. Nevertheless, there can exist significant potential for an acceptable rate of return even when recovery is low. Considering the average polymer requirement and the average costs of crude and polymer, it appears that polymer flooding should be a highly attractive EOR process. However, such costs should always be compared on a discounted basis, reflecting the time value of money. Such a comparison will decrease the apparent attractiveness of polymer flooding because of the decreased injectivity of the polymer solutions.

The most important property covered in this study is the non-Newtonian behaviour of polymer solutions, because such behavior impacts on the polymer requirements through the design of mobility ratio, and on the ability to accurately forecast the rate of polymer injection. Polymer injection rate determines project life which, in turn, determines the economic rate of return. Injectivity estimates along with estimates of mobile oil saturation are the most important determinants in polymer flooding success.

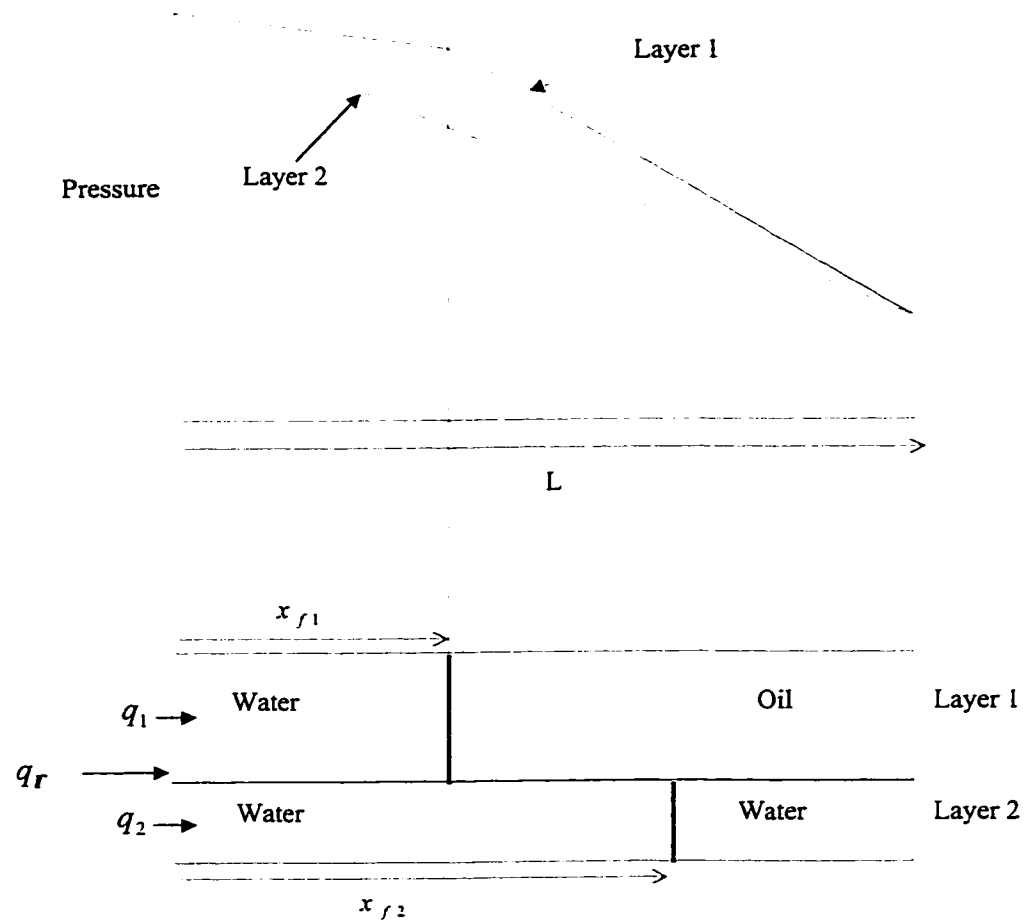


Figure 8-1: Driving Forces for Viscous Crossflow (no vertical communication)

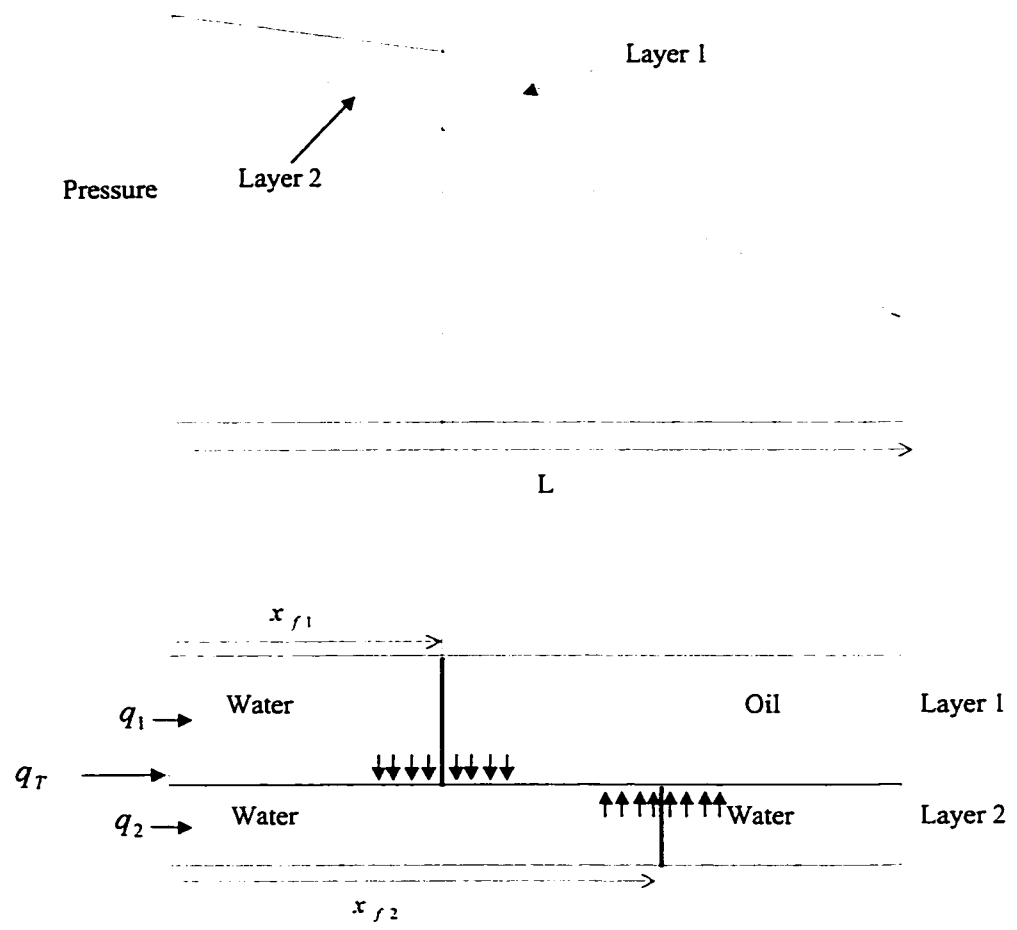


Figure 8-2: Driving Forces for Viscous Crossflow (vertical communication)

# Comparison of Polymer and Waterflood under Bottom-water Conditions

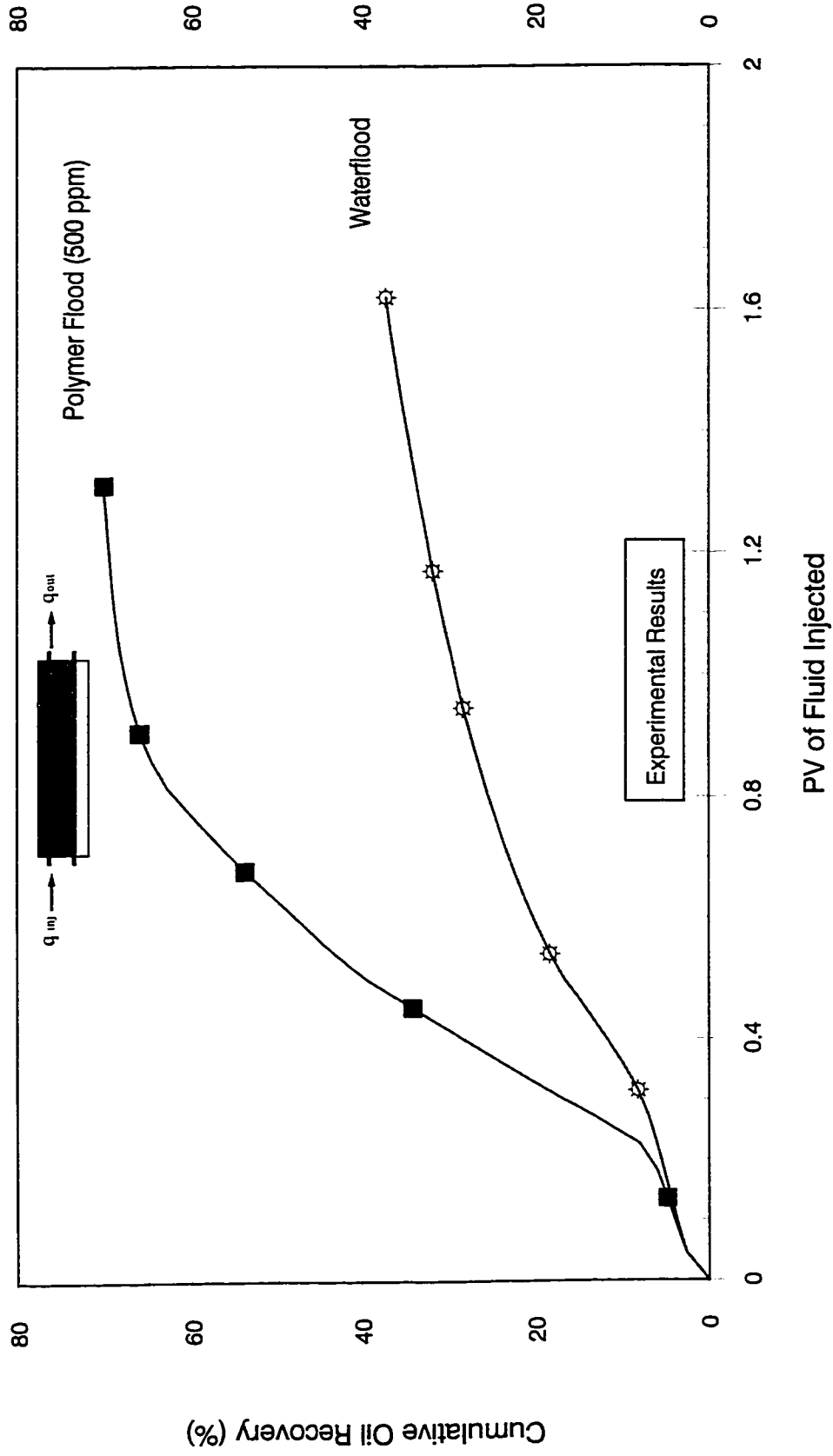


Figure 8-3: Bottom-Water Pack Water/Polymer Flood (  $q = 450$  cc/hr,  $hw/ho = 1/3$ , Oil Vis. =  $34.3$  mPa.s )

# Comparison of Polymer and Waterflood under Bottom-water Conditions

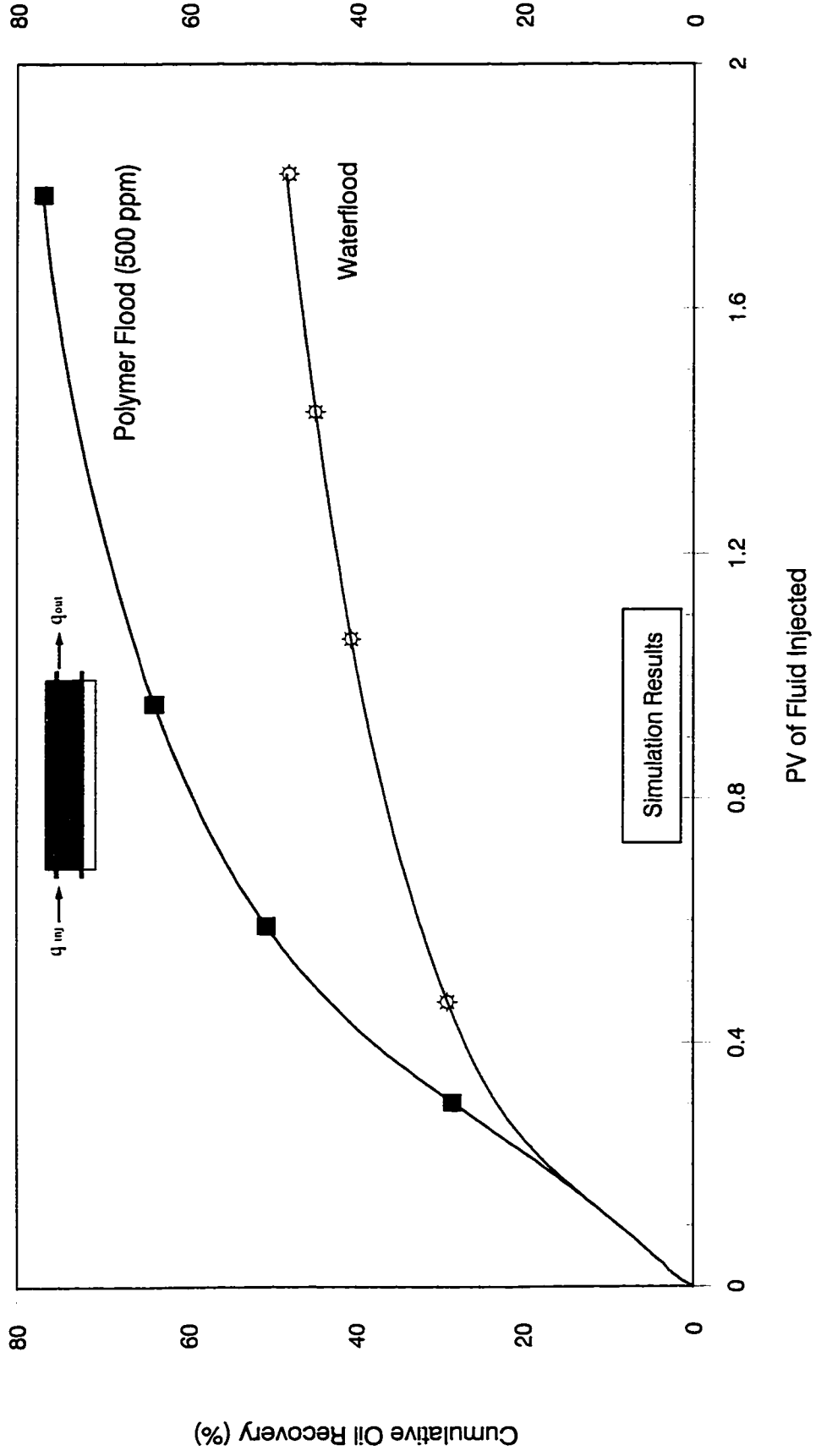


Figure 8-4: Bottom-Water Pack Water/Polymer Flood ( $q = 450 \text{ cc/hr}$ ,  $hw/h_o = 1/3$ , Oil Vis. =  $34.3 \text{ mPa.s}$ )

## Effect of Water Injection Rate on Oil Recovery

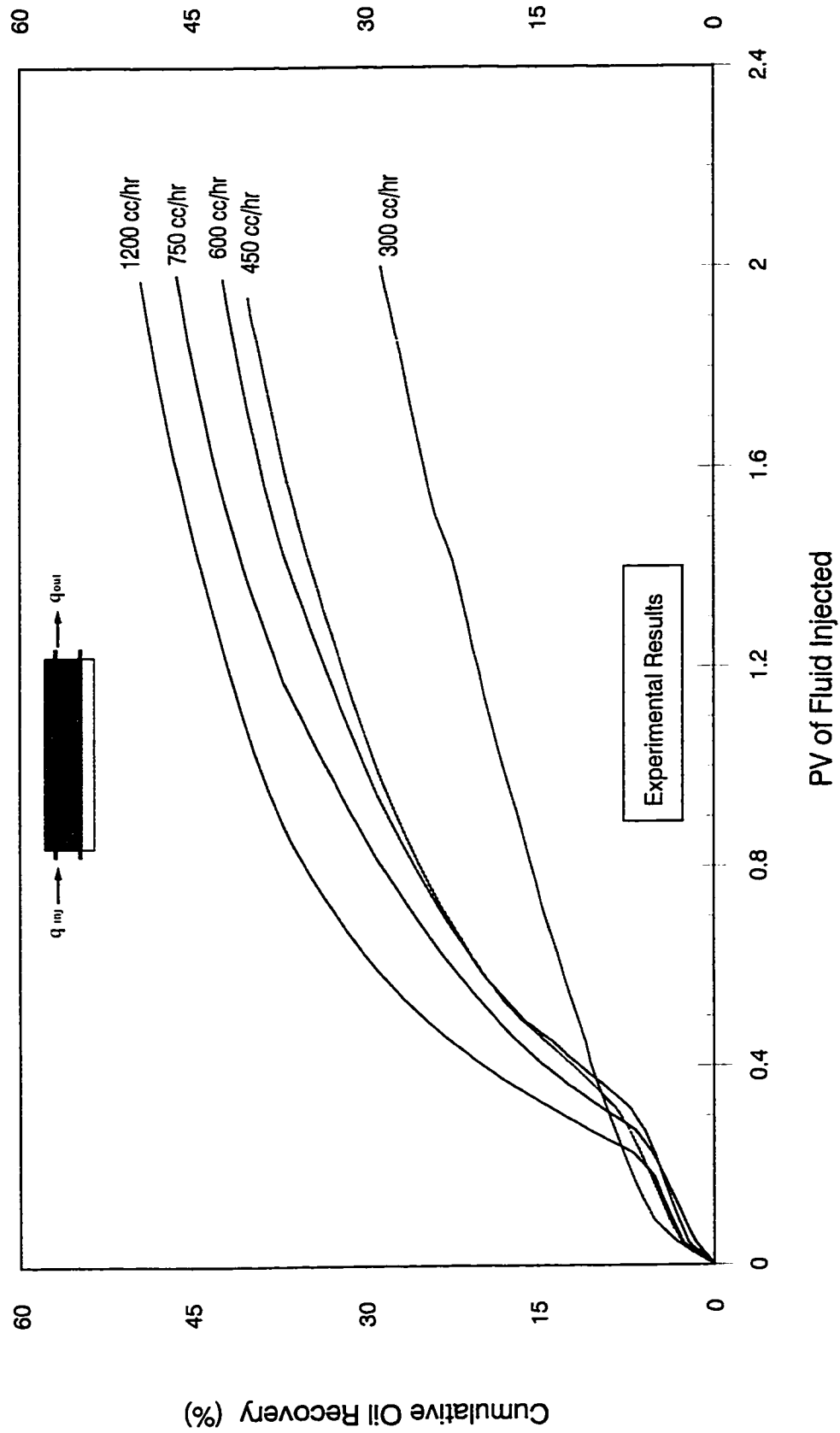


Figure 8-5: Bottom-Water Pack Waterflood (  $h_w/h_o = 1/3$ , Oil Viscosity = 34.3 mPa.s )

# Effect of Polymer Injection Rate on Oil Recovery

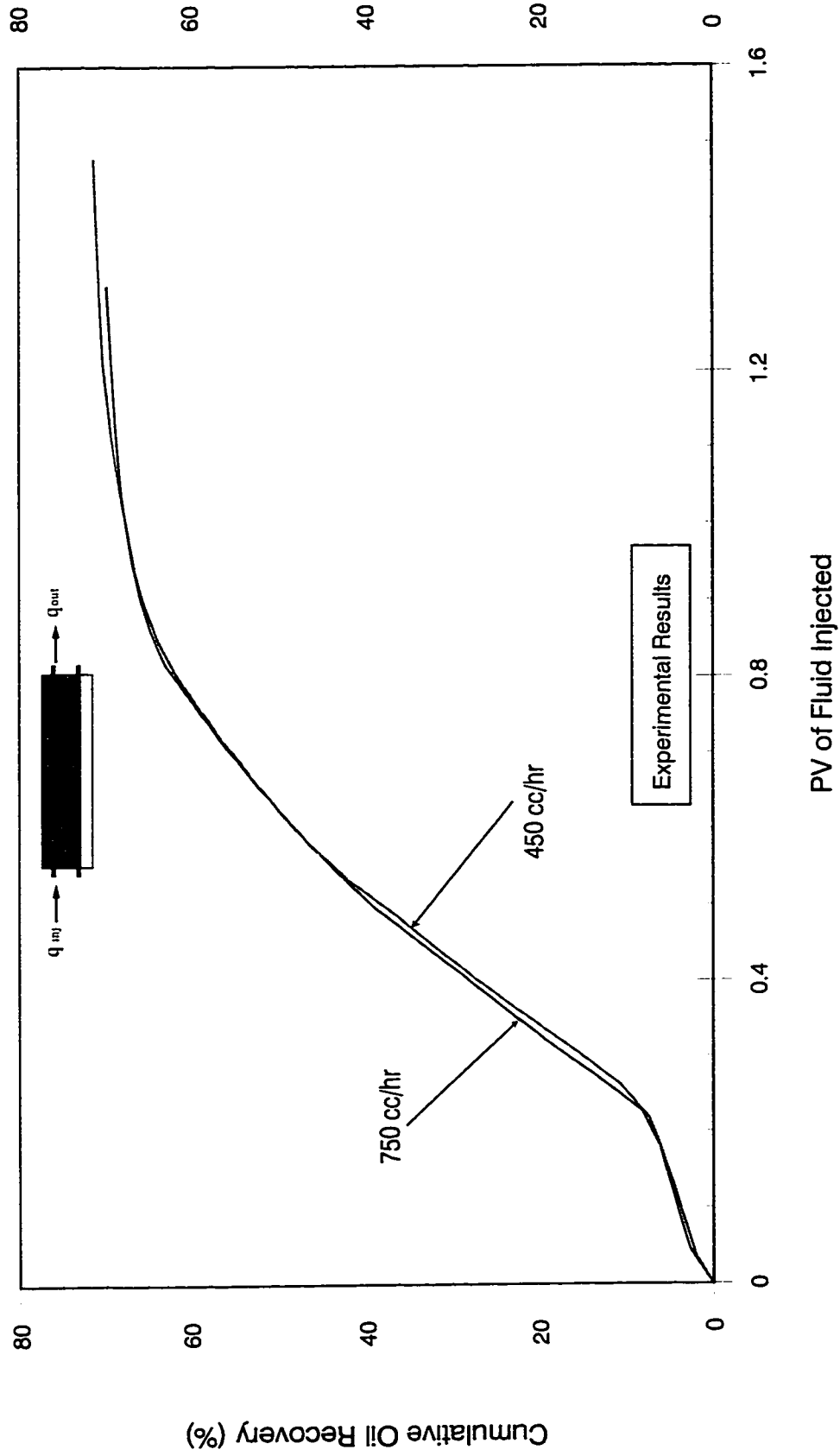


Figure 8-6: Bottom-Water Pack Polymer Flood ( Con. = 500 ppm,  $hw/ho = 1/3$ , Oil Vis. = 34.3 mPa.s )



# Effect of Injection Rate on Oil Recovery

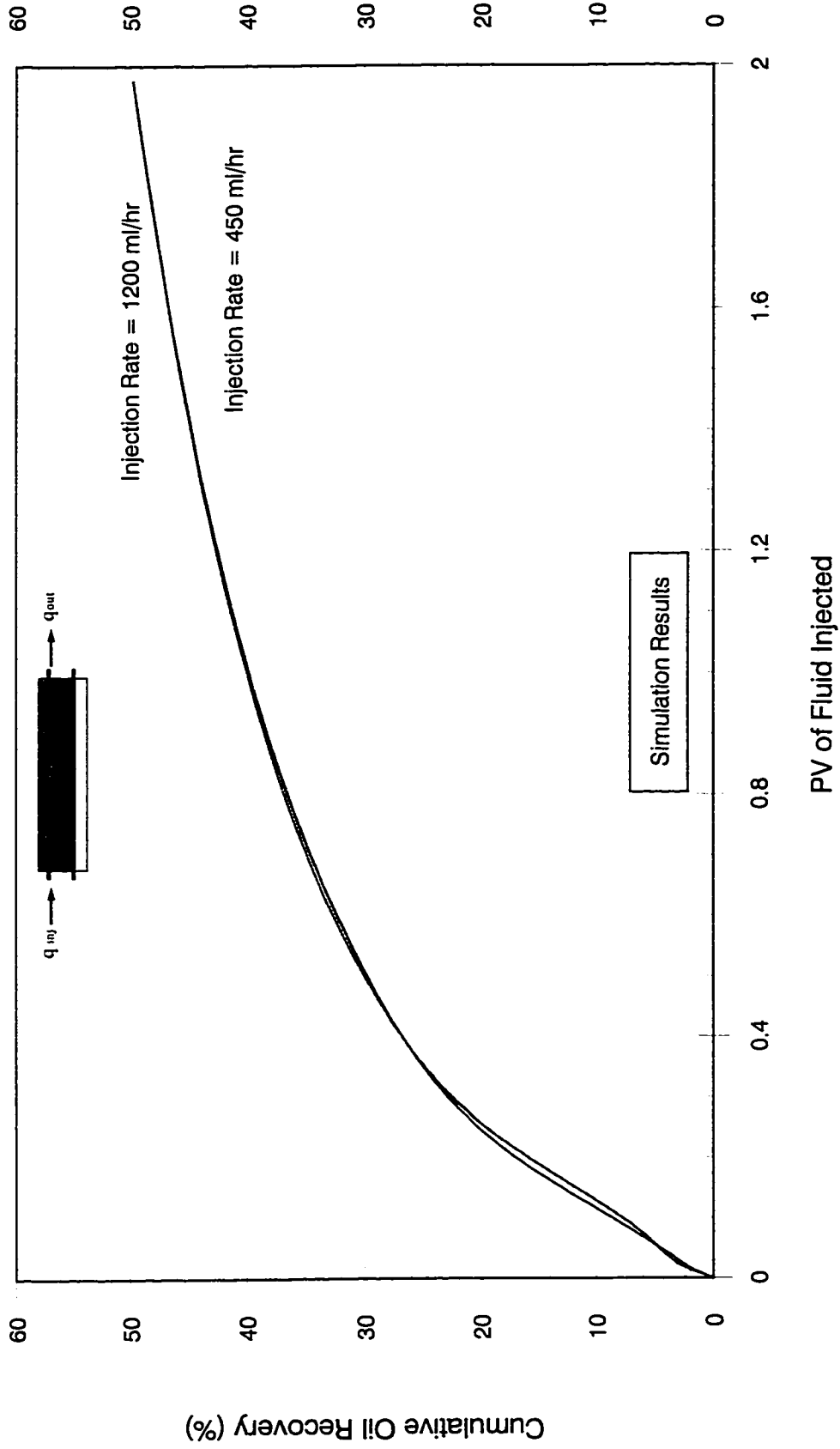


Figure 8-7: Bottom-Water Pack Waterflood ( $hw/ho = 1/3$ , Oil Viscosity = 34.3 mPa.s)

### Effect of Thickness ratio $hw/ho$ on Oil Recovery

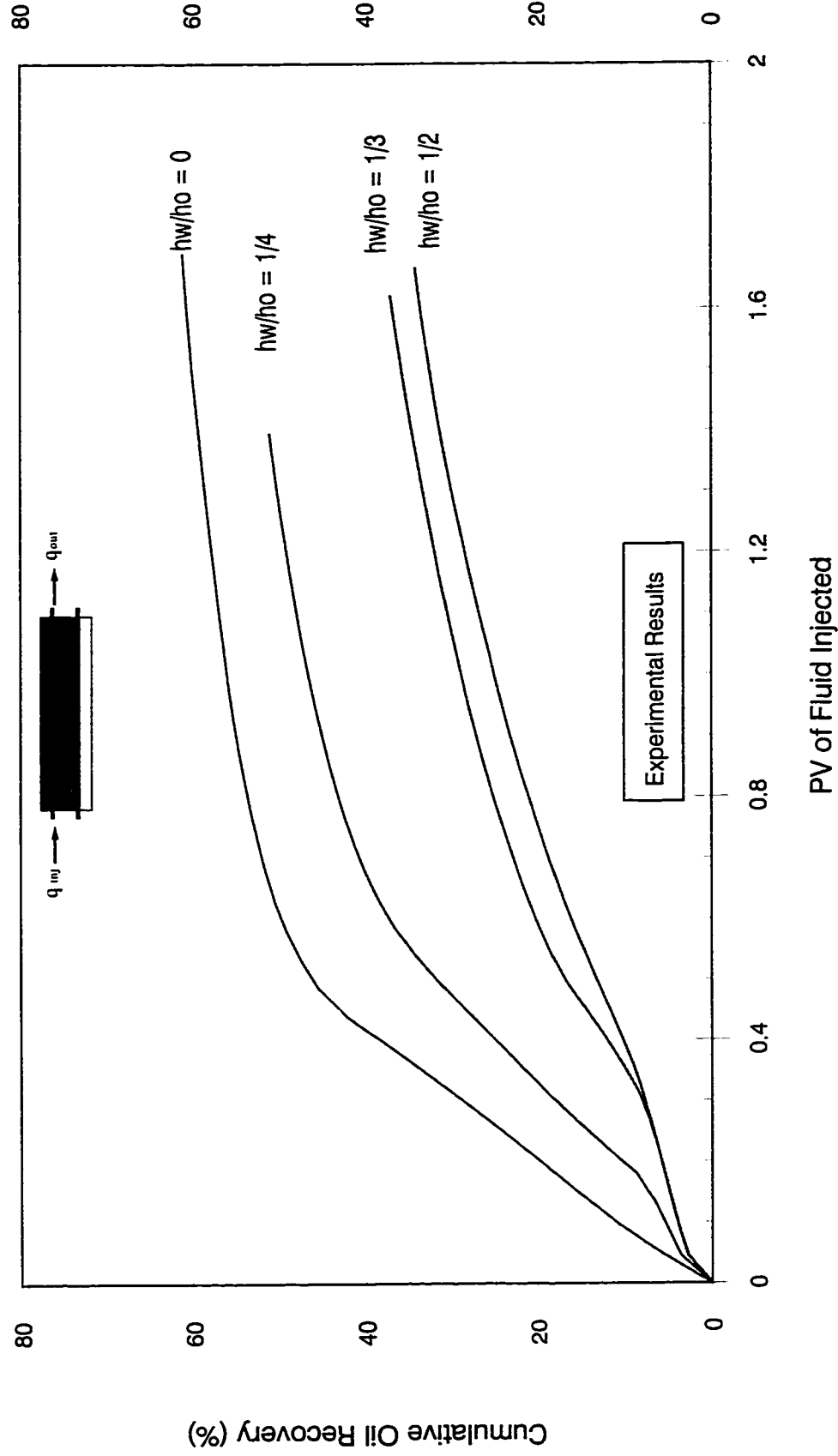


Figure 8-8: Bottom-Water Pack Waterflood ( Injection Rate = 450 cc/hr, Oil Vis. = 34.3 mPa.s )

### Effect of Thickness ratio $h_w/h_o$ on Oil Recovery

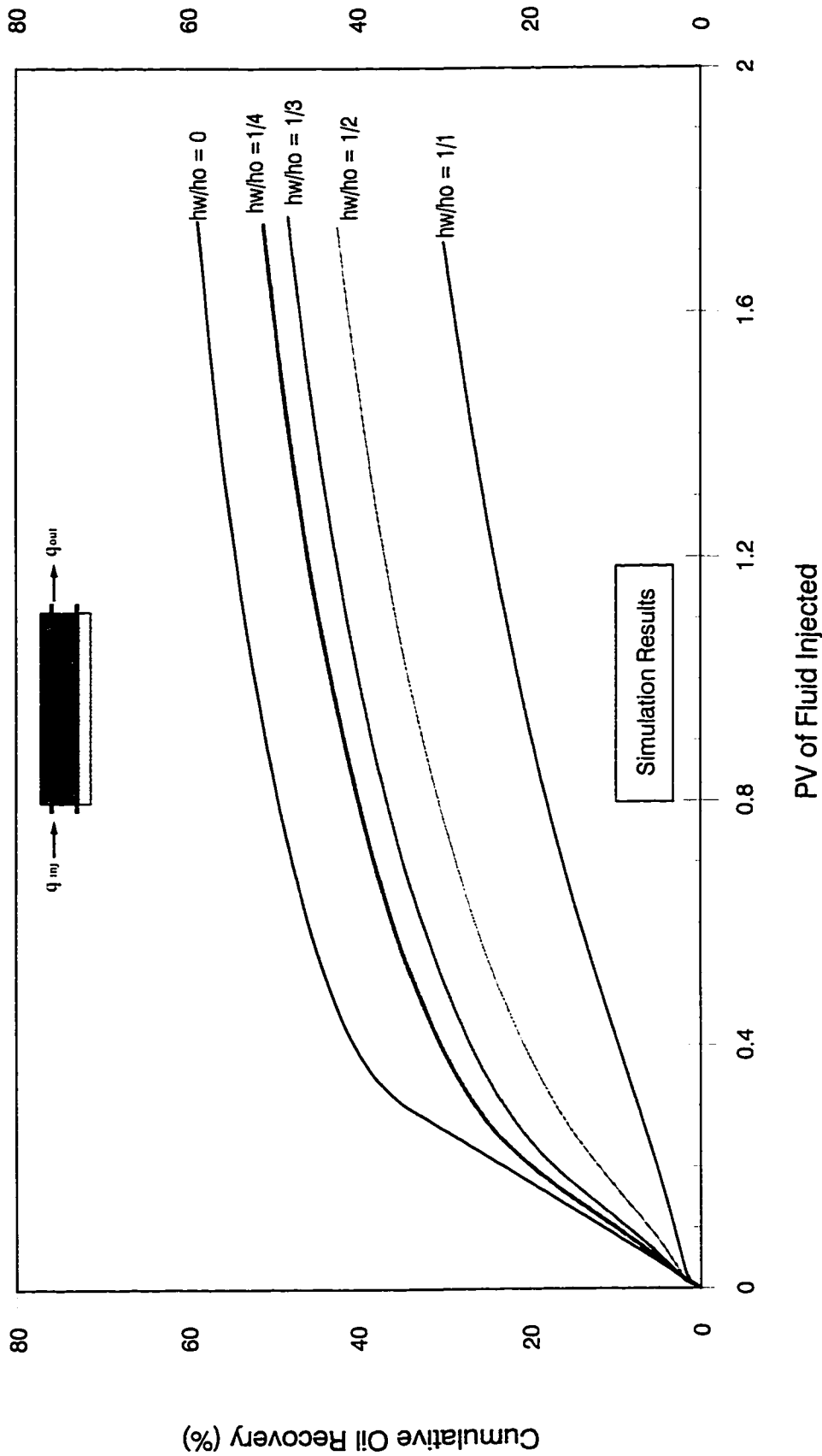


Figure 8-9: Bottom-Water Pack Waterflood ( Injection Rate = 450 cc/hr, Oil Viscosity = 34.3 mPa.s )

### Effect of Thickness ratio $hw/ho$ on Oil Recovery

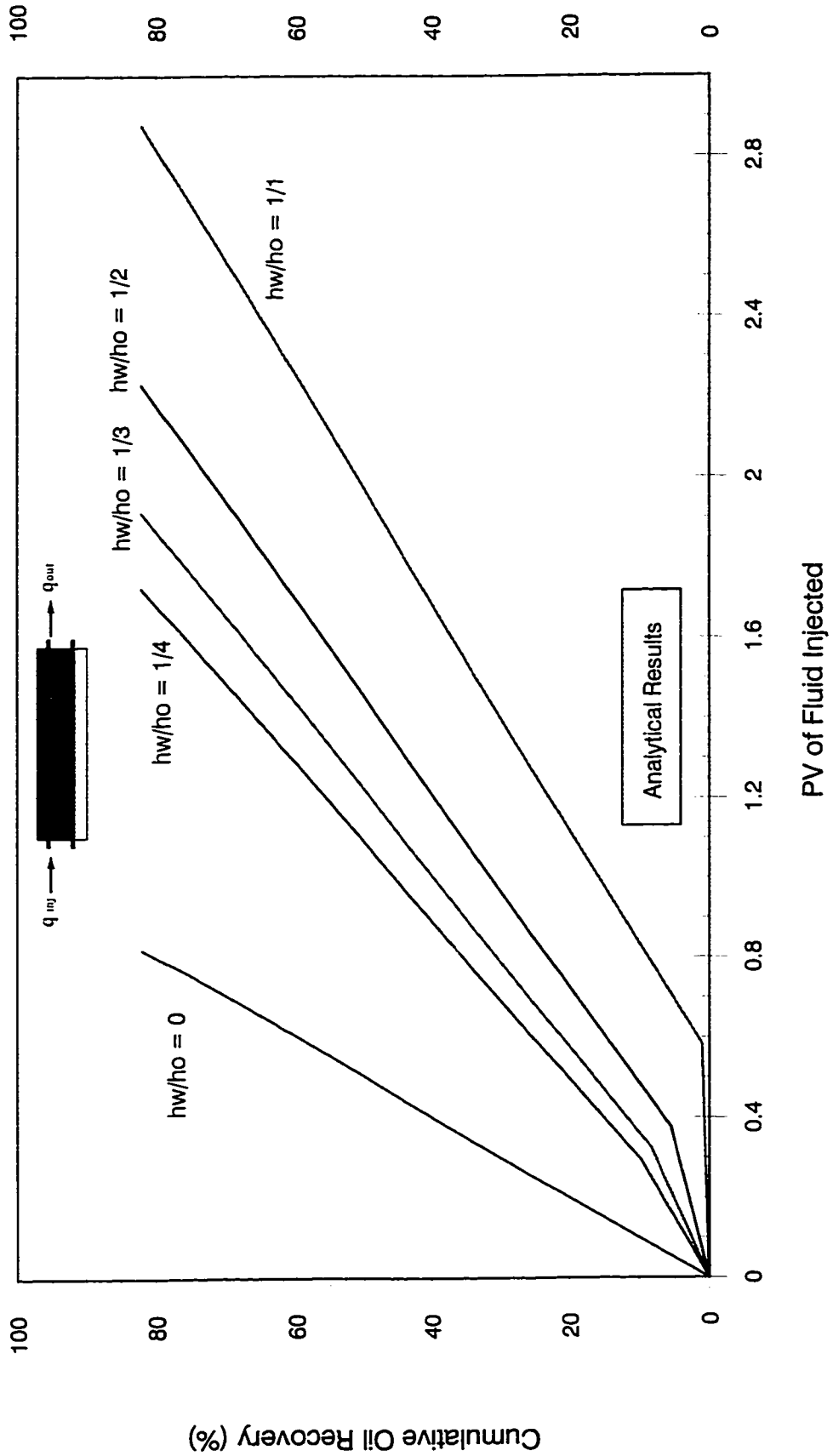


Figure 8-10: Bottom-Water Pack Waterflood (  $K1/K2 = 1/1$ , Oil Viscosity = 34.3 mPa.s )

# Effect of Thickness ratio $hw/ho$ on Oil Recovery

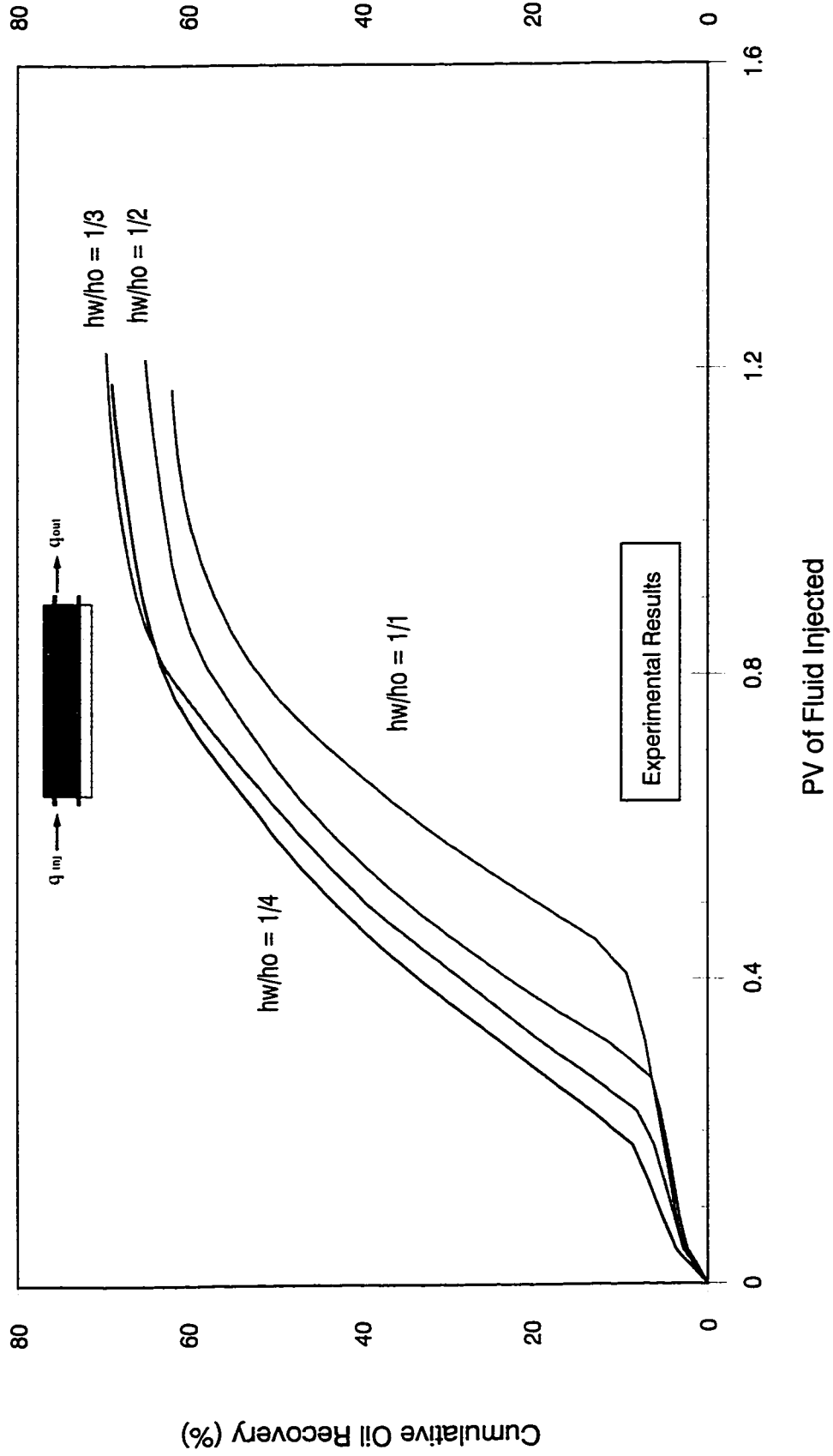


Figure 8-11: Bottom-Water Pack Polymer Flood ( Injection Rate = 450 cc/hr, Oil Vis. = 34.3 mPa.s )

### Effect of Thickness ratio $h_w/h_o$ on Oil Recovery

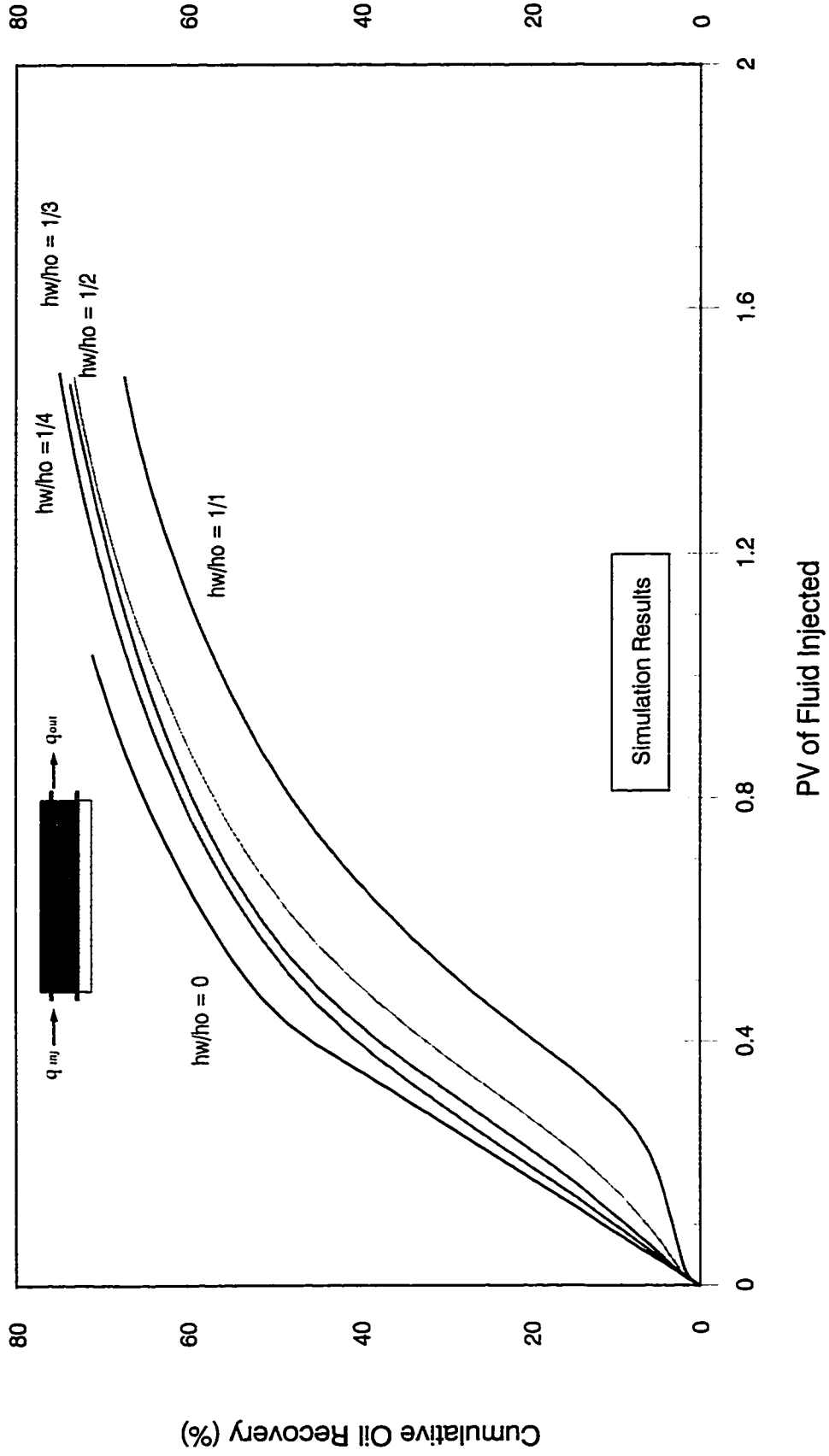


Figure 8-12: Bottom-Water Pack Polymer Flood ( Injection Rate = 450 cc/hr, Oil Viscosity = 34.3 mPa.s )

# Effect of Thickness Ratio $hw/ho$ on Oil Recovery

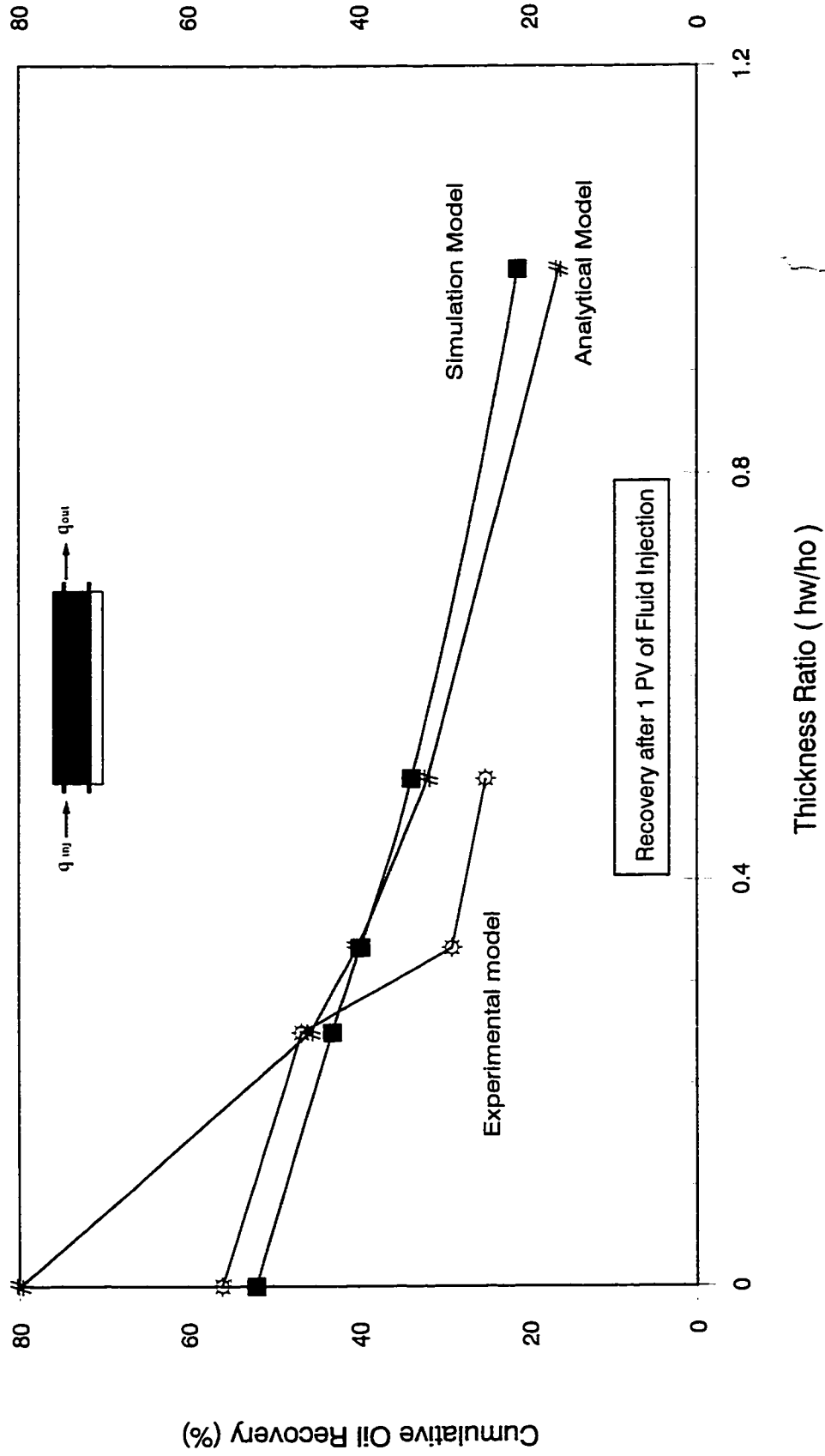


Figure 8-13: Bottom-Water Pack Waterflood ( Injection Rate = 450 cc/hr, Oil Vis. = 34.3 mPa.s )

# Effect of Thickness Ratio $hw/ho$ on Oil Recovery

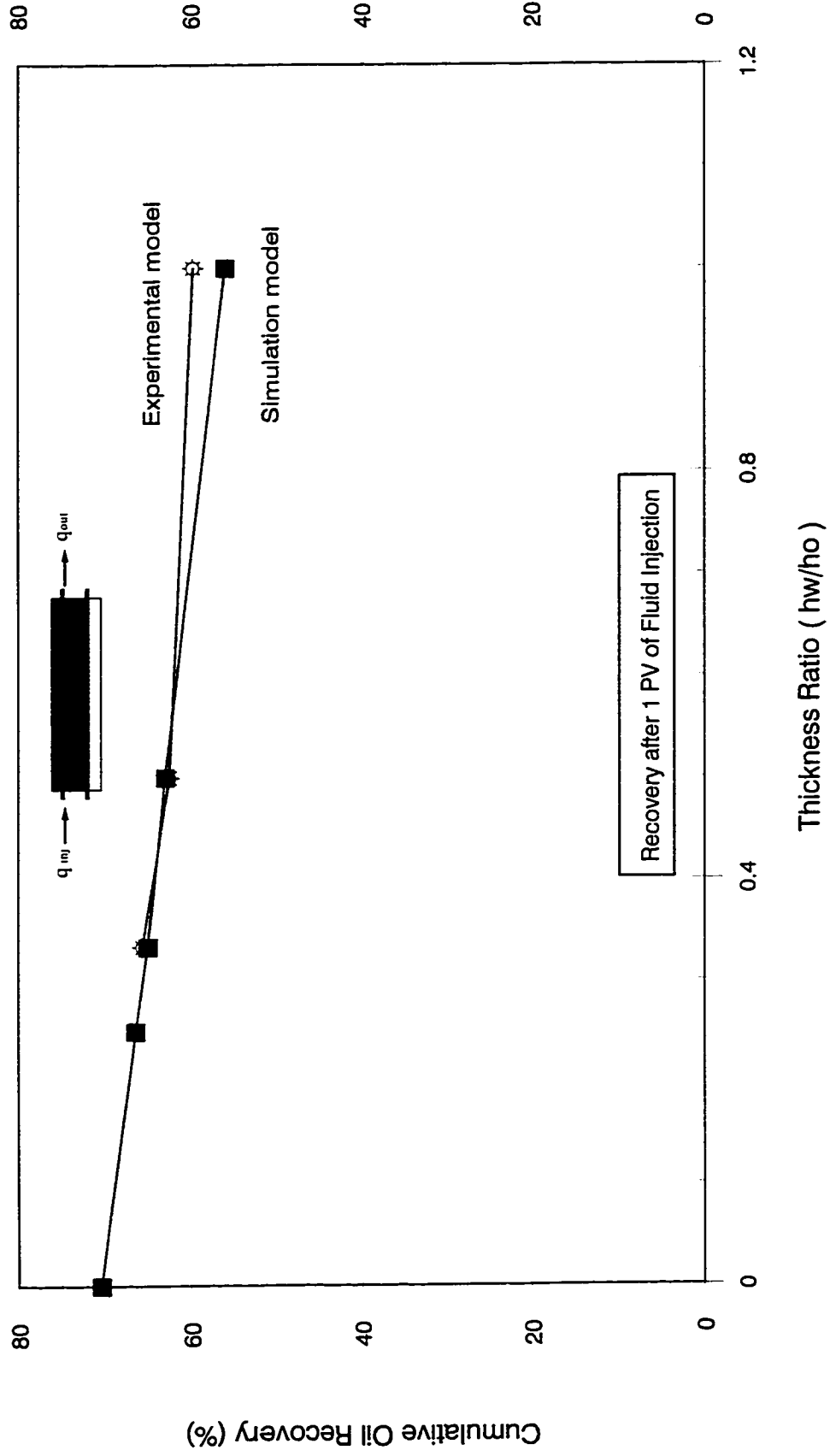


Figure 8-14: Bottom-Water Pack Polymer Flood ( Injection Rate = 450 cc/hr, Oil Vis. = 34.3 mPa.s )



# Effect of Oil Viscosity on Oil Recovery

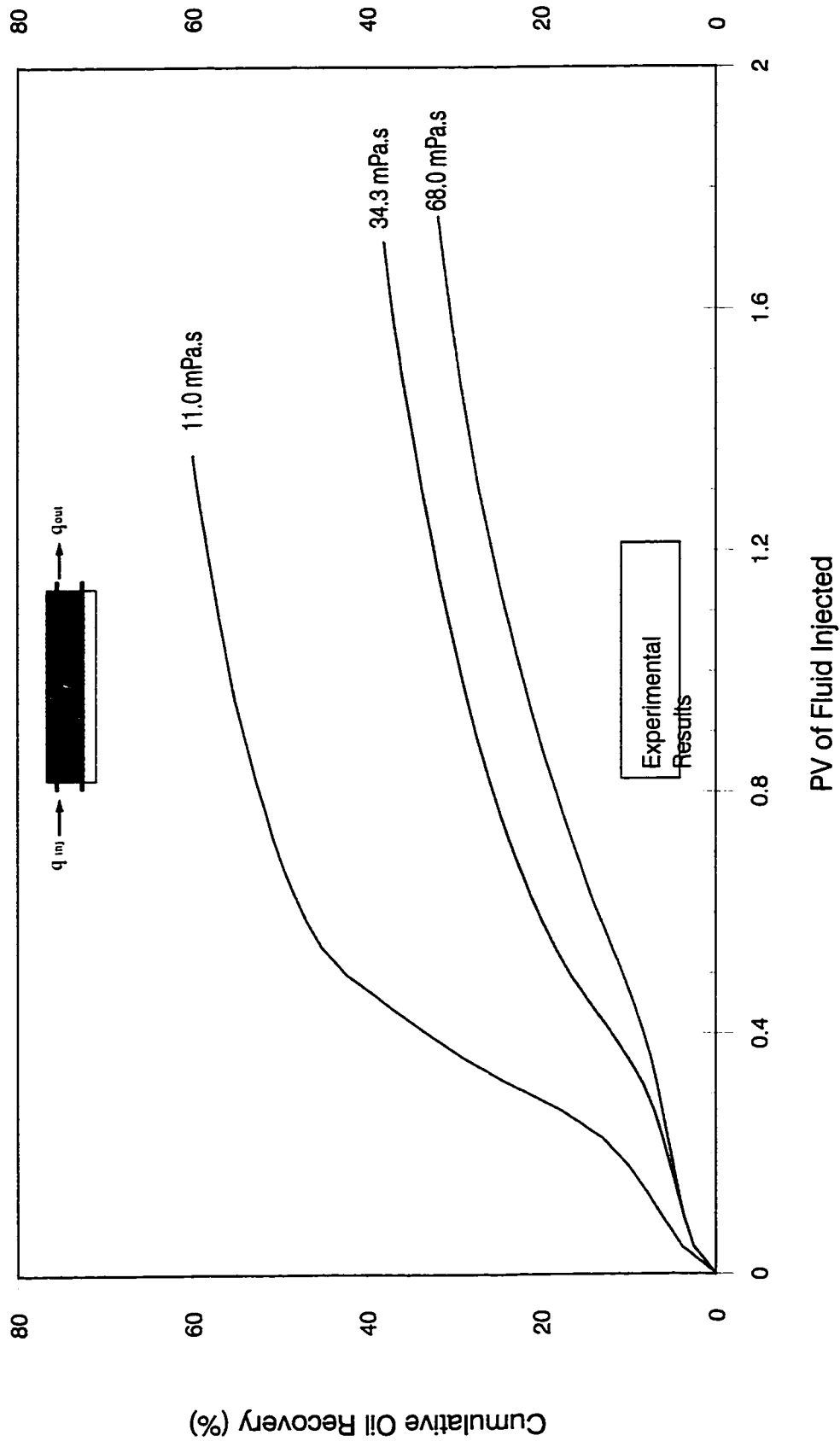


Figure 8-15: Bottom-Water Pack Waterflood ( Injection Rate = 450 cc/hr,  $hw/h_o = 1/3$  )

# Effect of Oil Viscosity on Oil Recovery

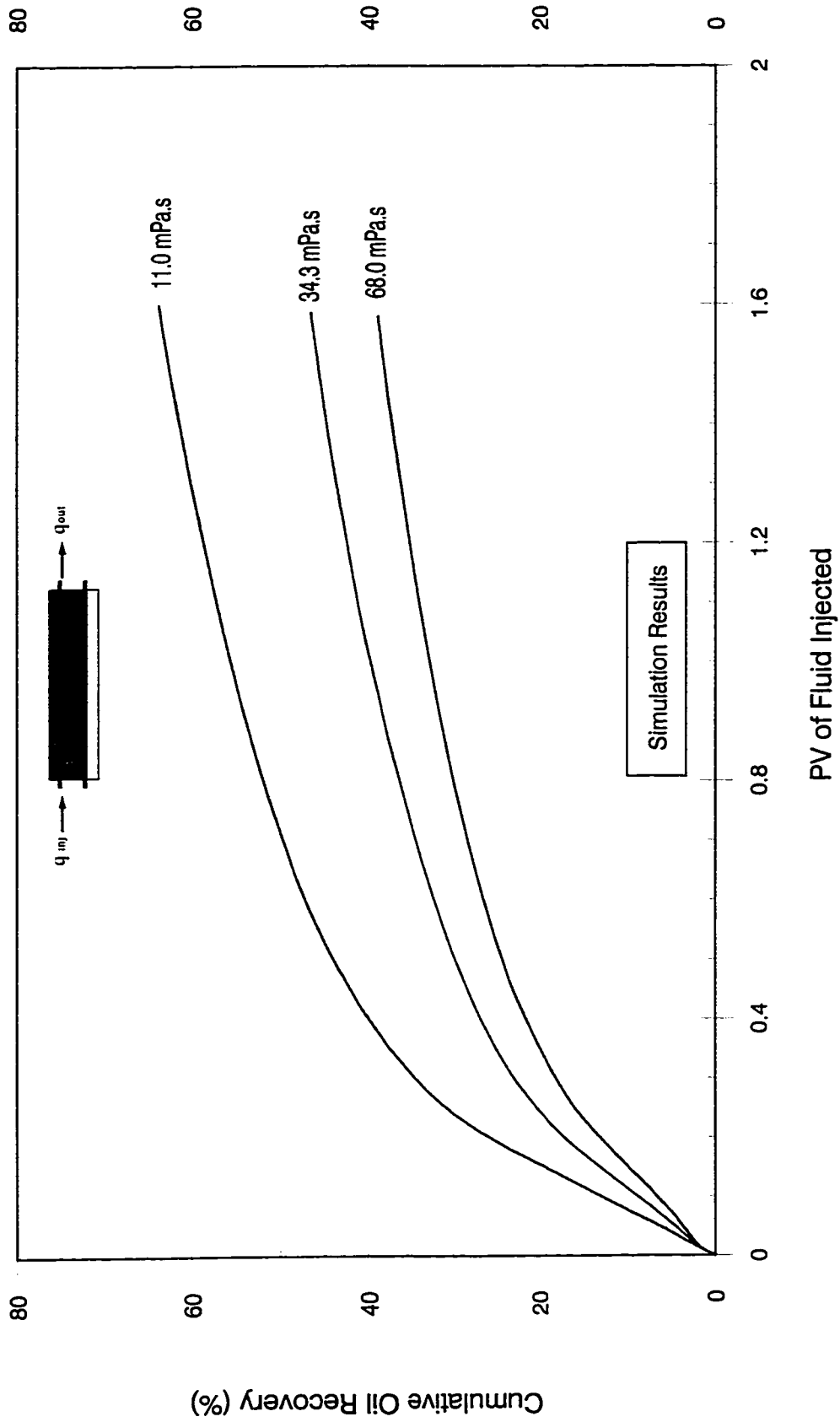


Figure 8-16: Bottom-Water Pack Waterflood ( Injection Rate = 450 cc/hr,  $h_w/h_o = 1/3$  )

# Effect of Oil Viscosity on Oil Recovery

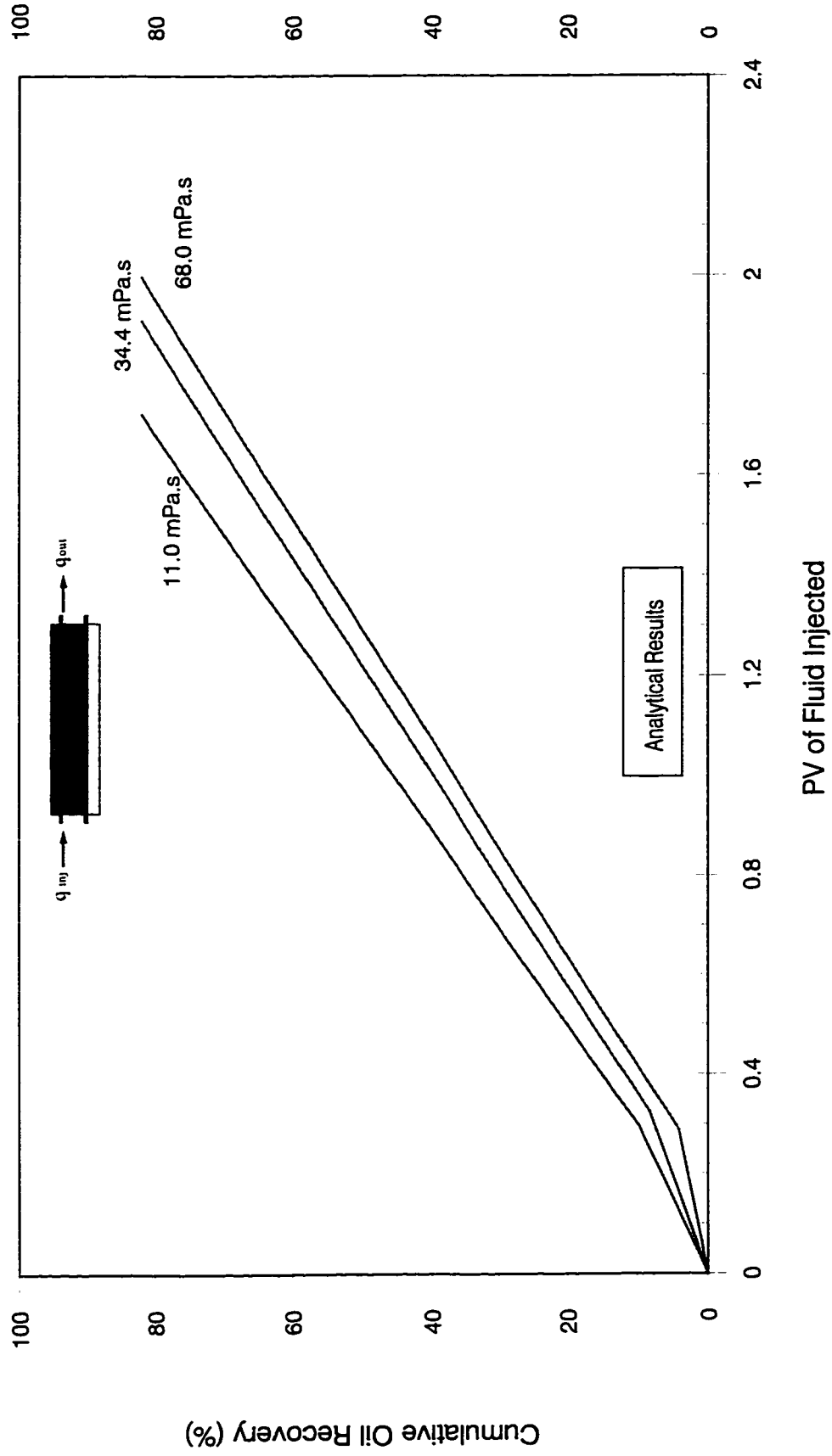


Figure 8-17: Bottom-Water Pack Waterflood ( $q = 450$  cc/hr,  $K1/K2 = 1/1$ ,  $hw/ho = 1/3$ )

# Effect of Oil Viscosity on Oil Recovery

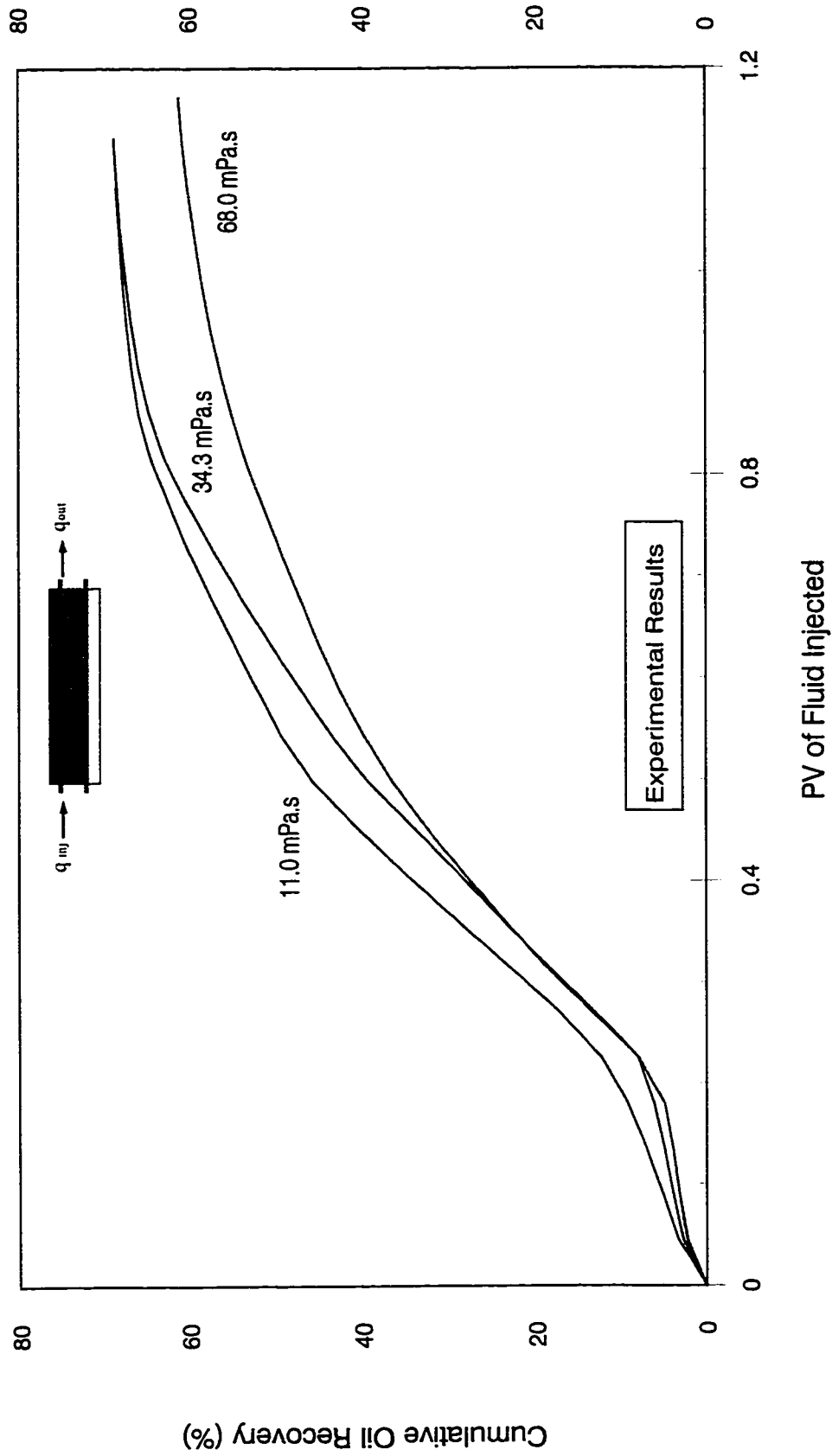


Figure 8-18: Bottom-Water Pack Polymer Flood (  $q = 450$  cc/hr,  $hw/ho = 1/3$ ,  $Con. = 500$  ppm )

# Effect of Oil Viscosity on Oil Recovery

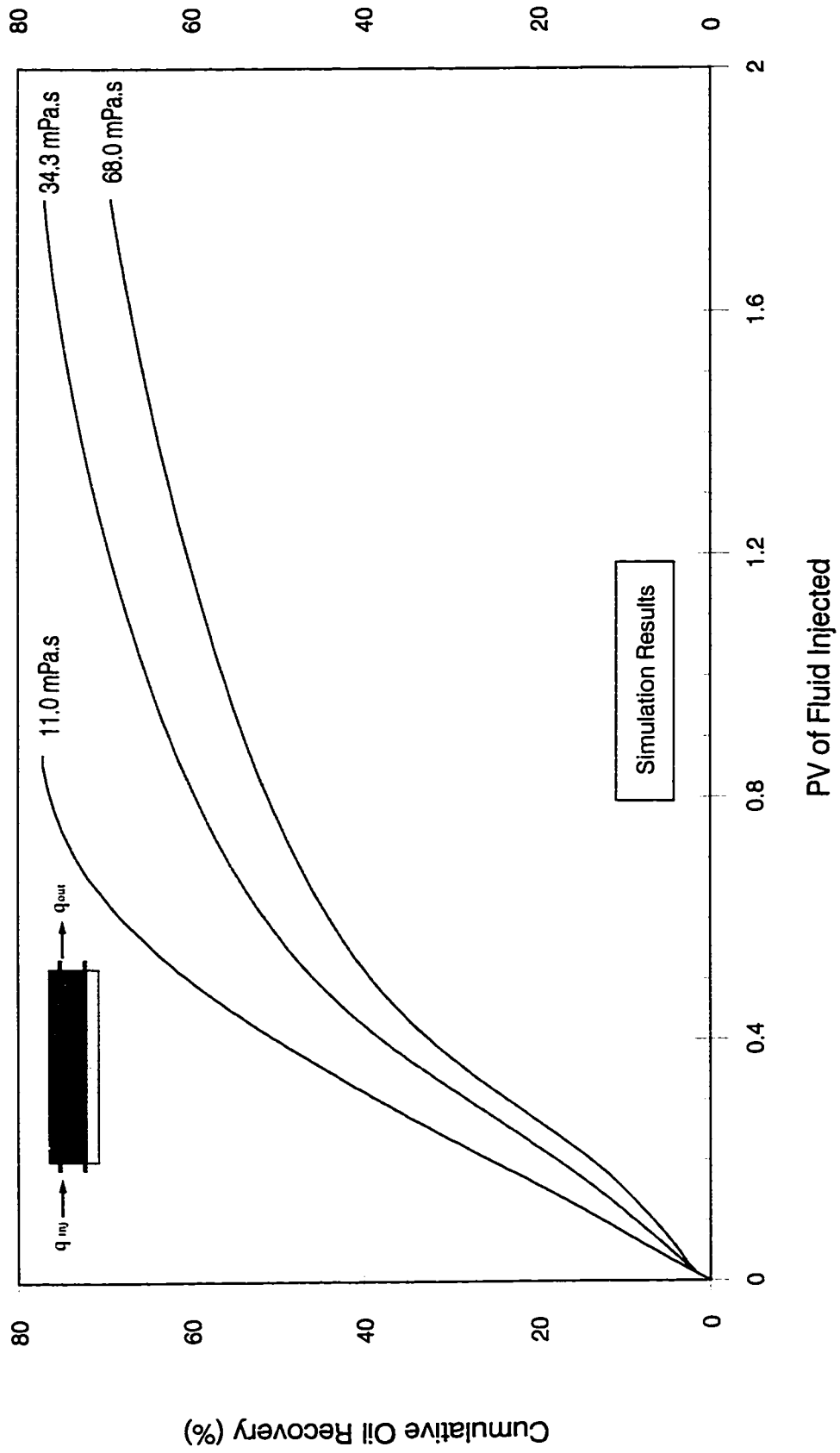


Figure 8-19: Bottom-Water Pack Polymer Flood (  $q = 450$  cc/hr,  $hw/ho = 1/3$ ,  $Con. = 500$  ppm )

# Effect of Oil Viscosity on Oil Recovery

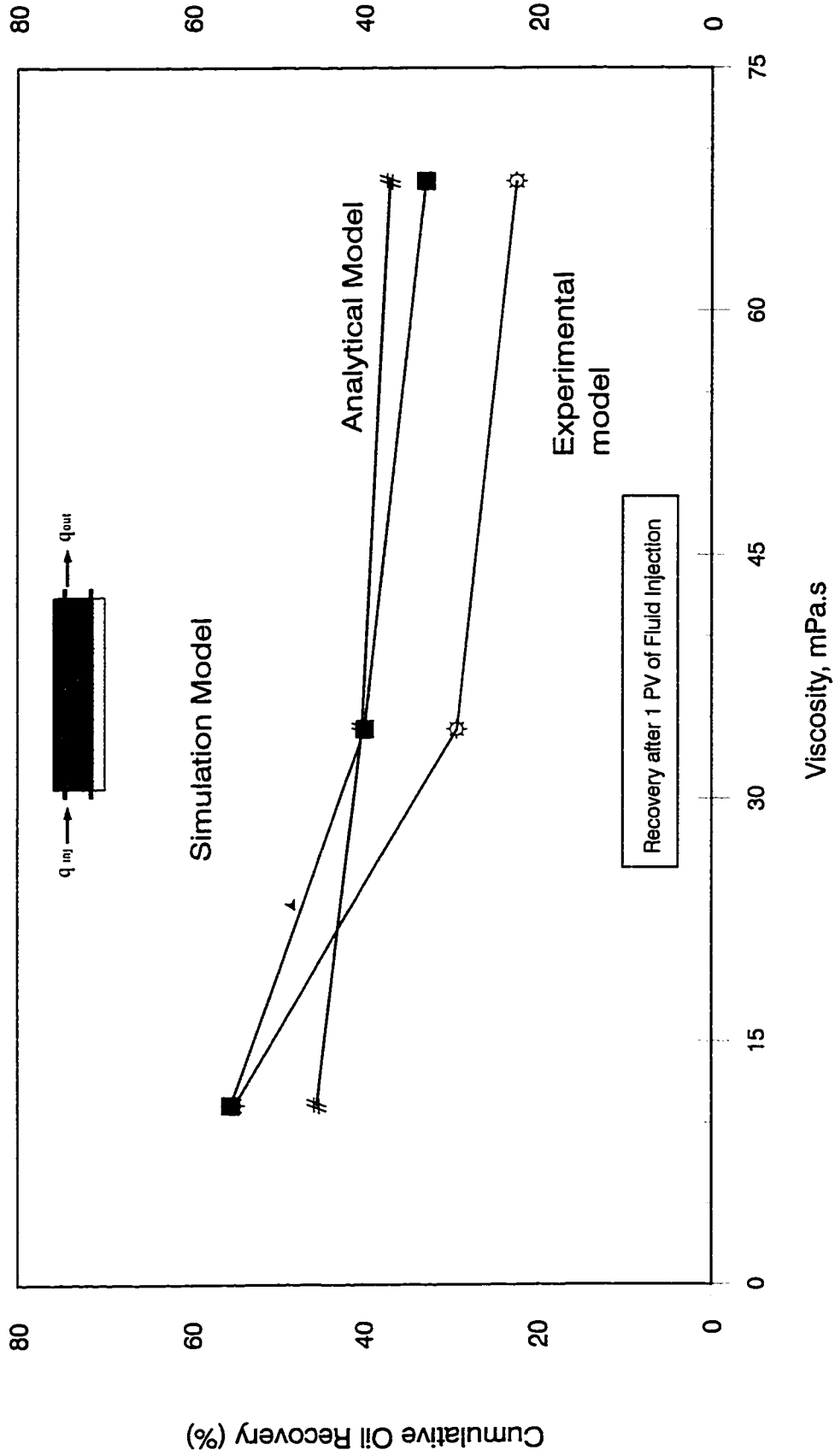


Figure 8-20: Bottom-Water Pack Waterflood ( Injection Rate = 450 cc/hr,  $h_w/h_o = 1/3$  )

# Effect of Oil Viscosity on Oil Recovery

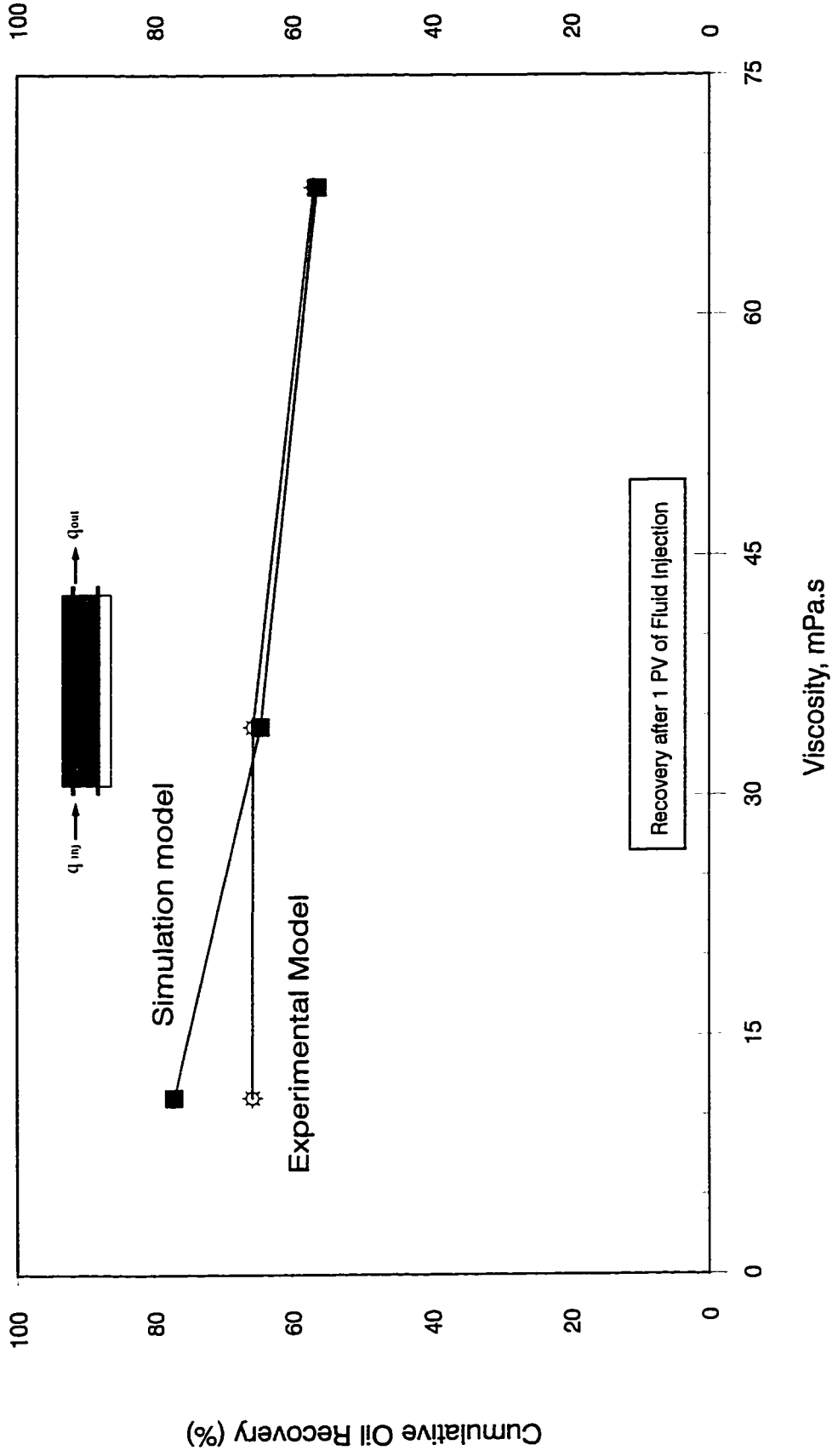


Figure 8-21: Bottom-Water Pack Polymer Flood ( Injection Rate = 450 cc/hr,  $hw/ho = 1/3$  )

# Dependence of Polymer Solution Viscosity on Polymer Concentration

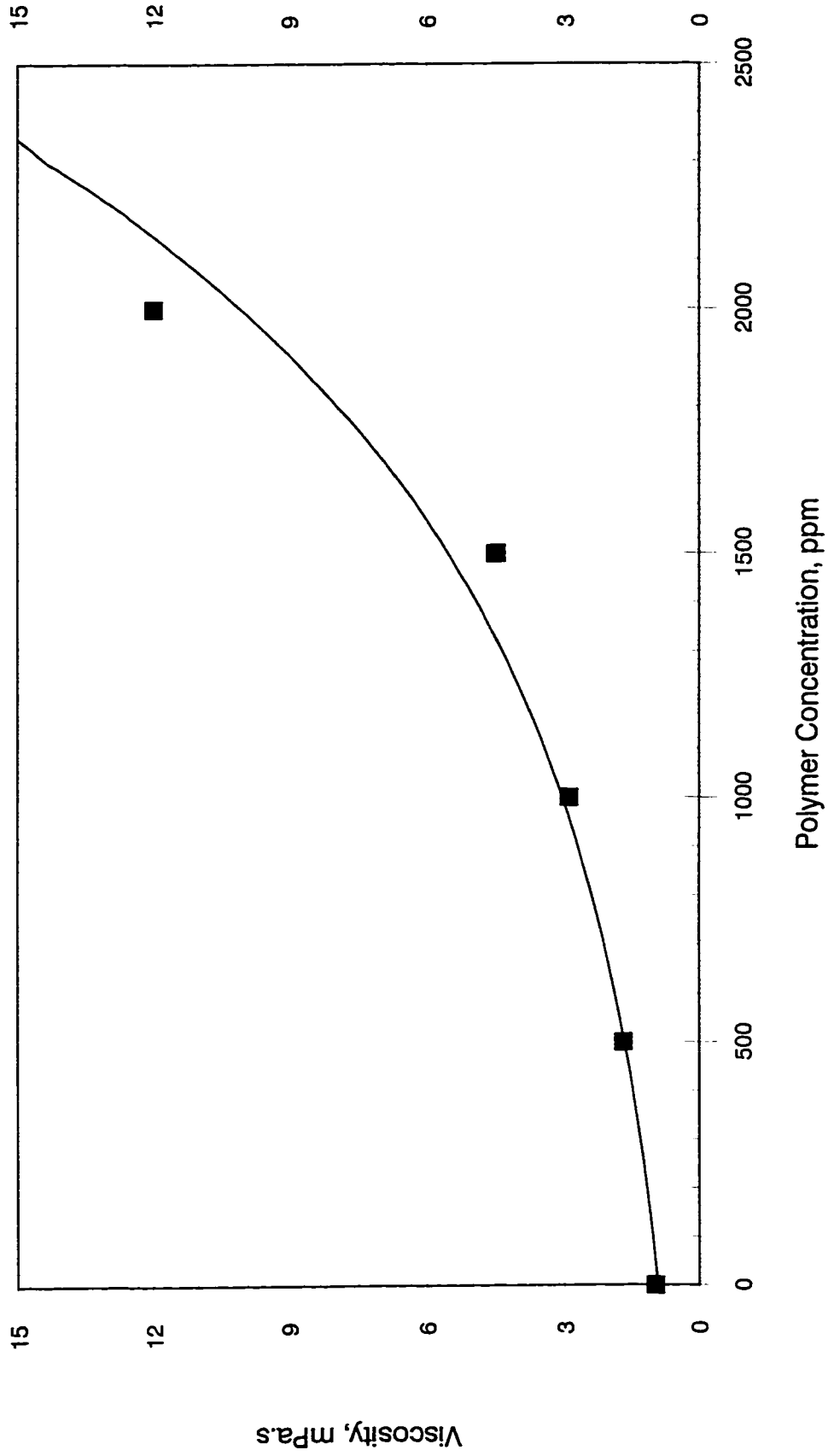


Figure 8-22: Polymer Solution Viscosity at Shear Rate = 10 Sec<sup>-1</sup>



### Effect of Polymer Concentration on Oil Recovery

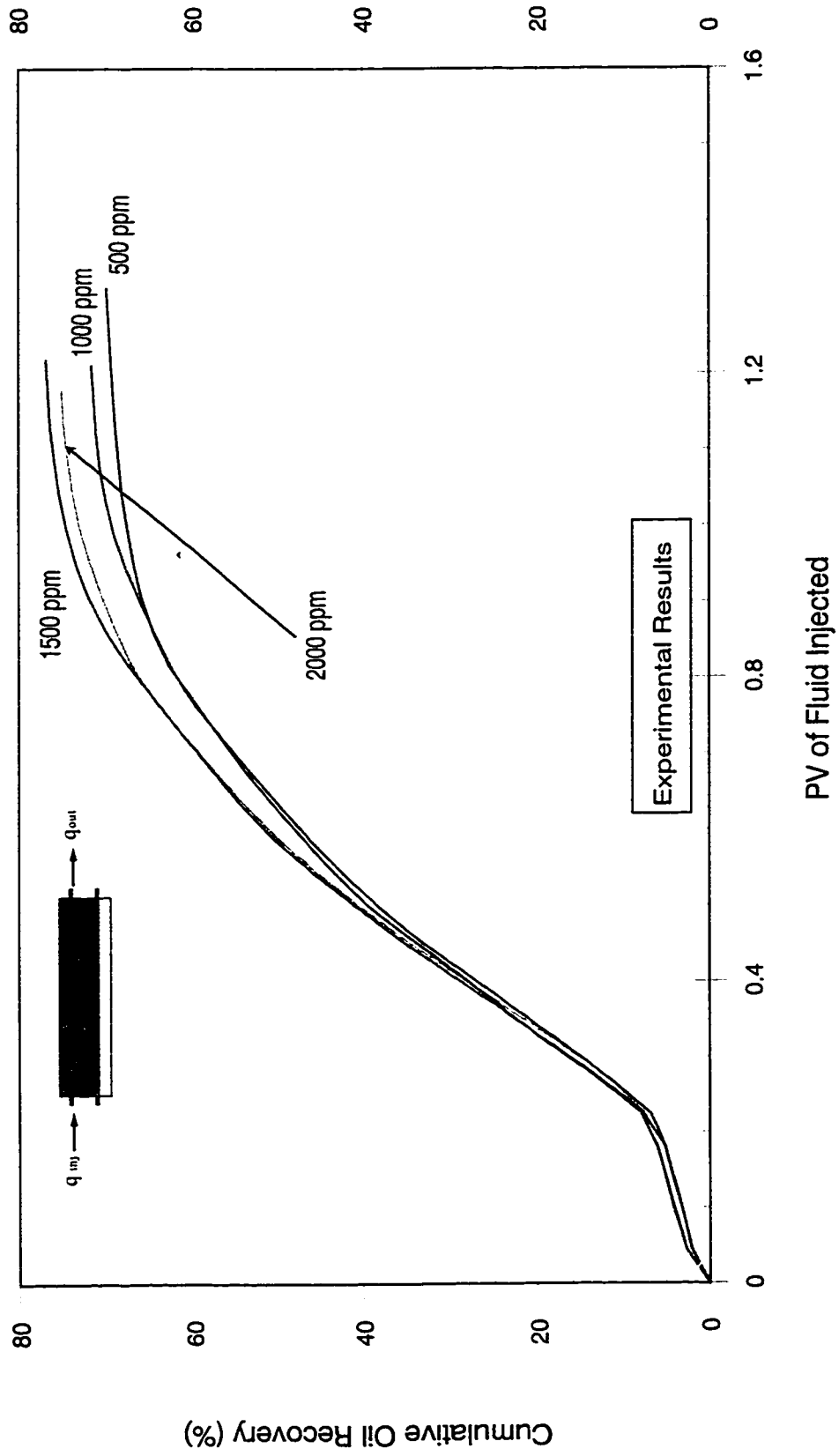


Figure 8-23: Bottom-Water Pack Polymer Flood ( $q = 450$  cc/hr,  $hw/h_o = 1/3$ , Oil Viscosity = 34.3 mPa.s)

## Effect of Polymer Concentration on Oil Recovery

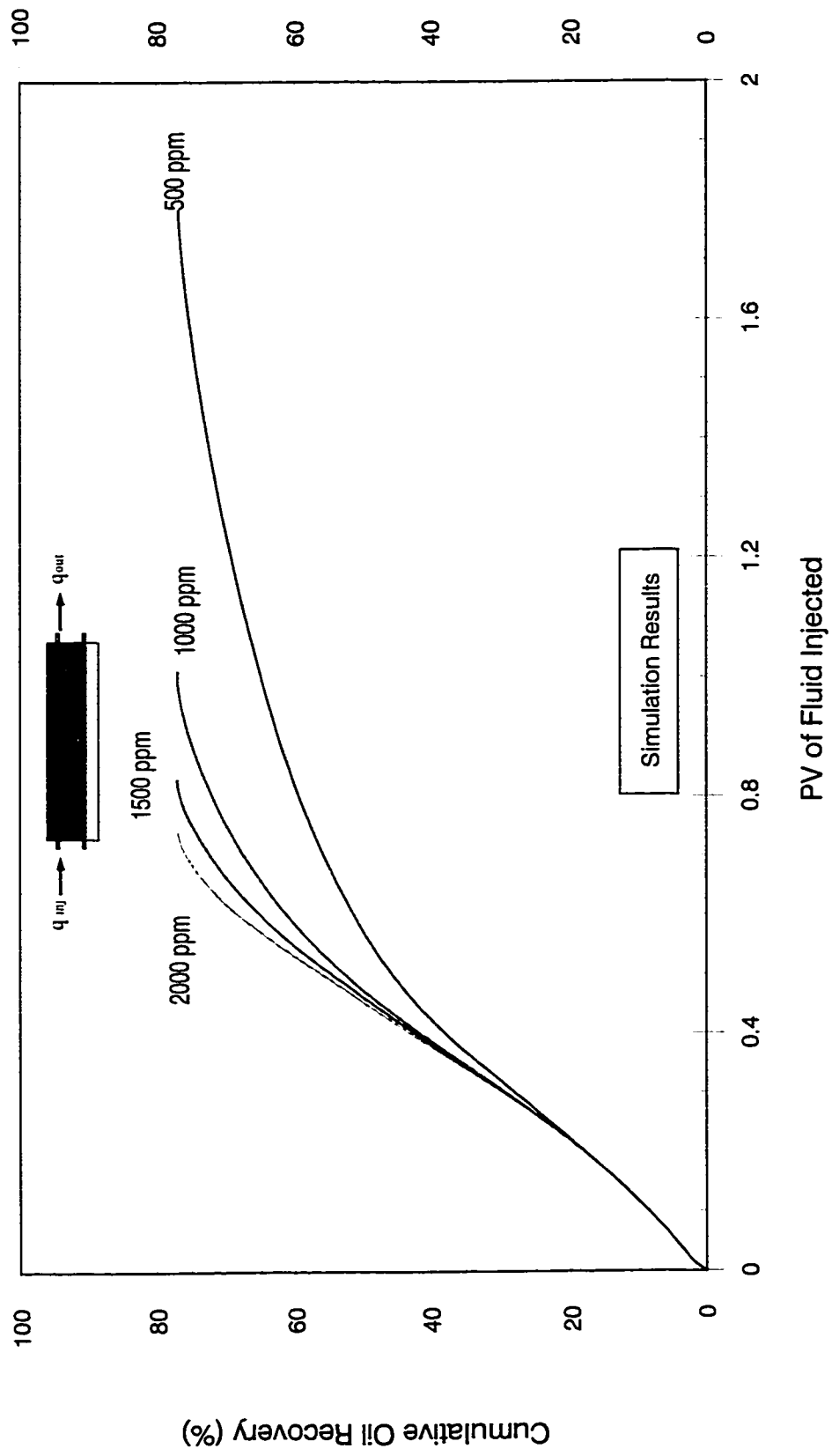


Figure 8-24: Bottom-Water Pack Polymer Flood ( $q = 450$  cc/hr,  $hw/ho = 1/3$ , Oil Viscosity =  $34.3$  mPa.s)

# Effect of Polymer Concentration on Oil Recovery

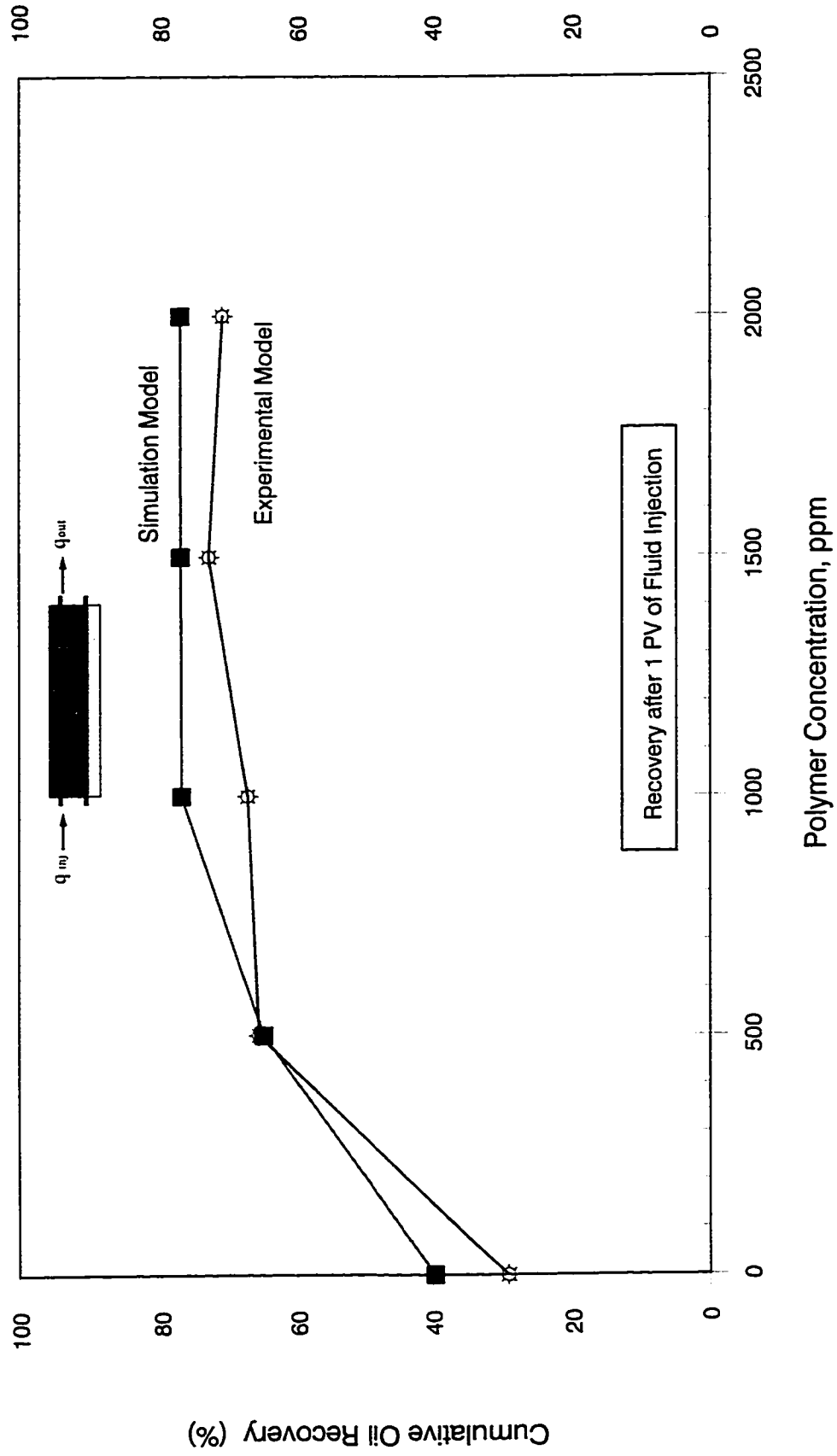


Figure 8-25: Bottom-Water Pack Polymer Flood ( $q = 450$  cc/hr,  $hw/ho = 1/3$ , Oil Vis. =  $34.3$  mPa.s)

### Effect of Barrier on Oil Recovery

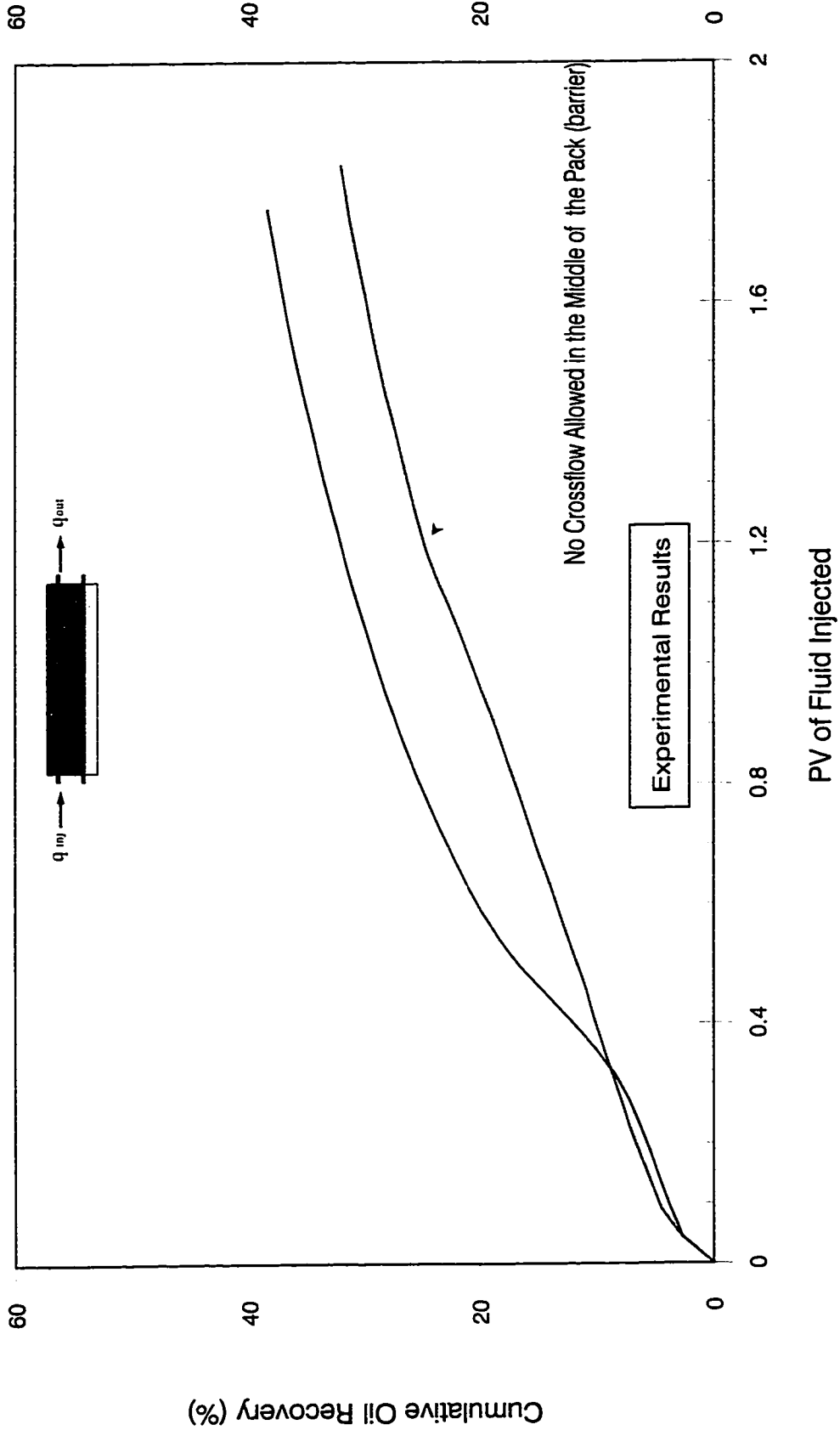


Figure 8-26: Bottom-Water Pack Waterflood (  $q = 450$  cc/hr,  $hw/ho = 1/3$ , Oil Viscosity =  $34.3$  mPa.s )

### Effect of Barrier on Oil Recovery

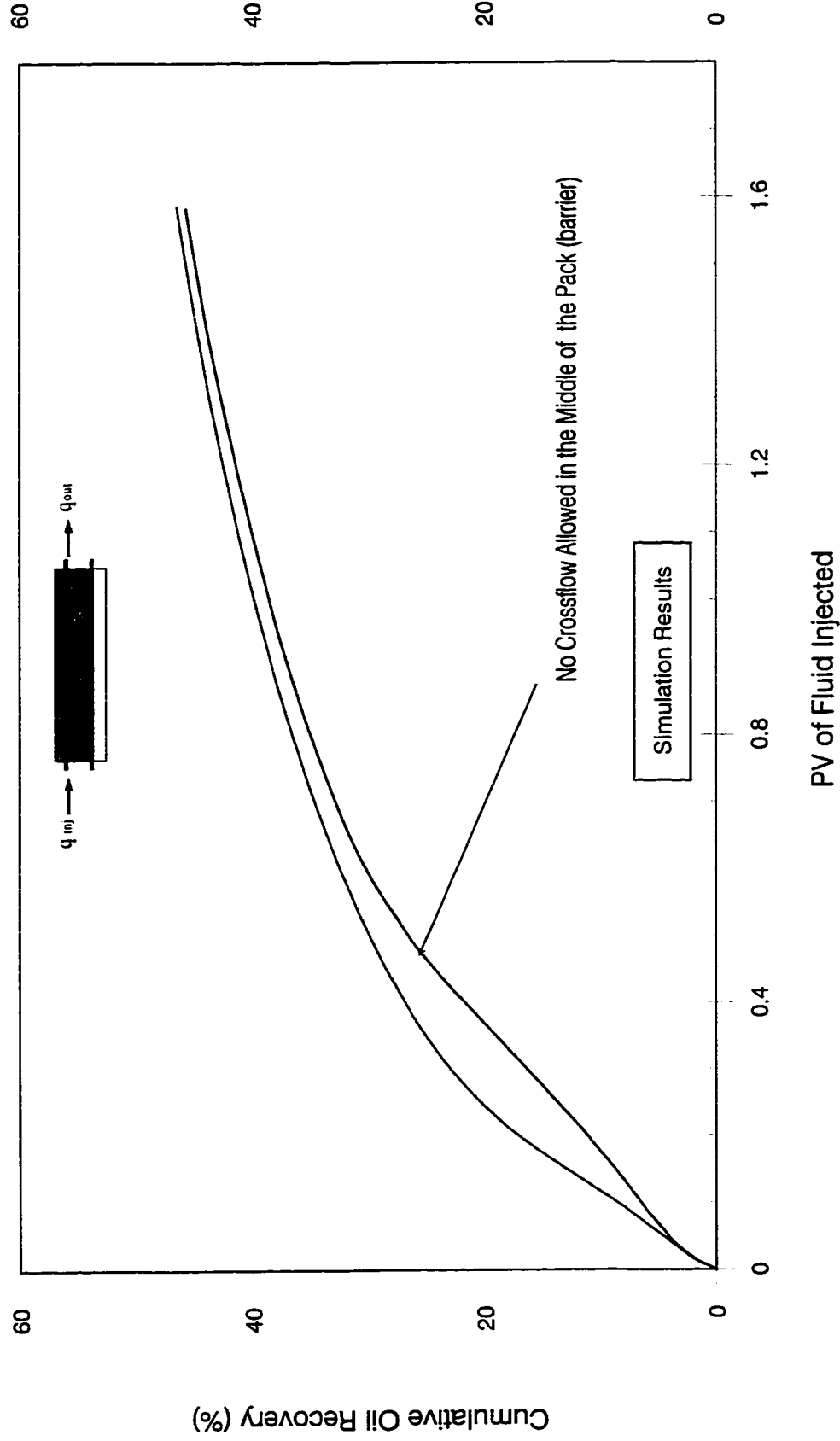


Figure 8-27: Bottom-Water Pack Waterflood ( $q = 450$  cc/hr,  $h_w/h_o = 1/3$ , Oil Viscosity =  $34.3$  mPa.s)

# Effect of Permeability Contrast on Oil Recovery

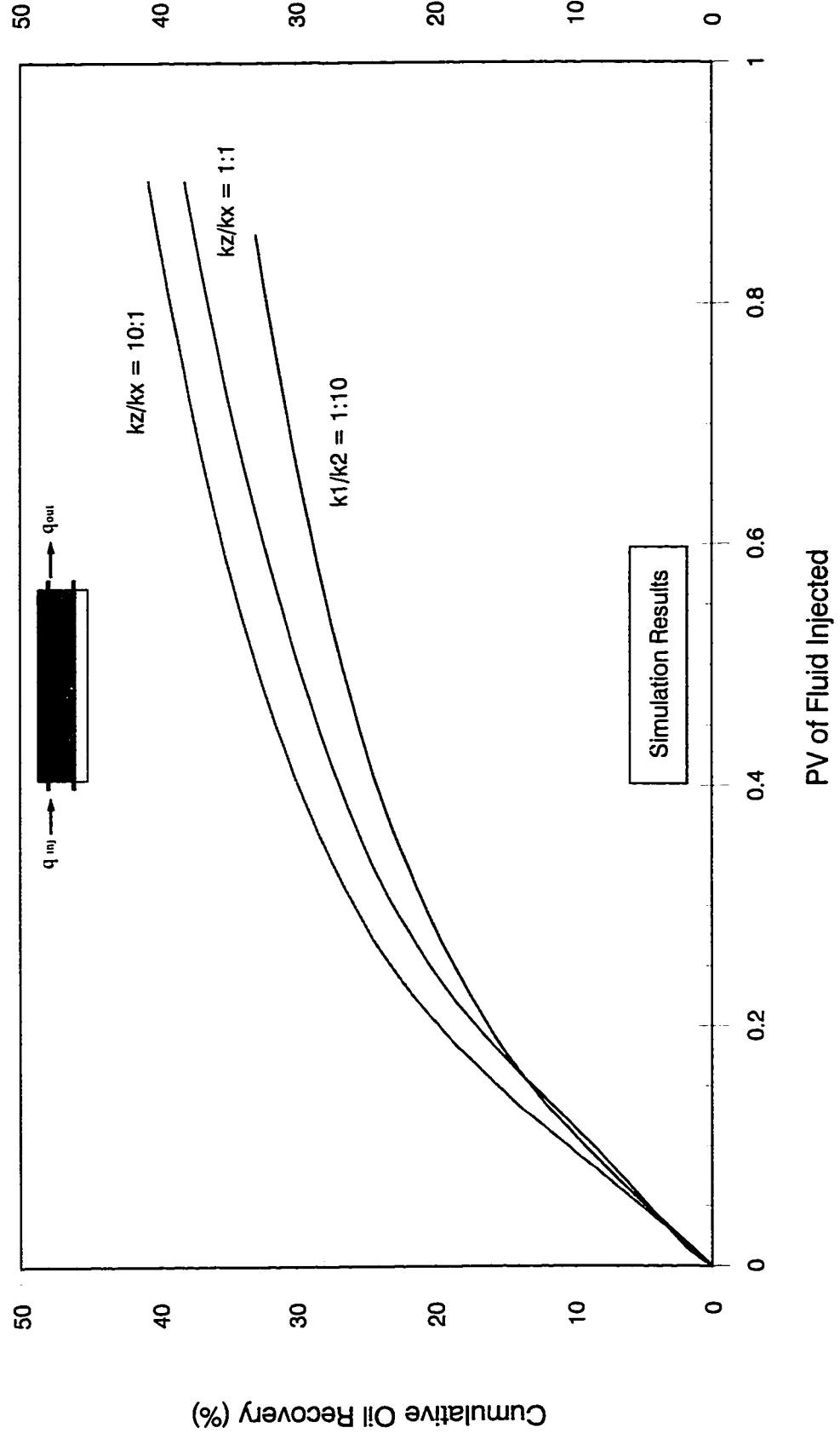


Figure 8-28: Bottom-Water Pack Waterflood (  $q = 450$  cc/hr,  $hw/h_o = 1/3$ , Oil Viscosity =  $34.3$  mPa.s )

# Effect of Permeability Contrast on Oil Recovery

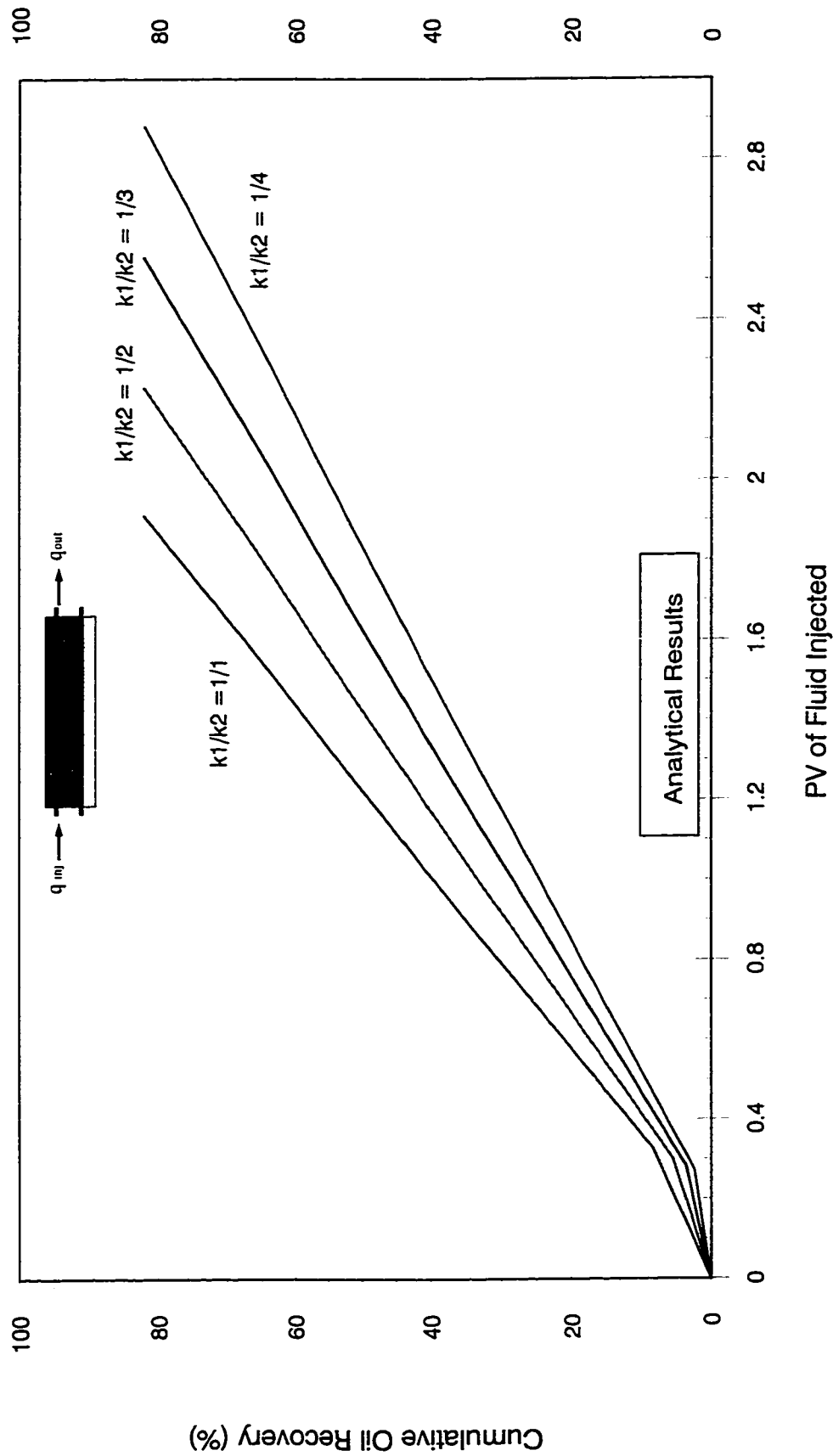


Figure 8-29: Bottom-Water Pack Waterflood ( $h_w/h_o = 1/3$ , Oil Viscosity = 34.3 mPa.s)

## Effect of Injection Strategy on Oil Recovery

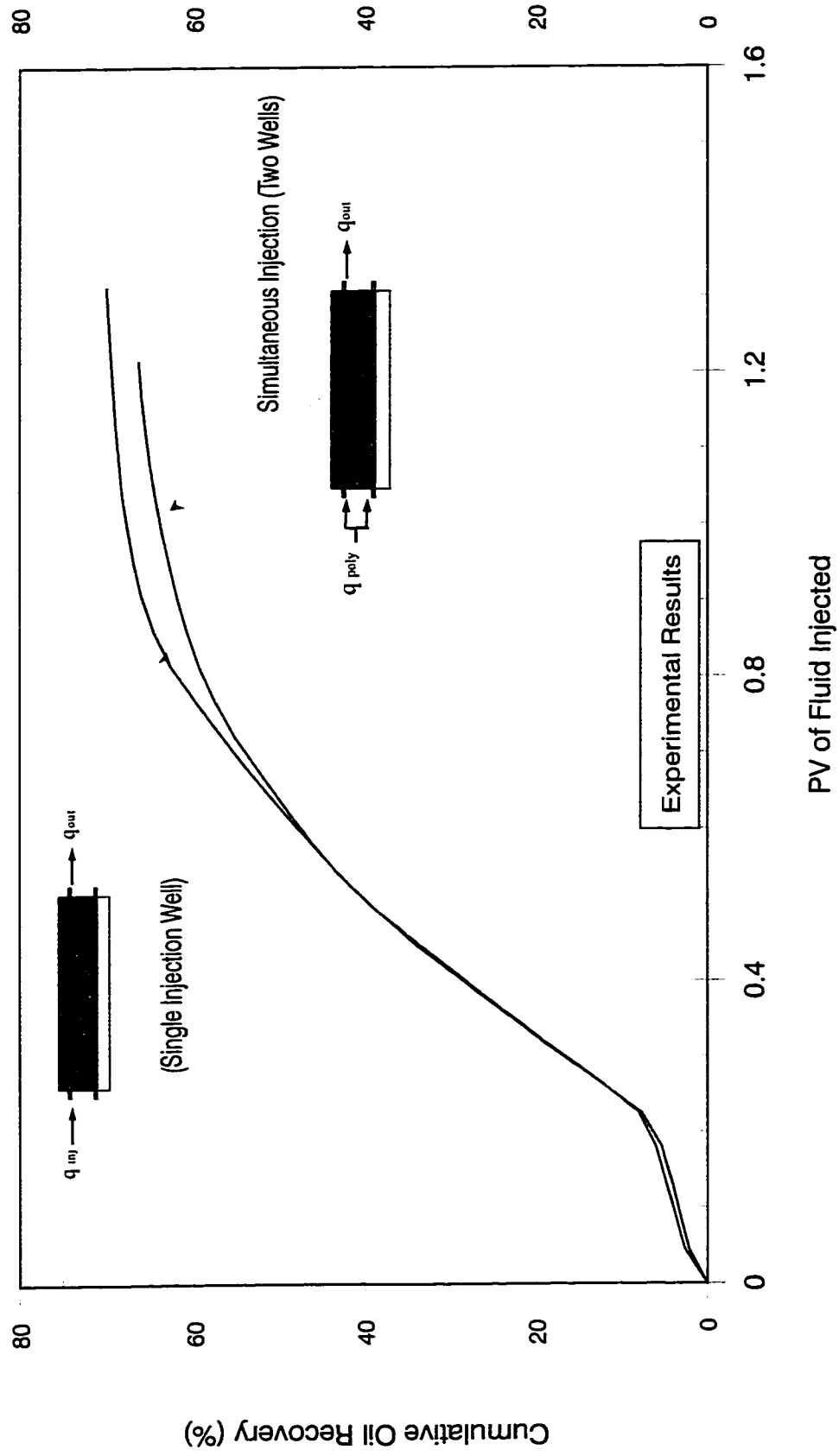


Figure 8-30: Bottom-Water Pack Polymer Flood ( $q = 450$  cc/hr, Con. = 500 ppm,  $hw/ho = 1/3$ , Oil Vis. = 34.3 mPa.s)



### Comparison of Oil Recovery for Horizontal and Vertical Wells

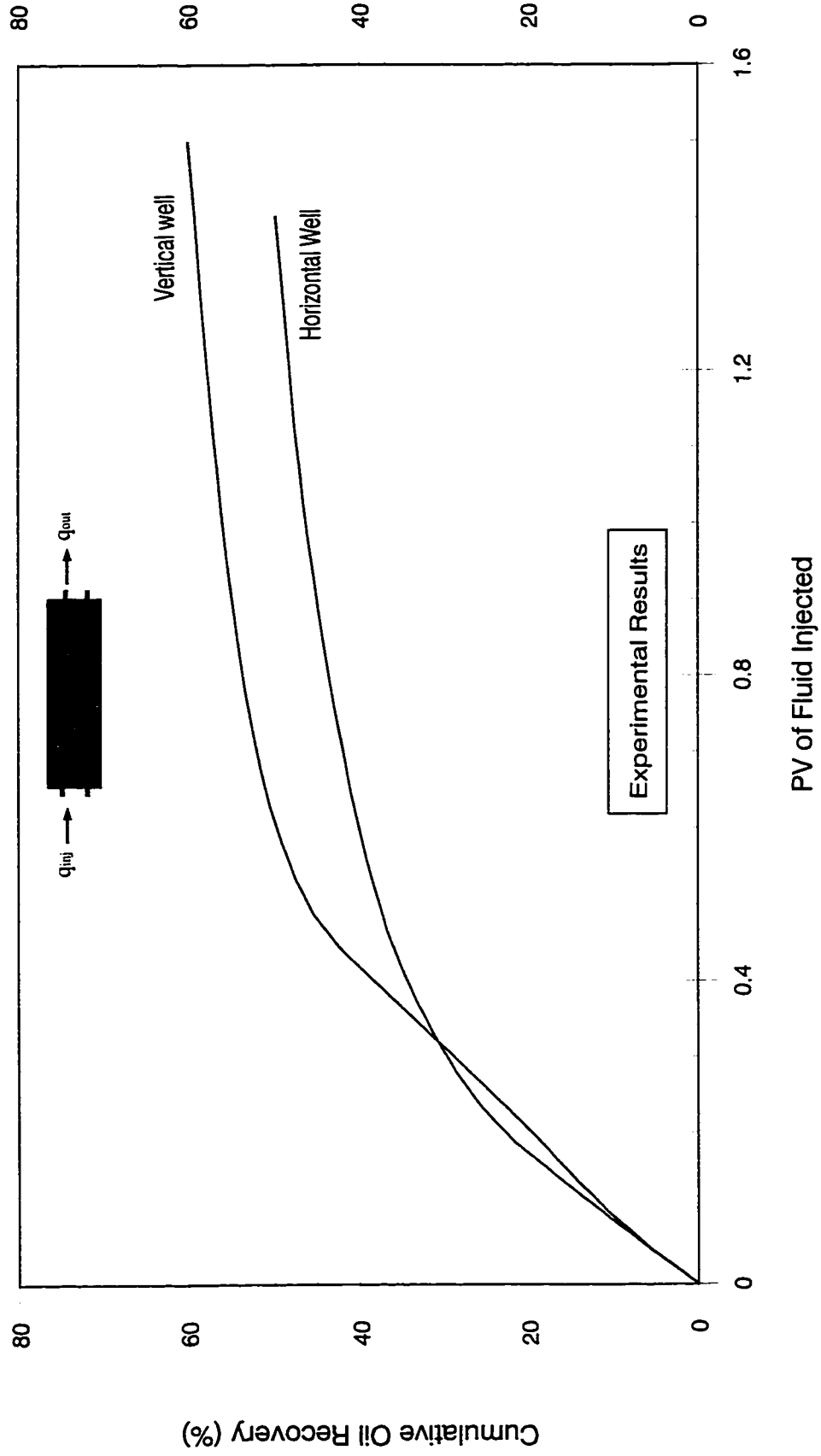


Figure 8-31: Homogeneous Pack Waterflood ( Injection Rate = 450 cc/hr,  $hw/ho = 1/3$ , Oil Viscosity = 34.3 mPa.s )

### Comparison of Oil Recovery for Horizontal and Vertical Wells

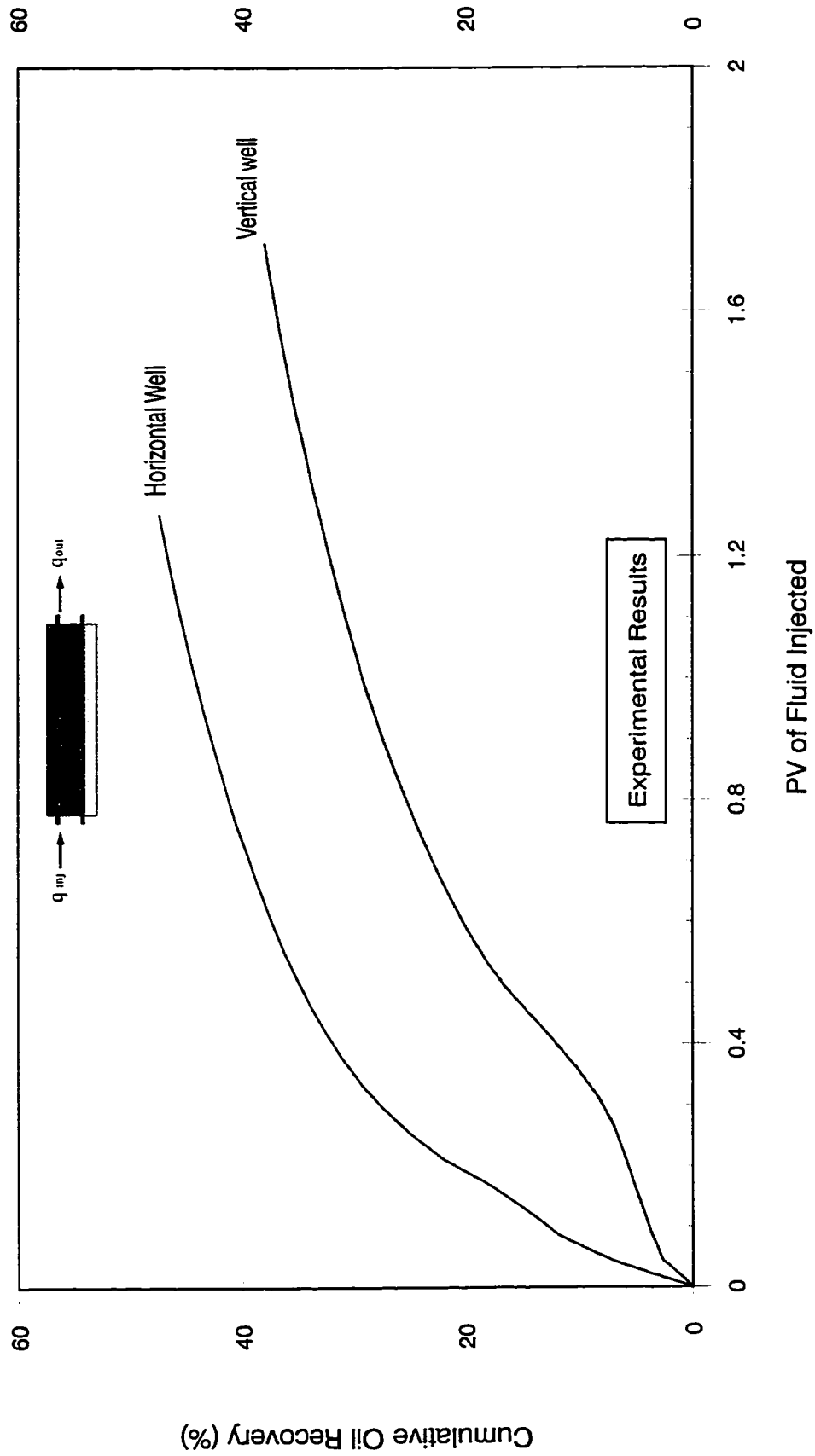


Figure 8-32: Bottom-Water Pack Waterflood ( Injection Rate = 450 cc/hr,  $h_w/h_o = 1/3$ , Oil Viscosity = 34.3 mPa.s)

### Effect of Horizontal/Vertical Wells Combination on Recovery

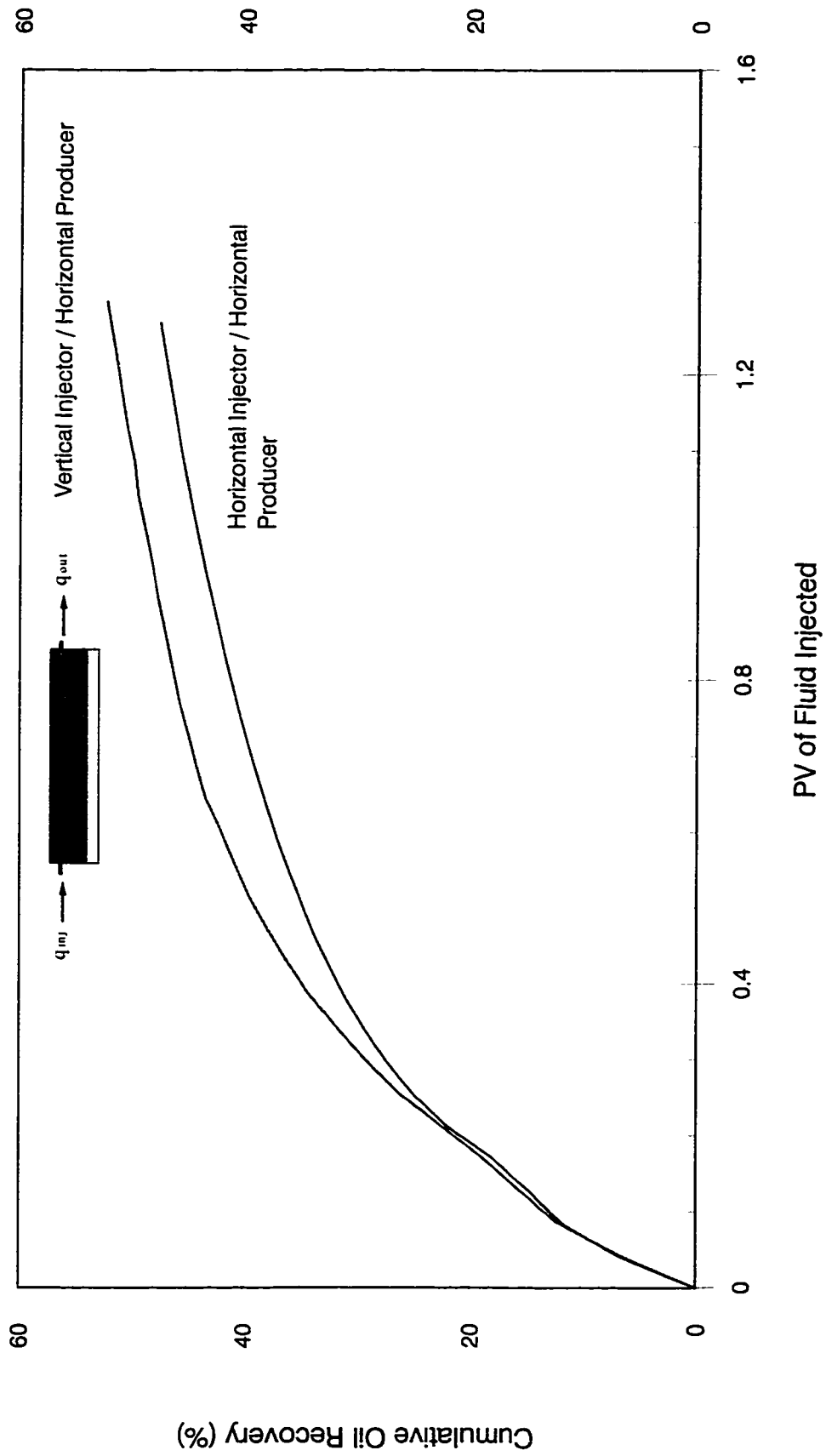


Figure 8-33: Bottom-Water Pack Waterflood (  $q = 450$  cc/hr,  $h_o/h_w = 3:1$ , Oil Vis. =  $34.3$  mPa.s )

## Chapter 9

### CONCLUSIONS AND RECOMMENDATIONS

This research examined waterflooding when a communicating water zone is present below the oil zone. Experimental runs were carried out for this purpose. Also a simple mathematical model describing two-phase flow of incompressible fluid in reservoirs under bottom-water conditions was presented. The mathematical model includes the influence of crossflow, together with the prediction of oil recovery as a function of fluid injection. Finally a three-dimensional, multiphase water/polymer flooding simulator was developed for this research. The effects of different variables and injection strategies for water and polymer floods the physical model, analytical model and numerical simulator were studied and compared for appropriate cases.

#### 9.1 Conclusions

Based on the theoretical and experimental results obtained in this study, the following conclusions are reached:

- 1) Oil recovery during a waterflood in a reservoir under bottom-water conditions with vertical communication is sensitive to injection rate, oil viscosity, crossflow, and water-to-oil formation thickness ratio.
- 2) Waterflooding a reservoir with a bottom-water zone shows poor performance, with a decrease in oil recovery as the thickness of the bottom-water zone and the oil viscosity increase, and the injection rate decreases.
- 3) In a two-layer reservoir, crossflow takes place around the flood fronts.
- 4) Oil recovery increases significantly when the mobility ratio is reduced when a bottom-water zone is present.
- 5) The polymer augmented waterflooding runs showed better oil recovery than waterflooding runs using vertical wells; however, the increase in oil recovery, in the presence of a bottom-water zone, was more significant. On the other hand, the worse the conventional waterflood is, the more effective is the polymer augmented

waterflood under bottom-water conditions.

- 6) Conventional waterflooding using horizontal production and vertical injection wells, showed better oil recoveries than vertical production/injection or horizontal production/injection wells cases in the presence of a bottom-water zone. However, in the absence of a bottom-water zone, oil recoveries for waterflooding runs with horizontal wells were lower than vertical wells due to insufficient and incomplete sweep of the reservoir model volume by the injected water.
- 7) Oil recovery during a polymer flood in a reservoir under bottom-water conditions is insensitive to injection rate and injection strategies.
- 8) Oil recovery during a polymer flood is sensitive to polymer solution concentrations. The lower the polymer solution concentration, the lower the oil recovery for both homogeneous and bottom-water conditions cases.
- 9) An analytical model and a numerical simulator were developed for the specific conditions used in the experiments. The predictions based upon both the analytical model and the numerical simulator were in good agreement with the experimental results.

## **9.2 Recommendations**

The following recommendations are made for further research:

1. The physical model should be modified for pattern floods.
2. Pressure transducers should be used along the length of the porous media to monitor the movement of the flood fronts.
3. Features such as the effect of salinity and the application of horizontal wells should be added to the simulator.
4. Gravity and capillary forces should be incorporated in the analytical model.

## REFERENCES

1. Stiles, W. E.: "Use of Permeability Distribution in Waterflood Calculations", *Trans., AIME* (1949) Vol. 186, 9-13.
2. Dykstra, H. and Parsons, H. L.: "The Prediction of Oil Recovery by Waterflooding", *Secondary Recovery of Oil in the United States*, 2nd ed., API, New York (1950), 160-74.
3. Johnson, C. E. Jr.: "Prediction of Oil Recovery by Waterflood - A Simplified Graphical Treatment of the Dykstra-Parsons Method", *Trans., AIME* (1956) Vol. 207, 345-46.
4. Snyder, R. W. and Ramey, H. J., Jr.: "Application of Buckley-Leverett Displacement Theory to Non-communicating Layered System", *J. Pet. Tech.* (November 1967) Vol. 204, 7-15.
5. Buckley, S. E. and Leverett, M. C.: "Mechanism of Fluid Displacement in Sand", *Trans., AIME* (1942) Vol. 146, 107-16.
6. Fayers, F. J. and Sheldon, J. W.: "The Effect of Capillary Pressure and Gravity on Two-Phase Flow in a Porous Medium", *Trans., AIME* (1959) Vol. 216, 147-55.
7. Katz, M. L. and Tek, M. R.: "A Theoretical Study of Pressure Distribution and Fluid Flux in Bounded Stratified Porous Systems with Crossflow", *Soc. Pet. Eng. J.* (March 1962) Vol. 2, 68-82.
8. Russell, D. G. and Prats, M.: "Performance of Layered Reservoirs With Crossflow-Single Compressible Fluid Case", *Soc. Pet. Eng. J.* (March 1962) Vol. 2, 53-68.
9. Pendergrass, J. D. and Berry, V. J.: "Pressure Transient Performance of a Multi-Layered Reservoir with Crossflow", *Soc. Pet. Eng. J.* (1962) Vol. 2, 347-54.
10. Hiatt, W. N.: "Injection-Fluid Coverage of Multi-Well Reservoirs With Permeability Stratification", *Drill. and Prod. Prac.*, API (1958), 165-94.
11. Russell, D. G. and Prats, M.: "The Practical Aspects of Interlayer Crossflow", *Soc. Pet. Eng. J.* (June 1962), 589-94.
12. Warren, J. E. and Cosgrove, J. J.: "Prediction of Waterflood Behavior in a Stratified System", *Soc. Pet. Eng. J.* (June 1964), 149-57.

13. Dietz, D. N.: "A Theoretical Approach to the Problem of Encroaching and by-Passing Edge Water", *Proc., Akad. van Wetenschappen, Amsterdam* (1953) Vol. 56-B 83-91.
14. Hearn, C. L.: "Simulation of Stratified Waterflooding by Pseudo-Relative Permeability Curves", *J. Pet. Tech.* (July 1971), 805-13.
15. Zapata, V. J. and Lake, L. W.: "A Theoretical Analysis of Viscous Crossflow", *SPE 10111, 56th Annual Fall Technical Conference*, San Antonio, Texas (October 1981).
16. Kereluk, M. J. and Crawford, P. B.: "Comparison Between Observed and Calculated Sweeps in oil Displacements from Stratified Reservoirs", paper presented at API Mid-Continent District Meeting, Amarillo, Texas (April 1968), 3-5.
17. Lewis, R. L.: "Vertical Permeability and Interstrata Flow", *J. Pet. Tech.* (August 1979), 1015-25.
18. Gaucher, D. H. and Lindley, D. C.: "Waterflood Performance in a Stratified, Five-Spot Reservoir - A Scaled-Model Study", *Trans., AIME* (1960) Vol. 219, 208-15.
19. Wright, R. J., Dawe, R. A. and Wall, C. G.: "Surfactant Slug Displacement Efficiency in Reservoirs Tracer Studies in 2-D Layered Models", *Proc.* (1981) European Symp. on EOR, Bournemouth, UK, 161-78.
20. Lambeth, N. and Dawe, R. A.: "Viscous Effects for Miscible Displacements in Regular Heterogeneous Porous Media", *Chem. Eng. Res. Des.* (January 1987), 52-62.
21. Wright, R. J., Wheat, M. R. and Dawe, R. A.: "Slug Size and Mobility Requirements for Chemically Enhanced Oil Recovery Within Heterogeneous Reservoirs", *Soc. Pet. Eng. J.* (February 1987), 92-102.
22. Ahmed, G., Castanier, L. M. and Brigham, W. E.: "An Experimental Study of Waterflooding From a Two-dimensional Layered Sand Model", *Soc. Pet. Eng. J.* (February 1988), 45-54.
23. Root, P. J. and Skiba, F. F.: "Cross-flow Effects During an Idealized Displacement Process in a Stratified Reservoir", *Soc. Pet. Eng. J.* (September. 1965), 229-38.
24. Goddin, C. S., Jr., Craig, F. F., Jr., Wilkes, J. O. and Tek, M. R.: "A Numerical Study of Waterflood Performance In a Stratified System With Cross-flow", *J. Pet. Tech.* (June 1966), 765-71.

25. Barnes, A. L.: "The Use of a Viscous Slug to Improve Waterflood Efficiency in a Reservoir Partially Invaded by Bottom Water", *J. Pet. Tech.* (October 1962), 1147-53.
26. Silva, Luis and Farouq Ali, S. M.: "Waterflood Performance in the Presence of Communicating Strata and Formation Plugging", *The Libyan Journal of Science* (1973) Vol. 3, 41-63.
27. El-Khatib, N.: "The Effect of Cross-flow on Waterflooding of Stratified Reservoirs", *Soc. Pet. Eng. J.* (April 1985), 291-302.
28. Pye, D. J.: "Improved Secondary Recovery by Control of Water Mobility", *J. Pet. Tech.* (August. 1964), 911-16.
29. Zaidel, Y. M.: "Polymer Flooding of Oil Formations With Bottom-water", *Izv. Akad. Nauk SSSR, Mekh. Zhidk. Gaza* (May-June 1986) No. 3, 84-90.
30. Islam, M. R.: "Mobility Control in Reservoirs With Bottom-Water", Ph.D. Dissertation, University of Alberta, Edmonton (1987).
31. Islam, M. R. and Farouq Ali, S. M.: "Mobility Control in Waterflooding Oil Reservoirs With a Bottom-Water Zone", *J. Can. Pet. Tech.* (Nov.-Dec. 1987), 40-53.
32. Farouq Ali, S. M., Islam, M. R., Kaleli, M. K., Yeung, K. and Thomas, S.: " Mobility Control", AOSTRA Contract 438C, Final Report (1988).
33. Islam, M. R. and Farouq Ali, S. M.: "Waterflooding Oil Reservoirs With Bottom-Water", *CIM 87-38-26, 38th Annual Technical Meeting*, Calgary (1987).
34. Islam, M. R. and Farouq Ali, S.M., "An Experimental and Numerical Study of Blocking of a Mobile Water Zone by an Emulsion," *Paper 133 presented at the Fourth UNITAR/UNDP Conference on Heavy Crude and Tar Sands* (1987).
35. Islam, M. R. and Farouq Ali, S.M., "The Use of Oil/Water Emulsion as a Blocking and Diverting Agent," Paper 5 Session 1, *presented at the Advances in Petroleum Recovery and Upgrading Technology Conference* (1987).
36. Yeung, K. and Farouq Ali, S. M.: "How to Waterflood Reservoirs with a Water Leg", *CIM 93-27, presented at the CIM Tech. Conf.*, Calgary, Alberta (May 9-12, 1993).
37. Yeung, K. and Farouq Ali, S. M.: "Waterflooding Bottom-water Formations Using the Dynamic Blocking Method", *Petroleum Society of CIM/AOSTRA Technical Conference*, Banff, Alberta (April 21-24, 1991).



38. Yeung, K.: "Mobility Control Under Bottom-Water Conditions", M. Sc. Thesis, University of Alberta, Edmonton, Alberta (1991).
39. Hassan, J. A.: "Mobility Control: Theory and Experimental Verification", M.Sc. Thesis, University of Alberta, Edmonton, Alberta (1994).
40. Lake, L. W. and Hirasaki, G. J.: "Taylor's Dispersion in Stratified Porous Media", *SPE 8436 Paper presented at the SPE Fall Meeting, Las Vegas, Nevada* (August 1981).
41. Yokoyama, Y. and Lake, L. W.: "The Effects of Capillary Pressure on Immiscible Displacements in Stratified Permeable Media", *SPE 10109, Paper presented at the SPE Fall Meeting, San Antonio, Texas* (1981).
42. Coats, K. H., Dempsey, J. R. and Henderson, J. H.: "The Use of Vertical Equilibrium in Two Dimensional Simulation of Three Dimensional Reservoir Performance", *Soc. Pet. Eng. J.* (March 1971) Vol. 11, 63-71.
43. Jacks, H. H., Smith, O. J. E. and Matlax, C. G.: "The Modeling of a Three-Dimensional Simulator - The Use of Dynamic Pseudo Functions", *Soc. Pet. Eng. J.* (June 1973) Vol. 13, 175-86.
44. Pope, G. A.: "The Application of Fractional Flow Theory to Enhanced Oil Recovery", *Soc. Pet. Eng. J.* (June 1980), 191-205.
45. Robertson, J. O., Jr., and Oelefein, F. H.: "Plugging Thief Zone in Water Injection Wells", *J. Pet. Tech.* (August 1967), 999-1004.
46. Sandiford, B. B.: "Laboratory and Field Studies of Waterfloods Using Polymer Solutions to Increase Oil Recoveries", *J. Pet. Tech.* (August 1964), 917-22.
47. Mungan, N., Smith, F. W. and Thompson, J. L.: "Some Aspects of Polymer Floods", *J. Pet. Tech.* (September 1966), 1143-50.
48. Fanchi, J. R., Harpole, K. J., Bujnowski, S. W. and Carrol, H. B., Jr.: "BOAST - A Three-Dimensional, Three-Phase Black Oil Applied Simulator Tool", Vol. I: Technical Description and Fortran Code, U.S. Dept. of Energy Report DOE/BC/10033-3, v. 1. (September 1982).
49. Fanchi, J. R., Harpole, K. J., Bujnowski, S. W. and Carrol, H. B., Jr.: "BOAST: A Three-Dimensional, Three-Phase Black Oil Applied Simulator Tool", Vol. II:

- Program User's Manual, U.S. Dept. of Energy Report No. DOE/BC/10033-3, v. 2. (September 1982).
50. Fanchi, J. R., Kennedy, J. E. and Dauben, D. L.: "BOAST II - A Three-Dimensional, Three-Phase Black Oil Applied Simulator Tool", (Releas 1.0), U.S. Dept. of Energy Report No. DOE/BC/88/2/SP (December 1987).
  51. Mungan, N.: "Rheology and Adsorption of Aqueous Polymer Solutions," *J. Can. Pet. Tech.* (1969) Vol. 8, 45-53.
  52. Meter, D. M. and Bird, R. B.: "Tube Flow of Non-Newtonian Polymer Solutions", Part I Laminar Flow and Rheological Models, *AIChE J.* (November 1964) Vol. 10, No. 6, 878-884.
  53. Gau, H. W., Lorenz, P. B. and Brock, S.: "Viscoelastic Behavior of Hydrolyzed Polyacrylamide Solutions in Porous Media", *Poly. Mater. Sci. Engr., Proc.* of the ACS Div. of Polymeric Materials: Sci. and Engr., Fall Mtg., Anaheim (1986) Vol. 55, 685-93.
  54. Camilleri, D.: "Micellar/Polymer Flooding Experiments and Comparisons with an Improved 1-D Simulator", M.Sc. Thesis, University of Texas-Austin (May 1983).
  55. Datta, G. A.: "Three-Dimensional Simulator of Chemical Flooding", M.Sc. Thesis, University of Texas-Austin (May 1985).
  56. Wang, B.: "Development of a 2-D Large-Scale Micellar/Polymer Simulator", Ph.D. Dissertation, University of Texas-Austin (May 1981).
  57. Jennings, R. R., Rogers, J. H. and West, T. J.: "Factors Influencing Mobility Control by Polymer Solutions", *J. Pet. Tech.* (March 1971), 391-401.
  58. Dawson, R. and Lantz, R. B.: "Inaccessible Pore Volume in Polymer Flooding", *Soc. Pet. Eng. J.* (October 1972), 448-452.
  59. Sorbie, K. S., Roberts, L. J. and Clifford, P. J.: "Calculation on the Behavior of Time-Setting Polymer Gel in Porous Media", *AIChE Mtg.* Houston, Texas (March 1985).
  60. Langmuir, I.: "The Constitution and Fundamental Properties of Solids and Liquids", *J. Am. Chem. Soc.* (September 1916) Vol. 38, 2221-95.

61. Liauh, W. C., Duda, J. L. and Klaus, E. E.: "An Investigation of the Inaccessible Pore Volume Phenomena", *Interfacial Phenomena in Enhanced Oil Recovery, AIChE Symp. Series* (1982) Vol. 78, No. 212, 70-76.
62. Stone, H. L.: "Estimation of Three-Phase Relative Permeability and Residual Oil Data", *J. Can. Pet. Tech.* (1973) Vol. 12, No. 4, 53-61.
63. Peaceman, D. W.: "Interpretation of Well-block Pressure in Numerical Reservoir Simulation", *Soc. Pet. Eng. J.* (June 1978) 183-94.
64. Aziz, K. and Settari, A.: "Petroleum Reservoir Simulation", Applied Science Publisher Ltd., London (1979) 10.
65. Sarma, H. K.: "A Study of the Impact of Instability on the Immiscible Displacement of One Fluid by Another", Ph.D. Dissertation, University of Alberta, Edmonton, Alberta (1988).

## Appendix A

### Calculation of the Unknown Saturations

All the terms in Equations (5.13) and (5.14) are known quantities of the system and fluid properties or functions of the unknown saturations  $S_{M1}$  and  $S_{M2}$ . Therefore, one has two equations and two unknowns, although both equations are non-linear.

In order to solve these Equations, a special computer program called saturation was developed which uses the Newton iterative technique.

Rearrange Equations (5.13) and (5.14) in the form

$$F(S_{M1} - S_{M2}) = 0 \quad (\text{A.1})$$

$$G(S_{M1} - S_{M2}) = 0 \quad (\text{A.2})$$

A Taylor's series expansion for both Equations (A.1) and (A.2) results in:

$$F(S_{M1}, S_{M2})^{k+1} = F(S_{M1}, S_{M2})^k + (S_{M1}^{k+1} - S_{M1}^k) \frac{\partial F}{\partial S_{M1}} \Big|_{(S_{M1}, S_{M2})^k} +$$

$$(S_{M2}^{k+1} - S_{M2}^k) \frac{\partial F}{\partial S_{M2}} \Big|_{(S_{M1}, S_{M2})^k} + \dots \quad (\text{A.3})$$

and

$$G(S_{M1}, S_{M2})^{k+1} = G(S_{M1}, S_{M2})^k + (S_{M1}^{k+1} - S_{M1}^k) \frac{\partial G}{\partial S_{M1}} \Big|_{(S_{M1}, S_{M2})^k} +$$

$$(S_{M2}^{k+1} - S_{M2}^k) \frac{\partial G}{\partial S_{M2}} \Big|_{(S_{M1}, S_{M2})^k} + \dots \quad (\text{A.4})$$

where

$$\frac{\partial F}{\partial S_{M1}} \Big|_{(S_{M1}, S_{M2})^k} = \text{the partial derivative of } F \text{ with respect to } S_{M1} \text{ evaluated at}$$

$$(S_{M1}, S_{M2})^k$$

$$\left. \frac{\partial F}{\partial S_{M2}} \right|_{(S_{M1}, S_{M2})^k} = \text{the partial derivative of } F \text{ with respect to } S_{M2} \text{ evaluated at } (S_{M1}, S_{M2})^k$$

$$\left. \frac{\partial G}{\partial S_{M1}} \right|_{(S_{M1}, S_{M2})^k} = \text{the partial derivative of } G \text{ with respect to } S_{M1} \text{ evaluated at } (S_{M1}, S_{M2})^k$$

$$\left. \frac{\partial G}{\partial S_{M2}} \right|_{(S_{M1}, S_{M2})^k} = \text{the partial derivative of } G \text{ with respect to } S_{M2} \text{ evaluated at } (S_{M1}, S_{M2})^k$$

k = iteration counter

Since the series is truncated after the first derivative term, one must iterate on the unknown saturations to obtain the roots of  $F$  and  $G$ . The two Equations implemented in the computer program are:

$$F(S_{M1}, S_{M2})^k = -\left(S_{M1}^{k+1} - S_{M1}^k\right) \left. \frac{\partial F}{\partial S_{M1}} \right|_{(S_{M1}, S_{M2})^k} - \left(S_{M2}^{k+1} - S_{M2}^k\right) \left. \frac{\partial F}{\partial S_{M2}} \right|_{(S_{M1}, S_{M2})^k} \quad (\text{A.5})$$

$$G(S_{M1}, S_{M2})^k = -\left(S_{M1}^{k+1} - S_{M1}^k\right) \left. \frac{\partial G}{\partial S_{M1}} \right|_{(S_{M1}, S_{M2})^k} - \left(S_{M2}^{k+1} - S_{M2}^k\right) \left. \frac{\partial G}{\partial S_{M2}} \right|_{(S_{M1}, S_{M2})^k} \quad (\text{A.6})$$

One now has two equations and two unknowns and they can be solved simultaneously by simple substitution once the four derivatives are determined. An alternative numerical technique is used to approximate these partial derivatives by recalculating the functions with a small perturbation ( $\delta$ ) to each of the saturations. Using finite differences to approximate the derivative results in:

$$\left. \frac{\partial F}{\partial S_{M1}} \right|_{(S_{M1}, S_{M2})^k} = \frac{F(S_{M1}^k + \delta, S_{M2}^k) - F(S_{M1}^k, S_{M2}^k)}{\delta} \quad (\text{A.7})$$

$$\left. \frac{\partial F}{\partial S_{M2}} \right|_{(S_{M1}, S_{M2})^k} = \frac{F(S_{M1}^k, S_{M2}^k + \delta) - F(S_{M1}^k, S_{M2}^k)}{\delta} \quad (\text{A.8})$$

$$\left. \frac{\partial G}{\partial S_{M1}} \right|_{(S_{M1}, S_{M2})^k} = \frac{G(S_{M1}^k + \delta, S_{M2}^k) - G(S_{M1}^k, S_{M2}^k)}{\delta} \quad (\text{A.9})$$

$$\left. \frac{\partial G}{\partial S_{M2}} \right|_{(S_{M1}, S_{M2})^k} = \frac{G(S_{M1}^k, S_{M2}^k + \delta) - G(S_{M1}^k, S_{M2}^k)}{\delta} \quad (\text{A.10})$$

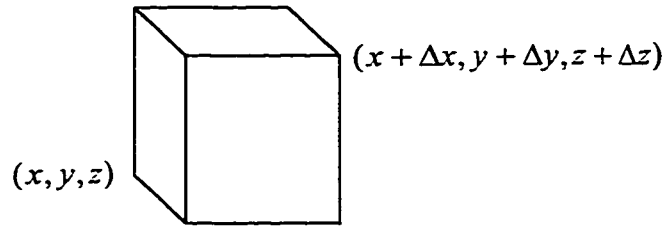
where  $\delta$  is a small change in saturation. With these definitions, Equations (A.5) and (A.6) become a chord-slope version of the technique.

This iterative solution converges when it meets certain tolerance requirements. The two real roots are the two unknown saturations  $S_{M1}$  and  $S_{M2}$ .

## Appendix B

### Derivation of Differential Equations

Consider the three-dimensional incremental system below, which is assumed to be located in a porous medium.



By conservation of mass, one has the equality:

$$\text{Mass in} - \text{Mass out} = \text{Accumulation of mass in the block} \quad (\text{B.1})$$

#### **B.1 Mass Balance of Oil**

A conservation of mass of oil over a time increment,  $\Delta t$ , may be expressed as:

$$\begin{aligned} & \left( \rho_o u_{ox} \Big|_x - \rho_o u_{ox} \Big|_{x+\Delta x} \right) \Delta y \Delta z \Delta t + \left( \rho_o u_{oy} \Big|_y - \rho_o u_{oy} \Big|_{y+\Delta y} \right) \Delta x \Delta z \Delta t + \\ & \left( \rho_o u_{oz} \Big|_z - \rho_o u_{oz} \Big|_{z+\Delta z} \right) \Delta x \Delta y \Delta t = \left( \rho_o \phi S_o \Big|_{t+\Delta t} - \rho_o \phi S_o \Big|_t \right) \Delta x \Delta y \Delta z \end{aligned} \quad (\text{B.2})$$

Combining terms in Equation (B.2), dividing through by  $\Delta x \Delta y \Delta z \Delta t$ , and taking the limit as  $\Delta x \Delta y \Delta z \Delta t$  approaches zero simultaneously yields:

$$-\frac{\partial}{\partial x}(\rho_o u_{ox}) - \frac{\partial}{\partial y}(\rho_o u_{oy}) - \frac{\partial}{\partial z}(\rho_o u_{oz}) = \frac{\partial}{\partial t}(\rho_o \phi S_o) \quad (\text{B.3})$$

From Darcy's law, the phase velocities can be expressed as:

$$u_{\ell} = \lambda_{\ell} (\Delta p_{\ell} - \rho_{\ell} g \Delta Z) \quad (\text{B.4})$$

where

- $\ell$  = phase,
- $u$  = Darcy velocity,
- $\rho$  = fluid density,
- $g$  = gravitational acceleration,
- $\Delta p$  = pressure gradient,
- $Z$  = elevation, and
- $\lambda_{\ell}$  = phase fluid mobility which may be expressed as:

$$\lambda_{\ell} = \frac{k k_{r\ell}}{\mu_{\ell}} \quad (\text{B.5})$$

where

- $k$  = absolute permeability,
- $k_{r\ell}$  = phase relative permeability, and
- $\mu_{\ell}$  = phase density.

Combining Equation (B.3), Darcy's law, the equation of state, introducing a sink or source term in the left-hand side of Equation (B.3), and expressing the oil density in terms of the oil formation volume factors<sup>64</sup>, results in:

$$\frac{\partial}{\partial x} \left( \frac{k_x k_{ro}}{\mu_o B_o} \frac{\partial \phi_o}{\partial x} \right) + \frac{\partial}{\partial y} \left( \frac{k_y k_{ro}}{\mu_o B_o} \frac{\partial \phi_o}{\partial y} \right) + \frac{\partial}{\partial z} \left( \frac{k_z k_{ro}}{\mu_o B_o} \frac{\partial \phi_o}{\partial z} \right) + q_o^* = \frac{\partial}{\partial t} \left( \frac{\phi S_o}{B_o} \right) \quad (\text{B.6})$$

where

- $\phi$  = fluid potential,
- $B_o$  = oil formation volume factor, and
- $S_o$  = oil saturation.



## B.2 Mass Balance of Water

The water phase contains two components (i.e., pure water and polymer), but it is assumed that the volume effects of changing polymer concentration is negligible, and that the polymer concentration is small in comparison with unity. Then for the water phase system under consideration, a conservation of mass of water may be written as:

$$\begin{aligned} & \left( \rho_w u_{wx} \Big|_x - \rho_w u_{wx} \Big|_{x+\Delta x} \right) \Delta y \Delta z \Delta t + \left( \rho_w u_{wy} \Big|_y - \rho_w u_{wy} \Big|_{y+\Delta y} \right) \Delta x \Delta z \Delta t + \\ & \left( \rho_w u_{wz} \Big|_z - \rho_w u_{wz} \Big|_{z+\Delta z} \right) \Delta x \Delta y \Delta t = \left( \rho_w \phi S_w \Big|_{t+\Delta t} - \rho_w \phi S_w \Big|_t \right) \Delta x \Delta y \Delta z \end{aligned} \quad (\text{B.7})$$

Rearranging and combining terms in Equation (B.7), dividing through by  $\Delta x \Delta y \Delta z \Delta t$ , and taking the limit as  $\Delta x \Delta y \Delta z \Delta t$  approaches zero simultaneously leads to:

$$-\frac{\partial}{\partial x}(\rho_w u_{wx}) - \frac{\partial}{\partial y}(\rho_w u_{wy}) - \frac{\partial}{\partial z}(\rho_w u_{wz}) = \frac{\partial}{\partial t}(\rho_w \phi S_w) \quad (\text{B.8})$$

Combining Equation (B.8), Darcy's law, the equation of state, introducing a sink or source term in the left-hand side of Equation (B.8), and expressing the water density in terms of the water formation volume factors<sup>64</sup> results in:

$$\begin{aligned} & \frac{\partial}{\partial x} \left( \frac{k_x k_{rw}}{\mu_w B_W} \frac{\partial \phi_w}{\partial x} \right) + \frac{\partial}{\partial y} \left( \frac{k_y k_{rw}}{\mu_w B_W} \frac{\partial \phi_w}{\partial y} \right) + \frac{\partial}{\partial z} \left( \frac{k_z k_{rw}}{\mu_w B_W} \frac{\partial \phi_w}{\partial z} \right) + q_w = \\ & \frac{\partial}{\partial t} \left( \frac{\phi S_w}{B_w} \right) \end{aligned} \quad (\text{B.9})$$

## B.3 Mass Balance of Gas

A mass balance of the gas phase must include all possible sources of gas (i.e., free gas, gas in oil, and gas in water). Applying the same procedures, arguments and assumptions as were used in the previous sections for water and oil results in the final gas Equation:

$$\begin{aligned}
& \frac{\partial}{\partial x} \left( R_{sw} \frac{k_x k_{rw}}{\mu_w B_w} \frac{\partial \phi_w}{\partial x} \right) + \frac{\partial}{\partial x} \left( R_{so} \frac{k_x k_{ro}}{\mu_o B_o} \frac{\partial \phi_o}{\partial x} \right) + \frac{\partial}{\partial x} \left( \frac{k_x k_{rg}}{\mu_g B_g} \frac{\partial \phi_g}{\partial x} \right) + \\
& \frac{\partial}{\partial y} \left( R_{sw} \frac{k_y k_{rw}}{\mu_w B_w} \frac{\partial \phi_w}{\partial y} \right) + \frac{\partial}{\partial y} \left( R_{so} \frac{k_y k_{ro}}{\mu_o B_o} \frac{\partial \phi_o}{\partial y} \right) + \frac{\partial}{\partial y} \left( \frac{k_y k_{rg}}{\mu_g B_g} \frac{\partial \phi_g}{\partial y} \right) + \\
& \frac{\partial}{\partial z} \left( R_{sw} \frac{k_z k_{rw}}{\mu_w B_w} \frac{\partial \phi_w}{\partial z} \right) + \frac{\partial}{\partial z} \left( R_{so} \frac{k_z k_{ro}}{\mu_o B_o} \frac{\partial \phi_o}{\partial z} \right) + \frac{\partial}{\partial z} \left( \frac{k_z k_{rg}}{\mu_g B_g} \frac{\partial \phi_g}{\partial z} \right) + \\
& R_{sw} q_w^* + R_{so} q_o^* + q_g^* = \frac{\partial}{\partial t} \left( R_{sw} \frac{\phi S_w}{B_w} + R_{so} \frac{\phi S_o}{B_o} + \frac{\phi S_g}{B_g} \right)
\end{aligned} \tag{B.10}$$

#### B.4 Mass Balance of Polymer

The mass balance of polymer may be written as:

$$\begin{aligned}
& (\text{Mass in} - \text{Mass out}) = \text{Mass accumulation in pore space} + \\
& \qquad \qquad \qquad \text{Mass accumulation on the rock surfaces}
\end{aligned} \tag{B.11}$$

where

$$\begin{aligned}
& (\text{Mass in} - \text{Mass out}) = \left( \dot{m}_{px} \Big|_x - \dot{m}_{px} \Big|_{x+\Delta x} \right) \Delta y \Delta z \Delta t + \\
& \qquad \qquad \qquad \left( \dot{m}_{py} \Big|_y - \dot{m}_{py} \Big|_{y+\Delta y} \right) \Delta x \Delta z \Delta t + \\
& \qquad \qquad \qquad \left( \dot{m}_{pz} \Big|_z - \dot{m}_{pz} \Big|_{z+\Delta z} \right) \Delta x \Delta y \Delta t
\end{aligned} \tag{B.12}$$

$$\begin{aligned}
& \left( \text{Mass accumulation} \right) \\
& \qquad \qquad \qquad \text{in pore space} = \rho_w \phi_p S_w C_p \Delta x \Delta y \Delta z \Big|_{t+\Delta t} - \rho_w \phi_p S_w C_p \Delta x \Delta y \Delta z \Big|_t,
\end{aligned} \tag{B.13}$$

and

$$\begin{aligned}
& \left( \text{Mass accumulation} \right) \\
& \qquad \qquad \qquad \text{on the rock} = \rho_{rm} (1 - \phi) C_s \Delta x \Delta y \Delta z \Big|_{t+\Delta t} - \rho_{rm} (1 - \phi) C_s \Delta x \Delta y \Delta z \Big|_t,
\end{aligned} \tag{B.14}$$

where

$\phi_p$  = effective porosity for polymer,

$C_p$  = mass concentration of polymer in water phase,

$C_s$  = mass concentration of polymer on the rock,  
 $\rho_{rm}$  = density of rock matrix, and  
 $\dot{m}_p$  = mass flux of polymer.

Substituting Equations (B.12) through (B.14) into Equation (B.11), rearranging and combining terms in Equation (B.11), dividing through by  $\Delta x \Delta y \Delta z \Delta t$ , and taking the limit as  $\Delta x \Delta y \Delta z \Delta t$  approaches zero simultaneously leads to:

$$-\frac{\partial \dot{m}_{px}}{\partial x} - \frac{\partial \dot{m}_{py}}{\partial y} - \frac{\partial \dot{m}_{pz}}{\partial z} = \frac{\partial}{\partial t} (\rho_w \phi_p S_w C_p) + \frac{\partial}{\partial t} (\rho_{rm} (1 - \phi) C_s) \quad (B.15)$$

The mass flux of polymer may be expressed as:

$$\dot{m}_{px} = \rho_w C_p u_{wx} - \rho_w D_{px} \frac{\partial C_p}{\partial x} \quad (B.16)$$

$$\dot{m}_{py} = \rho_w C_p u_{wy} - \rho_w D_{py} \frac{\partial C_p}{\partial y} \quad (B.17)$$

$$\dot{m}_{pz} = \rho_w C_p u_{wz} - \rho_w D_{pz} \frac{\partial C_p}{\partial z} \quad (B.18)$$

where  $D_p$  is the dispersion coefficient.

Substituting Equations (B.16) through (B.18) into Equation (B.15) leads to:

$$\begin{aligned}
 & -\frac{\partial}{\partial x} (\rho_w C_p u_{wx}) + \frac{\partial}{\partial x} \left( \rho_w D_{px} \frac{\partial C_p}{\partial x} \right) - \frac{\partial}{\partial y} (\rho_w C_p u_{wy}) + \\
 & \frac{\partial}{\partial y} \left( \rho_w D_{py} \frac{\partial C_p}{\partial y} \right) - \frac{\partial}{\partial z} (\rho_w C_p u_{wz}) + \frac{\partial}{\partial z} \left( \rho_w D_{pz} \frac{\partial C_p}{\partial z} \right) = \\
 & \frac{\partial}{\partial t} (\rho_w \phi_p S_w C_p) + \frac{\partial}{\partial t} (\rho_{rm} (1 - \phi) C_s)
 \end{aligned} \quad (B.19)$$

Rearranging and combining terms in Equation (B.19), expressing the density of the fluid

in terms of the formation volume factors and dividing through by the water density at standard conditions,  $\rho_{wsc}$ , results in the final polymer transport Equation:

$$\begin{aligned}
 & -\frac{\partial}{\partial x} \left( \frac{C_p u_{wx}}{B_w} \right) + \frac{\partial}{\partial x} \left( \frac{D_{px}}{B_w} \frac{\partial C_p}{\partial x} \right) - \frac{\partial}{\partial y} \left( \frac{C_p u_{wy}}{B_w} \right) + \frac{\partial}{\partial y} \left( \frac{D_{py}}{B_w} \frac{\partial C_p}{\partial y} \right) \\
 & -\frac{\partial}{\partial z} \left( \frac{C_p u_{wz}}{B_w} \right) + \frac{\partial}{\partial z} \left( \frac{D_{pz}}{B_w} \frac{\partial C_p}{\partial z} \right) = \frac{\partial}{\partial t} \left( \frac{\phi_p S_w C_p}{B_w} \right) + \frac{\partial}{\partial t} \left( \frac{\rho_{rm}}{\rho_{wsc}} (1-\phi) C_s \right)
 \end{aligned} \tag{B.20}$$

## Appendix C

### Finite Difference Approximation of Differential Equations

In this Appendix, the details of the finite difference approximation to the differential equations are presented. These differential equations are restated in terms of several primary variables through the use of the following auxiliary equations:

$$p_{cow} = p_o - p_w \quad (C.1)$$

$$p_{cgo} = p_g - p_o \quad (C.2)$$

$$S_o + S_w + S_g = 1 \quad (C.3)$$

$$\varphi_\ell = p_\ell - \rho_\ell gZ \quad \ell = o, w, g \quad (C.4)$$

$$C_s = C_s(C_p) \quad (C.5)$$

#### C.1 Oil Equation

Multiplying across Equation (B.6) by the cell volume of block  $V_{b_{i,j,k}}$  to convert it to a volumetric flow rate gives:

$$\begin{aligned} & \frac{\partial}{\partial x} \left( A_x \frac{k_x k_{ro}}{\mu_o B_o} \frac{\partial \varphi_o}{\partial x} \right) \Delta x + \frac{\partial}{\partial y} \left( A_y \frac{k_y k_{ro}}{\mu_o B_o} \frac{\partial \varphi_o}{\partial y} \right) \Delta y + \frac{\partial}{\partial z} \left( A_z \frac{k_z k_{ro}}{\mu_o B_o} \frac{\partial \varphi_o}{\partial z} \right) \Delta z \\ & + q_o = V_b \frac{\partial}{\partial t} \left( \frac{\phi S_o}{B_o} \right) \end{aligned} \quad (C.6)$$

Introducing the total inter-block phase transmissibility in the x, y and z-directions gives:

$$T_{ix}^n = \frac{2 A_{x_{i\pm 1,j,k}} A_{x_{i,j,k}} k_{x_{i\pm 1,j,k}} k_{x_{i,j,k}}}{A_{x_{i,j,k}} k_{x_{i,j,k}} \Delta x_{i\pm 1,j,k} + A_{x_{i\pm 1,j,k}} k_{x_{i\pm 1,j,k}} \Delta x_{i,j,k}} \left( \frac{k_{rt}}{\bar{\mu}_\ell \bar{B}_\ell} \right)_{upstream}^n \quad (C.7)$$

$$T_{iy}^n = \frac{2 A_{y_{i,j\pm 1,k}} A_{y_{i,j,k}} k_{y_{i,j\pm 1,k}} k_{y_{i,j,k}}}{A_{y_{i,j,k}} k_{y_{i,j,k}} \Delta y_{i,j\pm 1,k} + A_{y_{i,j\pm 1,k}} k_{y_{i,j\pm 1,k}} \Delta y_{i,j,k}} \left( \frac{k_{rt}}{\bar{\mu}_\ell \bar{B}_\ell} \right)_{upstream}^n \quad (C.8)$$

$$T_{t_{i,j,k=1}^n}^n = \frac{2A_{-i,j,k=1} A_{-i,j,k} k_{-i,j,k=1} k_{-i,j,k}}{A_{-i,j,k} k_{-i,j,k} \Delta z_{i,j,k=1} + A_{-i,j,k=1} k_{-i,j,k=1} \Delta z_{i,j,k}} \left( \frac{k_{r1}}{\bar{\mu}_\ell \bar{B}_\ell} \right)_{upstream}^n \quad (C.9)$$

Note that in the IMPES scheme, the non-linear coefficients (mobility) lag in time.

To discretize Equation (C.5), the time derivative is represented by a forward difference approximation and the space derivatives are represented by a centered difference approximation. Then the finite difference approximation to the LHS of Equation (C.5) becomes:

$$\begin{aligned} LHS = & T_{\alpha_{i+\frac{1}{2},j,k}^n}^n \left( \varphi_{o_{i+1,j,k}}^{n+1} - \varphi_{o_{i,j,k}}^{n+1} \right) - T_{\alpha_{i-\frac{1}{2},j,k}^n}^n \left( \varphi_{o_{i,j,k}}^{n+1} - \varphi_{o_{i-1,j,k}}^{n+1} \right) + \\ & T_{\alpha_{i,j+\frac{1}{2},k}^n}^n \left( \varphi_{o_{i,j+1,k}}^{n+1} - \varphi_{o_{i,j,k}}^{n+1} \right) - T_{\alpha_{i,j-\frac{1}{2},k}^n}^n \left( \varphi_{o_{i,j,k}}^{n+1} - \varphi_{o_{i,j-1,k}}^{n+1} \right) + \\ & T_{\alpha_{i,j,k+\frac{1}{2}}^n}^n \left( \varphi_{o_{i,j,k+1}}^{n+1} - \varphi_{o_{i,j,k}}^{n+1} \right) - T_{\alpha_{i,j,k-\frac{1}{2}}^n}^n \left( \varphi_{o_{i,j,k}}^{n+1} - \varphi_{o_{i,j,k-1}}^{n+1} \right) + q_{o_{i,j,k}} \end{aligned} \quad (C.10)$$

In order to reduce the round-off error, the following definition will be used throughout

$$\delta p_{i,j,k} = p_{i,j,k}^{n+1} - p_{i,j,k}^n$$

Relating potentials to pressures using auxiliary Equation (C.4) and the above definition results in:

$$\varphi_{o_{i+1,j,k}}^{n+1} - \varphi_{o_{i,j,k}}^{n+1} = \left( \delta p_{o_{i+1,j,k}} - \delta p_{o_{i,j,k}} \right) + \left( p_{o_{i+1,j,k}}^n - p_{o_{i,j,k}}^n \right) - \rho_{o_{i+\frac{1}{2},j,k}}^n g \left( Z_{i+1,j,k} - Z_{i,j,k} \right)$$

Then, Equation (C.10) may be written as:

$$\begin{aligned} LHS = & T_{\alpha_{i+\frac{1}{2},j,k}^n}^n \left( \delta p_{o_{i+1,j,k}} - \delta p_{o_{i,j,k}} \right) - T_{\alpha_{i-\frac{1}{2},j,k}^n}^n \left( \delta p_{o_{i,j,k}} - \delta p_{o_{i-1,j,k}} \right) + \\ & T_{\alpha_{i,j+\frac{1}{2},k}^n}^n \left( \delta p_{o_{i,j+1,k}} - \delta p_{o_{i,j,k}} \right) - T_{\alpha_{i,j-\frac{1}{2},k}^n}^n \left( \delta p_{o_{i,j,k}} - \delta p_{o_{i,j-1,k}} \right) + \\ & T_{\alpha_{i,j,k+\frac{1}{2}}^n}^n \left( \delta p_{o_{i,j,k+1}} - \delta p_{o_{i,j,k}} \right) - T_{\alpha_{i,j,k-\frac{1}{2}}^n}^n \left( \delta p_{o_{i,j,k}} - \delta p_{o_{i,j,k-1}} \right) + \\ & c_{o_{i,j,k}} + d_{o_{i,j,k}} + q_{o_{i,j,k}} \end{aligned} \quad (C.11)$$

where

$$\begin{aligned}
c_{o_{i,j,k}} &= T_{\alpha x_{i-\frac{1}{2},j,k}}^n (p_{o_{i+1,j,k}}^n - p_{o_{i,j,k}}^n) - T_{\alpha x_{i-\frac{1}{2},j,k}}^n (p_{o_{i,j,k}}^n - p_{o_{i-1,j,k}}^n) + \\
& T_{\alpha y_{i,j-\frac{1}{2},k}}^n (p_{o_{i,j-1,k}}^n - p_{o_{i,j,k}}^n) - T_{\alpha y_{i,j-\frac{1}{2},k}}^n (p_{o_{i,j,k}}^n - p_{o_{i,j-1,k}}^n) + \\
& T_{\alpha z_{i,j,k-\frac{1}{2}}}^n (p_{o_{i,j,k+1}}^n - p_{o_{i,j,k}}^n) - T_{\alpha z_{i,j,k-\frac{1}{2}}}^n (p_{o_{i,j,k}}^n - p_{o_{i,j,k-1}}^n) \\
d_{o_{i,j,k}} &= -T_{\alpha x_{i-\frac{1}{2},j,k}}^n \rho_{o_{i-\frac{1}{2},j,k}}^n g(Z_{i+1,j,k} - Z_{i,j,k}) + T_{\alpha x_{i-\frac{1}{2},j,k}}^n \rho_{o_{i-\frac{1}{2},j,k}}^n g(Z_{i,j,k} - Z_{i-1,j,k}) - \\
& T_{\alpha y_{i,j-\frac{1}{2},k}}^n \rho_{o_{i,j-\frac{1}{2},k}}^n g(Z_{i,j+1,k} - Z_{i,j,k}) + T_{\alpha y_{i,j-\frac{1}{2},k}}^n \rho_{o_{i,j-\frac{1}{2},k}}^n g(Z_{i,j,k} - Z_{i,j-1,k}) - \\
& T_{\alpha z_{i,j,k-\frac{1}{2}}}^n \rho_{o_{i,j,k-\frac{1}{2}}}^n g(Z_{i,j,k+1} - Z_{i,j,k}) + T_{\alpha z_{i,j,k-\frac{1}{2}}}^n \rho_{o_{i,j,k-\frac{1}{2}}}^n g(Z_{i,j,k} - Z_{i,j,k-1})
\end{aligned}$$

The LHS of the oil Equation (C.11) may be written as:

$$\Delta_x (T_{\alpha x}^n \Delta_x \delta p_o) + \Delta_y (T_{\alpha y}^n \Delta_y \delta p_o) + \Delta_z (T_{\alpha z}^n \Delta_z \delta p_o) + c_{o_{i,j,k}} + d_{o_{i,j,k}} + q_{o_{i,j,k}} \quad (C.12)$$

The finite difference approximation to the RHS of Equation (C.5) leads to the following discretization:

$$V_b \frac{\partial}{\partial t} \left( \frac{\phi S_o}{B_o} \right) = \frac{V_{b_{i,j,k}}}{\Delta t} \left( \frac{\phi_{i,j,k}}{B_o^{n+1}} \delta S_o + \phi_{i,j,k} S_o^n \left( \frac{1}{B_o} \right)^* \delta p_o \right)_{i,j,k} \quad (C.13)$$

where

$$\begin{aligned}
\delta S_o &= S_{o_{i,j,k}}^{n+1} - S_{o_{i,j,k}}^n \\
\left( \frac{1}{B_o} \right)^*_{i,j,k} &= \left( \frac{\frac{1}{B_o^{n+1}} - \frac{1}{B_o^n}}{p_o^{n+1} - p_o^n} \right)_{i,j,k}
\end{aligned}$$

The definition,  $\left( \frac{1}{B_o} \right)^*$  is the chord slope which may be estimated by the derivatives.

The RHS of Equation (C.13) may be written as:

$$RHS = a_{op_o} \delta p_o + a_{os_o} \delta S_o \quad (C.14)$$

Combining Equations (C.12) and (C.14), gives the final oil Equation:

$$\begin{aligned} \Delta_x (T_{\alpha x}^n \Delta_x \delta p_o) + \Delta_y (T_{\alpha y}^n \Delta_y \delta p_o) + \Delta_z (T_{\alpha z}^n \Delta_z \delta p_o) + \\ c_{o_{i,j,k}} + d_{o_{i,j,k}} + q_{o_{i,j,k}} = a_{op_o} \delta p_o + a_{os_o} \delta S_o \end{aligned} \quad (C.15)$$

## C.2 Water Equation

Multiplying across Equation (B.9) by the cell volume of block  $V_{b_{i,j,k}}$  to convert it to a volumetric flow rate gives:

$$\begin{aligned} \frac{\partial}{\partial x} \left( A_x \frac{k_x k_{rw}}{\mu_w B_w} \frac{\partial \phi_w}{\partial x} \right) \Delta x + \frac{\partial}{\partial y} \left( A_y \frac{k_y k_{rw}}{\mu_w B_w} \frac{\partial \phi_w}{\partial y} \right) \Delta y + \\ \frac{\partial}{\partial z} \left( A_z \frac{k_z k_{rw}}{\mu_w B_w} \frac{\partial \phi_w}{\partial z} \right) \Delta z + q_w = V_b \frac{\partial}{\partial t} \left( \frac{\phi S_w}{B_w} \right) \end{aligned} \quad (C.16)$$

The formulation of the finite difference approximation to LHS of Equation (C.16) is similar to that for the oil equation and it can be written as:

$$\begin{aligned} LHS = T_{wx}^n \left( \phi_{w_{i+1,j,k}}^{n+1} - \phi_{w_{i,j,k}}^{n+1} \right) - T_{wx}^n \left( \phi_{w_{i,j,k}}^{n+1} - \phi_{w_{i-1,j,k}}^{n+1} \right) + \\ T_{wy}^n \left( \phi_{w_{i,j+1,k}}^{n+1} - \phi_{w_{i,j,k}}^{n+1} \right) - T_{wy}^n \left( \phi_{w_{i,j,k}}^{n+1} - \phi_{w_{i,j-1,k}}^{n+1} \right) + \\ T_{wz}^n \left( \phi_{w_{i,j,k+1}}^{n+1} - \phi_{w_{i,j,k}}^{n+1} \right) - T_{wz}^n \left( \phi_{w_{i,j,k}}^{n+1} - \phi_{w_{i,j,k-1}}^{n+1} \right) + q_{w_{i,j,k}} \end{aligned} \quad (C.17)$$

Relating potentials to pressures by using the auxiliary Equation (C.4), and expressing the water pressure in terms of oil pressure using the capillary pressure relationship (C.1) results in the following Equation:



$$\begin{aligned} \phi_{w_{i+1,j,k}}^{n+1} - \phi_{w_{i,j,k}}^{n+1} &= (\delta p_{o_{i-1,j,k}} - \delta p_{o_{i,j,k}}) + (p_{o_{i-1,j,k}}^n - p_{o_{i,j,k}}^n) - \\ &\quad (p_{cow_{i+1,j,k}}^n - p_{cow_{i,j,k}}^n) - \rho_{w_{i+\frac{1}{2},j,k}}^n g(Z_{i+1,j,k} - Z_{i,j,k}) \end{aligned} \quad (C.18)$$

Combining Equations (C.17) and (C.18) results in:

$$\begin{aligned} LHS &= T_{wx_{i-\frac{1}{2},j,k}}^n (\delta p_{o_{i-1,j,k}} - \delta p_{o_{i,j,k}}) - T_{wx_{i-\frac{1}{2},j,k}}^n (\delta p_{o_{i,j,k}} - \delta p_{o_{i-1,j,k}}) + \\ &\quad T_{wy_{i,j-\frac{1}{2},k}}^n (\delta p_{o_{i,j-1,k}} - \delta p_{o_{i,j,k}}) - T_{wy_{i,j-\frac{1}{2},k}}^n (\delta p_{o_{i,j,k}} - \delta p_{o_{i,j-1,k}}) + \\ &\quad T_{wz_{i,j,k-\frac{1}{2}}^n} (\delta p_{o_{i,j,k+1}} - \delta p_{o_{i,j,k}}) - T_{wz_{i,j,k-\frac{1}{2}}^n} (\delta p_{o_{i,j,k}} - \delta p_{o_{i,j,k-1}}) + \\ &\quad c_{w_{i,j,k}} + d_{w_{i,j,k}} + e_{w_{i,j,k}} + q_{w_{i,j,k}} \end{aligned} \quad (C.19)$$

where

$$\begin{aligned} c_{w_{i,j,k}} &= T_{wx_{i-\frac{1}{2},j,k}}^n (p_{o_{i+1,j,k}}^n - p_{o_{i,j,k}}^n) - T_{wx_{i-\frac{1}{2},j,k}}^n (p_{o_{i,j,k}}^n - p_{o_{i-1,j,k}}^n) + \\ &\quad T_{wy_{i,j-\frac{1}{2},k}}^n (p_{o_{i,j-1,k}}^n - p_{o_{i,j,k}}^n) - T_{wy_{i,j-\frac{1}{2},k}}^n (p_{o_{i,j,k}}^n - p_{o_{i,j-1,k}}^n) + \\ &\quad T_{wz_{i,j,k-\frac{1}{2}}^n} (p_{o_{i,j,k+1}}^n - p_{o_{i,j,k}}^n) - T_{wz_{i,j,k-\frac{1}{2}}^n} (p_{o_{i,j,k}}^n - p_{o_{i,j,k-1}}^n) \\ d_{w_{i,j,k}} &= -T_{wx_{i-\frac{1}{2},j,k}}^n \rho_{w_{i-\frac{1}{2},j,k}}^n g(Z_{i+1,j,k} - Z_{i,j,k}) + T_{wx_{i-\frac{1}{2},j,k}}^n \rho_{w_{i-\frac{1}{2},j,k}}^n g(Z_{i,j,k} - Z_{i-1,j,k}) - \\ &\quad T_{wy_{i,j-\frac{1}{2},k}}^n \rho_{w_{i,j-\frac{1}{2},k}}^n g(Z_{i,j+1,k} - Z_{i,j,k}) + T_{wy_{i,j-\frac{1}{2},k}}^n \rho_{w_{i,j-\frac{1}{2},k}}^n g(Z_{i,j,k} - Z_{i,j-1,k}) - \\ &\quad T_{wz_{i,j,k-\frac{1}{2}}^n} \rho_{w_{i,j,k-\frac{1}{2}}^n} g(Z_{i,j,k+1} - Z_{i,j,k}) + T_{wz_{i,j,k-\frac{1}{2}}^n} \rho_{w_{i,j,k-\frac{1}{2}}^n} g(Z_{i,j,k} - Z_{i,j,k-1}) \\ e_{w_{i,j,k}} &= -T_{wx_{i+\frac{1}{2},j,k}}^n (p_{cow_{i-1,j,k}}^n - p_{cow_{i,j,k}}^n) + T_{wx_{i+\frac{1}{2},j,k}}^n (p_{cow_{i,j,k}}^n - p_{cow_{i-1,j,k}}^n) - \\ &\quad T_{wy_{i,j-\frac{1}{2},k}}^n (p_{cow_{i,j+1,k}}^n - p_{cow_{i,j,k}}^n) + T_{wy_{i,j-\frac{1}{2},k}}^n (p_{cow_{i,j,k}}^n - p_{cow_{i,j-1,k}}^n) - \\ &\quad T_{wz_{i,j,k-\frac{1}{2}}^n} (p_{cow_{i,j,k+1}}^n - p_{cow_{i,j,k}}^n) + T_{wz_{i,j,k-\frac{1}{2}}^n} (p_{cow_{i,j,k}}^n - p_{cow_{i,j,k-1}}^n) \end{aligned}$$

Thus, the LHS of the water Equation may be written as:

$$LHS = \Delta_x (T_{wx}^n \Delta_x \delta p_o) + \Delta_y (T_{wy}^n \Delta_y \delta p_o) + \Delta_z (T_{wz}^n \Delta_z \delta p_o) + c_{w_{i,j,k}} + d_{w_{i,j,k}} + e_{w_{i,j,k}} + q_{w_{i,j,k}} \quad (C.20)$$

The finite difference approximation to the RHS of Equation (C.16) is:

$$RHS = \frac{V_{b_{i,j,k}}}{\Delta t} \left( + \frac{\phi_{i,j,k}}{B_w^{n+1}} \delta S_w + \phi_{i,j,k} S_w^n \left( \frac{1}{B_w} \right)^* (\delta p_o - \delta p_{cow}) \right)_{i,j,k} \quad (C.21)$$

where

$$\delta S_w = S_{w_{i,j,k}}^{n+1} - S_{w_{i,j,k}}^n$$

$$\left( \frac{1}{B_w} \right)^*_{i,j,k} = \left( \frac{\frac{1}{B_w^{n+1}} - \frac{1}{B_w^n}}{p_w^{n+1} - p_w^n} \right)_{i,j,k}$$

Equation (C.21) may be written as:

$$RHS = a_{wp_o} \delta p_o + a_{ws_w} \delta S_w + a_{wp_{cow}} \delta p_{cow} \quad (C.22)$$

Combining Equations (C.20) and (C.21) gives the final water Equation:

$$\Delta_x (T_{wx}^n \Delta_x \delta p_o) + \Delta_y (T_{wy}^n \Delta_y \delta p_o) + \Delta_z (T_{wz}^n \Delta_z \delta p_o) + c_{w_{i,j,k}} + d_{w_{i,j,k}} + e_{w_{i,j,k}} + q_{w_{i,j,k}} = a_{wp_o} \delta p_o + a_{ws_w} \delta S_w + a_{wp_{cow}} \delta p_{cow} \quad (C.23)$$

### C.3 Gas Equation

Multiplying across the gas Equation (B.9) by the cell volume of block  $V_{b_{i,j,k}}$  yields:

$$\begin{aligned}
& \frac{\partial}{\partial x} \left( R_{s_w} A_x \frac{k_x k_{rw}}{\mu_w B_w} \frac{\partial \phi_w}{\partial x} \right) \Delta x + \frac{\partial}{\partial x} \left( R_{s_o} A_x \frac{k_x k_{ro}}{\mu_o B_o} \frac{\partial \phi_o}{\partial x} \right) \Delta x + \\
& \frac{\partial}{\partial x} \left( A_x \frac{k_x k_{rg}}{\mu_g B_g} \frac{\partial \phi_g}{\partial x} \right) \Delta x + \frac{\partial}{\partial y} \left( R_{s_w} A_y \frac{k_y k_{rw}}{\mu_w B_w} \frac{\partial \phi_w}{\partial y} \right) \Delta y + \\
& \frac{\partial}{\partial y} \left( R_{s_o} A_y \frac{k_y k_{ro}}{\mu_o B_o} \frac{\partial \phi_o}{\partial y} \right) \Delta y + \frac{\partial}{\partial y} \left( A_y \frac{k_y k_{rg}}{\mu_g B_g} \frac{\partial \phi_g}{\partial y} \right) \Delta y + \\
& \frac{\partial}{\partial z} \left( R_{s_w} A_z \frac{k_z k_{rw}}{\mu_w B_w} \frac{\partial \phi_w}{\partial z} \right) \Delta z + \frac{\partial}{\partial z} \left( R_{s_o} A_z \frac{k_z k_{ro}}{\mu_o B_o} \frac{\partial \phi_o}{\partial z} \right) \Delta z + \\
& \frac{\partial}{\partial z} \left( A_z \frac{k_z k_{rg}}{\mu_g B_g} \frac{\partial \phi_g}{\partial z} \right) \Delta z + R_{s_w} q_w + R_{s_o} q_o + q_g = \\
& V_b \frac{\partial}{\partial t} \left( R_{s_w} \frac{\phi S_w}{B_w} + R_{s_o} \frac{\phi S_o}{B_o} + \frac{\phi S_g}{B_g} \right)
\end{aligned} \tag{C.24}$$

The finite difference approximation to LHS of the gas Equation (C.24) becomes:

$$\begin{aligned}
LHS = & T_{gx}^n \left( \phi_{g_{i+1,j,k}}^{n+1} - \phi_{g_{i,j,k}}^{n+1} \right) - T_{gx}^n \left( \phi_{g_{i,j,k}}^{n+1} - \phi_{g_{i-1,j,k}}^{n+1} \right) + \\
& T_{gy}^n \left( \phi_{g_{i,j+1,k}}^{n+1} - \phi_{g_{i,j,k}}^{n+1} \right) - T_{gy}^n \left( \phi_{g_{i,j,k}}^{n+1} - \phi_{g_{i,j-1,k}}^{n+1} \right) + \\
& T_{gz}^n \left( \phi_{g_{i,j,k+1}}^{n+1} - \phi_{g_{i,j,k}}^{n+1} \right) - T_{gz}^n \left( \phi_{g_{i,j,k}}^{n+1} - \phi_{g_{i,j,k-1}}^{n+1} \right) + \\
& T_{ox}^n R_{s_o}^n \left( \phi_{o_{i+1,j,k}}^{n+1} - \phi_{o_{i,j,k}}^{n+1} \right) - T_{ox}^n R_{s_o}^n \left( \phi_{o_{i,j,k}}^{n+1} - \phi_{o_{i-1,j,k}}^{n+1} \right) + \\
& T_{oy}^n R_{s_o}^n \left( \phi_{o_{i,j+1,k}}^{n+1} - \phi_{o_{i,j,k}}^{n+1} \right) - T_{oy}^n R_{s_o}^n \left( \phi_{o_{i,j,k}}^{n+1} - \phi_{o_{i,j-1,k}}^{n+1} \right) + \\
& T_{oz}^n R_{s_o}^n \left( \phi_{o_{i,j,k+1}}^{n+1} - \phi_{o_{i,j,k}}^{n+1} \right) - T_{oz}^n R_{s_o}^n \left( \phi_{o_{i,j,k}}^{n+1} - \phi_{o_{i,j,k-1}}^{n+1} \right) + \\
& T_{wx}^n R_{s_w}^n \left( \phi_{w_{i+1,j,k}}^{n+1} - \phi_{w_{i,j,k}}^{n+1} \right) - T_{wx}^n R_{s_w}^n \left( \phi_{w_{i,j,k}}^{n+1} - \phi_{w_{i-1,j,k}}^{n+1} \right) + \\
& T_{wy}^n R_{s_w}^n \left( \phi_{w_{i,j+1,k}}^{n+1} - \phi_{w_{i,j,k}}^{n+1} \right) - T_{wy}^n R_{s_w}^n \left( \phi_{w_{i,j,k}}^{n+1} - \phi_{w_{i,j-1,k}}^{n+1} \right) + \\
& T_{wz}^n R_{s_w}^n \left( \phi_{w_{i,j,k+1}}^{n+1} - \phi_{w_{i,j,k}}^{n+1} \right) - T_{wz}^n R_{s_w}^n \left( \phi_{w_{i,j,k}}^{n+1} - \phi_{w_{i,j,k-1}}^{n+1} \right) + \\
& R_{s_{o_{i,j,k}}} q_{o_{i,j,k}} + R_{s_{w_{i,j,k}}} q_{w_{i,j,k}} + q_{g_{i,j,k}}
\end{aligned} \tag{C.25}$$

Relating potentials to pressures and expressing the gas pressure in terms of oil pressure using the auxiliary Equation (C.4) and the capillary pressure Equation (C.2) results in:

$$\begin{aligned} \phi_{g_{i-1,j,k}}^{n+1} - \phi_{g_{i,j,k}}^{n+1} = & \left( \delta p_{o_{i-1,j,k}} - \delta p_{o_{i,j,k}} \right) + \left( p_{o_{i-1,j,k}}^n - p_{o_{i,j,k}}^n \right) + \\ & \left( p_{cow_{i-1,j,k}}^n - p_{cow_{i,j,k}}^n \right) - \rho_{g_{i-1,j,k}}^n g \left( Z_{i+1,j,k} - Z_{i,j,k} \right) \end{aligned} \quad (C.26)$$

Combining Equations (C.25) and (C.26), the LHS of the gas Equation (C.24) can be written as:

$$\begin{aligned} LHS = & \left( T_{gx}^n + T_{\alpha x}^n R_{s_o}^n + T_{wx}^n R_{s_w}^n \right)_{i+\frac{1}{2},j,k} \left( \delta p_{o_{i-1,j,k}} - \delta p_{o_{i,j,k}} \right) - \\ & \left( T_{gx}^n + T_{\alpha x}^n R_{s_o}^n + T_{wx}^n R_{s_w}^n \right)_{i-\frac{1}{2},j,k} \left( \delta p_{o_{i,j,k}} - \delta p_{o_{i-1,j,k}} \right) + \\ & \left( T_{gy}^n + T_{\alpha y}^n R_{s_o}^n + T_{wy}^n R_{s_w}^n \right)_{i,j+\frac{1}{2},k} \left( \delta p_{o_{i,j-1,k}} - \delta p_{o_{i,j,k}} \right) - \\ & \left( T_{gy}^n + T_{\alpha y}^n R_{s_o}^n + T_{wy}^n R_{s_w}^n \right)_{i,j-\frac{1}{2},k} \left( \delta p_{o_{i,j,k}} - \delta p_{o_{i,j-1,k}} \right) + \\ & \left( T_{gz}^n + T_{\alpha z}^n R_{s_o}^n + T_{wz}^n R_{s_w}^n \right)_{i,j,k+\frac{1}{2}} \left( \delta p_{o_{i,j,k-1}} - \delta p_{o_{i,j,k}} \right) - \\ & \left( T_{gz}^n + T_{\alpha z}^n R_{s_o}^n + T_{wz}^n R_{s_w}^n \right)_{i,j,k-\frac{1}{2}} \left( \delta p_{o_{i,j,k}} - \delta p_{o_{i,j,k-1}} \right) + \\ & c_{g_{i,j,k}} + d_{g_{i,j,k}} + e_{g_{w_{i,j,k}}} + e_{g_{g_{i,j,k}}} + R_{s_{o_{i,j,k}}} q_{o_{i,j,k}} + R_{s_{w_{i,j,k}}} q_{w_{i,j,k}} + q_{g_{i,j,k}} \end{aligned} \quad (C.27)$$

where

$$\begin{aligned} c_{oo_{i,j,k}} = & \left( T_{gx}^n + T_{\alpha x}^n R_{s_o}^n + T_{wx}^n R_{s_w}^n \right)_{i+\frac{1}{2},j,k} \left( p_{o_{i-1,j,k}}^n - p_{o_{i,j,k}}^n \right) - \\ & \left( T_{gx}^n + T_{\alpha x}^n R_{s_o}^n + T_{wx}^n R_{s_w}^n \right)_{i-\frac{1}{2},j,k} \left( p_{o_{i,j,k}}^n - p_{o_{i-1,j,k}}^n \right) + \\ & \left( T_{gy}^n + T_{\alpha y}^n R_{s_o}^n + T_{wy}^n R_{s_w}^n \right)_{i,j+\frac{1}{2},k} \left( p_{o_{i,j-1,k}}^n - p_{o_{i,j,k}}^n \right) - \\ & \left( T_{gy}^n + T_{\alpha y}^n R_{s_o}^n + T_{wy}^n R_{s_w}^n \right)_{i,j-\frac{1}{2},k} \left( p_{o_{i,j,k}}^n - p_{o_{i,j-1,k}}^n \right) + \\ & \left( T_{gz}^n + T_{\alpha z}^n R_{s_o}^n + T_{wz}^n R_{s_w}^n \right)_{i,j,k+\frac{1}{2}} \left( p_{o_{i,j,k-1}}^n - p_{o_{i,j,k}}^n \right) - \\ & \left( T_{gz}^n + T_{\alpha z}^n R_{s_o}^n + T_{wz}^n R_{s_w}^n \right)_{i,j,k-\frac{1}{2}} \left( p_{o_{i,j,k}}^n - p_{o_{i,j,k-1}}^n \right) \end{aligned}$$

$$\begin{aligned}
d_{g_{o_i,j,k}} &= \left( T_{gx}^n \rho_g^n + T_{ox}^n R_{s_o}^n \rho_o^n + T_{wx}^n R_{s_w}^n \rho_w^n \right)_{i+\frac{1}{2},j,k} g(Z_{i+1,j,k} - Z_{i,j,k}) - \\
&\quad \left( T_{gx}^n \rho_g^n + T_{ox}^n R_{s_o}^n \rho_o^n + T_{wx}^n R_{s_w}^n \rho_w^n \right)_{i-\frac{1}{2},j,k} g(Z_{i,j,k} - Z_{i-1,j,k}) + \\
&\quad \left( T_{gy}^n \rho_g^n + T_{oy}^n R_{s_o}^n \rho_o^n + T_{wy}^n R_{s_w}^n \rho_w^n \right)_{i,j+\frac{1}{2},k} g(Z_{i,j+1,k} - Z_{i,j,k}) - \\
&\quad \left( T_{gy}^n \rho_g^n + T_{oy}^n R_{s_o}^n \rho_o^n + T_{wy}^n R_{s_w}^n \rho_w^n \right)_{i,j-\frac{1}{2},k} g(Z_{i,j,k} - Z_{i,j-1,k}) + \\
&\quad \left( T_{gz}^n \rho_g^n + T_{oz}^n R_{s_o}^n \rho_o^n + T_{wz}^n R_{s_w}^n \rho_w^n \right)_{i,j,k+\frac{1}{2}} g(Z_{i,j,k+1} - Z_{i,j,k}) - \\
&\quad \left( T_{gz}^n \rho_g^n + T_{oz}^n R_{s_o}^n \rho_o^n + T_{wz}^n R_{s_w}^n \rho_w^n \right)_{i,j,k-\frac{1}{2}} g(Z_{i,j,k} - Z_{i,j,k-1}) \\
e_{g_{w_i,j,k}} &= -\left( T_{wx}^n R_{s_w}^n \right)_{i+\frac{1}{2},j,k} \left( p_{cow_{i-1,j,k}}^n - p_{cow_{i,j,k}}^n \right) + \left( T_{wx}^n R_{s_w}^n \right)_{i-\frac{1}{2},j,k} \left( p_{cow_{i,j,k}}^n - p_{cow_{i-1,j,k}}^n \right) - \\
&\quad \left( T_{wy}^n R_{s_w}^n \right)_{i,j+\frac{1}{2},k} \left( p_{cow_{i,j-1,k}}^n - p_{cow_{i,j,k}}^n \right) + \left( T_{wy}^n R_{s_w}^n \right)_{i,j-\frac{1}{2},k} \left( p_{cow_{i,j,k}}^n - p_{cow_{i,j-1,k}}^n \right) - \\
&\quad \left( T_{wz}^n R_{s_w}^n \right)_{i,j,k+\frac{1}{2}} \left( p_{cow_{i,j,k-1}}^n - p_{cow_{i,j,k}}^n \right) + \left( T_{wz}^n R_{s_w}^n \right)_{i,j,k-\frac{1}{2}} \left( p_{cow_{i,j,k}}^n - p_{cow_{i,j,k-1}}^n \right) \\
e_{g_{g_i,j,k}} &= T_{wx}^n \left( p_{cgo_{i-1,j,k}}^n - p_{cgo_{i,j,k}}^n \right) - T_{wx}^n \left( p_{cgo_{i,j,k}}^n - p_{cgo_{i-1,j,k}}^n \right) + \\
&\quad T_{wy}^n \left( p_{cgo_{i,j+1,k}}^n - p_{cgo_{i,j,k}}^n \right) - T_{wy}^n \left( p_{cgo_{i,j,k}}^n - p_{cgo_{i,j-1,k}}^n \right) + \\
&\quad T_{wz}^n \left( p_{cgo_{i,j,k-1}}^n - p_{cgo_{i,j,k}}^n \right) - T_{wz}^n \left( p_{cgo_{i,j,k}}^n - p_{cgo_{i,j,k-1}}^n \right)
\end{aligned}$$

Equation (C.27) can be written in a compact form as:

$$\begin{aligned}
LHS &= \Delta_x \left( \left( T_{gx}^n + T_{ox}^n R_{s_o}^n + T_{wx}^n R_{s_w}^n \right) \Delta_x \delta p_o \right) + \\
&\quad \Delta_y \left( \left( T_{gy}^n + T_{oy}^n R_{s_o}^n + T_{wy}^n R_{s_w}^n \right) \Delta_y \delta p_o \right) + \\
&\quad \Delta_z \left( \left( T_{gz}^n + T_{oz}^n R_{s_o}^n + T_{wz}^n R_{s_w}^n \right) \Delta_z \delta p_o \right) + \\
&\quad c_{g_{i,j,k}} + d_{g_{i,j,k}} + e_{g_{w_i,j,k}} + e_{g_{g_i,j,k}} + R_{s_{o_i,j,k}} q_{o_i,j,k} + \\
&\quad R_{s_{w_i,j,k}} q_{w_i,j,k} + q_{g_{i,j,k}}
\end{aligned} \tag{C.28}$$

The finite difference approximation to the RHS of Equation (C.24) is

$$RHS = \frac{\phi_{i,j,k} V_{b_{i,j,k}}}{\Delta t} \left( \begin{array}{l} +R_{s_o}^* \frac{S_o^{n+1}}{B_o^{n+1}} \delta p_o + R_{s_w}^* \frac{S_w^{n+1}}{B_w^{n+1}} \delta p_o + R_{s_o}^n S_o^n \left( \frac{1}{B_o} \right)^* \delta p_o + \\ R_{s_w}^n S_w^n \left( \frac{1}{B_w} \right)^* \delta p_o + S_g^n \left( \frac{1}{B_g} \right)^* \delta p_o + \frac{S_o^{n+1} R_{s_o}^n}{B_o^{n+1}} \delta S_o + \\ \frac{R_{s_w}^{n+1}}{B_w^{n+1}} \delta S_w + \frac{1}{B_g^{n+1}} \delta S_g - \frac{S_o^{n+1}}{B_o^{n+1}} (R_{s_w})^* \delta p_{cow} - \\ R_{s_w}^n S_w^n \left( \frac{1}{B_w} \right)^* \delta p_{cow} + S_g^n \left( \frac{1}{B_g} \right)^* \delta p_{cgo} \end{array} \right)_{i,j,k} \quad (C.29)$$

where

$$R_{s_{oi,j,k}}^* = \left( \frac{R_{s_o}^{n+1} - R_{s_o}^n}{p_o^{n+1} - p_o^n} \right)_{i,j,k}$$

$$R_{s_{wi,j,k}}^* = \left( \frac{R_{s_w}^{n+1} - R_{s_w}^n}{p_w^{n+1} - p_w^n} \right)_{i,j,k}$$

$$\left( \frac{1}{B_g} \right)^*_{i,j,k} = \left( \frac{\frac{1}{B_g^{n+1}} - \frac{1}{B_g^n}}{p_g^{n+1} - p_g^n} \right)_{i,j,k}$$

Equation (C.29) can be written in a compact form as:

$$RHS = a_{gp_o} \delta p_o + a_{gs_o} \delta S_o + a_{gs_w} \delta S_w + a_{gs_g} \delta S_g + a_{gp_{cow}} \delta p_{cow} + a_{gp_{cgo}} \delta p_{cgo} \quad (C.30)$$

Combining Equations (C.28) and (C.30) gives the final gas Equation:

$$\begin{aligned}
& \Delta_x \left( (T_{gx}^n + T_{ox}^n R_{s_o}^n + T_{wx}^n R_{s_w}^n) \Delta_x \delta p_o \right) + \\
& \Delta_y \left( (T_{gy}^n + T_{oy}^n R_{s_o}^n + T_{wy}^n R_{s_w}^n) \Delta_y \delta p_o \right) + \\
& \Delta_z \left( (T_{gz}^n + T_{oz}^n R_{s_o}^n + T_{wz}^n R_{s_w}^n) \Delta_z \delta p_o \right) + c_{\bar{g}_{i,j,k}} + d_{\bar{g}_{i,j,k}} + e_{\bar{g}_{i,j,k}} + e_{\bar{g}_{i,j,k}} + \quad (C.31) \\
& R_{s_{oi,j,k}} q_{oi,j,k} + R_{s_{wi,j,k}} q_{wi,j,k} + q_{\bar{g}_{i,j,k}} = a_{\bar{g}^o} \delta p_o + a_{\bar{g}^s_o} \delta S_o + a_{\bar{g}^s_w} \delta S_w + \\
& a_{\bar{g}^s_g} \delta S_g + a_{\bar{g}^p_{cow}} \delta p_{cow} + a_{\bar{g}^p_{cgo}} \delta p_{cgo}
\end{aligned}$$

It is desired to combine the oil, water and gas Equations in such a way that all terms with  $\delta S$  disappear. This is achieved by multiplying the oil Equation (C.15) by  $\frac{1}{a_{\bar{g}^s_g}}$ , the water Equation (C.23) by  $\frac{a_{\bar{g}^s_g} - a_{\bar{g}^s_w}}{a_{\bar{g}^s_g} a_{\bar{g}^s_w}}$ , and the gas Equation (C.31) by  $\frac{a_{\bar{g}^s_g} - a_{\bar{g}^s_o}}{a_{\bar{g}^s_g} a_{\bar{g}^s_o}}$  and adding the three Equations which yields the final pressure Equation:

$$\begin{aligned}
& \hat{Z}_{i,j,k} \delta p_{oi,j,k-1} + \hat{B}_{i,j,k} \delta p_{oi,j-1,k} + \hat{D}_{i,j,k} \delta p_{oi+1,j,k} + \hat{E}_{i,j,k} \delta p_{oi,j,k} + \\
& \hat{F}_{i,j,k} \delta p_{oi+1,j,k} + \hat{H}_{i,j,k} \delta p_{oi,j+1,k} + \hat{S}_{i,j,k} \delta p_{oi,j,k-1} = \hat{q}_{i,j,k} \quad (C.32)
\end{aligned}$$

where the coefficients are defined as follow:

$$\begin{aligned}
\hat{Z}_{i,j,k} &= -\frac{a_{\bar{g}^s_g} - a_{\bar{g}^s_o}}{a_{\bar{g}^s_g} a_{\bar{g}^s_o}} T_{oz}^n_{i,j,k-\frac{1}{2}} - \frac{a_{\bar{g}^s_g} - a_{\bar{g}^s_w}}{a_{\bar{g}^s_g} a_{\bar{g}^s_w}} T_{wz}^n_{i,j,k-\frac{1}{2}} - \frac{1}{a_{\bar{g}^s_g}} \left( R_{s_o} T_{oz} + R_{s_w} T_{wz} + T_{gz} \right)_{i,j,k-\frac{1}{2}} \\
\hat{B}_{i,j,k} &= -\frac{a_{\bar{g}^s_g} - a_{\bar{g}^s_o}}{a_{\bar{g}^s_g} a_{\bar{g}^s_o}} T_{oy}^n_{i,j-\frac{1}{2},k} - \frac{a_{\bar{g}^s_g} - a_{\bar{g}^s_w}}{a_{\bar{g}^s_g} a_{\bar{g}^s_w}} T_{wy}^n_{i,j-\frac{1}{2},k} - \frac{1}{a_{\bar{g}^s_g}} \left( R_{s_o} T_{oy} + R_{s_w} T_{wy} + T_{gy} \right)_{i,j-\frac{1}{2},k} \\
\hat{D}_{i,j,k} &= -\frac{a_{\bar{g}^s_g} - a_{\bar{g}^s_o}}{a_{\bar{g}^s_g} a_{\bar{g}^s_o}} T_{ox}^n_{i-\frac{1}{2},j,k} - \frac{a_{\bar{g}^s_g} - a_{\bar{g}^s_w}}{a_{\bar{g}^s_g} a_{\bar{g}^s_w}} T_{wx}^n_{i-\frac{1}{2},j,k} - \frac{1}{a_{\bar{g}^s_g}} \left( R_{s_o} T_{ox} + R_{s_w} T_{wx} + T_{gx} \right)_{i-\frac{1}{2},j,k}
\end{aligned}$$

$$\hat{F}_{i,j,k} = \frac{a_{g^x} - a_{as_o}}{a_{g^x} a_{g^o}} T_{ax}^{n,i-\frac{1}{2},j,k} + \frac{a_{g^x} - a_{as_w}}{a_{g^x} a_{g^w}} T_{wx}^{n,i-\frac{1}{2},j,k} + \frac{1}{a_{g^x}} \left( R_{s_o} T_{ax} + R_{s_w} T_{wx} + T_{gx} \right)_{i-\frac{1}{2},j,k}$$

$$\hat{H}_{i,j,k} = \frac{a_{g^x} - a_{as_o}}{a_{g^x} a_{g^o}} T_{oy}^{n,i,j-\frac{1}{2},k} + \frac{a_{g^x} - a_{as_w}}{a_{g^x} a_{g^w}} T_{wy}^{n,i,j-\frac{1}{2},k} + \frac{1}{a_{g^x}} \left( R_{s_o} T_{oy} + R_{s_w} T_{wy} + T_{gy} \right)_{i,j-\frac{1}{2},k}$$

$$\hat{S}_{i,j,k} = \frac{a_{g^x} - a_{as_o}}{a_{g^x} a_{g^o}} T_{oz}^{n,i,j,k-\frac{1}{2}} + \frac{a_{g^x} - a_{as_w}}{a_{g^x} a_{g^w}} T_{wz}^{n,i,j,k-\frac{1}{2}} + \frac{1}{a_{g^x}} \left( R_{s_o} T_{oz} + R_{s_w} T_{wz} + T_{gz} \right)_{i,j,k-\frac{1}{2}}$$

$$\hat{E}_{i,j,k} = \frac{a_{g^x} - a_{as_o}}{a_{g^x} a_{g^o}} \left( T_{ax}^{n,i-\frac{1}{2},j,k} - T_{ax}^{n,i-\frac{1}{2},j,k} + T_{oy}^{n,i,j-\frac{1}{2},k} - T_{oy}^{n,i,j-\frac{1}{2},k} + T_{oz}^{n,i,j,k-\frac{1}{2}} - T_{oz}^{n,i,j,k-\frac{1}{2}} \right) +$$

$$\frac{a_{g^x} - a_{as_w}}{a_{g^x} a_{g^w}} \left( T_{wx}^{n,i-\frac{1}{2},j,k} - T_{wx}^{n,i-\frac{1}{2},j,k} + T_{wy}^{n,i,j-\frac{1}{2},k} - T_{wy}^{n,i,j-\frac{1}{2},k} + T_{wz}^{n,i,j,k-\frac{1}{2}} - T_{wz}^{n,i,j,k-\frac{1}{2}} \right) +$$

$$\frac{1}{a_{g^x}} \left( \left( R_{s_o} T_{ax} + R_{s_w} T_{wx} + T_{gx} \right)_{i-\frac{1}{2},j,k} - \left( R_{s_o} T_{ax} + R_{s_w} T_{wx} + T_{gx} \right)_{i-\frac{1}{2},j,k} \right) +$$

$$\frac{1}{a_{g^x}} \left( \left( R_{s_o} T_{oy} + R_{s_w} T_{wy} + T_{gy} \right)_{i,j-\frac{1}{2},k} - \left( R_{s_o} T_{oy} + R_{s_w} T_{wy} + T_{gy} \right)_{i,j-\frac{1}{2},k} \right) +$$

$$\frac{1}{a_{g^x}} \left( \left( R_{s_o} T_{oz} + R_{s_w} T_{wz} + T_{gz} \right)_{i,j,k-\frac{1}{2}} - \left( R_{s_o} T_{oz} + R_{s_w} T_{wz} + T_{gz} \right)_{i,j,k-\frac{1}{2}} \right)$$

$$\hat{q}_{i,j,k} = \frac{a_{g^x} - a_{as_o}}{a_{g^x} a_{g^o}} (d_o + c_o + q_o) + \frac{a_{g^x} - a_{as_w}}{a_{g^x} a_{g^w}} (d_w + c_w + E_w + q_w + a_{wp_{cow}} \delta p_{cow}) +$$

$$\frac{1}{a_{g^x}} (d_g + c_g + E_g + R_{s_o} q_o + R_{s_w} q_w + q_g - a_{gp_{cow}} \delta p_{cow} - a_{gp_{cgo}} \delta p_{cgo})$$

### C.1 Polymer Equation

A simplified form of the three-dimensional polymer transport Equation in three-phase flow, in which the polymer is found only in the aqueous phase, is given by the following generalized convection-dispersion Equation:



$$\begin{aligned}
& -\frac{\partial}{\partial x} \left( \frac{C_p u_{wx}}{B_w} \right) + \frac{\partial}{\partial x} \left( \frac{D_{px}}{B_w} \frac{\partial C_p}{\partial x} \right) - \frac{\partial}{\partial y} \left( \frac{C_p u_{wy}}{B_w} \right) + \frac{\partial}{\partial y} \left( \frac{D_{py}}{B_w} \frac{\partial C_p}{\partial y} \right) - \\
& \frac{\partial}{\partial z} \left( \frac{C_p u_{wz}}{B_w} \right) + \frac{\partial}{\partial z} \left( \frac{D_{pz}}{B_w} \frac{\partial C_p}{\partial z} \right) = \frac{\partial}{\partial t} \left( \frac{\phi_p S_w C_p}{B_w} \right) + \frac{\partial}{\partial t} \left( \frac{\rho_{wm}}{\rho_{ws}} (1-\phi) C_p \right)
\end{aligned} \tag{C.33}$$

This partial differential equation is stated in terms of several variables. However, it was assumed that at any time the velocities are known as functions of position. Then this equation is restated in terms of one primary variable,  $C_p$ , through the use of the auxiliary Equation (C.5).

Several schemes can be used to discretize Equation (C.33). A backward in distance (upstream) forward in time (explicit) discretization is used. This gives the following explicit update equation for polymer concentration to be solved after the saturation update equation.

Assuming a constant dispersion coefficient, the finite difference approximation to the LHS of Equation (C.33) becomes:

$$\begin{aligned}
LHS = & -\frac{1}{\Delta x} \left( \frac{C_{p_{i,j,k}}^n u_{w_{i+\frac{1}{2},j,k}}^n}{B_{w_{i,j,k}}^n} - \frac{C_{p_{i-1,j,k}}^n u_{w_{i-\frac{1}{2},j,k}}^n}{B_{w_{i-1,j,k}}^n} \right) \\
& -\frac{1}{\Delta y} \left( \frac{C_{p_{i,j,k}}^n u_{w_{i,j-\frac{1}{2},k}}^n}{B_{w_{i,j,k}}^n} - \frac{C_{p_{i,j-1,k}}^n u_{w_{i,j-\frac{1}{2},k}}^n}{B_{w_{i,j-1,k}}^n} \right) \\
& -\frac{1}{\Delta z} \left( \frac{C_{p_{i,j,k}}^n u_{w_{i,j,k-\frac{1}{2}}}^n}{B_{w_{i,j,k}}^n} - \frac{C_{p_{i,j,k-1}}^n u_{w_{i,j,k-\frac{1}{2}}}^n}{B_{w_{i,j,k-1}}^n} \right) + \\
& T_{Px_{i-\frac{1}{2},j,k}} \left( C_{p_{i-1,j,k}}^n - C_{p_{i,j,k}}^n \right) - T_{Px_{i-\frac{1}{2},j,k}} \left( C_{p_{i,j,k}}^n - C_{p_{i-1,j,k}}^n \right) + \\
& T_{Py_{i,j-\frac{1}{2},k}} \left( C_{p_{i,j+1,k}}^n - C_{p_{i,j,k}}^n \right) - T_{Py_{i,j-\frac{1}{2},k}} \left( C_{p_{i,j,k}}^n - C_{p_{i,j-1,k}}^n \right) + \\
& T_{Pz_{i,j,k-\frac{1}{2}}} \left( C_{p_{i,j,k+1}}^n - C_{p_{i,j,k}}^n \right) - T_{Pz_{i,j,k-\frac{1}{2}}} \left( C_{p_{i,j,k}}^n - C_{p_{i,j,k-1}}^n \right)
\end{aligned} \tag{C.34}$$

Where the polymer total inter-block transmissibility in the x-direction is:

$$T_{Px} = \left( \frac{D_{px}}{B_w} \right) \quad (C.35)$$

The finite difference approximation to the RHS of Equation (C.33) is:

$$RHS = \frac{\phi_{pi,j,k}}{\Delta t} \left( \frac{S_w^{n+1} C_p^{n+1}}{B_w^{n+1}} - \frac{S_w^n C_p^n}{B_w^n} \right)_{i,j,k} + \frac{\rho_{rmi,j,k}}{\rho_{wsc}} (1 - \phi_{i,j,k}) \left( \frac{C_s^{n+1} - C_s^n}{\Delta t} \right)_{i,j,k} \quad (C.36)$$

In Equation (C.36), the unknown variables are  $C_p^{n+1}$ , and  $C_s^{n+1}$ ; however, there is a functional relationship between  $C_p$  and  $C_s$ :

$$C_s = C_s(C_p) = \frac{A_{ad} C_p}{1 + B_{ad} C_p} \quad (C.37)$$

where  $A_{ad}$  and  $B_{ad}$  are constants at a particular time and position.

Combining Equations (C.36) and (C.37) results in:

$$RHS = \frac{\phi_{pi,j,k}}{\Delta t} \left( \frac{S_w^{n+1} C_p^{n+1}}{B_w^{n+1}} - \frac{S_w^n C_p^n}{B_w^n} \right)_{i,j,k} + \frac{\rho_{rmi,j,k}}{\rho_{wsc}} (1 - \phi_{i,j,k}) \left( \frac{\frac{A_{ad}^n C_p^{n+1}}{1 + B_{ad} C_p^{n+1}} - C_s^n}{\Delta t} \right)_{i,j,k} \quad (C.38)$$

Combining Equations (C.34) and (C.38) gives the final polymer transport Equation:

$$\begin{aligned}
& -\frac{1}{\Delta x} \left( \frac{C_{p_{i,j,k}}^n u_{w_{i+\frac{1}{2},j,k}}^n}{B_{w_{i,j,k}}^n} - \frac{C_{p_{i-1,j,k}}^n u_{w_{i-\frac{1}{2},j,k}}^n}{B_{w_{i-1,j,k}}^n} \right) - \frac{1}{\Delta y} \left( \frac{C_{p_{i,j,k}}^n u_{w_{i,j+\frac{1}{2},k}}^n}{B_{w_{i,j,k}}^n} - \frac{C_{p_{i,j-1,k}}^n u_{w_{i,j-\frac{1}{2},k}}^n}{B_{w_{i,j-1,k}}^n} \right) \\
& - \frac{1}{\Delta z} \left( \frac{C_{p_{i,j,k}}^n u_{w_{i,j,k+\frac{1}{2}}}^n}{B_{w_{i,j,k}}^n} - \frac{C_{p_{i,j,k-1}}^n u_{w_{i,j,k-\frac{1}{2}}}^n}{B_{w_{i,j,k-1}}^n} \right) + T_{P_x_{i+\frac{1}{2},j,k}} \left( C_{p_{i-1,j,k}}^n - C_{p_{i,j,k}}^n \right) - \\
& T_{P_x_{i-\frac{1}{2},j,k}} \left( C_{p_{i,j,k}}^n - C_{p_{i-1,j,k}}^n \right) + T_{P_y_{i,j+\frac{1}{2},k}} \left( C_{p_{i,j-1,k}}^n - C_{p_{i,j,k}}^n \right) - \\
& T_{P_y_{i,j-\frac{1}{2},k}} \left( C_{p_{i,j,k}}^n - C_{p_{i,j-1,k}}^n \right) + T_{P_z_{i,j,k+\frac{1}{2}}} \left( C_{p_{i,j,k-1}}^n - C_{p_{i,j,k}}^n \right) - \\
& T_{P_z_{i,j,k-\frac{1}{2}}} \left( C_{p_{i,j,k}}^n - C_{p_{i,j,k-1}}^n \right) = \frac{\phi_{p_{i,j,k}}}{\Delta t} \left( \frac{S_w^{n+1} C_p^{n+1}}{B_w^{n+1}} - \frac{S_w^n C_p^n}{B_w^n} \right)_{i,j,k} \\
& + \frac{\rho_{rm_{i,j,k}}}{\rho_{wsc}} (1 - \phi_{i,j,k}) \left( \frac{\frac{A_{ad}^n C_p^{n+1}}{1 + B_{ad} C_p^{n+1}} - C_s^n}{\Delta t} \right)_{i,j,k}
\end{aligned} \tag{C.39}$$

**Appendix D**  
**Flow Charts**

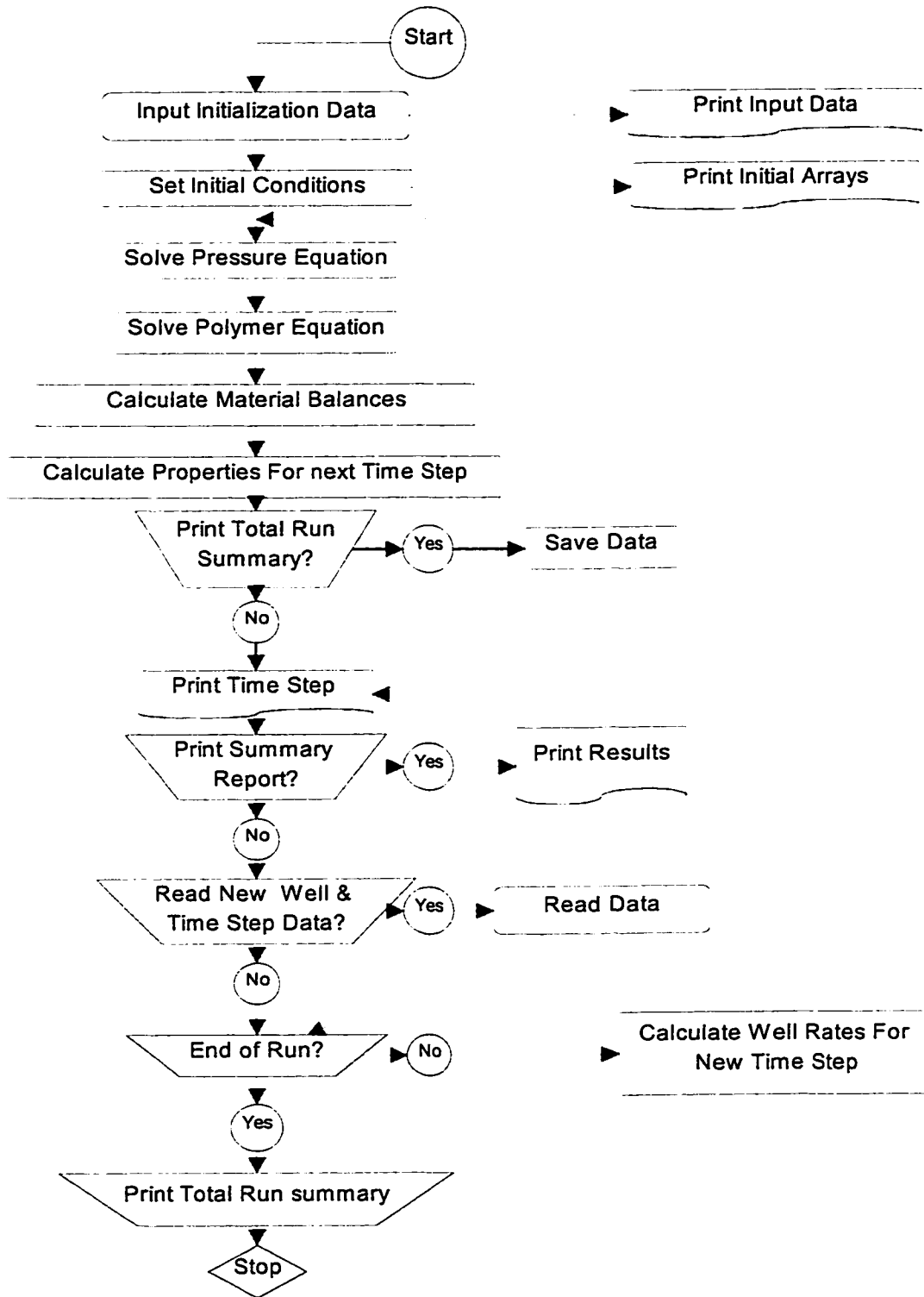


Figure D-1: Main Program Flow Chart

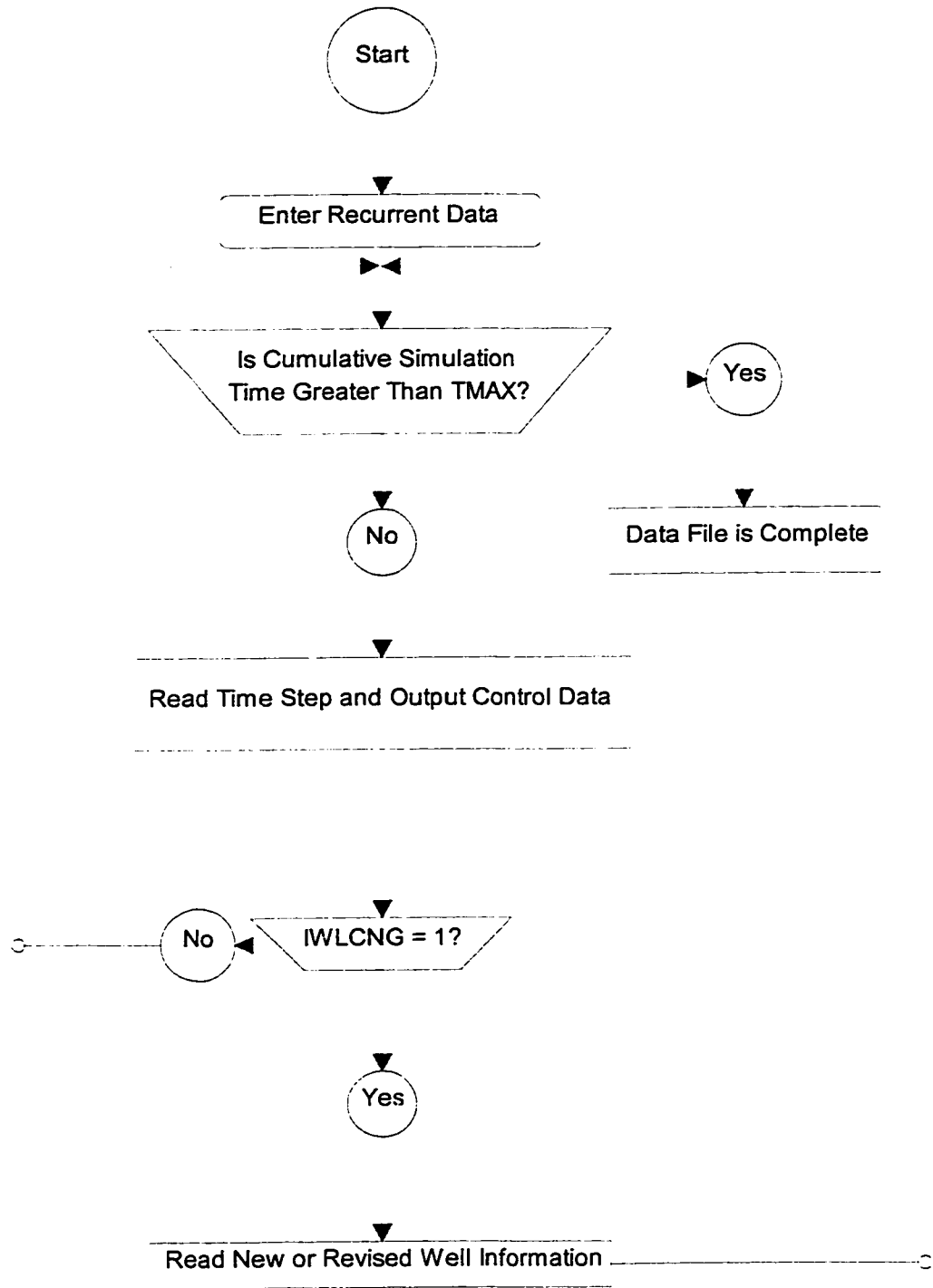


Figure D-2: Recurrent Data Flow Chart

## **Appendix E**

### **Production History Of All Experimental Runs In Tabulated Form**

**Table E-1**

**PRODUCTION HISTORY FOR RUN 1**

$$k_{abs} = 10.554 \mu m^2 \quad k_{owr} = 9.361 \mu m^2 \quad k_{wor} = 4.125 \mu m^2$$

$$IOIP = 908 \text{ ml} \quad \phi = 36.27 \quad S_{or} = 0.23 \quad S_{wc} = 0.129$$

Sample Vol. (ml)	Cum. Vol.	Water Vol.	Cum. water	Oil Vol.	Cum. Oil Vol.	PV Injected	Cum. Oil Rec. %	Oil Cut %	WOR
0.0	0.0	0.0	0.0	0.0	0.0	0.000	0.00	0.00	0.00
50.0	50.0	0.0	0.0	50.0	50.0	0.048	5.51	100.00	0.00
50.0	100.0	5.0	5.0	45.0	95.0	0.096	10.46	90.00	0.11
50.0	150.0	11.2	16.2	38.8	133.8	0.144	14.74	77.60	0.29
50.0	200.0	11.9	28.1	38.1	171.9	0.192	18.93	76.20	0.31
53.0	253.0	10.5	38.6	42.5	214.4	0.243	23.61	80.19	0.25
53.0	306.0	10.5	49.1	42.5	256.9	0.294	28.29	80.19	0.25
50.0	356.0	9.4	58.5	40.6	297.5	0.342	32.76	81.20	0.23
50.0	406.0	8.4	66.9	41.6	339.1	0.390	37.35	83.20	0.20
50.0	456.0	7.8	74.7	42.2	381.3	0.438	41.99	84.40	0.18
50.0	506.0	18.9	93.6	31.1	412.4	0.486	45.42	62.20	0.61
50.0	556.0	31.0	124.6	19.0	431.4	0.534	47.51	38.00	1.63
50.0	606.0	34.8	159.4	15.2	446.6	0.582	49.19	30.40	2.29
50.0	656.0	38.0	197.4	12.0	458.6	0.630	50.51	24.00	3.17
50.0	706.0	40.5	237.9	9.5	468.1	0.678	51.55	19.00	4.26
50.0	756.0	42.0	279.9	8.0	476.1	0.726	52.43	16.00	5.25
55.3	811.3	47.5	327.4	7.8	483.9	0.779	53.29	14.10	6.09
50.0	861.3	43.9	371.3	6.1	490.0	0.827	53.96	12.20	7.20
49.5	910.8	43.9	415.2	5.6	495.6	0.874	54.58	11.31	7.84
52.0	962.8	46.5	461.7	5.5	501.1	0.924	55.19	10.58	8.45
50.0	1012.8	45.2	506.9	4.8	505.9	0.972	55.72	9.60	9.42
50.2	1063.0	46.0	552.9	4.2	510.1	1.020	56.18	8.37	10.95
50.0	1113.0	46.3	599.2	3.7	513.8	1.068	56.59	7.40	12.51
50.2	1163.2	46.0	645.2	4.2	518.0	1.116	57.05	8.37	10.95
50.0	1213.2	46.6	691.8	3.4	521.4	1.164	57.42	6.80	13.71
50.0	1263.2	46.0	737.8	4.0	525.4	1.212	57.86	8.00	11.50
100.0	1363.2	93.0	830.8	7.0	532.4	1.308	58.63	7.00	13.29
100.0	1463.2	93.9	924.7	6.1	538.5	1.404	59.31	6.10	15.39
100.0	1563.2	93.2	1017.9	6.8	545.3	1.500	60.06	6.80	13.71
100.0	1663.2	95.0	1112.9	5.0	550.3	1.596	60.61	5.00	19.00
100.0	1763.2	95.5	1208.4	4.5	554.8	1.692	61.10	4.50	21.22
100.0	1863.2	95.8	1304.2	4.2	559.0	1.788	61.56	4.20	22.81
100.0	1963.2	95.5	1399.7	4.5	563.5	1.884	62.06	4.50	21.22
100.0	2063.2	95.5	1495.2	4.5	568.0	1.980	62.56	4.50	21.22
87.2	2150.4	85.0	1580.2	2.2	570.2	2.064	62.80	2.52	38.64



Table E-2

PRODUCTION HISTORY FOR RUN 2

$$k_{abs} = 11.152 \mu m^2 \quad k_{owr} = 10.679 \mu m^2$$

$$IOIP = 977 \text{ ml} \quad \phi = 36.06 \quad S_{wc} = 0.12$$

Sample Vol. (ml)	Cum. Vol.	Water Vol.	Cum. water	Oil Vol.	Cum. Oil Vol.	PV Injected	Cum. Oil Rec. %	Oil Cut %	WOR
0.0	0.0	0.0	0.0	0.0	0.0	0.000	0.00	0.00	0.00
48.0	48.0	0.0	0.0	48.0	48.0	0.043	4.91	100.00	0.00
48.0	96.0	1.0	1.0	47.0	95.0	0.086	9.73	97.92	0.02
50.0	146.0	8.4	9.4	41.6	136.6	0.132	13.98	83.20	0.20
50.0	196.0	9.5	18.9	40.5	177.1	0.177	18.13	81.00	0.23
50.0	246.0	10.0	28.9	40.0	217.1	0.222	22.23	80.00	0.25
50.0	296.0	10.2	39.1	39.8	256.9	0.267	26.30	79.60	0.26
50.0	346.0	9.2	48.3	40.8	297.7	0.312	30.48	81.60	0.23
50.0	396.0	8.5	56.8	41.5	339.2	0.357	34.73	83.00	0.20
50.0	446.0	8.6	65.4	41.4	380.6	0.402	38.96	82.80	0.21
50.0	496.0	21.0	86.4	29.0	409.6	0.447	41.93	58.00	0.72
50.0	546.0	35.0	121.4	15.0	424.6	0.492	43.47	30.00	2.33
50.0	596.0	38.2	159.6	11.8	436.4	0.537	44.68	23.60	3.24
50.2	646.2	39.6	199.2	10.6	447.0	0.582	45.76	21.12	3.74
50.2	696.4	40.9	240.1	9.3	456.3	0.627	46.71	18.53	4.40
50.0	746.4	41.2	281.3	8.8	465.1	0.672	47.61	17.60	4.68
50.1	796.5	42.2	323.5	7.9	473.0	0.718	48.42	15.77	5.34
50.0	846.5	42.7	366.2	7.3	480.3	0.763	49.17	14.60	5.85
50.0	896.5	43.0	409.2	7.0	487.3	0.808	49.89	14.00	6.14
50.0	946.5	43.5	452.7	6.5	493.8	0.853	50.55	13.00	6.69
50.0	996.5	44.0	496.7	6.0	499.8	0.898	51.17	12.00	7.33
50.0	1046.5	44.2	540.9	5.8	505.6	0.943	51.76	11.60	7.62
50.0	1096.5	45.0	585.9	5.0	510.6	0.988	52.27	10.00	9.00
50.0	1146.5	45.1	631.0	4.9	515.5	1.033	52.77	9.80	9.20
49.9	1196.4	45.3	676.3	4.6	520.1	1.078	53.25	9.22	9.85
50.1	1246.5	45.5	721.8	4.6	524.7	1.123	53.72	9.18	9.89
50.0	1296.5	45.6	767.4	4.4	529.1	1.168	54.17	8.80	10.36
50.0	1346.5	46.2	813.6	3.8	532.9	1.213	54.56	7.60	12.16
50.2	1396.7	46.1	859.7	4.1	537.0	1.258	54.98	8.17	11.24
50.0	1446.7	46.2	905.9	3.8	540.8	1.303	55.36	7.60	12.16
50.0	1496.7	46.5	952.4	3.5	544.3	1.348	55.72	7.00	13.29
50.1	1546.8	46.1	998.5	4.0	548.3	1.394	56.13	7.98	11.53
50.0	1596.8	47.0	1045.5	3.0	551.3	1.439	56.44	6.00	15.67
50.0	1646.8	47.1	1092.6	2.9	554.2	1.484	56.74	5.80	16.24
50.0	1696.8	47.0	1139.6	3.0	557.2	1.529	57.04	6.00	15.67
100.0	1796.8	93.5	1233.1	6.5	563.7	1.619	57.71	6.50	14.38
100.0	1896.8	93.7	1326.8	6.3	570.0	1.709	58.35	6.30	14.87
100.0	1996.8	94.0	1420.8	6.0	576.0	1.799	58.97	6.00	15.67
100.0	2096.8	94.0	1514.8	6.0	582.0	1.889	59.58	6.00	15.67
100.0	2196.8	94.2	1609.0	5.8	587.8	1.979	60.18	5.80	16.24
100.0	2296.8	94.8	1703.8	5.2	593.0	2.069	60.71	5.20	18.23
100.0	2396.8	95.2	1799.0	4.8	597.8	2.159	61.20	4.80	19.83
100.0	2496.8	95.5	1894.5	4.5	602.3	2.249	61.66	4.50	21.22

**Table E-3**

**PRODUCTION HISTORY FOR RUN 3**

$$k_{abs} = 10.066 \mu m^2 \quad k_{owr} = 9.228 \mu m^2$$

$$IOIP = 898 \text{ ml} \quad \phi = 35.87 \quad S_{wc} = 0.117$$

Sample Vol. (ml)	Cum. Vol.	Water Vol.	Cum. water	Oil Vol.	Cum. Oil Vol.	PV Injected	Cum. Oil Rec. %	Oil Cut %	WOR
0.0	0.0	0.0	0.0	0.0	0.0	0.000	0.00	0.00	0.00
50.0	50.0	0.0	0.0	50.0	50.0	0.049	5.57	100.00	0.00
50.0	100.0	0.0	0.0	50.0	100.0	0.098	11.14	100.00	0.00
50.0	150.0	7.0	7.0	43.0	143.0	0.147	15.92	86.00	0.16
50.0	200.0	9.8	16.8	40.2	183.2	0.197	20.40	80.40	0.24
50.0	250.0	10.0	26.8	40.0	223.2	0.246	24.86	80.00	0.25
50.0	300.0	11.0	37.8	39.0	262.2	0.295	29.20	78.00	0.28
50.0	350.0	10.5	48.3	39.5	301.7	0.344	33.60	79.00	0.27
50.0	400.0	10.0	58.3	40.0	341.7	0.393	38.05	80.00	0.25
50.0	450.0	9.0	67.3	41.0	382.7	0.442	42.62	82.00	0.22
50.0	500.0	20.0	87.3	30.0	412.7	0.492	45.96	60.00	0.67
50.0	550.0	33.6	120.9	16.4	429.1	0.541	47.78	32.80	2.05
50.0	600.0	38.0	158.9	12.0	441.1	0.590	49.12	24.00	3.17
50.0	650.0	41.5	200.4	8.5	449.6	0.639	50.07	17.00	4.88
50.0	700.0	42.5	242.9	7.5	457.1	0.688	50.90	15.00	5.67
50.0	750.0	43.2	286.1	6.8	463.9	0.737	51.66	13.60	6.35
50.0	800.0	44.0	330.1	6.0	469.9	0.787	52.33	12.00	7.33
50.0	850.0	44.6	374.7	5.4	475.3	0.836	52.93	10.80	8.26
50.0	900.0	45.0	419.7	5.0	480.3	0.885	53.49	10.00	9.00
50.0	950.0	45.3	465.0	4.7	485.0	0.934	54.01	9.40	9.64
50.0	1000.0	46.0	511.0	4.0	489.0	0.983	54.45	8.00	11.50
50.0	1050.0	45.7	556.7	4.3	493.3	1.032	54.93	8.60	10.63
50.0	1100.0	46.6	603.3	3.4	496.7	1.082	55.31	6.80	13.71
50.0	1150.0	46.7	650.0	3.3	500.0	1.131	55.68	6.60	14.15
50.0	1200.0	47.0	697.0	3.0	503.0	1.180	56.01	6.00	15.67
50.0	1250.0	46.6	743.6	3.4	506.4	1.229	56.39	6.80	13.71
50.0	1300.0	46.9	790.5	3.1	509.5	1.278	56.74	6.20	15.13
100.0	1400.0	93.2	883.7	6.8	516.3	1.377	57.49	6.80	13.71
100.0	1500.0	93.2	976.9	6.8	523.1	1.475	58.25	6.80	13.71
100.2	1600.2	95.1	1072.0	5.1	528.2	1.573	58.82	5.09	18.65
100.1	1700.3	95.2	1167.2	4.9	533.1	1.672	59.37	4.90	19.43
100.0	1800.3	95.0	1262.2	5.0	538.1	1.770	59.92	5.00	19.00
100.0	1900.3	95.1	1357.3	4.9	543.0	1.869	60.47	4.90	19.41
100.1	2000.4	95.4	1452.7	4.7	547.7	1.967	60.99	4.70	20.30
100.2	2100.6	96.0	1548.7	4.2	551.9	2.065	61.46	4.19	22.86
100.0	2200.6	96.0	1644.7	4.0	555.9	2.164	61.90	4.00	24.00

**Table E-4**

**PRODUCTION HISTORY FOR RUN 4**

$$k_{abs} = 9.953 \mu m^2 \quad k_{owr} = 9.229 \mu m^2$$

$$IOIP = 710 \text{ ml} \quad \phi = 36.06 \quad S_{wc} = 0.147$$

Sample Vol. (ml)	Cum. Vol.	Water Vol.	Cum. water	Oil Vol.	Cum. Oil Vol.	PV Injected	Cum. Oil Rec. %	Oil Cut %	WOR
0.0	0.0	0.0	0.0	0.0	0.0	0.000	0.00	0.00	0.00
50.0	50.0	31.3	31.3	18.7	18.7	0.045	2.64	37.40	1.67
50.0	100.0	43.0	74.3	7.0	25.7	0.090	3.62	14.00	6.14
50.0	150.0	44.1	118.4	6.0	31.7	0.135	4.46	11.90	7.40
50.0	200.0	44.2	162.6	5.8	37.5	0.180	5.28	11.60	7.62
50.0	250.0	44.1	206.7	5.9	43.4	0.225	6.11	11.80	7.47
50.0	300.0	43.5	250.1	6.6	49.9	0.270	7.03	13.10	6.63
50.0	350.0	41.1	291.2	8.9	58.8	0.315	8.29	17.80	4.62
50.0	400.0	37.3	328.5	12.7	71.5	0.360	10.08	25.40	2.94
50.0	450.0	35.5	364.0	14.5	86.0	0.405	12.12	29.00	2.45
50.0	500.0	34.6	398.6	15.4	101.4	0.450	14.29	30.80	2.25
50.0	550.0	34.5	433.1	15.6	117.0	0.495	16.48	31.10	2.22
50.0	600.0	37.3	470.3	12.8	129.7	0.541	18.28	25.50	2.92
50.0	650.0	39.4	509.7	10.7	140.4	0.586	19.78	21.30	3.69
50.0	700.0	40.5	550.2	9.5	149.9	0.631	21.12	19.00	4.26
50.0	750.0	41.5	591.6	8.6	158.4	0.676	22.32	17.10	4.85
50.0	800.0	42.0	633.6	8.0	166.4	0.721	23.45	16.00	5.25
50.0	850.0	42.6	676.2	7.5	173.9	0.766	24.50	14.90	5.71
50.0	900.0	42.9	719.1	7.1	181.0	0.811	25.50	14.20	6.04
50.0	950.0	43.5	762.5	6.6	187.5	0.856	26.42	13.10	6.63
50.0	1000.0	43.9	806.4	6.2	193.7	0.901	27.29	12.30	7.13
50.0	1050.0	44.2	850.6	5.8	199.5	0.946	28.11	11.60	7.62
50.0	1100.0	44.5	895.1	5.5	205.0	0.991	28.88	11.00	8.09
50.0	1150.0	45.0	940.1	5.0	210.0	1.036	29.59	10.00	9.00
50.0	1200.0	44.9	985.0	5.1	215.1	1.081	30.31	10.20	8.80
50.0	1250.0	45.1	1030.0	5.0	220.0	1.126	31.00	9.90	9.10
50.0	1300.0	45.4	1075.4	4.6	224.6	1.171	31.65	9.20	9.87
50.0	1350.0	45.7	1121.1	4.4	229.0	1.216	32.26	8.70	10.49
50.0	1400.0	45.7	1166.7	4.4	233.3	1.261	32.88	8.70	10.49
50.0	1450.0	45.6	1212.3	4.4	237.7	1.306	33.50	8.80	10.36
50.0	1500.0	46.0	1258.3	4.0	241.7	1.351	34.06	8.00	11.50
50.0	1550.0	46.0	1304.3	4.0	245.7	1.396	34.62	8.00	11.50
50.0	1600.0	46.0	1350.3	4.0	249.7	1.441	35.19	8.00	11.50
50.0	1650.0	46.2	1396.5	3.8	253.5	1.486	35.72	7.60	12.16
50.0	1700.0	46.6	1443.1	3.4	256.9	1.532	36.20	6.80	13.71
50.0	1750.0	46.4	1489.5	3.6	260.5	1.577	36.71	7.20	12.89
50.0	1800.0	47.0	1536.5	3.0	263.5	1.622	37.13	6.00	15.67
50.0	1850.0	47.0	1583.5	3.0	266.5	1.667	37.56	6.00	15.67
50.0	1900.0	47.0	1630.5	3.0	269.5	1.712	37.98	6.00	15.67
50.0	1950.0	47.0	1677.5	3.0	272.5	1.757	38.40	6.00	15.67
50.0	2000.0	47.2	1724.7	2.8	275.3	1.802	38.80	5.60	16.86
52.0	2052.0	49.0	1773.7	3.0	278.3	1.849	39.22	5.77	16.33

**Table E-5**

**PRODUCTION HISTORY FOR RUN 5**

$$k_{abs} = 10.388 \mu m^2 \quad k_{owr} = 9.894 \mu m^2$$

$$IOIP = 728 \text{ ml} \quad \phi = 36.05 \quad S_{wc} = 0.124$$

Sample Vol. (ml)	Cum. Vol.	Water Vol.	Cum. water	Oil Vol.	Cum. Oil Vol.	PV Injected	Cum. Oil Rec. %	Oil Cut %	WOR
0.0	0.0	0.0	0.0	0.0	0.0	0.000	0.00	0.00	0.00
50.0	50.0	29.0	29.0	21.0	21.0	0.045	2.88	42.00	1.38
50.0	100.0	36.0	65.0	14.0	35.0	0.090	4.80	28.00	2.57
50.0	150.0	43.0	108.0	7.0	42.0	0.135	5.76	14.00	6.14
50.0	200.0	44.0	152.0	6.0	48.0	0.180	6.59	12.00	7.33
50.0	250.0	44.2	196.2	5.8	53.8	0.225	7.38	11.60	7.62
50.0	300.0	45.0	241.2	5.0	58.8	0.270	8.07	10.00	9.00
50.0	350.0	45.0	286.2	5.0	63.8	0.315	8.76	10.00	9.00
50.0	400.0	45.0	331.2	5.0	68.8	0.361	9.44	10.00	9.00
50.0	450.0	45.2	376.4	4.8	73.6	0.406	10.10	9.60	9.42
47.0	497.0	44.0	420.4	3.0	76.6	0.448	10.51	6.38	14.67
49.7	546.7	45.2	465.6	4.5	81.1	0.493	11.13	9.05	10.04
50.0	596.7	45.5	511.1	4.5	85.6	0.538	11.75	9.00	10.11
49.8	646.5	45.5	556.6	4.3	89.9	0.583	12.34	8.63	10.58
60.0	706.5	55.0	611.6	5.0	94.9	0.637	13.03	8.33	11.00
49.7	756.2	45.2	656.8	4.5	99.4	0.682	13.64	9.05	10.04
50.0	806.2	46.0	702.8	4.0	103.4	0.727	14.19	8.00	11.50
50.0	856.2	46.5	749.3	3.5	106.9	0.772	14.67	7.00	13.29
50.0	906.2	46.0	795.3	4.0	110.9	0.817	15.22	8.00	11.50
51.2	957.4	47.4	842.7	3.8	114.7	0.863	15.74	7.42	12.47
51.4	1008.8	47.7	890.4	3.7	118.4	0.909	16.25	7.20	12.89
52.5	1061.3	48.0	938.4	4.5	122.9	0.957	16.87	8.57	10.67
56.8	1118.1	52.2	990.6	4.6	127.5	1.008	17.50	8.10	11.35
50.0	1168.1	46.0	1036.6	4.0	131.5	1.053	18.05	8.00	11.50
49.7	1217.8	46.0	1082.6	3.7	135.2	1.098	18.56	7.44	12.43
52.0	1269.8	48.0	1130.6	4.0	139.2	1.144	19.11	7.69	12.00
52.3	1322.1	49.0	1179.6	3.3	142.5	1.192	19.56	6.31	14.85
52.0	1374.1	48.0	1227.6	4.0	146.5	1.238	20.11	7.69	12.00
51.5	1425.6	48.6	1276.2	2.9	149.4	1.285	20.51	5.63	16.76
45.0	1470.6	41.7	1317.9	3.3	152.7	1.325	20.96	7.33	12.64
50.0	1520.6	47.0	1364.9	3.0	155.7	1.371	21.37	6.00	15.67
49.5	1570.1	46.2	1411.1	3.3	159.0	1.415	21.82	6.67	14.00
38.8	1608.9	35.2	1446.3	3.6	162.6	1.450	22.32	9.28	9.78
66.0	1674.9	59.0	1505.3	7.0	169.6	1.510	23.28	10.61	8.43
50.0	1724.9	46.5	1551.8	3.5	173.1	1.555	23.76	7.00	13.29
50.0	1774.9	47.0	1598.8	3.0	176.1	1.600	24.17	6.00	15.67
49.6	1824.5	46.3	1645.1	3.3	179.4	1.644	24.62	6.65	14.03
49.6	1874.1	46.7	1691.8	2.9	182.3	1.689	25.02	5.85	16.10
50.0	1924.1	47.0	1738.8	3.0	185.3	1.734	25.43	6.00	15.67
49.6	1973.7	47.0	1785.8	2.6	187.9	1.779	25.79	5.24	18.08
50.0	2023.7	47.1	1832.9	2.9	190.8	1.824	26.19	5.80	16.24
49.5	2073.2	46.3	1879.2	3.2	194.0	1.869	26.63	6.46	14.47
50.0	2123.2	47.2	1926.4	2.8	196.8	1.914	27.01	5.60	16.86
50.0	2173.2	46.5	1972.9	3.5	200.3	1.959	27.49	7.00	13.29
50.0	2223.2	47.4	2020.3	2.6	202.9	2.004	27.85	5.20	18.23
49.7	2272.9	47.2	2067.5	2.5	205.4	2.049	28.19	5.03	18.88

**Table E-6**

**PRODUCTION HISTORY FOR RUN 6**

$$k_{abs} = 11.503 \mu m^2 \quad k_{owr} = 10.589 \mu m^2$$

$$IOIP = 751 \text{ ml} \quad \phi = 36.24 \quad S_{wc} = 0.102$$

Sample Vol. (ml)	Cum. Vol.	Water Vol.	Cum. water	Oil Vol.	Cum. Oil Vol.	PV Injected	Cum. Oil Rec. %	Oil Cut %	WOR
0.0	0.0	0.0	0.0	0.0	0.0	0.000	0.00	0.00	0.00
50.0	50.0	35.0	35.0	15.0	15.0	0.045	2.00	30.00	2.33
50.0	100.0	44.0	79.0	6.0	21.0	0.090	2.79	12.00	7.33
50.0	150.0	44.8	123.8	5.2	26.2	0.134	3.49	10.40	8.62
50.0	200.0	45.0	168.8	5.0	31.2	0.179	4.15	10.00	9.00
50.0	250.0	45.0	213.8	5.0	36.2	0.224	4.82	10.00	9.00
50.0	300.0	44.0	257.8	6.0	42.2	0.269	5.62	12.00	7.33
50.0	350.0	41.2	299.0	8.8	51.0	0.314	6.79	17.60	4.68
50.0	400.0	34.0	333.0	16.0	67.0	0.359	8.92	32.00	2.13
50.0	450.0	32.4	365.4	17.6	84.6	0.403	11.26	35.20	1.84
50.0	500.0	34.5	399.9	15.5	100.1	0.448	13.32	31.00	2.23
50.0	550.0	31.1	431.0	18.9	119.0	0.493	15.83	37.80	1.65
50.2	600.2	37.7	468.7	12.5	131.5	0.538	17.50	24.90	3.02
50.0	650.2	36.0	504.7	14.0	145.5	0.583	19.36	28.00	2.57
50.0	700.2	40.2	544.9	9.8	155.3	0.628	20.66	19.60	4.10
50.3	750.5	40.4	585.3	9.9	165.2	0.673	21.98	19.68	4.08
54.5	805.0	45.0	630.3	9.5	174.7	0.722	23.25	17.43	4.74
50.0	855.0	41.7	672.0	8.3	183.0	0.766	24.35	16.60	5.02
50.0	905.0	42.0	714.0	8.0	191.0	0.811	25.41	16.00	5.25
50.0	955.0	42.0	756.0	8.0	199.0	0.856	26.48	16.00	5.25
50.0	1005.0	42.8	798.8	7.2	206.2	0.901	27.44	14.40	5.94
50.0	1055.0	43.1	841.9	6.9	213.1	0.946	28.36	13.80	6.25
50.0	1105.0	43.8	885.7	6.2	219.3	0.991	29.18	12.40	7.06
50.0	1155.0	43.8	929.5	6.2	225.5	1.035	30.01	12.40	7.06
50.0	1205.0	44.0	973.5	6.0	231.5	1.080	30.80	12.00	7.33
50.0	1255.0	44.0	1017.5	6.0	237.5	1.125	31.60	12.00	7.33
50.0	1305.0	44.8	1062.3	5.2	242.7	1.170	32.29	10.40	8.62
50.0	1355.0	44.8	1107.1	5.2	247.9	1.215	32.99	10.40	8.62
50.0	1405.0	44.8	1151.9	5.2	253.1	1.259	33.68	10.40	8.62
50.0	1455.0	45.1	1197.0	4.9	258.0	1.304	34.33	9.80	9.20
50.0	1505.0	44.8	1241.8	5.2	263.2	1.349	35.02	10.40	8.62
50.0	1555.0	45.1	1286.9	4.9	268.1	1.394	35.67	9.80	9.20
50.0	1605.0	45.5	1332.4	4.5	272.6	1.439	36.27	9.00	10.11
50.0	1655.0	45.8	1378.2	4.2	276.8	1.484	36.83	8.40	10.90
50.0	1705.0	46.1	1424.3	3.9	280.7	1.528	37.35	7.80	11.82
50.0	1755.0	46.1	1470.4	3.9	284.6	1.573	37.87	7.80	11.82
50.1	1805.1	47.0	1517.4	3.1	287.7	1.618	38.28	6.19	15.16
50.0	1855.1	47.0	1564.4	3.0	290.7	1.663	38.68	6.00	15.67
52.3	1907.4	48.7	1613.1	3.6	294.3	1.710	39.16	6.88	13.53
50.0	1957.4	47.2	1660.3	2.8	297.1	1.755	39.53	5.60	16.86
50.0	2007.4	47.0	1707.3	3.0	300.1	1.799	39.93	6.00	15.67
50.0	2057.4	47.5	1754.8	2.5	302.6	1.844	40.26	5.00	19.00
50.0	2107.4	47.2	1802.0	2.8	305.4	1.889	40.64	5.60	16.86
50.0	2157.4	47.5	1849.5	2.5	307.9	1.934	40.97	5.00	19.00
50.0	2207.4	47.6	1897.1	2.4	310.3	1.979	41.29	4.80	19.83
50.0	2257.4	47.9	1945.0	2.1	312.4	2.024	41.57	4.20	22.81
50.0	2307.4	48.0	1993.0	2.0	314.4	2.068	41.83	4.00	24.00

**Table E-7**

**PRODUCTION HISTORY FOR RUN 7**

$$k_{abs} = 13.268 \mu m^2 \quad k_{owr} = 11.118 \mu m^2$$

$$IOIP = 735 \text{ ml} \quad \phi = 36.22 \quad S_{wc} = 0.121$$

Sample Vol. (ml)	Cum. Vol.	Water Vol.	Cum. water	Oil Vol.	Cum. Oil Vol.	PV Injected	Cum. Oil Rec. %	Oil Cut %	WOR
0.0	0.0	0.0	0.0	0.0	0.0	0.000	0.00	0.00	0.00
50.0	50.0	39.5	39.5	10.5	10.5	0.045	1.43	21.00	3.76
50.4	100.4	44.0	83.5	6.4	16.9	0.090	2.30	12.70	6.88
50.0	150.4	44.0	127.5	6.0	22.9	0.135	3.12	12.00	7.33
50.0	200.4	43.5	171.0	6.5	29.4	0.180	4.00	13.00	6.69
50.4	250.8	43.5	214.5	6.9	36.3	0.225	4.94	13.69	6.30
50.2	301.0	40.0	254.5	10.2	46.5	0.270	6.33	20.32	3.92
50.1	351.1	29.0	283.5	21.1	67.6	0.315	9.20	42.12	1.37
50.3	401.4	31.0	314.5	19.3	86.9	0.360	11.82	38.37	1.61
50.3	451.7	33.0	347.5	17.3	104.2	0.405	14.18	34.39	1.91
50.1	501.8	34.8	382.3	15.3	119.5	0.450	16.26	30.54	2.27
50.0	551.8	37.0	419.3	13.0	132.5	0.495	18.03	26.00	2.85
50.1	601.9	37.0	456.3	13.1	145.6	0.540	19.81	26.15	2.82
50.0	651.9	38.5	494.8	11.5	157.1	0.585	21.37	23.00	3.35
50.0	701.9	39.5	534.3	10.5	167.6	0.630	22.80	21.00	3.76
50.2	752.1	40.2	574.5	10.0	177.6	0.675	24.16	19.92	4.02
50.0	802.1	40.4	614.9	9.6	187.2	0.719	25.47	19.20	4.21
50.3	852.4	41.2	656.1	9.1	196.3	0.764	26.71	18.09	4.53
50.2	902.6	41.2	697.3	9.0	205.3	0.810	27.93	17.93	4.58
50.0	952.6	42.0	739.3	8.0	213.3	0.854	29.02	16.00	5.25
50.0	1002.6	42.0	781.3	8.0	221.3	0.899	30.11	16.00	5.25
50.1	1052.7	42.5	823.8	7.6	228.9	0.944	31.14	15.17	5.59
50.0	1102.7	42.8	866.6	7.2	236.1	0.989	32.12	14.40	5.94
50.0	1152.7	43.0	909.6	7.0	243.1	1.034	33.07	14.00	6.14
50.1	1202.8	43.6	953.2	6.5	249.6	1.079	33.96	12.97	6.71
50.1	1252.9	43.6	996.8	6.5	256.1	1.124	34.84	12.97	6.71
50.1	1303.0	43.6	1040.4	6.5	262.6	1.169	35.73	12.97	6.71
50.0	1353.0	45.1	1085.5	4.9	267.5	1.213	36.39	9.80	9.20
50.1	1403.1	45.1	1130.6	5.0	272.5	1.258	37.07	9.98	9.02
50.0	1453.1	45.0	1175.6	5.0	277.5	1.303	37.76	10.00	9.00
50.0	1503.1	45.1	1220.7	4.9	282.4	1.348	38.42	9.80	9.20
50.0	1553.1	45.5	1266.2	4.5	286.9	1.393	39.03	9.00	10.11
50.1	1603.2	46.1	1312.3	4.0	290.9	1.438	39.58	7.98	11.53
50.0	1653.2	46.1	1358.4	3.9	294.8	1.483	40.11	7.80	11.82
50.0	1703.2	46.0	1404.4	4.0	298.8	1.528	40.65	8.00	11.50
50.0	1753.2	46.2	1450.6	3.8	302.6	1.572	41.17	7.60	12.16
50.0	1803.2	46.4	1497.0	3.6	306.2	1.617	41.66	7.20	12.89
50.0	1853.2	46.9	1543.9	3.1	309.3	1.662	42.08	6.20	15.13
50.0	1903.2	47.0	1590.9	3.0	312.3	1.707	42.49	6.00	15.67
50.0	1953.2	47.0	1637.9	3.0	315.3	1.752	42.90	6.00	15.67
51.0	2004.2	47.9	1685.8	3.1	318.4	1.797	43.32	6.08	15.45
50.0	2054.2	47.1	1732.9	2.9	321.3	1.842	43.71	5.80	16.24
50.2	2104.4	47.5	1780.4	2.7	324.0	1.887	44.08	5.38	17.59
50.0	2154.4	47.5	1827.9	2.5	326.5	1.932	44.42	5.00	19.00
50.0	2204.4	47.5	1875.4	2.5	329.0	1.977	44.76	5.00	19.00
100.5	2304.9	95.0	1970.4	5.5	334.5	2.067	45.51	5.47	17.27
100.0	2404.9	95.0	2065.4	5.0	339.5	2.157	46.19	5.00	19.00

**Table E-8**

**PRODUCTION HISTORY FOR RUN 8**

$$k_{abs} = 11.815 \mu m^2 \quad k_{owr} = 9.198 \mu m^2$$

$$IOIP = 737 \text{ ml} \quad \phi = 36.20 \quad S_{wc} = 0.118$$

Sample Vol. (ml)	Cum. Vol.	Water Vol.	Cum. water	Oil Vol.	Cum. Oil Vol.	PV Injected	Cum. Oil Rec. %	Oil Cut %	WOR
0.0	0.0	0.0	0.0	0.0	0.0	0.000	0.00	0.00	0.00
50.0	50.0	32.0	32.0	18.0	18.0	0.045	2.44	36.00	1.78
50.0	100.0	43.7	75.7	6.3	24.3	0.090	3.30	12.60	6.94
50.0	150.0	44.2	119.9	5.8	30.1	0.135	4.08	11.60	7.62
50.0	200.0	44.5	164.4	5.5	35.6	0.179	4.83	11.00	8.09
50.0	250.0	38.0	202.4	12.0	47.6	0.224	6.46	24.00	3.17
50.0	300.0	23.7	226.1	26.3	73.9	0.269	10.02	52.60	0.90
50.0	350.0	26.0	252.1	24.0	97.9	0.314	13.28	48.00	1.08
50.0	400.0	27.0	279.1	23.0	120.9	0.359	16.40	46.00	1.17
50.0	450.0	28.0	307.1	22.0	142.9	0.404	19.38	44.00	1.27
50.0	500.0	31.4	338.5	18.6	161.5	0.449	21.90	37.20	1.69
50.0	550.0	34.0	372.5	16.0	177.5	0.494	24.07	32.00	2.13
50.0	600.0	35.5	408.0	14.5	192.0	0.538	26.04	29.00	2.45
50.0	650.0	37.4	445.4	12.6	204.6	0.583	27.75	25.20	2.97
50.0	700.0	38.5	483.9	11.5	216.1	0.628	29.31	23.00	3.35
50.0	750.0	39.5	523.4	10.5	226.6	0.673	30.73	21.00	3.76
50.0	800.0	40.6	564.0	9.4	236.0	0.718	32.01	18.80	4.32
50.0	850.0	41.2	605.2	8.8	244.8	0.763	33.20	17.60	4.68
50.0	900.0	42.0	647.2	8.0	252.8	0.808	34.28	16.00	5.25
50.0	950.0	42.5	689.7	7.5	260.3	0.853	35.30	15.00	5.67
50.0	1000.0	44.0	733.7	6.0	266.3	0.897	36.12	12.00	7.33
50.0	1050.0	44.0	777.7	6.0	272.3	0.942	36.93	12.00	7.33
50.0	1100.0	44.7	822.4	5.3	277.6	0.987	37.65	10.60	8.43
50.0	1150.0	45.0	867.4	5.0	282.6	1.032	38.33	10.00	9.00
50.0	1200.0	45.5	912.9	4.5	287.1	1.077	38.94	9.00	10.11
50.0	1250.0	45.6	958.5	4.4	291.5	1.122	39.53	8.80	10.36
50.0	1300.0	46.0	1004.5	4.0	295.5	1.167	40.08	8.00	11.50
50.0	1350.0	46.0	1050.5	4.0	299.5	1.212	40.62	8.00	11.50
50.0	1400.0	46.0	1096.5	4.0	303.5	1.256	41.16	8.00	11.50
50.0	1450.0	46.0	1142.5	4.0	307.5	1.301	41.70	8.00	11.50
50.0	1500.0	46.0	1188.5	4.0	311.5	1.346	42.25	8.00	11.50
100.0	1600.0	92.4	1280.9	7.6	319.1	1.436	43.28	7.60	12.16
100.0	1700.0	93.1	1374.0	6.9	326.0	1.526	44.21	6.90	13.49
100.0	1800.0	93.2	1467.2	6.8	332.8	1.615	45.13	6.80	13.71
100.0	1900.0	94.0	1561.2	6.0	338.8	1.705	45.95	6.00	15.67
100.0	2000.0	94.1	1655.3	5.9	344.7	1.795	46.75	5.90	15.95
100.0	2100.0	94.9	1750.2	5.1	349.8	1.885	47.44	5.10	18.61
100.0	2200.0	94.8	1845.0	5.2	355.0	1.974	48.14	5.20	18.23
100.0	2300.0	94.9	1939.9	5.1	360.1	2.064	48.84	5.10	18.61
100.0	2400.0	95.0	2034.9	5.0	365.1	2.154	49.51	5.00	19.00
100.0	2500.0	95.7	2130.6	4.3	369.4	2.244	50.10	4.30	22.26

**Table E-9**

**PRODUCTION HISTORY FOR RUN 9**

$$k_{abs} = 10.221 \mu m^2 \quad k_{owr} = 9.865 \mu m^2$$

$$IOIP = 766 \text{ ml} \quad \phi = 36.06 \quad S_{wc} = 0.138$$

Sample Vol. (ml)	Cum. Vol.	Water Vol.	Cum. water	Oil Vol.	Cum. Oil Vol.	PV Injected	Cum. Oil Rec. %	Oil Cut %	WOR
0.0	0.0	0.0	0.0	0.0	0.0	0.000	0.00	0.00	0.00
50.0	50.0	23.6	23.6	26.4	26.4	0.045	3.45	52.80	0.89
50.0	100.0	38.5	62.1	11.5	37.9	0.090	4.95	23.00	3.35
50.0	150.0	38.1	100.2	11.9	49.8	0.135	6.51	23.80	3.20
50.0	200.0	34.2	134.4	15.8	65.6	0.180	8.57	31.60	2.16
50.0	250.0	22.1	156.5	27.9	93.5	0.225	12.22	55.80	0.79
50.0	300.0	23.9	180.4	26.1	119.6	0.270	15.63	52.20	0.92
50.0	350.0	24.5	204.9	25.5	145.1	0.315	18.96	51.00	0.96
50.0	400.0	25.0	229.9	25.0	170.1	0.360	22.22	50.00	1.00
50.0	450.0	25.5	255.4	24.5	194.6	0.405	25.43	49.00	1.04
50.0	500.0	26.0	281.4	24.0	218.6	0.450	28.56	48.00	1.08
50.0	550.0	26.6	308.0	23.4	242.0	0.495	31.62	46.80	1.14
50.0	600.0	29.0	337.0	21.0	263.0	0.541	34.36	42.00	1.38
50.0	650.0	32.0	369.0	18.0	281.0	0.586	36.71	36.00	1.78
50.0	700.0	36.0	405.0	14.0	295.0	0.631	38.54	28.00	2.57
50.0	750.0	38.9	443.9	11.1	306.1	0.676	39.99	22.20	3.50
50.0	800.0	40.5	484.4	9.5	315.6	0.721	41.23	19.00	4.26
50.0	850.0	41.5	525.9	8.5	324.1	0.766	42.35	17.00	4.88
50.0	900.0	42.4	568.3	7.6	331.7	0.811	43.34	15.20	5.58
50.0	950.0	43.2	611.5	6.8	338.5	0.856	44.23	13.60	6.35
50.0	1000.0	44.0	655.5	6.0	344.5	0.901	45.01	12.00	7.33
50.0	1050.0	44.4	699.9	5.6	350.1	0.946	45.74	11.20	7.93
50.0	1100.0	44.6	744.5	5.4	355.5	0.991	46.45	10.80	8.26
50.0	1150.0	45.0	789.5	5.0	360.5	1.036	47.10	10.00	9.00
51.0	1201.0	46.3	835.8	4.7	365.2	1.082	47.72	9.22	9.85
50.0	1251.0	46.0	881.8	4.0	369.2	1.127	48.24	8.00	11.50
50.0	1301.0	46.0	927.8	4.0	373.2	1.172	48.76	8.00	11.50
50.0	1351.0	46.1	973.9	3.9	377.1	1.217	49.27	7.80	11.82
50.0	1401.0	46.1	1020.0	3.9	381.0	1.262	49.78	7.80	11.82
50.0	1451.0	46.5	1066.5	3.5	384.5	1.307	50.24	7.00	13.29
50.0	1501.0	46.5	1113.0	3.5	388.0	1.352	50.69	7.00	13.29
50.0	1551.0	47.0	1160.0	3.0	391.0	1.397	51.09	6.00	15.67



**Table E-10**

**PRODUCTION HISTORY FOR RUN 10**

$$k_{abs} = 9.953 \mu m^2 \quad k_{owr} = 9.229 \mu m^2$$

$$IOIP = 647 \text{ ml} \quad \phi = 36.06 \quad S_{wc} = 0.147$$

Sample Vol. (ml)	Cum. Vol.	Water Vol.	Cum. water	Oil Vol.	Cum. Oil Vol.	PV Injected	Cum. Oil Rec. %	Oil Cut %	WOR
0.0	0.0	0.0	0.0	0.0	0.0	0.000	0.00	0.00	0.00
50.0	50.0	31.0	31.0	16.0	16.0	0.045	2.47	32.00	1.94
50.0	100.0	43.0	74.0	7.0	23.0	0.090	3.55	14.00	6.14
50.0	150.0	44.0	118.0	6.0	29.0	0.135	4.48	12.00	7.33
50.0	200.0	44.2	162.2	5.5	34.5	0.180	5.33	11.00	8.04
50.0	250.0	44.4	206.6	5.0	39.5	0.225	6.11	10.00	8.88
50.0	300.0	44.2	250.8	5.0	44.5	0.270	6.88	10.00	8.84
50.0	350.0	43.6	294.4	6.0	50.5	0.315	7.81	12.00	7.27
50.0	400.0	42.6	337.0	6.5	57.0	0.360	8.81	13.00	6.55
50.0	450.0	41.0	378.0	8.5	65.5	0.405	10.12	17.00	4.82
50.0	500.0	40.2	418.2	9.5	75.0	0.450	11.59	19.00	4.23
50.0	550.0	40.0	458.2	9.5	84.5	0.495	13.06	19.00	4.21
50.0	600.0	40.4	498.6	9.0	93.5	0.541	14.45	18.00	4.49
50.0	650.0	40.8	539.4	8.8	102.3	0.586	15.81	17.60	4.64
50.0	700.0	41.0	580.4	8.5	110.8	0.631	17.13	17.00	4.82
50.0	750.0	41.8	622.2	8.2	119.0	0.676	18.39	16.40	5.10
50.0	800.0	41.9	664.1	8.0	127.0	0.721	19.63	16.00	5.24
50.0	850.0	42.2	706.3	7.5	134.5	0.766	20.79	15.00	5.63
50.0	900.0	42.6	748.9	7.1	141.6	0.811	21.89	14.20	6.00
50.0	950.0	42.6	791.5	7.0	148.6	0.856	22.97	14.00	6.09
50.0	1000.0	43.2	834.7	6.0	154.6	0.901	23.89	12.00	7.20
50.0	1050.0	43.8	878.5	6.0	160.6	0.946	24.82	12.00	7.30
50.0	1100.0	44.0	922.5	6.0	166.6	0.991	25.75	12.00	7.33
50.0	1150.0	44.5	967.0	5.0	171.6	1.036	26.52	10.00	8.90
50.0	1200.0	44.3	1011.3	5.1	176.7	1.081	27.31	10.20	8.69
50.0	1250.0	44.4	1055.7	5.0	181.7	1.126	28.08	10.00	8.88
50.0	1300.0	44.8	1100.5	5.1	186.8	1.171	28.87	10.20	8.78
50.0	1350.0	45.0	1145.5	5.0	191.8	1.216	29.64	10.00	9.00
50.0	1400.0	45.0	1190.5	5.0	196.8	1.261	30.42	10.00	9.00
50.0	1450.0	45.0	1235.5	5.0	201.8	1.306	31.19	10.00	9.00
50.0	1500.0	45.8	1281.3	4.2	206.0	1.351	31.84	8.40	10.90
50.0	1550.0	46.0	1327.3	4.0	210.0	1.396	32.46	8.00	11.50
50.0	1600.0	46.0	1373.3	3.8	213.8	1.441	33.04	7.60	12.11
50.0	1650.0	46.2	1419.5	3.8	217.6	1.486	33.63	7.60	12.16
50.0	1700.0	46.6	1466.1	3.4	221.0	1.532	34.16	6.80	13.71
50.0	1750.0	46.4	1512.5	3.4	224.4	1.577	34.68	6.80	13.65
50.0	1800.0	47.0	1559.5	3.0	227.4	1.622	35.15	6.00	15.67
50.0	1850.0	47.0	1606.5	3.0	230.4	1.667	35.61	6.00	15.67
50.0	1900.0	47.0	1653.5	3.0	233.4	1.712	36.07	6.00	15.67
50.0	1950.0	47.0	1700.5	2.8	236.2	1.757	36.51	5.60	16.79
50.0	2000.0	47.2	1747.7	2.8	239.0	1.802	36.94	5.60	16.86
52.0	2052.0	49.0	1796.7	3.0	242.0	1.849	37.40	5.77	16.33
51.0	2103.0	47.5	1844.2	3.5	245.5	1.895	37.94	6.86	13.57
50.0	2153.0	47.6	1891.8	2.4	247.9	1.940	38.32	4.80	19.83

**Table E-11**

**PRODUCTION HISTORY FOR RUN 11**

$$k_{abs} = 10.306 \mu m^2 \quad k_{owr} = 9.754 \mu m^2 \quad k_{wor} = 2.936 \mu m^2$$

$$IOIP = 922 \text{ ml} \quad \phi = 35.93 \quad S_{wc} = 0.119$$

Sample Vol. (ml)	Cum. Vol.	Water Vol.	Cum. water	Oil Vol.	Cum. Oil Vol.	PV Injected	Cum. Oil Rec. %	Oil Cut %	WOR
0.0	0.0	0.0	0.0	0.0	0.0	0.000	0.00	0.00	0.00
50.0	50.0	0.0	0.0	50.0	50.0	0.048	5.42	100.00	0.00
50.0	100.0	0.0	0.0	50.0	100.0	0.096	10.85	100.00	0.00
50.0	150.0	2.0	2.0	48.0	148.0	0.143	16.05	96.00	0.04
50.0	200.0	8.9	10.9	41.1	189.1	0.191	20.51	82.20	0.22
50.1	250.1	10.0	20.9	40.1	229.2	0.239	24.86	80.04	0.25
50.1	300.2	9.7	30.6	40.4	269.6	0.287	29.24	80.54	0.24
50.1	350.3	10.0	40.6	40.1	309.7	0.335	33.59	80.04	0.25
50.1	400.4	12.0	52.6	38.1	347.8	0.383	37.72	76.05	0.31
50.1	450.5	27.0	79.6	23.1	370.9	0.431	40.23	46.11	1.17
50.0	500.5	32.7	112.3	17.3	388.2	0.478	42.10	34.60	1.89
50.0	550.5	26.8	139.1	23.2	411.4	0.526	44.62	46.40	1.16
50.0	600.5	39.0	178.1	11.0	422.4	0.574	45.81	22.00	3.55
50.0	650.5	41.5	219.6	8.5	430.9	0.622	46.74	17.00	4.88
50.0	700.5	42.8	262.4	7.2	438.1	0.670	47.52	14.40	5.94
50.0	750.5	43.0	305.4	7.0	445.1	0.717	48.28	14.00	6.14
50.0	800.5	43.5	348.9	6.5	451.6	0.765	48.98	13.00	6.69
53.0	853.5	47.2	396.1	5.8	457.4	0.816	49.61	10.94	8.14
50.0	903.5	44.5	440.6	5.5	462.9	0.864	50.21	11.00	8.09
50.0	953.5	45.0	485.6	5.0	467.9	0.912	50.75	10.00	9.00
50.0	1003.5	45.0	530.6	5.0	472.9	0.959	51.29	10.00	9.00
50.0	1053.5	45.0	575.6	5.0	477.9	1.007	51.83	10.00	9.00
50.0	1103.5	46.9	622.5	3.1	481.0	1.055	52.17	6.20	15.13
50.0	1153.5	45.8	668.3	4.2	485.2	1.103	52.62	8.40	10.90
50.0	1203.5	46.5	714.8	3.5	488.7	1.151	53.00	7.00	13.29
50.0	1253.5	46.7	761.5	3.3	492.0	1.198	53.36	6.60	14.15
50.1	1303.6	46.0	807.5	4.1	496.1	1.246	53.81	8.18	11.22

**Table E-12**

**PRODUCTION HISTORY FOR RUN 12**

$$k_{abs} = 10.362 \mu m^2 \quad k_{owr} = 9.978 \mu m^2$$

$$IOIP = 746 \text{ ml} \quad \phi = 36.10 \quad S_{wc} = 0.104$$

Sample Vol. (ml)	Cum. Vol.	Water Vol.	Cum. water	Oil Vol.	Cum. Oil Vol.	PV Injected	Cum. Oil Rec. %	Oil Cut %	WOR
0.0	0.0	0.0	0.0	0.0	0.0	0.000	0.00	0.00	0.00
50.0	50.0	30.4	30.4	19.6	19.6	0.045	2.63	39.20	1.55
50.0	100.0	42.6	73.0	7.4	27.0	0.090	3.62	14.80	5.76
50.0	150.0	44.9	117.9	5.1	32.1	0.135	4.30	10.20	8.80
50.0	200.0	45.2	163.1	4.8	36.9	0.180	4.94	9.60	9.42
50.0	250.0	45.5	208.6	4.5	41.4	0.225	5.55	9.00	10.11
50.0	300.0	45.6	254.2	4.4	45.8	0.270	6.14	8.80	10.36
50.0	350.0	45.5	299.7	4.5	50.3	0.315	6.74	9.00	10.11
50.0	400.0	44.8	344.5	5.2	55.5	0.360	7.43	10.40	8.62
50.0	450.0	43.3	387.8	6.7	62.2	0.405	8.33	13.40	6.46
50.0	500.0	42.1	429.9	7.9	70.1	0.450	9.39	15.80	5.33
50.0	550.0	41.6	471.5	8.4	78.5	0.495	10.52	16.80	4.95
50.0	600.0	40.4	511.9	9.6	88.1	0.540	11.80	19.20	4.21
50.0	650.0	40.8	552.7	9.2	97.3	0.585	13.03	18.40	4.43
50.0	700.0	41.0	593.7	9.0	106.3	0.630	14.24	18.00	4.56
50.0	750.0	41.8	635.5	8.2	114.5	0.675	15.34	16.40	5.10
50.0	800.0	41.9	677.4	8.1	122.6	0.720	16.42	16.20	5.17
50.0	850.0	42.2	719.6	7.8	130.4	0.765	17.47	15.60	5.41
50.0	900.0	42.6	762.2	7.4	137.8	0.810	18.46	14.80	5.76
50.0	950.0	42.6	804.8	7.4	145.2	0.855	19.45	14.80	5.76
50.0	1000.0	43.2	848.0	6.8	152.0	0.900	20.36	13.60	6.35
50.0	1050.0	43.8	891.8	6.2	158.2	0.945	21.19	12.40	7.06
50.0	1100.0	44.0	935.8	6.0	164.2	0.990	22.00	12.00	7.33
50.0	1150.0	44.5	980.3	5.5	169.7	1.035	22.73	11.00	8.09
50.0	1200.0	44.3	1024.6	5.7	175.4	1.080	23.50	11.40	7.77
50.0	1250.0	44.4	1069.0	5.6	181.0	1.125	24.25	11.20	7.93
50.0	1300.0	44.8	1113.8	5.2	186.2	1.170	24.94	10.40	8.62
50.0	1350.0	45.0	1158.8	5.0	191.2	1.215	25.61	10.00	9.00
50.0	1400.0	45.0	1203.8	5.0	196.2	1.260	26.28	10.00	9.00
50.0	1450.0	45.0	1248.8	5.0	201.2	1.305	26.95	10.00	9.00
50.0	1500.0	45.8	1294.6	4.2	205.4	1.350	27.51	8.40	10.90
50.0	1550.0	46.0	1340.6	4.0	209.4	1.395	28.05	8.00	11.50
50.0	1600.0	46.0	1386.6	4.0	213.4	1.440	28.59	8.00	11.50
50.0	1650.0	46.2	1432.8	3.8	217.2	1.485	29.10	7.60	12.16
50.0	1700.0	46.6	1479.4	3.4	220.6	1.530	29.55	6.80	13.71
50.0	1750.0	46.4	1525.8	3.6	224.2	1.575	30.03	7.20	12.89
50.0	1800.0	47.0	1572.8	3.0	227.2	1.620	30.43	6.00	15.67
50.0	1850.0	47.0	1619.8	3.0	230.2	1.665	30.84	6.00	15.67
50.0	1900.0	47.0	1666.8	3.0	233.2	1.710	31.24	6.00	15.67
50.0	1950.0	47.0	1713.8	3.0	236.2	1.755	31.64	6.00	15.67
50.0	2000.0	47.2	1761.0	2.8	239.0	1.800	32.02	5.60	16.86

**Table E-13**

**PRODUCTION HISTORY FOR RUN 13**

$$k_{abs} = 10.127 \mu m^2 \quad k_{owr} = 8.635 \mu m^2$$

$$IOIP = 724 \text{ ml} \quad \phi = 35.88 \quad S_{wc} = 0.126$$

Sample Vol. (ml)	Cum. Vol.	Water Vol.	Cum. water	Oil Vol.	Cum. Oil Vol.	PV Injected	Cum. Oil Rec. %	Oil Cut %	WOR
0.0	0.0	0.0	0.0	0.0	0.0	0.000	0.00	0.00	0.00
50.0	50.0	22.3	22.3	27.7	27.7	0.045	3.83	55.40	0.81
50.0	100.0	35.8	58.1	14.2	41.9	0.091	5.79	28.40	2.52
50.0	150.0	36.5	94.6	13.5	55.4	0.136	7.65	27.00	2.70
50.0	200.0	34.5	129.1	15.5	70.9	0.181	9.79	31.00	2.23
50.0	250.0	29.5	158.6	20.5	91.4	0.226	12.63	41.00	1.44
50.1	300.1	17.6	176.2	32.5	123.9	0.272	17.12	64.87	0.54
50.0	350.1	8.4	184.6	41.6	165.5	0.317	22.86	83.20	0.20
50.0	400.1	12.5	197.1	37.5	203.0	0.362	28.04	75.00	0.33
50.0	450.1	17.6	214.7	32.4	235.4	0.408	32.52	64.80	0.54
50.1	500.2	18.9	233.6	31.2	266.6	0.453	36.83	62.28	0.61
50.1	550.3	19.7	253.3	30.4	297.0	0.498	41.03	60.68	0.65
50.1	600.4	30.0	283.3	20.1	317.1	0.544	43.80	40.12	1.49
50.0	650.4	37.0	320.3	13.0	330.1	0.589	45.60	26.00	2.85
50.0	700.4	40.0	360.3	10.0	340.1	0.634	46.98	20.00	4.00
50.1	750.5	41.2	401.5	8.9	349.0	0.680	48.21	17.76	4.63
50.1	800.6	42.3	443.8	7.8	356.8	0.725	49.29	15.57	5.42
50.0	850.6	43.8	487.6	6.2	363.0	0.770	50.14	12.40	7.06
50.1	900.7	43.5	531.1	6.6	369.6	0.816	51.06	13.17	6.59
50.0	950.7	43.9	575.0	6.1	375.7	0.861	51.90	12.20	7.20
50.0	1000.7	44.0	619.0	6.0	381.7	0.906	52.73	12.00	7.33
50.1	1050.8	44.4	663.4	5.7	387.4	0.952	53.51	11.38	7.79
50.0	1100.8	45.8	709.2	4.2	391.6	0.997	54.09	8.40	10.90
50.0	1150.8	45.8	755.0	4.2	395.8	1.042	54.67	8.40	10.90
50.1	1200.9	45.8	800.8	4.3	400.1	1.087	55.27	8.58	10.65
50.1	1251.0	46.3	847.1	3.8	403.9	1.133	55.79	7.58	12.18
52.0	1303.0	48.0	895.1	4.0	407.9	1.180	56.35	7.69	12.00
50.0	1353.0	46.5	941.6	3.5	411.4	1.225	56.83	7.00	13.29
50.0	1403.0	46.3	987.9	3.7	415.1	1.271	57.34	7.40	12.51
50.0	1453.0	46.6	1034.5	3.4	418.5	1.316	57.81	6.80	13.71
50.1	1503.1	47.2	1081.7	2.9	421.4	1.361	58.21	5.79	16.28

**Table E-14**

**PRODUCTION HISTORY FOR RUN 14**

$$k_{abs} = 10.703 \mu m^2 \quad k_{owr} = 8.002 \mu m^2$$

$$IOIP = 954 \text{ ml} \quad \phi = 36.04 \quad S_{wc} = 0.140$$

Sample Vol. (ml)	Cum. Vol.	Water Vol.	Cum. water	Oil Vol.	Cum. Oil Vol.	PV Injected	Cum. Oil Rec. %	Oil Cut %	WOR
0.0	0.0	0.0	0.0	0.0	0.0	0.000	0.00	0.00	0.00
50.0	50.0	0.0	0.0	50.0	50.0	0.046	5.24	100.00	0.00
50.0	100.0	0.0	0.0	50.0	100.0	0.092	10.48	100.00	0.00
50.0	150.0	0.0	0.0	50.0	150.0	0.138	15.72	100.00	0.00
50.0	200.0	0.0	0.0	50.0	200.0	0.184	20.96	100.00	0.00
50.0	250.0	0.0	0.0	50.0	250.0	0.230	26.21	100.00	0.00
50.1	300.1	1.0	1.0	49.1	299.1	0.277	31.35	98.00	0.02
50.0	350.1	2.0	3.0	48.0	347.1	0.323	36.38	96.00	0.04
50.1	400.2	2.5	5.5	47.6	394.7	0.369	41.37	95.01	0.05
50.0	450.2	2.0	7.5	48.0	442.7	0.415	46.41	96.00	0.04
50.0	500.2	2.0	9.5	48.0	490.7	0.461	51.44	96.00	0.04
50.0	550.2	5.5	15.0	44.5	535.2	0.507	56.10	89.00	0.12
50.2	600.4	26.3	41.3	23.9	559.1	0.553	58.61	47.61	1.10
50.0	650.4	38.4	79.7	11.6	570.7	0.599	59.82	23.20	3.31
50.0	700.4	42.0	121.7	8.0	578.7	0.646	60.66	16.00	5.25
50.1	750.5	42.8	164.5	7.3	586.0	0.692	61.43	14.57	5.86
50.0	800.5	43.5	208.0	6.5	592.5	0.738	62.11	13.00	6.69
50.0	850.5	44.0	252.0	6.0	598.5	0.784	62.74	12.00	7.33
50.0	900.5	45.0	297.0	5.0	603.5	0.830	63.26	10.00	9.00
50.0	950.5	45.1	342.1	4.9	608.4	0.876	63.77	9.80	9.20
50.1	1000.6	45.3	387.4	4.8	613.2	0.922	64.28	9.58	9.44
50.0	1050.6	45.8	433.2	4.2	617.4	0.968	64.72	8.40	10.90
51.0	1101.6	46.5	479.7	4.5	621.9	1.015	65.19	8.82	10.33
50.1	1151.7	46.3	526.0	3.8	625.7	1.061	65.59	7.58	12.18
50.1	1201.8	46.5	572.5	3.6	629.3	1.108	65.97	7.19	12.92

Table E-15

PRODUCTION HISTORY FOR RUN 15

$$k_{abs} = 9.975 \mu m^2 \quad k_{owr} = 9.073 \mu m^2$$

$$IOIP = 700 \text{ ml} \quad \phi = 36.06 \quad S_{wc} = 0.159$$

Sample Vol. (ml)	Cum. Vol.	Water Vol.	Cum. water	Oil Vol.	Cum. Oil Vol.	PV Injected	Cum. Oil Rec. %	Oil Cut %	WOR
0.0	0.0	0.0	0.0	0.0	0.0	0.000	0.00	0.00	0.00
50.0	50.0	30.9	30.9	19.1	19.1	0.045	2.73	38.20	1.62
50.0	100.0	38.3	69.2	11.8	30.9	0.090	4.41	23.50	3.26
50.0	150.0	43.5	112.7	6.5	37.4	0.135	5.34	12.99	6.70
50.0	200.1	44.2	156.9	5.8	43.2	0.180	6.17	11.59	7.63
50.0	250.1	44.2	201.1	5.8	49.0	0.225	7.00	11.59	7.63
50.0	300.1	44.8	246.0	5.2	54.2	0.270	7.74	10.39	8.62
50.0	350.1	44.7	290.7	5.3	59.5	0.315	8.50	10.64	8.39
50.0	400.2	44.6	335.2	5.5	65.0	0.360	9.28	10.94	8.14
50.0	450.2	44.6	379.8	5.4	70.4	0.406	10.05	10.79	8.26
47.8	497.9	43.5	423.3	4.3	74.6	0.449	10.66	8.95	10.17
49.8	547.7	44.2	467.5	5.6	80.2	0.493	11.46	11.20	7.93
50.0	597.7	44.4	511.9	5.6	85.8	0.538	12.27	11.25	7.89
49.9	647.6	44.4	556.3	5.5	91.3	0.583	13.05	10.98	8.11
57.5	705.1	51.3	607.6	6.2	97.5	0.635	13.93	10.74	8.31
49.8	754.9	43.9	651.5	5.9	103.4	0.680	14.77	11.80	7.48
50.0	804.9	44.5	696.0	5.5	108.9	0.725	15.56	11.00	8.09
50.0	854.9	44.7	740.7	5.3	114.2	0.770	16.32	10.65	8.39
50.0	904.9	44.2	784.9	5.8	120.0	0.815	17.14	11.55	7.66
50.9	955.8	45.1	830.0	5.8	125.8	0.861	17.97	11.39	7.78
51.1	1006.8	45.2	875.2	5.9	131.7	0.907	18.81	11.56	7.65
51.9	1058.7	45.2	920.3	6.7	138.4	0.954	19.77	12.96	6.72
55.1	1113.8	48.2	968.5	6.9	145.3	1.003	20.76	12.57	6.96
50.0	1163.8	43.4	1011.9	6.6	151.9	1.048	21.71	13.20	6.58
49.8	1213.6	42.8	1054.7	7.0	158.9	1.093	22.71	14.11	6.09
51.5	1265.1	44.0	1098.6	7.6	166.5	1.140	23.79	14.66	5.82
51.7	1316.8	45.3	1143.9	6.4	172.9	1.186	24.71	12.37	7.08
51.5	1368.3	46.6	1190.5	5.0	177.8	1.233	25.41	9.63	9.38
51.1	1419.5	47.0	1237.5	4.1	182.0	1.279	26.01	8.09	11.36
46.3	1465.7	42.4	1279.9	3.9	185.8	1.320	26.56	8.35	10.97
50.0	1515.7	45.8	1325.7	4.2	190.0	1.365	27.16	8.40	10.90
49.6	1565.3	45.5	1371.2	4.1	194.2	1.410	27.75	8.31	11.03
50.1	1615.4	46.0	1417.2	4.1	198.3	1.455	28.33	8.18	11.22
62.0	1677.4	57.5	1474.7	4.5	202.8	1.511	28.98	7.26	12.78
50.0	1727.4	46.6	1521.3	3.4	206.2	1.556	29.46	6.80	13.71
51.3	1778.7	48.1	1569.4	3.2	209.3	1.602	29.92	6.19	15.16
51.0	1829.7	47.6	1617.0	3.4	212.7	1.648	30.40	6.67	14.00
49.7	1879.5	46.7	1663.6	3.1	215.8	1.693	30.84	6.18	15.17
50.0	1929.5	46.9	1710.5	3.2	219.0	1.738	31.29	6.30	14.88
49.6	1979.1	47.0	1757.5	2.6	221.6	1.783	31.66	5.24	18.08
50.0	2029.1	47.1	1804.6	2.9	224.5	1.828	32.08	5.80	16.24
49.5	2078.6	46.3	1850.9	3.2	227.7	1.873	32.53	6.46	14.47
50.0	2128.6	47.2	1898.1	2.8	230.5	1.918	32.93	5.60	16.86

Table E-16

**PRODUCTION HISTORY FOR RUN 16**

$k_{abs} = 10.227 \mu m^2$        $k_{owr} = 8.947 \mu m^2$        $\phi = 35.92$   
 IOIP = 733 ml       $S_{wc} = 0.116$       Polymer Concentration = 500 PPM

Sample Vol. (ml)	Cum. Vol.	Water Vol.	Cum. water	Oil Vol.	Cum. Oil Vol.	PV Injected	Cum. Oil Rec. %	Oil Cut %	WOR
0.0	0.0	0.0	0.0	0.0	0.0	0.000	0.00	0.00	0.00
50.0	50.0	31.0	31.0	19.0	19.0	0.045	2.59	38.00	1.63
50.0	100.0	41.7	72.7	8.3	27.3	0.090	3.73	16.60	5.02
50.0	150.0	42.3	115.0	7.7	35.0	0.136	4.78	15.40	5.49
50.0	200.0	41.6	156.6	8.4	43.4	0.181	5.92	16.80	4.95
50.0	250.0	35.8	192.4	14.2	57.6	0.226	7.86	28.40	2.52
50.1	300.1	13.6	206.0	36.5	94.1	0.271	12.84	72.85	0.37
50.2	350.3	11.0	217.0	39.2	133.3	0.317	18.19	78.09	0.28
50.0	400.3	13.5	230.5	36.5	169.8	0.362	23.17	73.00	0.37
50.0	450.3	14.7	245.2	35.3	205.1	0.407	27.99	70.60	0.42
50.0	500.3	13.1	258.3	36.9	242.0	0.452	33.02	73.80	0.36
50.0	550.3	13.2	271.5	36.8	278.8	0.498	38.04	73.60	0.36
50.0	600.3	21.1	292.6	28.9	307.7	0.543	41.99	57.80	0.73
50.0	650.3	24.0	316.6	26.0	333.7	0.588	45.53	52.00	0.92
50.2	700.5	25.0	341.6	25.2	358.9	0.634	48.97	50.20	0.99
50.0	750.5	26.0	367.6	24.0	382.9	0.679	52.25	48.00	1.08
51.5	802.0	28.5	396.1	23.0	405.9	0.725	55.39	44.66	1.24
50.0	852.0	29.3	425.4	20.7	426.6	0.771	58.21	41.40	1.42
50.0	902.0	30.0	455.4	20.0	446.6	0.816	60.94	40.00	1.50
50.0	952.0	37.0	492.4	13.0	459.6	0.861	62.71	26.00	2.85
50.0	1002.0	40.7	533.1	9.3	468.9	0.906	63.98	18.60	4.38
50.0	1052.0	43.5	576.6	6.5	475.4	0.951	64.87	13.00	6.69
50.0	1102.0	45.0	621.6	5.0	480.4	0.997	65.55	10.00	9.00
50.3	1152.3	46.0	667.6	4.3	484.7	1.042	66.14	8.55	10.70
50.0	1202.3	47.3	714.9	2.7	487.4	1.087	66.51	5.40	17.52
50.0	1252.3	47.4	762.3	2.6	490.0	1.133	66.86	5.20	18.23
100.2	1352.5	96.2	858.5	4.0	494.0	1.223	67.41	3.99	24.05
100.0	1452.5	96.7	955.2	3.3	497.3	1.314	67.86	3.30	29.30

**Table E-17**

**PRODUCTION HISTORY FOR RUN 17**

$k_{abs} = 12.533 \mu m^2$        $k_{owr} = 11.264 \mu m^2$        $\phi = 35.98$   
 IOIP = 746 ml       $S_{wc} = 0.115$       Polymer Concentration = 1000 PPM

Sample Vol. (ml)	Cum. Vol.	Water Vol.	Cum. water	Oil Vol.	Cum. Oil Vol.	PV Injected	Cum. Oil Rec. %	Oil Cut %	WOR
0.0	0.0	0.0	0.0	0.0	0.0	0.000	0.00	0.00	0.00
50.0	50.0	35.5	35.5	14.5	14.5	0.045	1.94	29.00	2.45
50.0	100.0	42.9	78.4	7.1	21.6	0.090	2.90	14.20	6.04
50.0	150.0	42.6	121.0	7.4	29.0	0.135	3.89	14.80	5.76
50.0	200.0	42.3	163.3	7.7	36.7	0.179	4.92	15.40	5.49
50.0	250.0	37.0	200.3	13.0	49.7	0.224	6.66	26.00	2.85
50.1	300.1	15.3	215.6	34.8	84.5	0.269	11.33	69.46	0.44
50.0	350.1	12.8	228.4	37.2	121.7	0.314	16.32	74.40	0.34
51.8	401.9	12.0	240.4	39.8	161.5	0.361	21.66	76.83	0.30
48.7	450.6	10.6	251.0	38.1	199.6	0.404	26.77	78.23	0.28
50.0	500.6	11.0	262.0	39.0	238.6	0.449	32.00	78.00	0.28
50.0	550.6	15.5	277.5	34.5	273.1	0.494	36.62	69.00	0.45
50.1	600.7	19.3	296.8	30.8	303.9	0.539	40.75	61.48	0.63
50.1	650.8	22.0	318.8	28.1	332.0	0.584	44.52	56.09	0.78
50.1	700.9	24.1	342.9	26.0	358.0	0.629	48.01	51.90	0.93
50.0	750.9	24.8	367.7	25.2	383.2	0.674	51.39	50.40	0.98
50.0	800.9	24.8	392.5	25.2	408.4	0.719	54.77	50.40	0.98
50.0	850.9	25.7	418.2	24.3	432.7	0.764	58.02	48.60	1.06
50.0	900.9	32.0	450.2	18.0	450.7	0.809	60.44	36.00	1.78
50.0	950.9	36.0	486.2	14.0	464.7	0.853	62.32	28.00	2.57
50.0	1000.9	37.0	523.2	13.0	477.7	0.898	64.06	26.00	2.85
50.0	1050.9	38.0	561.2	12.0	489.7	0.943	65.67	24.00	3.17
50.0	1100.9	40.0	601.2	10.0	499.7	0.988	67.01	20.00	4.00
50.1	1151.0	43.0	644.2	7.1	506.8	1.033	67.96	14.17	6.06
50.0	1201.0	45.0	689.2	5.0	511.8	1.078	68.63	10.00	9.00
50.0	1251.0	46.7	735.9	3.3	515.1	1.123	69.07	6.60	14.15
50.0	1301.0	48.0	783.9	2.0	517.1	1.168	69.34	4.00	24.00
50.0	1351.0	48.1	832.0	1.9	519.0	1.212	69.60	3.80	25.32



**Table E-18**

**PRODUCTION HISTORY FOR RUN 18**

$k_{abs} = 10.994 \mu m^2$        $k_{owr} = 9.132 \mu m^2$        $\phi = 36.20$   
 IOIP = 734 ml       $S_{wc} = 0.108$       Polymer Concentration = 1500 PPM

Sample Vol. (ml)	Cum. Vol.	Water Vol.	Cum. water	Oil Vol.	Cum. Oil Vol.	PV Injected	Cum. Oil Rec. %	Oil Cut %	WOR
0.0	0.0	0.0	0.0	0.0	0.0	0.000	0.00	0.00	0.00
50.0	50.0	35.0	35.0	15.0	15.0	0.045	2.04	30.00	2.33
50.0	100.0	43.1	78.1	6.9	21.9	0.090	2.98	13.80	6.25
50.0	150.0	42.6	120.7	7.4	29.3	0.135	3.99	14.80	5.76
50.0	200.0	42.0	162.7	8.0	37.3	0.181	5.08	16.00	5.25
50.0	250.0	32.0	194.7	18.0	55.3	0.226	7.53	36.00	1.78
50.0	300.0	13.2	207.9	36.8	92.1	0.271	12.54	73.60	0.36
50.0	350.0	10.8	218.7	39.2	131.3	0.316	17.87	78.40	0.28
50.0	400.0	10.0	228.7	40.0	171.3	0.361	23.32	80.00	0.25
50.0	450.0	9.7	238.4	40.3	211.6	0.406	28.80	80.60	0.24
50.2	500.2	10.0	248.4	40.2	251.8	0.452	34.27	80.08	0.25
50.0	550.2	12.6	261.0	37.4	289.2	0.497	39.37	74.80	0.34
50.1	600.3	14.0	275.0	36.1	325.3	0.542	44.28	72.06	0.39
50.0	650.3	16.6	291.6	33.4	358.7	0.587	48.83	66.80	0.50
50.2	700.5	22.0	313.6	28.2	386.9	0.633	52.66	56.18	0.78
50.0	750.5	25.0	338.6	25.0	411.9	0.678	56.07	50.00	1.00
45.0	795.5	23.7	362.3	21.3	433.2	0.718	58.97	47.33	1.11
55.0	850.5	30.5	392.8	24.5	457.7	0.768	62.30	44.55	1.24
50.1	900.6	28.5	421.3	21.6	479.3	0.813	65.24	43.11	1.32
50.1	950.7	31.1	452.4	19.0	498.3	0.859	67.83	37.92	1.64
50.0	1000.7	35.3	487.7	14.7	513.0	0.904	69.83	29.40	2.40
50.0	1050.7	39.2	526.9	10.8	523.8	0.949	71.30	21.60	3.63
50.0	1100.7	42.2	569.1	7.8	531.6	0.994	72.36	15.60	5.41
50.0	1150.7	44.4	613.5	5.6	537.2	1.039	73.12	11.20	7.93
50.1	1200.8	46.0	659.5	4.1	541.3	1.084	73.68	8.18	11.22
50.0	1250.8	46.5	706.0	3.5	544.8	1.129	74.16	7.00	13.29
50.2	1301.0	48.6	754.6	1.6	546.4	1.175	74.37	3.19	30.38
49.9	1350.9	48.2	802.8	1.7	548.1	1.220	74.61	3.41	28.35

Table E-19

PRODUCTION HISTORY FOR RUN 19

$k_{abs} = 10.758 \mu m^2$        $k_{owr} = 9.205 \mu m^2$        $\phi = 35.85$   
 IOIP = 730 ml       $S_{wc} = 0.118$       Polymer Concentration = 2000 PPM

Sample Vol. (ml)	Cum. Vol.	Water Vol.	Cum. water	Oil Vol.	Cum. Oil Vol.	PV Injected	Cum. Oil Rec. %	Oil Cut %	WOR
0.0	0.0	0.0	0.0	0.0	0.0	0.000	0.00	0.00	0.00
50.0	50.0	30.0	30.0	20.0	20.0	0.045	2.74	40.00	1.50
50.0	100.0	41.5	71.5	8.5	28.5	0.091	3.91	17.00	4.88
50.0	150.0	42.0	113.5	8.0	36.5	0.136	5.00	16.00	5.25
50.0	200.0	42.0	155.5	8.0	44.5	0.181	6.10	16.00	5.25
50.0	250.0	39.6	195.1	10.4	54.9	0.227	7.52	20.80	3.81
50.2	300.2	21.0	216.1	29.2	84.1	0.272	11.53	58.17	0.72
50.0	350.2	10.0	226.1	40.0	124.1	0.317	17.01	80.00	0.25
50.0	400.2	9.0	235.1	41.0	165.1	0.363	22.63	82.00	0.22
50.0	450.2	8.0	243.1	42.0	207.1	0.408	28.38	84.00	0.19
50.0	500.2	10.0	253.1	40.0	247.1	0.453	33.87	80.00	0.25
50.0	550.2	11.5	264.6	38.5	285.6	0.499	39.14	77.00	0.30
50.0	600.2	14.7	279.3	35.3	320.9	0.544	43.98	70.60	0.42
50.0	650.2	17.2	296.5	32.8	353.7	0.589	48.48	65.60	0.52
50.0	700.2	21.6	318.1	28.4	382.1	0.634	52.37	56.80	0.76
50.0	750.2	23.8	341.9	26.2	408.3	0.680	55.96	52.40	0.91
51.2	801.4	25.7	367.6	25.5	433.8	0.726	59.45	49.80	1.01
50.0	851.4	26.7	394.3	23.3	457.1	0.771	62.65	46.60	1.15
50.0	901.4	32.6	426.9	17.4	474.5	0.817	65.03	34.80	1.87
50.0	951.4	37.1	464.0	12.9	487.4	0.862	66.80	25.80	2.88
50.0	1001.4	38.1	502.1	11.9	499.3	0.907	68.43	23.80	3.20
50.0	1051.4	40.0	542.1	10.0	509.3	0.953	69.80	20.00	4.00
50.0	1101.4	42.1	584.2	7.9	517.2	0.998	70.88	15.80	5.33
50.0	1151.4	44.1	628.3	5.9	523.1	1.043	71.69	11.80	7.47
50.0	1201.4	46.0	674.3	4.0	527.1	1.089	72.24	8.00	11.50
50.0	1251.4	46.8	721.1	3.2	530.3	1.134	72.68	6.40	14.63
50.1	1301.5	48.5	769.6	1.6	531.9	1.179	72.90	3.19	30.31

**Table E-20**

**PRODUCTION HISTORY FOR RUN 20**

$$k_{abs} = 10.257 \mu m^2 \quad k_{owr} = 8.868 \mu m^2 \quad \phi = 36.03$$

$$IOIP = 725 \text{ ml} \quad S_{wc} = 0.129 \quad \text{Polymer Concentration} = 500 \text{ PPM}$$

Sample Vol. (ml)	Cum. Vol.	Water Vol.	Cum. water	Oil Vol.	Cum. Oil Vol.	PV Injected	Cum. Oil Rec. %	Oil Cut %	WOR
0.0	0.0	0.0	0.0	0.0	0.0	0.000	0.00	0.00	0.00
41.0	41.0	27.1	27.1	13.9	13.9	0.037	1.92	33.90	1.95
50.0	91.0	41.2	68.3	8.8	22.7	0.082	3.13	17.60	4.68
50.0	141.0	41.5	109.8	8.5	31.2	0.127	4.30	17.00	4.88
50.0	191.0	41.1	150.9	8.9	40.1	0.172	5.53	17.80	4.62
50.0	241.0	39.0	189.9	11.0	51.1	0.217	7.05	22.00	3.55
50.0	291.0	25.4	215.3	24.6	75.7	0.262	10.44	49.20	1.03
50.0	341.0	13.9	229.2	36.1	111.8	0.308	15.42	72.20	0.39
50.0	391.0	11.0	240.2	39.0	150.8	0.353	20.81	78.00	0.28
50.0	441.0	12.2	252.4	37.8	188.6	0.398	26.02	75.60	0.32
50.0	491.0	14.4	266.8	35.6	224.2	0.443	30.93	71.20	0.40
50.0	541.0	15.4	282.2	34.6	258.8	0.488	35.71	69.20	0.45
50.2	591.2	13.1	295.3	37.1	295.9	0.533	40.82	73.90	0.35
50.0	641.2	21.0	316.3	29.0	324.9	0.578	44.82	58.00	0.72
50.0	691.2	24.9	341.2	25.1	350.0	0.623	48.29	50.20	0.99
50.0	741.2	27.6	368.8	22.4	372.4	0.668	51.38	44.80	1.23
50.1	791.3	28.0	396.8	22.1	394.5	0.714	54.43	44.11	1.27
50.0	841.3	30.0	426.8	20.0	414.5	0.759	57.19	40.00	1.50
50.0	891.3	31.0	457.8	19.0	433.5	0.804	59.81	38.00	1.63
50.0	941.3	35.3	493.1	14.7	448.2	0.849	61.84	29.40	2.40
50.0	991.3	38.8	531.9	11.2	459.4	0.894	63.38	22.40	3.46
50.0	1041.3	41.5	573.4	8.5	467.9	0.939	64.55	17.00	4.88
50.0	1091.3	44.8	618.2	5.2	473.1	0.984	65.27	10.40	8.62
50.1	1141.4	44.3	662.5	5.8	478.9	1.029	66.07	11.58	7.64
50.0	1191.4	45.0	707.5	5.0	483.9	1.074	66.76	10.00	9.00
50.6	1242.0	46.0	753.5	4.6	488.5	1.120	67.40	9.09	10.00
100.0	1342.0	94.0	847.5	6.0	494.5	1.210	68.22	6.00	15.67
100.0	1442.0	97.0	944.5	3.0	497.5	1.300	68.64	3.00	32.33
100.0	1542.0	97.3	1041.8	2.7	500.2	1.391	69.01	2.70	36.04
100.0	1642.0	98.0	1139.8	2.0	502.2	1.481	69.29	2.00	49.00

**Table E-21**

**PRODUCTION HISTORY FOR RUN 21**

$$k_{abs} = 10.115 \mu m^2 \quad k_{owr} = 8.924 \mu m^2 \quad \phi = 36.06$$

$$IOIP = 737 \text{ ml} \quad S_{wc} = 0.114 \quad \text{Polymer Concentration} = 500 \text{ PPM}$$

Sample Vol. (ml)	Cum. Vol.	Water Vol.	Cum. water	Oil Vol.	Cum. Oil Vol.	PV Injected	Cum. Oil Rec. %	Oil Cut %	WOR
0.0	0.0	0.0	0.0	0.0	0.0	0.000	0.00	0.00	0.00
50.0	50.0	34.5	34.5	15.5	15.5	0.045	2.10	31.00	2.23
50.0	100.0	42.4	76.9	7.6	23.1	0.090	3.13	15.20	5.58
50.0	150.0	42.6	119.5	7.4	30.5	0.135	4.14	14.80	5.76
50.0	200.0	42.0	161.5	8.0	38.5	0.180	5.22	16.00	5.25
50.0	250.0	32.9	194.4	17.1	55.6	0.225	7.54	34.20	1.92
50.1	300.1	11.0	205.4	39.1	94.7	0.270	12.84	78.04	0.28
50.0	350.1	10.0	215.4	40.0	134.7	0.315	18.27	80.00	0.25
50.1	400.2	13.8	229.2	36.3	171.0	0.361	23.19	72.46	0.38
50.1	450.3	13.8	243.0	36.3	207.3	0.406	28.11	72.46	0.38
50.0	500.3	12.5	255.5	37.5	244.8	0.451	33.20	75.00	0.33
50.1	550.4	16.0	271.5	34.1	278.9	0.496	37.82	68.06	0.47
50.0	600.4	20.0	291.5	30.0	308.9	0.541	41.89	60.00	0.67
50.0	650.4	25.6	317.1	24.4	333.3	0.586	45.20	48.80	1.05
50.1	700.5	28.5	345.6	21.6	354.9	0.631	48.13	43.11	1.32
50.0	750.5	29.4	375.0	20.6	375.5	0.676	50.92	41.20	1.43
50.1	800.6	30.0	405.0	20.1	395.6	0.721	53.65	40.12	1.49
50.1	850.7	33.9	438.9	16.2	411.8	0.766	55.85	32.34	2.09
50.0	900.7	37.0	475.9	13.0	424.8	0.811	57.61	26.00	2.85
50.0	950.7	40.0	515.9	10.0	434.8	0.856	58.97	20.00	4.00
50.0	1000.7	42.0	557.9	8.0	442.8	0.902	60.05	16.00	5.25
50.0	1050.7	43.0	600.9	7.0	449.8	0.947	61.00	14.00	6.14
50.0	1100.7	43.6	644.5	6.4	456.2	0.992	61.87	12.80	6.81
50.0	1150.7	44.9	689.4	5.1	461.3	1.037	62.56	10.20	8.80
50.0	1200.7	45.6	735.0	4.4	465.7	1.082	63.16	8.80	10.36
50.0	1250.7	46.6	781.6	3.4	469.1	1.127	63.62	6.80	13.71
50.0	1300.7	47.1	828.7	2.9	472.0	1.172	64.01	5.80	16.24
50.0	1350.7	47.7	876.4	2.3	474.3	1.217	64.32	4.60	20.74

**Table E-22**

**PRODUCTION HISTORY FOR RUN 22**

$k_{abs} = 10.153 \mu m^2$        $k_{owr} = 9.001 \mu m^2$        $\phi = 36.26$   
 IOIP = 653 ml       $S_{wc} = 0.123$       Polymer Concentration = 500 PPM

Sample Vol. (ml)	Cum. Vol.	Water Vol.	Cum. water	Oil Vol.	Cum. Oil Vol.	PV Injected	Cum. Oil Rec. %	Oil Cut %	WOR
0.0	0.0	0.0	0.0	0.0	0.0	0.000	0.00	0.00	0.00
50.0	50.0	35.3	35.3	14.7	14.7	0.045	2.25	29.40	2.40
50.0	100.0	44.0	79.3	6.0	20.7	0.090	3.17	12.00	7.33
50.0	150.0	45.3	124.6	4.7	25.4	0.134	3.89	9.40	9.64
50.0	200.0	45.5	170.1	4.5	29.9	0.179	4.58	9.00	10.11
50.1	250.1	45.2	215.3	4.9	34.8	0.224	5.33	9.78	9.22
50.0	300.1	43.0	258.3	7.0	41.8	0.269	6.40	14.00	6.14
50.1	350.2	20.2	278.5	29.9	71.7	0.314	10.98	59.68	0.68
50.0	400.2	10.0	288.5	40.0	111.7	0.359	17.11	80.00	0.25
50.0	450.2	11.3	299.8	38.7	150.4	0.403	23.04	77.40	0.29
50.0	500.2	14.9	314.7	35.1	185.5	0.448	28.42	70.20	0.42
50.0	550.2	15.8	330.5	34.2	219.7	0.493	33.66	68.40	0.46
50.0	600.2	18.7	349.2	31.3	251.0	0.538	38.45	62.60	0.60
50.0	650.2	22.2	371.4	27.8	278.8	0.583	42.71	55.60	0.80
52.5	702.7	27.4	398.8	25.1	303.9	0.630	46.55	47.81	1.09
50.0	752.7	29.1	427.9	20.9	324.8	0.674	49.76	41.80	1.39
51.8	804.5	33.0	460.9	18.8	343.6	0.721	52.64	36.29	1.76
50.0	854.5	33.0	493.9	17.0	360.6	0.766	55.24	34.00	1.94
50.0	904.5	33.8	527.7	16.2	376.8	0.811	57.72	32.40	2.09
50.0	954.5	38.2	565.9	11.8	388.6	0.855	59.53	23.60	3.24
50.0	1004.5	42.0	607.9	8.0	396.6	0.900	60.76	16.00	5.25
50.0	1054.5	44.0	651.9	6.0	402.6	0.945	61.67	12.00	7.33
50.0	1104.5	45.5	697.4	4.5	407.1	0.990	62.36	9.00	10.11
50.1	1154.6	46.1	743.5	4.0	411.1	1.035	62.98	7.98	11.53
51.4	1206.0	47.8	791.3	3.6	414.7	1.081	63.53	7.00	13.28
50.0	1256.0	46.5	837.8	3.5	418.2	1.125	64.06	7.00	13.29
50.0	1306.0	47.3	885.1	2.7	420.9	1.170	64.48	5.40	17.52
50.0	1356.0	47.6	932.7	2.4	423.3	1.215	64.85	4.80	19.83
50.1	1406.1	48.3	981.0	1.8	425.1	1.260	65.12	3.59	26.83
100.1	1506.2	96.2	1077.2	3.9	429.0	1.350	65.72	3.90	24.67

**Table E-23**

**PRODUCTION HISTORY FOR RUN 23**

$k_{abs} = 9.674 \mu m^2$        $k_{owr} = 8.263 \mu m^2$        $\phi = 35.85$   
 IOIP = 773 ml       $S_{wc} = 0.124$       Polymer Concentration = 500 PPM

Sample Vol. (ml)	Cum. Vol.	Water Vol.	Cum. water	Oil Vol.	Cum. Oil Vol.	PV Injected	Cum. Oil Rec. %	Oil Cut %	WOR
0.0	0.0	0.0	0.0	0.0	0.0	0.000	0.00	0.00	0.00
50.0	50.0	22.4	22.4	27.6	27.6	0.045	3.57	55.20	0.81
50.0	100.0	37.3	59.7	12.7	40.3	0.091	5.21	25.40	2.94
50.0	150.0	37.6	97.3	12.4	52.7	0.136	6.82	24.80	3.03
50.0	200.0	36.5	133.8	13.5	66.2	0.181	8.56	27.00	2.70
50.1	250.1	14.0	147.8	36.1	102.3	0.227	13.23	72.06	0.39
50.0	300.1	10.6	158.4	39.4	141.7	0.272	18.33	78.80	0.27
50.0	350.1	10.0	168.4	40.0	181.7	0.317	23.50	80.00	0.25
50.0	400.1	9.2	177.6	40.8	222.5	0.363	28.78	81.60	0.23
50.0	450.1	10.7	188.3	39.3	261.8	0.408	33.86	78.60	0.27
50.0	500.1	12.5	200.8	37.5	299.3	0.453	38.71	75.00	0.33
50.0	550.1	17.1	217.9	32.9	332.2	0.498	42.97	65.80	0.52
50.1	600.2	21.0	238.9	29.1	361.3	0.544	46.73	58.08	0.72
50.0	650.2	23.9	262.8	26.1	387.4	0.589	50.11	52.20	0.92
50.1	700.3	26.5	289.3	23.6	411.0	0.635	53.16	47.11	1.12
50.0	750.3	26.4	315.7	23.6	434.6	0.680	56.21	47.20	1.12
50.0	800.3	28.5	344.2	21.5	456.1	0.725	58.99	43.00	1.33
50.0	850.3	32.0	376.2	18.0	474.1	0.770	61.32	36.00	1.78
50.0	900.3	36.3	412.5	13.7	487.8	0.816	63.09	27.40	2.65
50.0	950.3	40.9	453.4	9.1	496.9	0.861	64.27	18.20	4.49
51.7	1002.0	44.3	497.7	7.4	504.3	0.908	65.23	14.31	5.99
51.1	1053.1	44.8	542.5	6.3	510.6	0.954	66.04	12.33	7.11
52.0	1105.1	47.0	589.5	5.0	515.6	1.001	66.69	9.62	9.40
50.0	1155.1	45.4	634.9	4.6	520.2	1.047	67.28	9.20	9.87
50.0	1205.1	45.6	680.5	4.4	524.6	1.092	67.85	8.80	10.36
50.0	1255.1	46.0	726.5	4.0	528.6	1.137	68.37	8.00	11.50
50.0	1305.1	47.1	773.6	2.9	531.5	1.183	68.75	5.80	16.24

**Table E-24**

**PRODUCTION HISTORY FOR RUN 24**

$k_{abs} = 10.890 \mu m^2$        $k_{owr} = 9.388 \mu m^2$        $\phi = 35.95$   
 IOIP = 491 ml       $S_{wc} = 0.112$       Polymer Concentration = 500 PPM

Sample Vol. (ml)	Cum. Vol.	Water Vol.	Cum. water	Oil Vol.	Cum. Oil Vol.	PV Injected	Cum. Oil Rec. %	Oil Cut %	WOR
0.0	0.0	0.0	0.0	0.0	0.0	0.000	0.00	0.00	0.00
50.0	50.0	37.2	37.2	12.8	12.8	0.045	2.61	25.60	2.91
50.0	100.0	45.3	82.5	4.7	17.5	0.090	3.57	9.40	9.64
50.0	150.0	46.6	129.1	3.4	20.9	0.136	4.26	6.80	13.71
50.0	200.0	46.8	175.9	3.2	24.1	0.181	4.91	6.40	14.63
50.0	250.0	46.3	222.2	3.7	27.8	0.226	5.67	7.40	12.51
50.0	300.0	46.2	268.4	3.8	31.6	0.271	6.44	7.60	12.16
50.0	350.0	46.6	315.0	3.4	35.0	0.317	7.13	6.80	13.71
50.0	400.0	45.2	360.2	4.8	39.8	0.362	8.11	9.60	9.42
50.0	450.0	44.2	404.4	5.8	45.6	0.407	9.29	11.60	7.62
50.0	500.0	33.0	437.4	17.0	62.6	0.452	12.76	34.00	1.94
50.0	550.0	20.5	457.9	29.5	92.1	0.497	18.77	59.00	0.69
50.0	600.0	19.6	477.5	30.4	122.5	0.543	24.96	60.80	0.64
50.0	650.0	21.0	498.5	29.0	151.5	0.588	30.87	58.00	0.72
50.0	700.0	23.6	522.1	26.4	177.9	0.633	36.25	52.80	0.89
50.0	750.0	26.0	548.1	24.0	201.9	0.678	41.14	48.00	1.08
50.0	800.0	27.8	575.9	22.2	224.1	0.724	45.67	44.40	1.25
50.0	850.0	30.8	606.7	19.2	243.3	0.769	49.58	38.40	1.60
50.0	900.0	34.6	641.3	15.4	258.7	0.814	52.72	30.80	2.25
50.0	950.0	38.3	679.6	11.7	270.4	0.859	55.10	23.40	3.27
50.0	1000.0	40.8	720.4	9.2	279.6	0.904	56.98	18.40	4.43
50.0	1050.0	42.6	763.0	7.4	287.0	0.950	58.49	14.80	5.76
50.0	1100.0	44.3	807.3	5.7	292.7	0.995	59.65	11.40	7.77
50.0	1150.0	46.0	853.3	4.0	296.7	1.040	60.46	8.00	11.50
50.0	1200.0	47.1	900.4	2.9	299.6	1.085	61.05	5.80	16.24
50.0	1250.0	48.0	948.4	2.0	301.6	1.130	61.46	4.00	24.00
50.0	1300.0	48.6	997.0	1.4	303.0	1.176	61.75	2.80	34.71

**Table E-25**

**PRODUCTION HISTORY FOR RUN 25**

$k_{abs} = 9.994 \mu m^2$        $k_{owr} = 9.746 \mu m^2$        $\phi = 36.17$   
 IOIP = 741 ml       $S_{wc} = 0.112$       Polymer Concentration = 500 PPM

Sample Vol. (ml)	Cum. Vol.	Water Vol.	Cum. water	Oil Vol.	Cum. Oil Vol.	PV Injected	Cum. Oil Rec. %	Oil Cut %	WOR
0.0	0.0	0.0	0.0	0.0	0.0	0.000	0.00	0.00	0.00
50.0	50.0	33.8	33.8	16.2	16.2	0.045	2.19	32.40	2.09
50.0	100.0	44.0	77.8	6.0	22.2	0.090	3.00	12.00	7.33
50.0	150.0	44.7	122.5	5.3	27.5	0.135	3.71	10.60	8.43
50.0	200.0	42.8	165.3	7.2	34.7	0.180	4.68	14.40	5.94
50.1	250.1	27.9	193.2	22.2	56.9	0.225	7.68	44.31	1.26
51.3	301.4	11.0	204.2	40.3	97.2	0.271	13.12	78.56	0.27
50.1	351.5	11.5	215.7	38.6	135.8	0.316	18.33	77.05	0.30
50.0	401.5	16.7	232.4	33.3	169.1	0.361	22.82	66.60	0.50
50.1	451.6	17.3	249.7	32.8	201.9	0.406	27.25	65.47	0.53
50.1	501.7	19.0	268.7	31.1	233.0	0.451	31.45	62.08	0.61
50.0	551.7	22.1	290.8	27.9	260.9	0.496	35.21	55.80	0.79
50.0	601.7	26.8	317.6	23.2	284.1	0.541	38.35	46.40	1.16
50.1	651.8	30.0	347.6	20.1	304.2	0.586	41.06	40.12	1.49
50.0	701.8	32.8	380.4	17.2	321.4	0.630	43.38	34.40	1.91
50.0	751.8	34.3	414.7	15.7	337.1	0.675	45.50	31.40	2.18
50.0	801.8	34.5	449.2	15.5	352.6	0.720	47.59	31.00	2.23
50.0	851.8	35.0	484.2	15.0	367.6	0.765	49.62	30.00	2.33
50.0	901.8	35.4	519.6	14.6	382.2	0.810	51.59	29.20	2.42
50.0	951.8	38.0	557.6	12.0	394.2	0.855	53.21	24.00	3.17
50.1	1001.9	40.2	597.8	9.9	404.1	0.900	54.54	19.76	4.06
50.0	1051.9	41.3	639.1	8.7	412.8	0.945	55.72	17.40	4.75
53.8	1105.7	46.2	685.3	7.6	420.4	0.993	56.74	14.13	6.08
50.0	1155.7	44.1	729.4	5.9	426.3	1.038	57.54	11.80	7.47
50.0	1205.7	44.7	774.1	5.3	431.6	1.083	58.25	10.60	8.43
50.0	1255.7	45.8	819.9	4.2	435.8	1.128	58.82	8.40	10.90
50.0	1305.7	46.5	866.4	3.5	439.3	1.173	59.29	7.00	13.29



**Table E-26**

**PRODUCTION HISTORY FOR RUN 26**

$$k_{abs} = 8.975 \mu m^2 \quad k_{owr} = 7.926 \mu m^2 \quad \phi = 36.11$$

$$IOIP = 726 \text{ ml} \quad S_{wc} = 0.129 \quad \text{Polymer Concentration} = 500 \text{ PPM}$$

Sample Vol. (ml)	Cum. Vol.	Water Vol.	Cum. water	Oil Vol.	Cum. Oil Vol.	PV Injected	Cum. Oil Rec. %	Oil Cut %	WOR
0.0	0.0	0.0	0.0	0.0	0.0	0.000	0.00	0.00	0.00
50.2	50.2	27.5	27.5	22.7	22.7	0.045	3.13	45.22	1.21
50.1	100.3	37.1	64.6	13.0	35.7	0.090	4.92	25.95	2.85
50.1	150.4	36.5	101.1	13.6	49.3	0.135	6.79	27.15	2.68
50.1	200.5	33.9	135.0	16.2	65.5	0.180	9.02	32.34	2.09
50.2	250.7	28.7	163.7	21.5	87.0	0.226	11.98	42.83	1.33
50.0	300.7	15.6	179.3	34.4	121.4	0.271	16.72	68.80	0.45
51.8	352.5	10.0	189.3	41.8	163.2	0.317	22.47	80.69	0.24
50.3	402.8	8.5	197.8	41.8	205.0	0.362	28.23	83.10	0.20
50.1	452.9	9.0	206.8	41.1	246.1	0.407	33.89	82.04	0.22
51.9	504.8	13.0	219.8	38.9	285.0	0.454	39.24	74.95	0.33
50.3	555.1	14.9	234.7	35.4	320.4	0.499	44.12	70.38	0.42
50.0	605.1	24.8	259.5	25.2	345.6	0.544	47.59	50.40	0.98
50.1	655.2	30.4	289.9	19.7	365.3	0.589	50.30	39.32	1.54
50.0	705.2	31.3	321.2	18.7	384.0	0.634	52.88	37.40	1.67
50.2	755.4	31.8	353.0	18.4	402.4	0.680	55.41	36.65	1.73
50.0	805.4	32.3	385.3	17.7	420.1	0.725	57.85	35.40	1.82
50.2	855.6	34.0	419.3	16.2	436.3	0.770	60.08	32.27	2.10
50.0	905.6	34.8	454.1	15.2	451.5	0.815	62.17	30.40	2.29
50.0	955.6	39.0	493.1	11.0	462.5	0.860	63.68	22.00	3.55
50.0	1005.6	44.0	537.1	6.0	468.5	0.905	64.51	12.00	7.33
50.0	1055.6	45.6	582.7	4.4	472.9	0.950	65.12	8.80	10.36
50.0	1105.6	46.5	629.2	3.5	476.4	0.995	65.60	7.00	13.29
50.1	1155.7	47.5	676.7	2.6	479.0	1.040	65.96	5.19	18.27
50.0	1205.7	47.4	724.1	2.6	481.6	1.085	66.31	5.20	18.23

**Table E-27**

**PRODUCTION HISTORY FOR RUN 27**

$$k_{abs} = 9.22 \mu m^2 \quad k_{owr} = 8.901 \mu m^2 \quad \phi = 36.30$$

$$IOIP = 920 \text{ ml} \quad S_{wc} = 0.140 \quad \text{Horizontal Wells}$$

Sample Vol. (ml)	Cum. Vol.	Water Vol.	Cum. water	Oil Vol.	Cum. Oil Vol.	PV Injected	Cum. Oil Rec. %	Oil Cut %	WOR
0.0	0.0	0.0	0.0	0.0	0.0	0.000	0.00	0.00	0.00
50.0	50.0	0.0	0.0	50.0	50.0	0.047	5.43	100.00	0.00
50.0	100.0	0.0	0.0	50.0	100.0	0.093	10.87	100.00	0.00
50.0	150.0	0.0	0.0	50.0	150.0	0.140	16.30	100.00	0.00
50.0	200.0	0.0	0.0	50.0	200.0	0.187	21.74	100.00	0.00
50.0	250.0	14.1	14.1	35.9	235.9	0.234	25.64	71.80	0.39
50.0	300.0	21.9	36.0	28.1	264.0	0.280	28.70	56.20	0.78
50.0	350.0	27.8	63.8	22.2	286.2	0.327	31.11	44.40	1.25
50.0	400.0	29.9	93.7	20.1	306.3	0.374	33.29	40.20	1.49
50.0	450.0	32.9	126.6	17.1	323.4	0.421	35.15	34.20	1.92
50.0	500.0	34.8	161.4	15.2	338.6	0.467	36.80	30.40	2.29
50.0	550.0	38.5	199.9	11.5	350.1	0.514	38.05	23.00	3.35
50.0	600.0	38.9	238.8	11.1	361.2	0.561	39.26	22.20	3.50
50.0	650.0	40.9	279.7	9.1	370.3	0.607	40.25	18.20	4.49
50.0	700.0	41.3	321.0	8.7	379.0	0.654	41.20	17.40	4.75
50.0	750.0	42.8	363.8	7.2	386.2	0.701	41.98	14.40	5.94
50.0	800.0	42.5	406.3	7.5	393.7	0.748	42.79	15.00	5.67
50.0	850.0	43.0	449.3	7.0	400.7	0.794	43.55	14.00	6.14
50.0	900.0	43.7	493.0	6.3	407.0	0.841	44.24	12.60	6.94
50.0	950.0	43.8	536.8	6.2	413.2	0.888	44.91	12.40	7.06
50.0	1000.0	44.7	581.5	5.3	418.5	0.935	45.49	10.60	8.43
50.0	1050.0	44.3	625.8	5.7	424.2	0.981	46.11	11.40	7.77
50.0	1100.0	45.1	670.9	4.9	429.1	1.028	46.64	9.80	9.20
50.0	1150.0	46.0	716.9	4.0	433.1	1.075	47.08	8.00	11.50
51.0	1201.0	46.0	762.9	5.0	438.1	1.122	47.62	9.80	9.20
50.0	1251.0	46.5	809.4	3.5	441.6	1.169	48.00	7.00	13.29
50.1	1301.1	46.7	856.1	3.4	445.0	1.216	48.37	6.79	13.74
50.0	1351.1	46.6	902.7	3.4	448.4	1.263	48.74	6.80	13.71
50.0	1401.1	46.7	949.4	3.3	451.7	1.309	49.10	6.60	14.15
100.0	1501.1	93.0	1042.4	7.0	458.7	1.403	49.86	7.00	13.29

**Table E-28**

**PRODUCTION HISTORY FOR RUN 28**

$k_{abs} = 9.983 \mu m^2$        $k_{owr} = 9.606 \mu m^2$        $\phi = 38.45$   
 IOIP = 753 ml       $S_{wc} = 0.151$       Horizontal Wells

Sample Vol. (ml)	Cum. Vol.	Water Vol.	Cum. water	Oil Vol.	Cum. Oil Vol.	PV Injected	Cum. Oil Rec. %	Oil Cut %	WOR
0.0	0.0	0.0	0.0	0.0	0.0	0.000	0.00	0.00	0.00
50.0	50.0	0.0	0.0	50.0	50.0	0.042	6.64	100.00	0.00
50.0	100.0	15.0	15.0	35.0	85.0	0.084	11.28	70.00	0.43
50.0	150.0	28.5	43.5	21.5	106.5	0.127	14.14	43.00	1.33
50.0	200.0	26.1	69.6	23.9	130.4	0.169	17.31	47.80	1.09
50.0	250.0	19.8	89.4	30.2	160.6	0.211	21.32	60.40	0.66
50.0	300.0	28.0	117.4	22.0	182.6	0.253	24.24	44.00	1.27
50.0	350.0	32.8	150.2	17.2	199.8	0.296	26.52	34.40	1.91
50.0	400.0	35.5	185.7	14.5	214.3	0.338	28.45	29.00	2.45
50.0	450.0	37.4	223.1	12.6	226.9	0.380	30.12	25.20	2.97
50.0	500.0	39.4	262.5	10.6	237.5	0.422	31.53	21.20	3.72
50.0	550.0	40.0	302.5	10.0	247.5	0.465	32.86	20.00	4.00
50.0	600.0	41.6	344.1	8.4	255.9	0.507	33.97	16.80	4.95
50.0	650.0	42.0	386.1	8.0	263.9	0.549	35.03	16.00	5.25
50.0	700.0	42.7	428.8	7.3	271.2	0.591	36.00	14.60	5.85
50.0	750.0	43.5	472.3	6.5	277.7	0.634	36.87	13.00	6.69
50.0	800.0	43.7	516.0	6.3	284.0	0.676	37.70	12.60	6.94
50.0	850.0	44.0	560.0	6.0	290.0	0.718	38.50	12.00	7.33
50.0	900.0	44.0	604.0	6.0	296.0	0.760	39.30	12.00	7.33
50.0	950.0	44.6	648.6	5.4	301.4	0.803	40.01	10.80	8.26
61.3	1011.3	55.0	703.6	6.3	307.7	0.854	40.85	10.28	8.73
100.0	1111.3	90.0	793.6	10.0	317.7	0.939	42.18	10.00	9.00
100.0	1211.3	91.5	885.1	8.5	326.2	1.023	43.30	8.50	10.76
100.0	1311.3	92.0	977.1	8.0	334.2	1.108	44.37	8.00	11.50
100.0	1411.3	93.0	1070.1	7.0	341.2	1.192	45.30	7.00	13.29
91.0	1502.3	84.6	1154.7	6.4	347.6	1.269	46.15	7.03	13.22

**Table E-29**

**PRODUCTION HISTORY FOR RUN 29**

$k_{abs} = 9.847 \mu m^2$        $k_{avr} = 8.532 \mu m^2$        $\phi = 37.79$   
 IOIP = 751 ml       $S_{wc} = 0.139$       Vertical Injector/Horizontal Producer

Sample Vol. (ml)	Cum. Vol.	Water Vol.	Cum. water	Oil Vol.	Cum. Oil Vol.	PV Injected	Cum. Oil Rec. %	Oil Cut %	WOR
0.0	0.0	0.0	0.0	0.0	0.0	0.000	0.00	0.00	0.00
50.0	50.0	0.0	0.0	50.0	50.0	0.043	6.66	100.00	0.00
50.0	100.0	9.4	9.4	40.6	90.6	0.086	12.07	81.20	0.23
50.0	150.0	24.1	33.5	25.9	116.5	0.129	15.52	51.80	0.93
50.0	200.0	23.9	57.4	26.1	142.6	0.172	19.00	52.20	0.92
50.0	250.0	22.0	79.4	28.0	170.6	0.215	22.73	56.00	0.79
50.0	300.0	21.9	101.3	28.1	198.7	0.258	26.47	56.20	0.78
50.0	350.0	28.0	129.3	22.0	220.7	0.301	29.40	44.00	1.27
50.0	400.0	31.0	160.3	19.0	239.7	0.344	31.93	38.00	1.63
50.0	450.0	32.0	192.3	18.0	257.7	0.387	34.33	36.00	1.78
49.2	499.2	34.9	227.2	14.3	272.0	0.429	36.24	29.07	2.44
50.0	549.2	37.5	264.7	12.5	284.5	0.472	37.90	25.00	3.00
50.0	599.2	38.0	302.7	12.0	296.5	0.515	39.50	24.00	3.17
50.0	649.2	40.0	342.7	10.0	306.5	0.558	40.83	20.00	4.00
50.0	699.2	41.0	383.7	9.0	315.5	0.601	42.03	18.00	4.56
50.0	749.2	39.5	423.2	10.5	326.0	0.644	43.43	21.00	3.76
50.0	799.2	43.9	467.1	6.1	332.1	0.687	44.24	12.20	7.20
50.0	849.2	44.5	511.6	5.5	337.6	0.730	44.97	11.00	8.09
50.3	899.5	44.2	555.8	6.1	343.7	0.773	45.79	12.13	7.25
50.0	949.5	45.5	601.3	4.5	348.2	0.816	46.39	9.00	10.11
50.0	999.5	45.6	646.9	4.4	352.6	0.859	46.97	8.80	10.36
55.5	1055.0	50.5	697.4	5.0	357.6	0.907	47.64	9.01	10.10
50.0	1105.0	45.9	743.3	4.1	361.7	0.950	48.18	8.20	11.20
50.0	1155.0	45.4	788.7	4.6	366.3	0.993	48.80	9.20	9.87
56.9	1211.9	51.8	840.5	5.1	371.4	1.042	49.48	8.96	10.16
50.0	1261.9	47.7	888.2	2.3	373.7	1.085	49.78	4.60	20.74
49.8	1311.7	45.4	933.6	4.4	378.1	1.128	50.37	8.84	10.32
50.0	1361.7	46.0	979.6	4.0	382.1	1.171	50.90	8.00	11.50
50.2	1411.9	47.0	1026.6	3.2	385.3	1.214	51.33	6.37	14.69
95.5	1507.4	88.6	1115.2	6.9	392.2	1.296	52.25	7.23	12.84

## Appendix F

### Production History Of All Experimental Runs

# Production History for Experimental Run 1

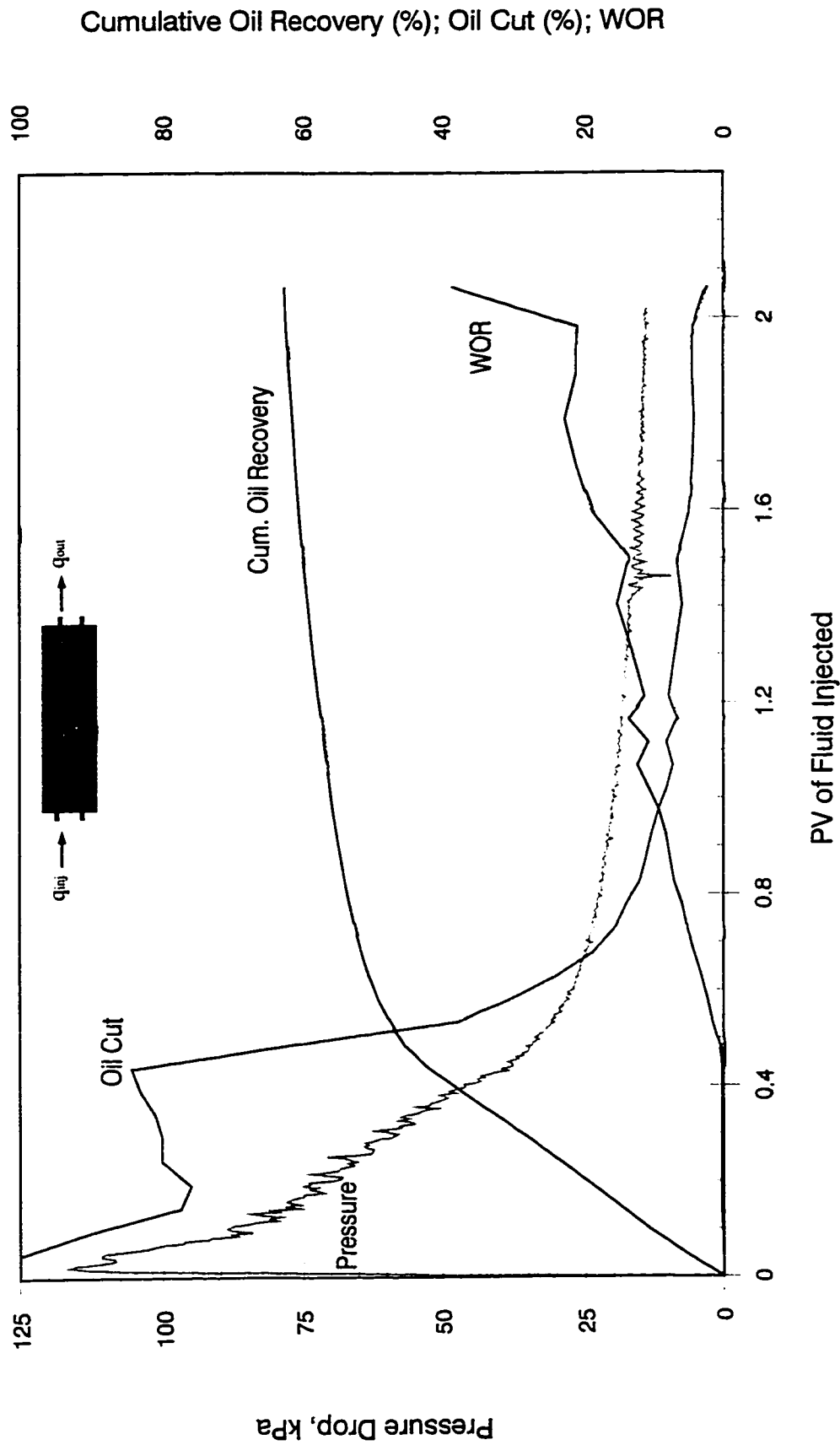


Figure F-i: Homogeneous Pack Waterflood ( Injection Rate = 450 cc/hr, Oil Viscosity = 34.3 mPa.s )

# Production History for Experimental Run 2

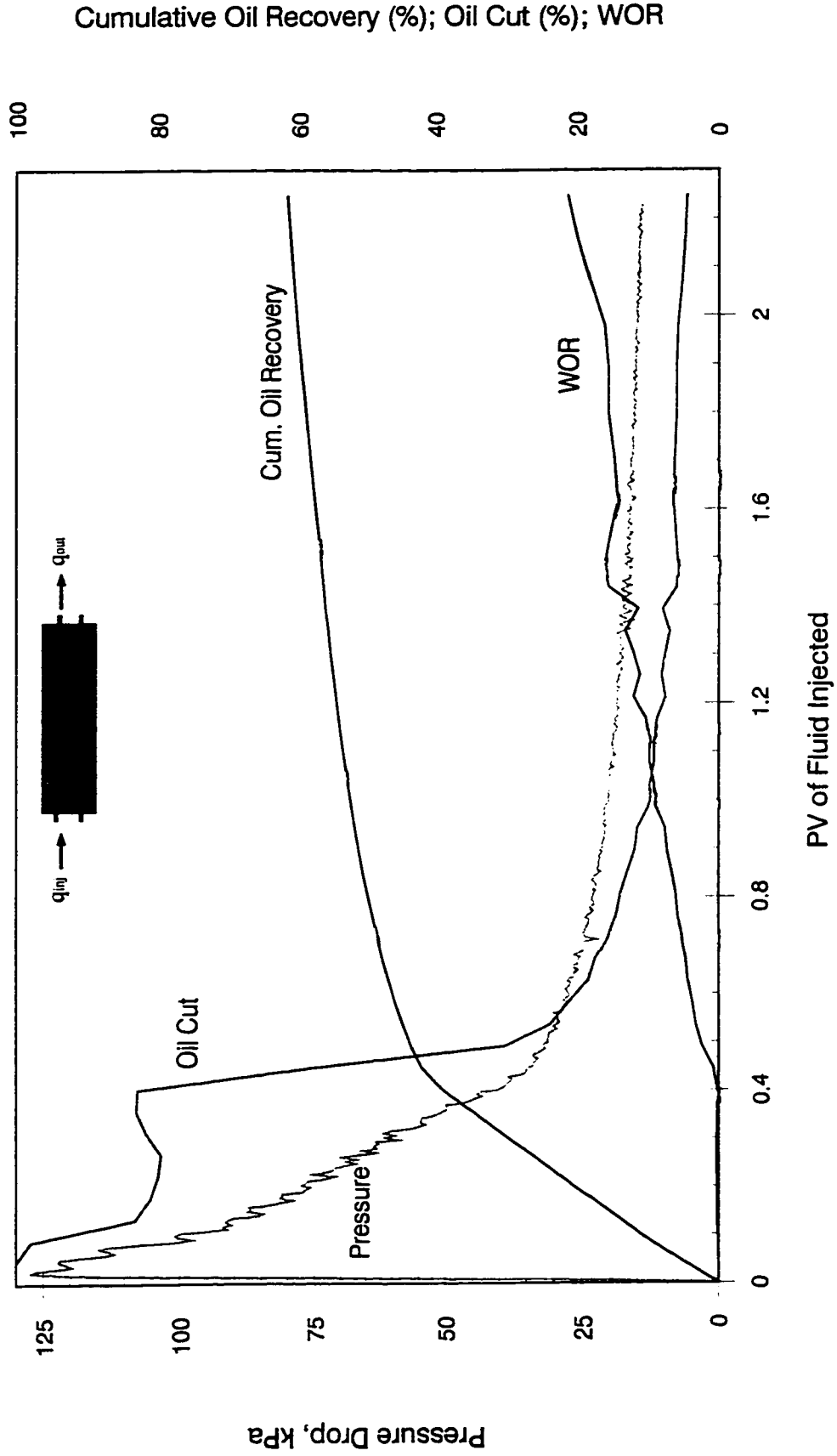


Figure F-2: Homogeneous Pack Waterflood ( Injection Rate = 600 cc/hr, Oil Viscosity = 34.3 mPa.s )

### Production History for Experimental Run 3

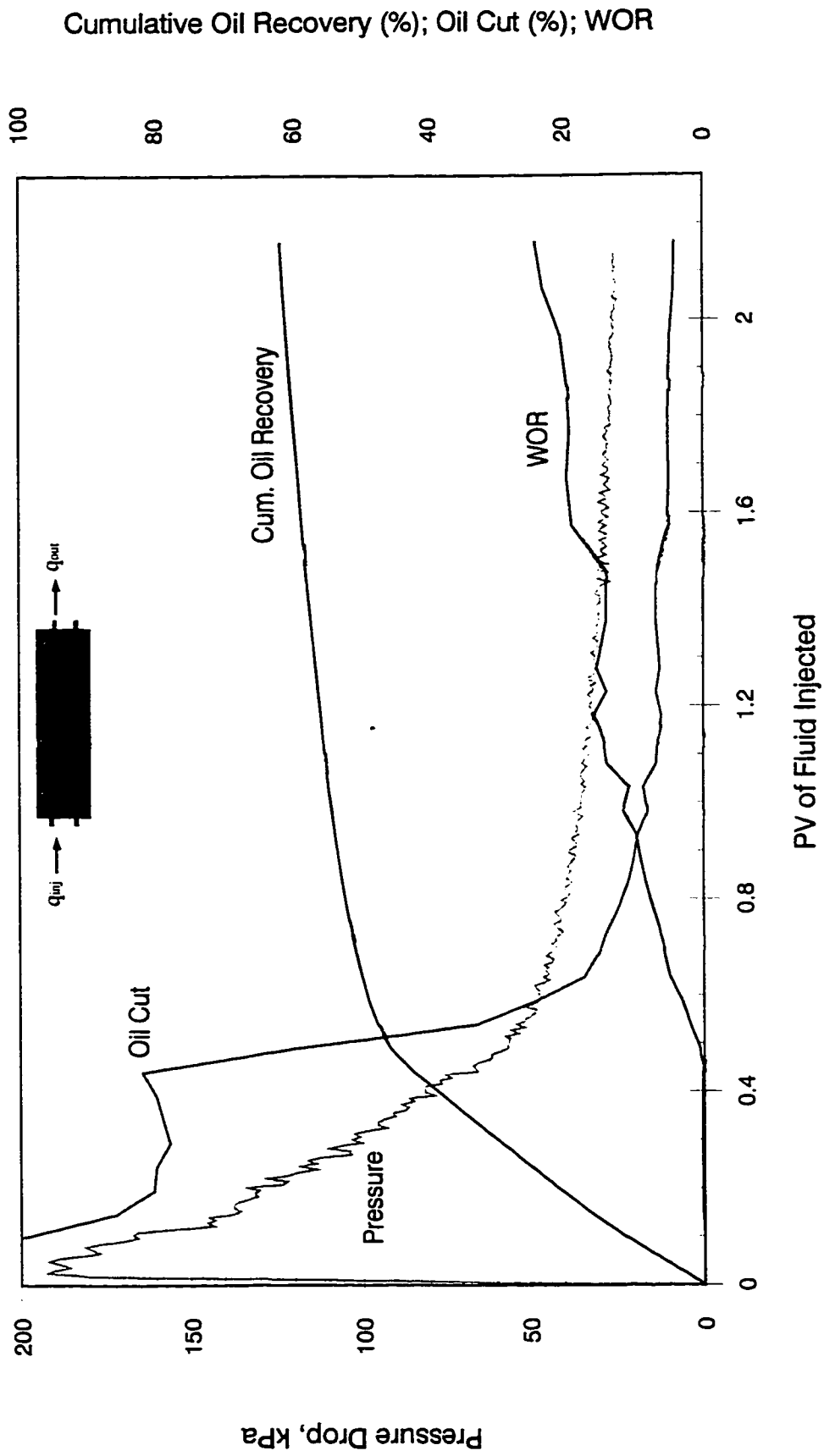


Figure F-3: Homogeneous Pack Waterflood ( Injection Rate = 750 cc/hr, Oil Viscosity = 34.3 mPa.s )



### Production History for Experimental Run 4

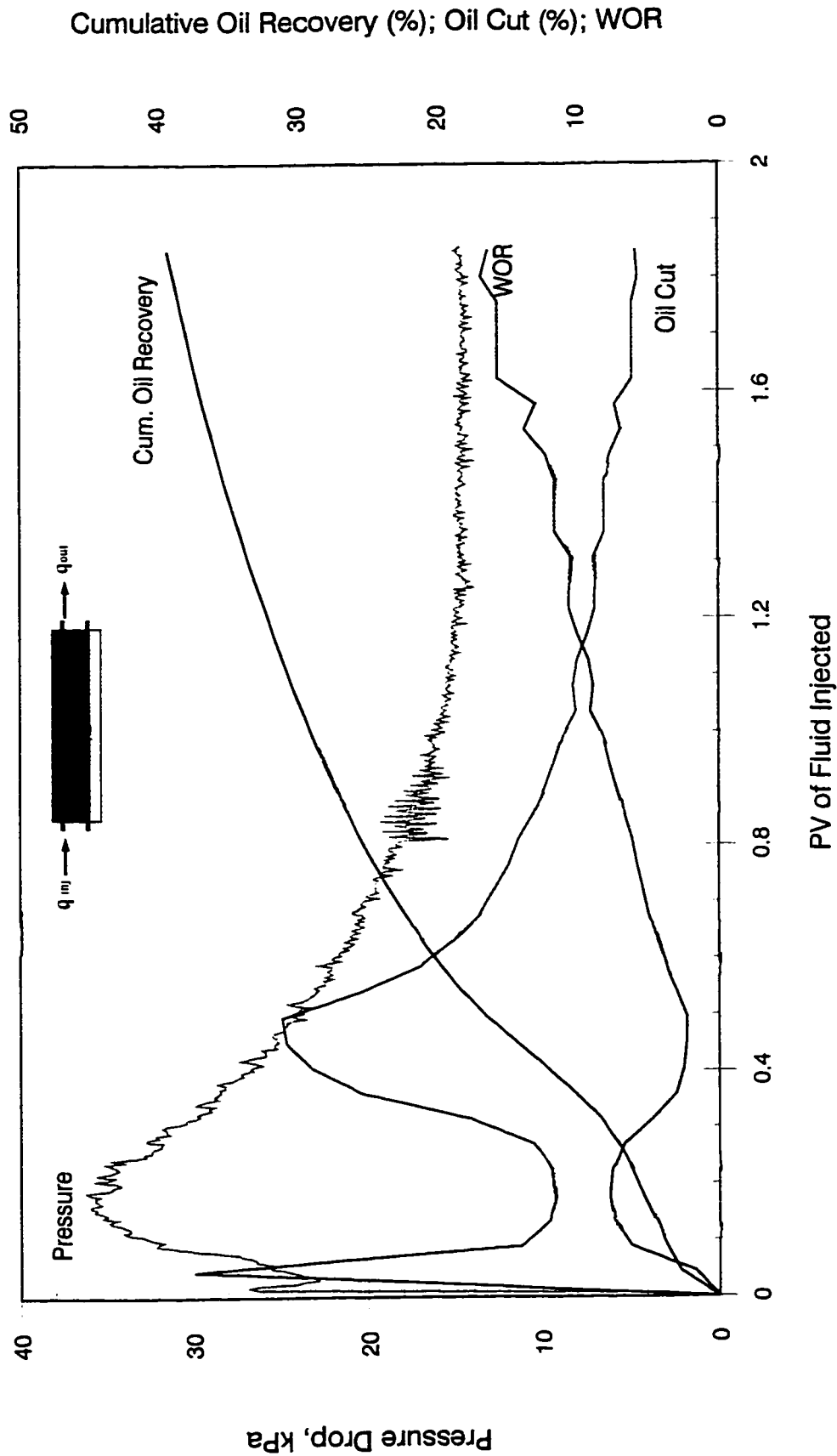


Figure F-4: Bottom-Water Pack Waterflood (  $q = 450$  cc/hr,  $h_w/h_o = 1/3$ , Oil Viscosity =  $34.3$  mPa.s )

# Production History for Experimental Run 5

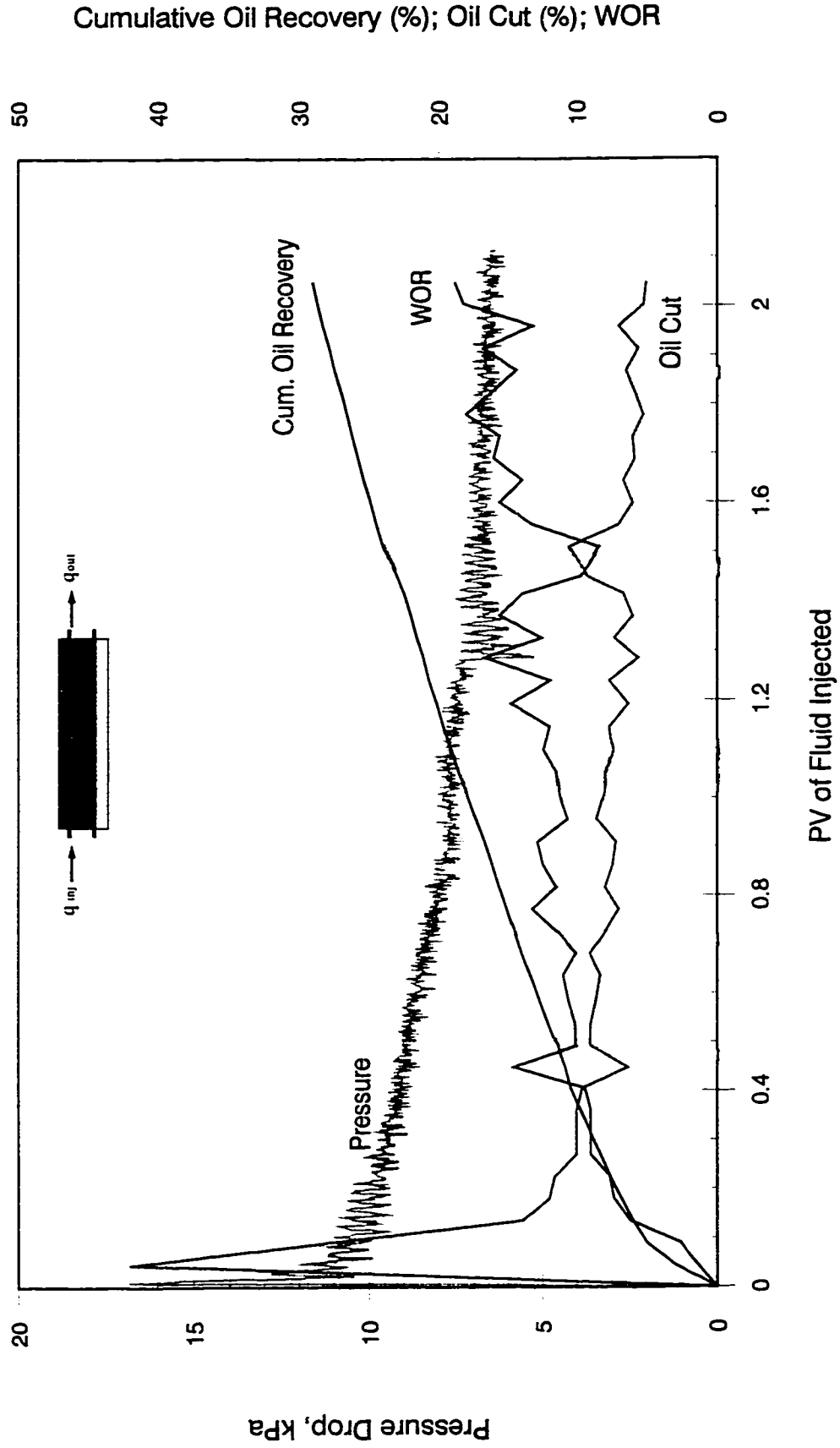


Figure F-5: Bottom-Water Pack Waterflood (  $q = 300$  cc/hr,  $hw/ho = 1/3$ , Oil Viscosity =  $34.3$  mPa.s )

# Production History for Experimental Run 6

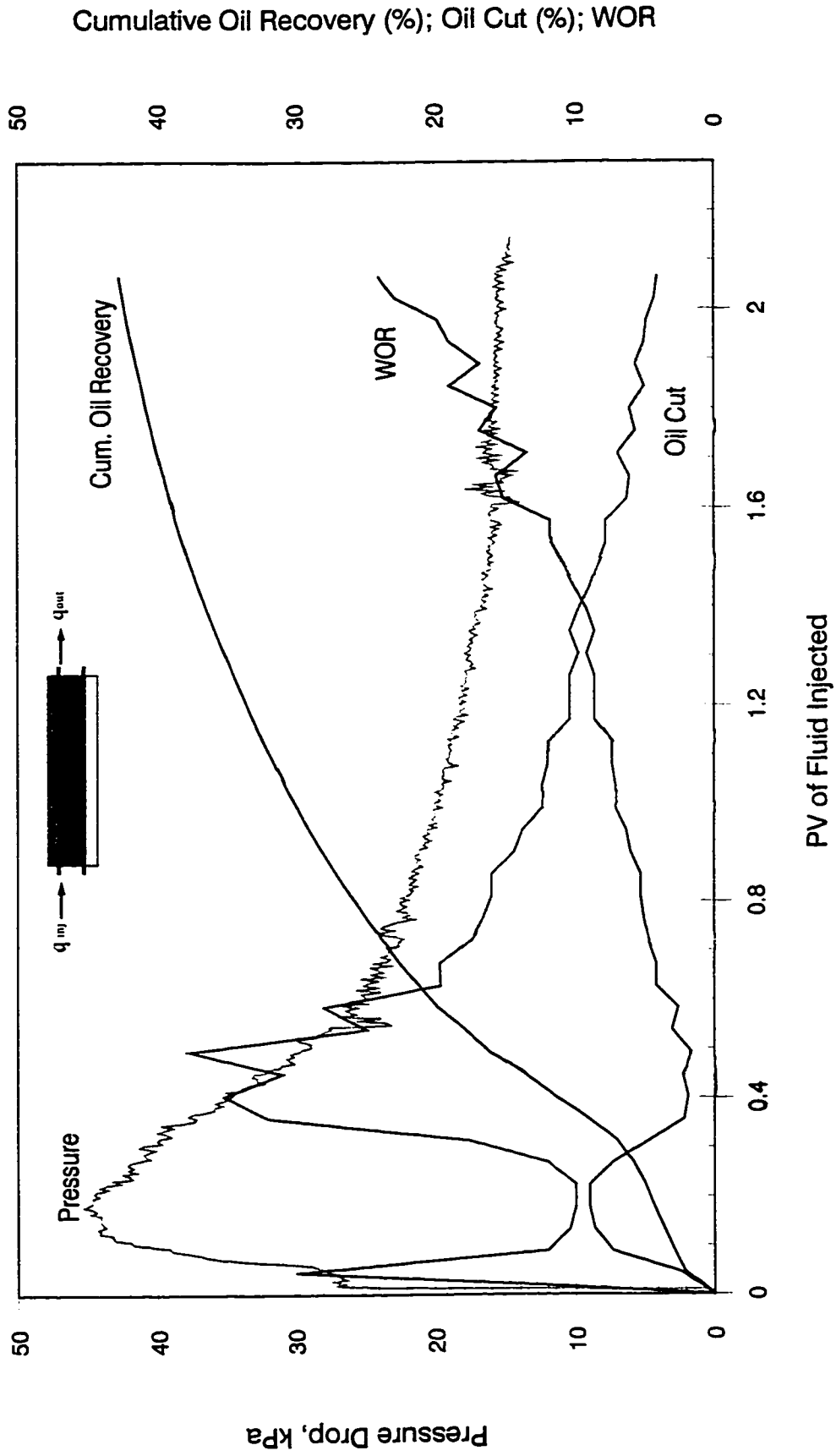


Figure F-6: Bottom-Water Pack Waterflood (  $q = 600$  cc/hr,  $h_w/h_o = 1/3$ , Oil Viscosity =  $34.3$  mPa.s )

# Production History for Experimental Run 7

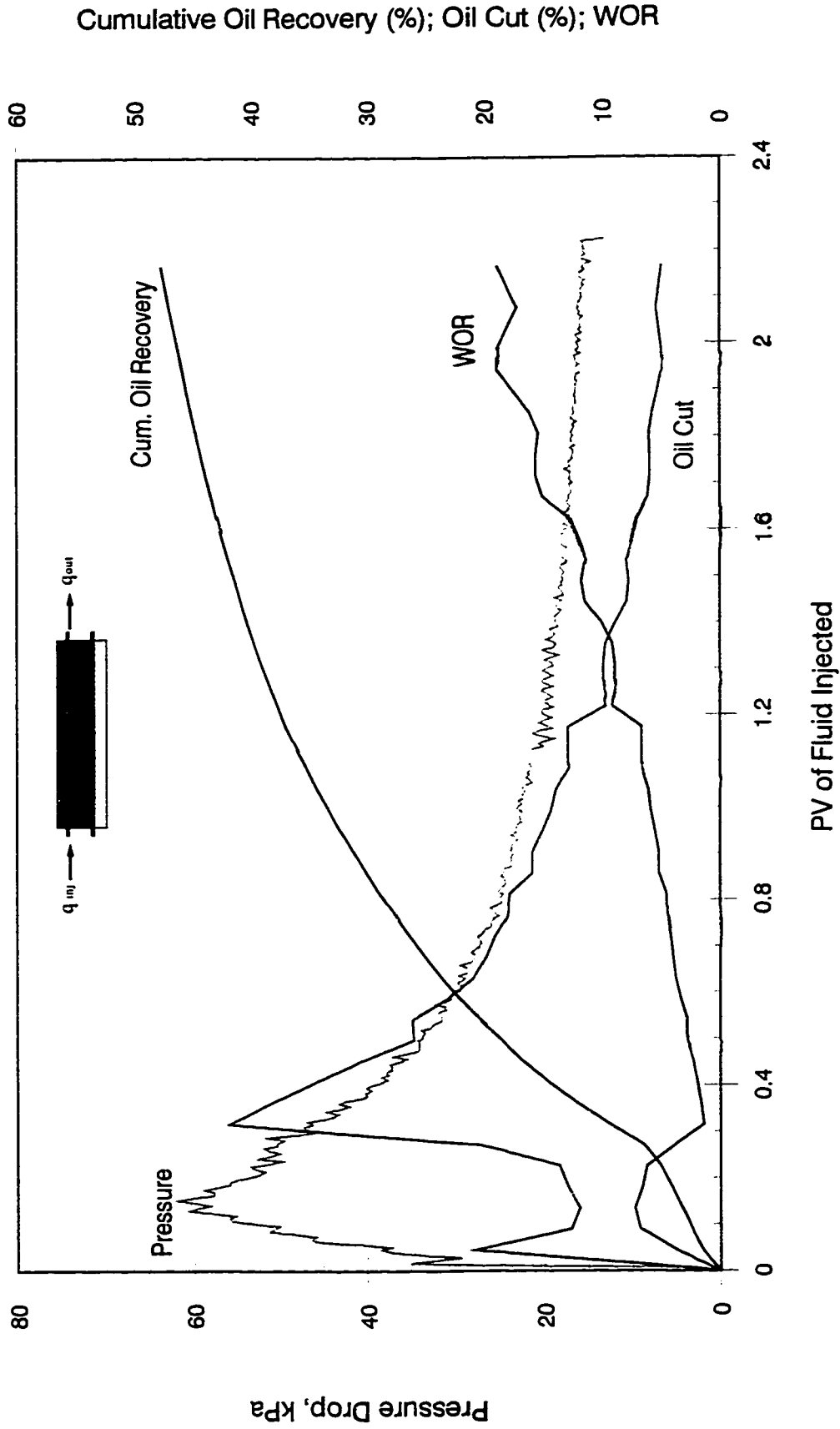


Figure F-7: Bottom-Water Pack Waterflood ( $q = 750$  cc/hr,  $h_w/h_o = 1/3$ , Oil Viscosity =  $34.3$  mPa.s)

# Production History for Experimental Run 8

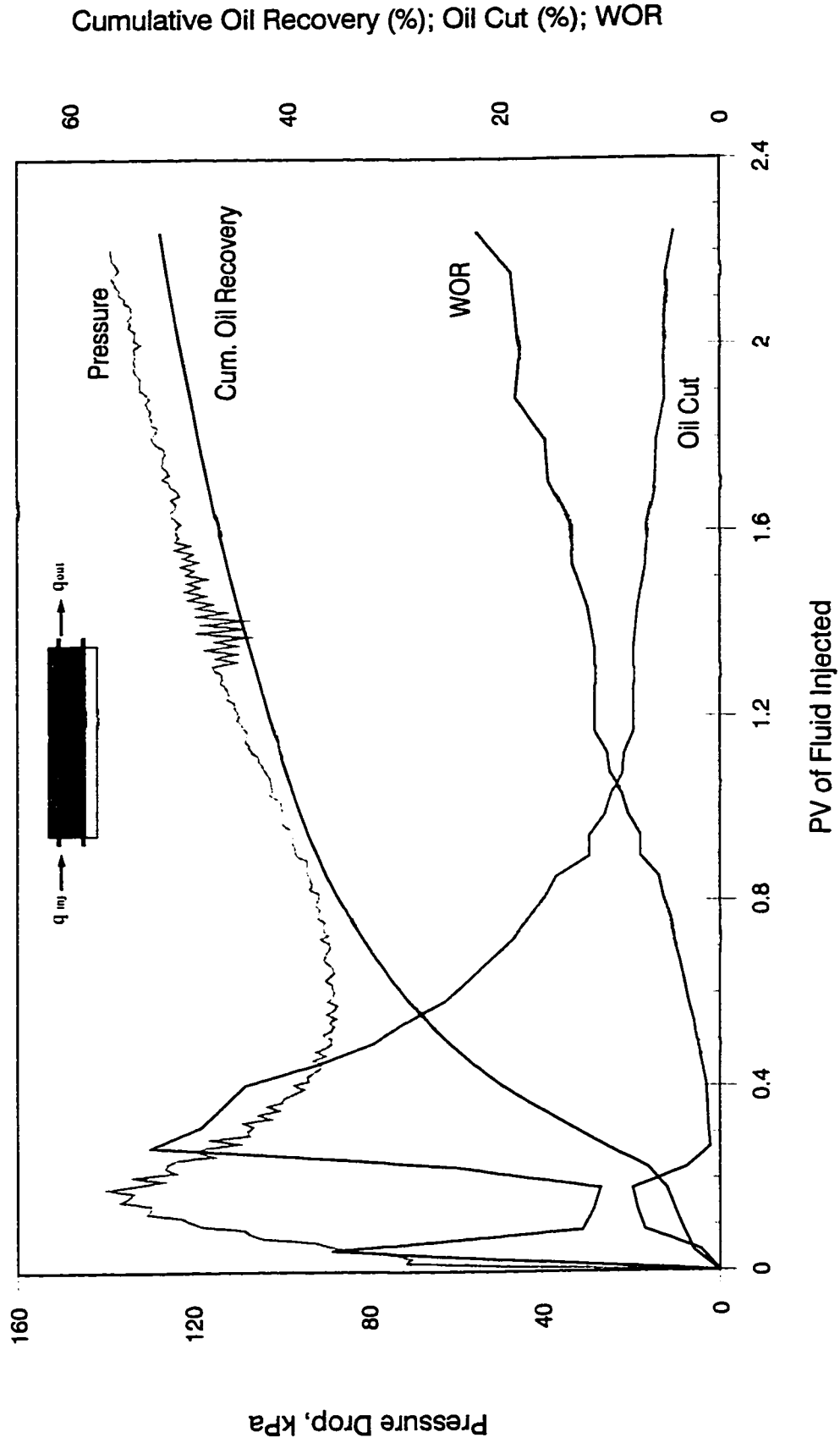


Figure F-8: Bottom-Water Pack Waterflood (  $q = 1200$  cc/hr,  $hw/ho = 1/3$ , Oil Viscosity =  $34.3$  mPa.s )

# Production History for Experimental Run 9

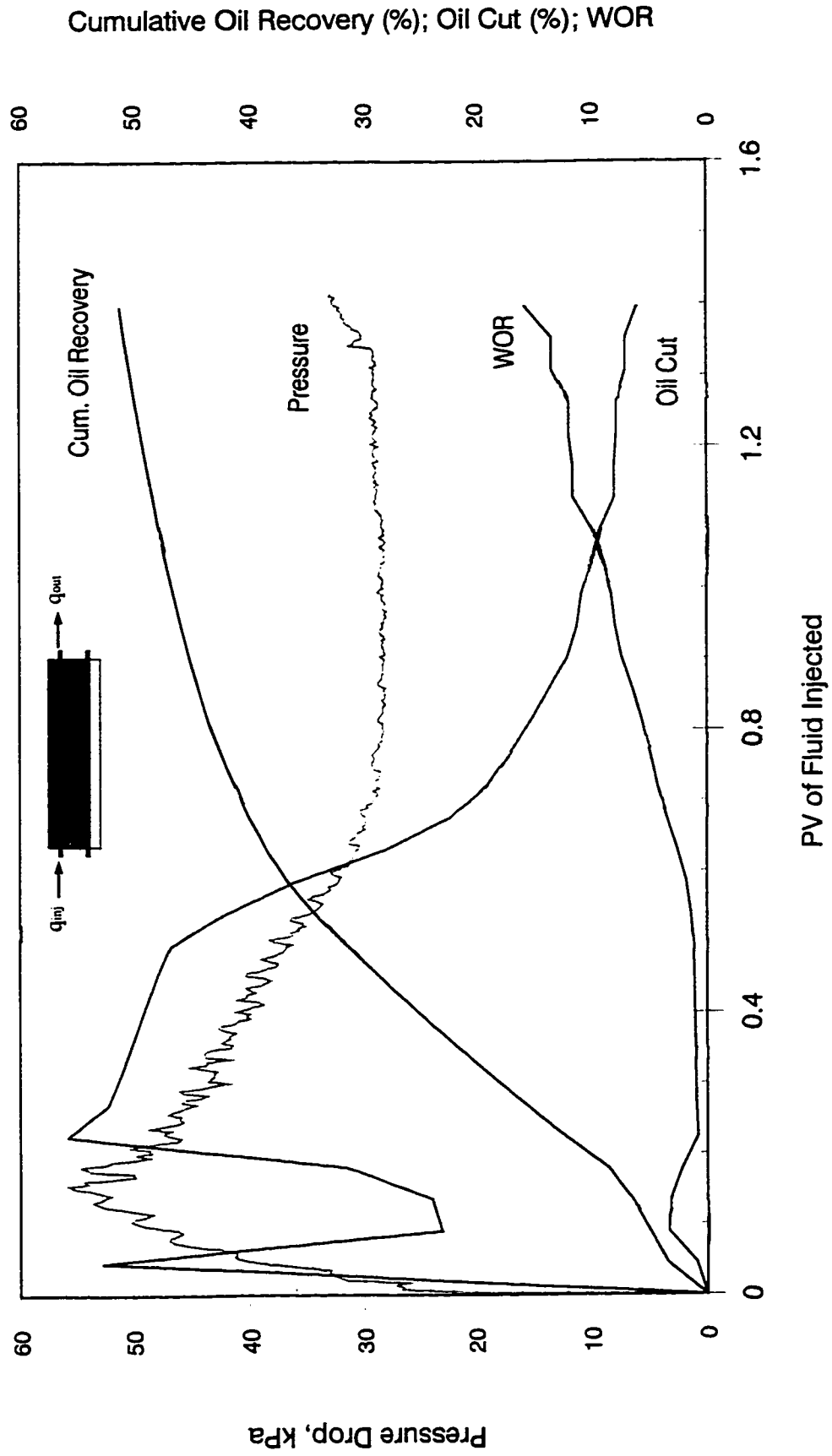
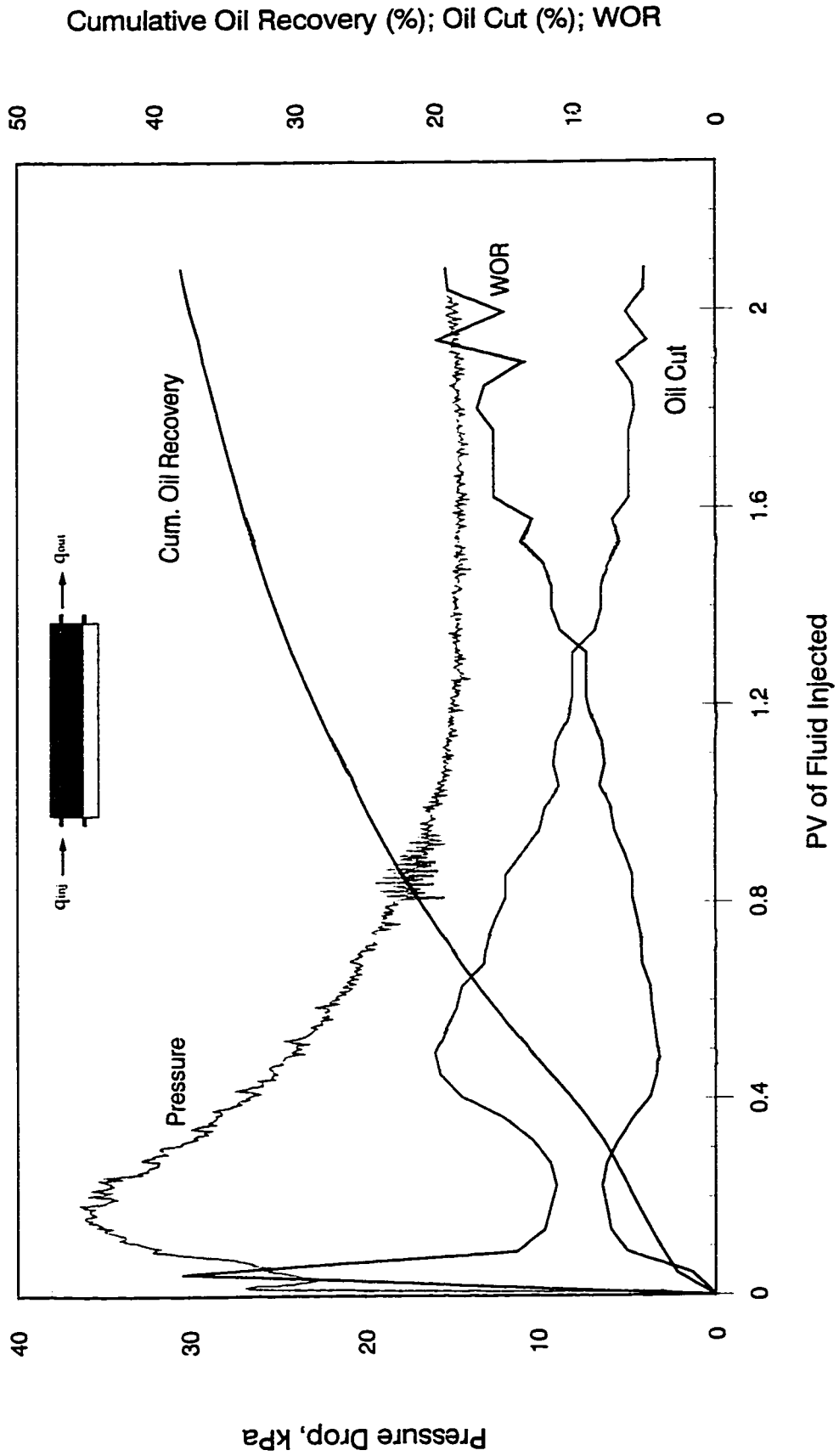


Figure F-9: Bottom-Water Pack Waterflood (Injection Rate = 450 cc/hr,  $h_w/h_o = 1/4$ , Oil Viscosity = 34.3 mPa.s)

# Production History for Experimental Run 10



Cumulative Oil Recovery (%); Oil Cut (%); WOR

Figure F-10: Bottom-Water Pack Waterflood ( $q = 450$  cc/hr,  $hw/ho = 1/2$ , Oil Viscosity =  $34.3$  mPa.s)

# Production History for Experimental Run 10

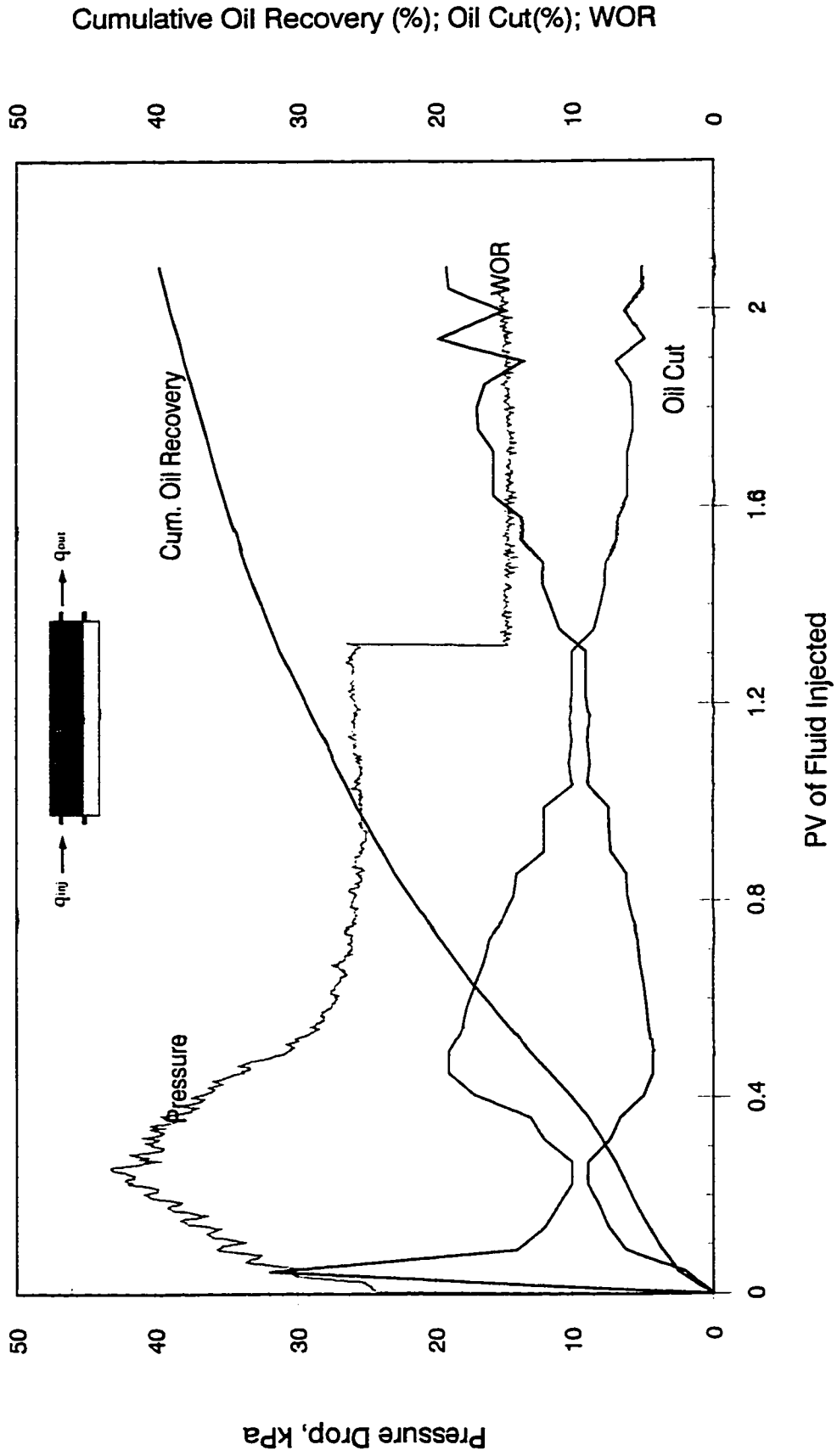


Figure F-10: Bottom-Water Pack Waterflood (  $q = 450$  cc/hr,  $h_w/h_o = 1/2$ , Oil Viscosity =  $34.3$  mPa.s )



# Production History for Experimental Run 11

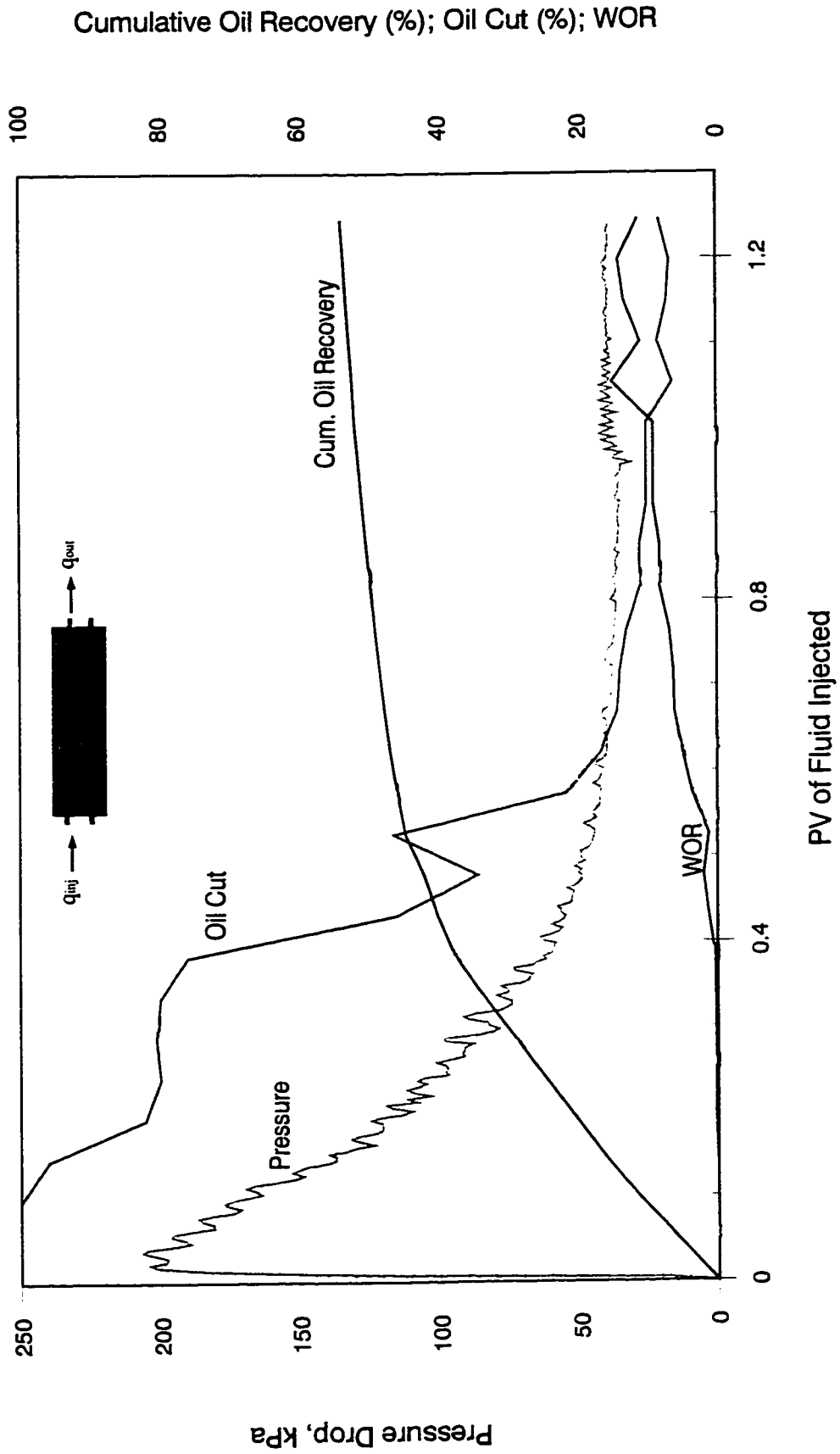


Figure F-11: Homogeneous Pack Waterflood ( Injection Rate = 450 cc/hr, Oil Viscosity = 68.0 mPa.s )

# Production History for Experimental Run 12

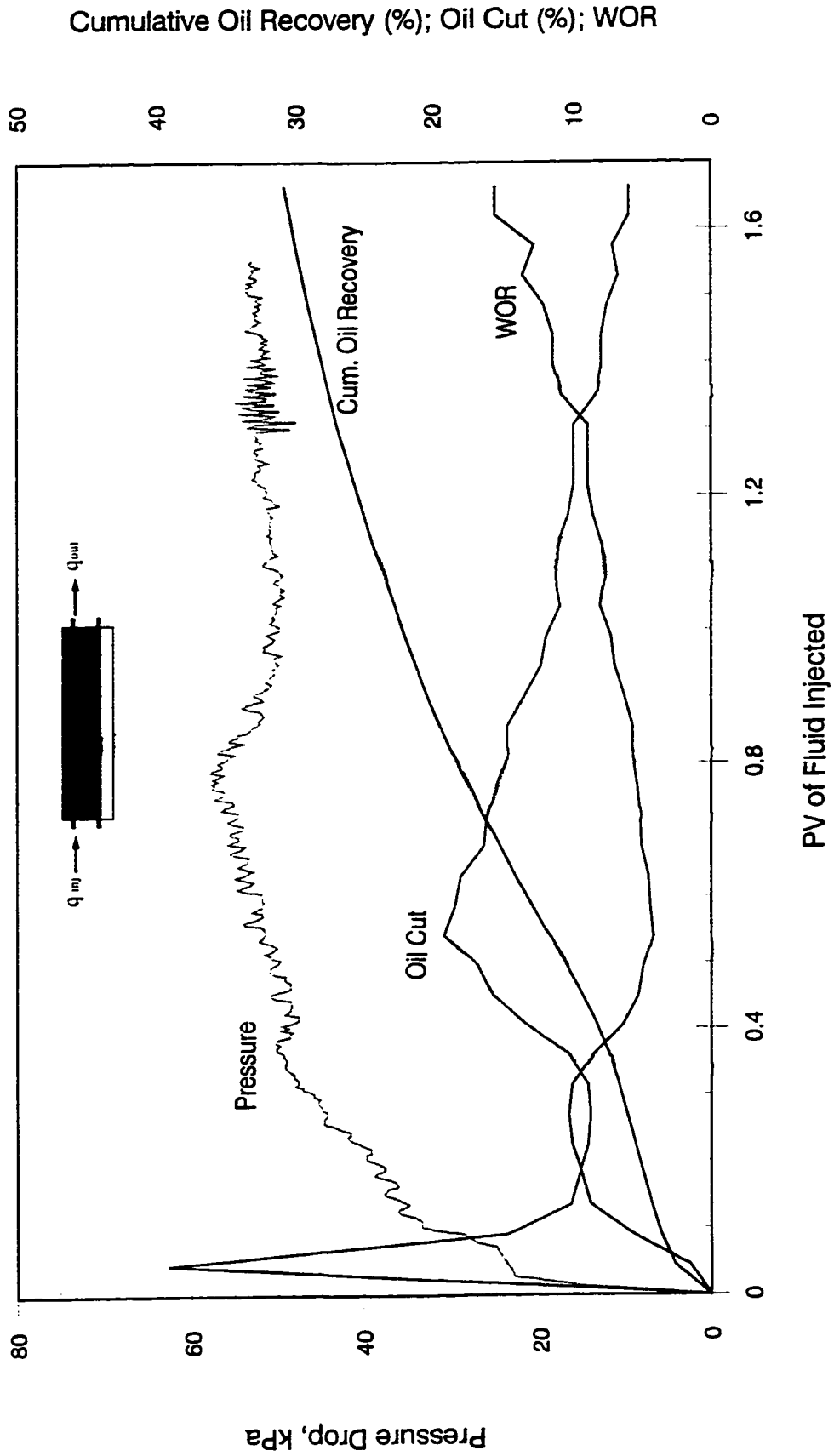


Figure F-12: Bottom-Water Pack Waterflood (Injection Rate = 450 cc/hr,  $hw/h_o = 1/3$ , Oil Viscosity = 68.0 mPa.s)

# Production History for Experimental Run 13

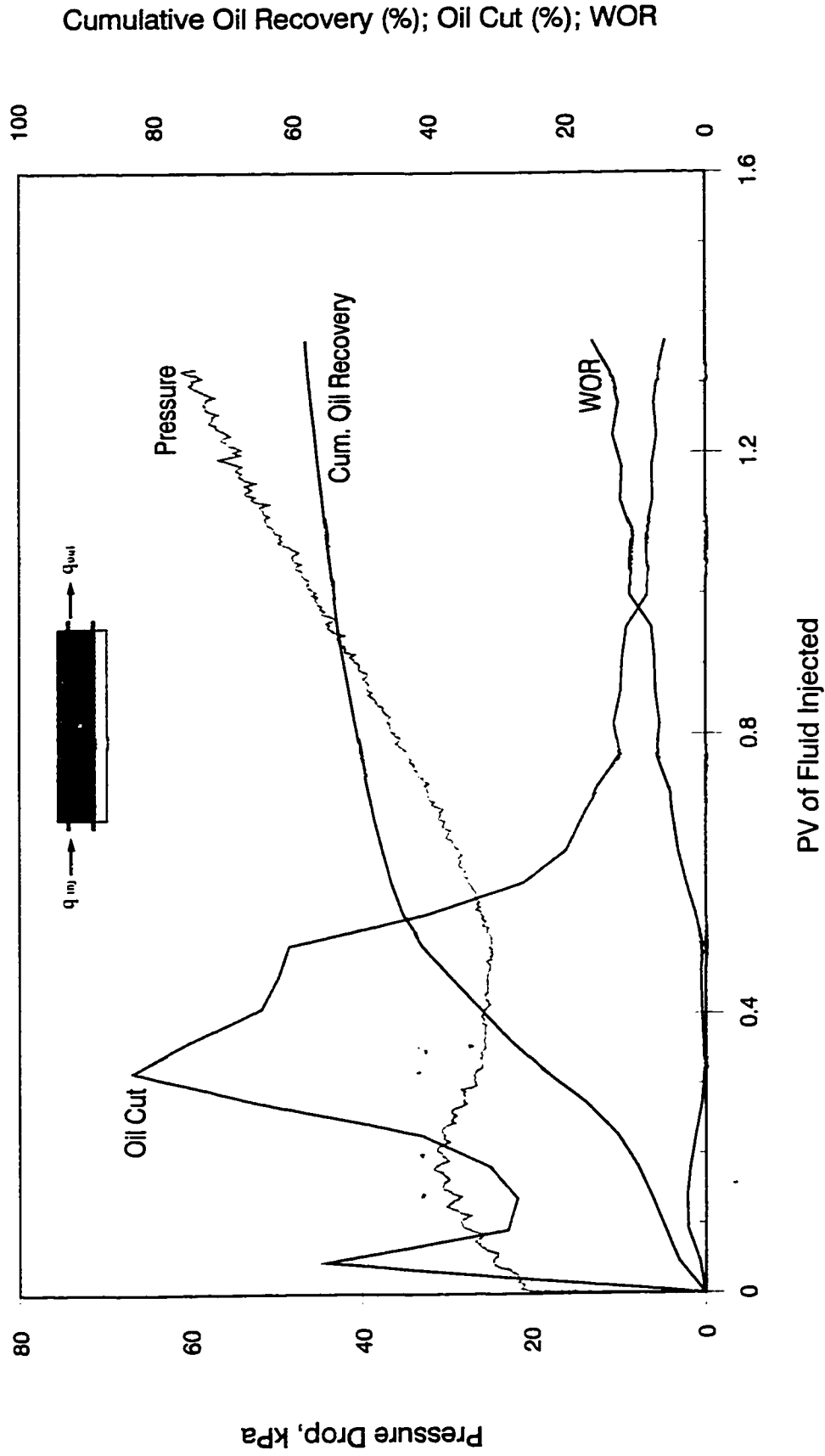


Figure F-13: Bottom-Water Pack Waterflood (Injection Rate = 450 cc/hr,  $h_w/h_o = 1/3$ , Oil Viscosity = 11.0 mPa.s)

# Production History for Experimental Run 14

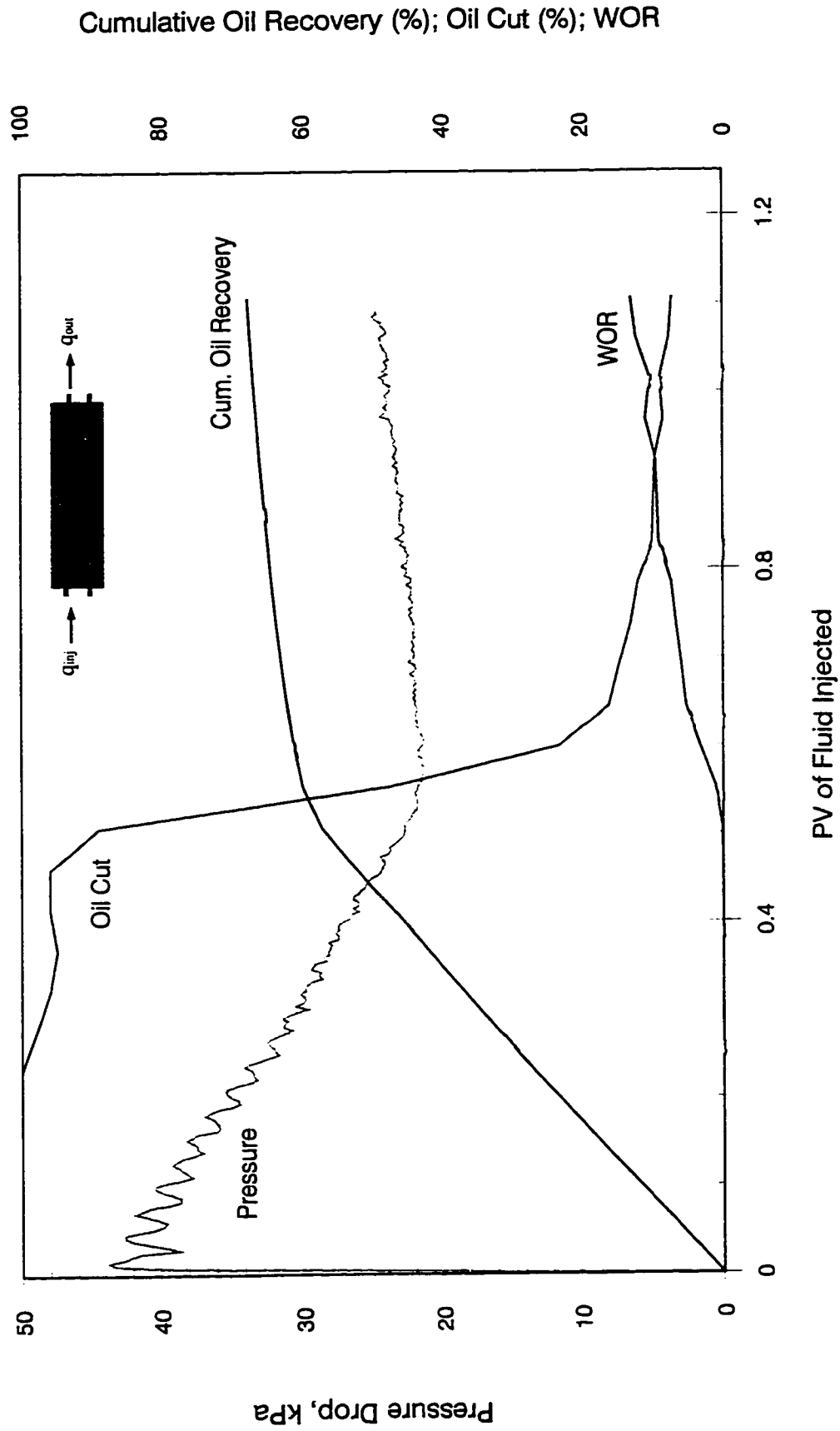


Figure F-14: Homogeneous Pack Waterflood ( Injection Rate = 450 cc/hr, Oil Viscosity = 11.0 mPa.s )

# Production History for Experimental Run 15

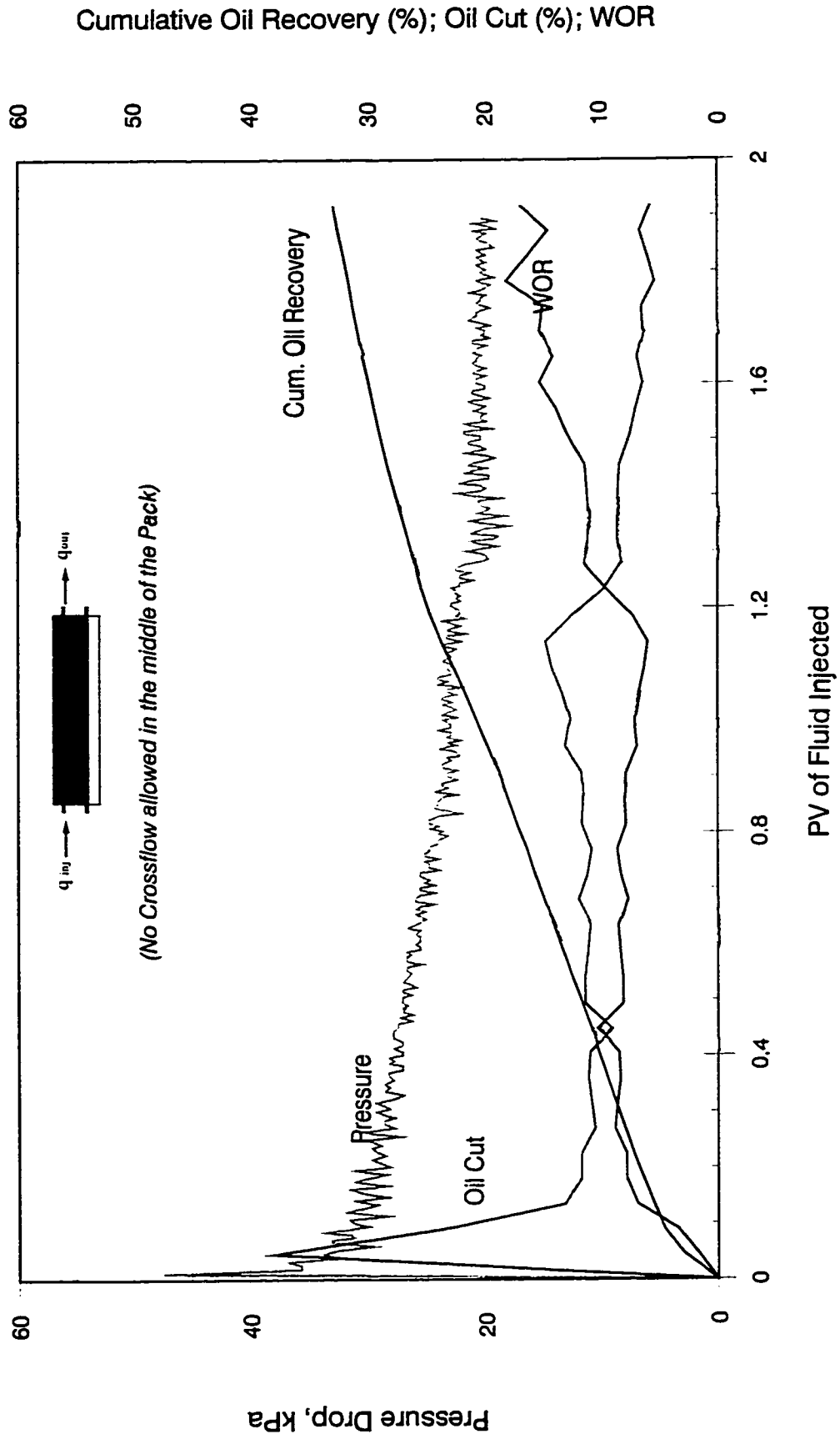


Figure F-15: Bottom-Water Pack Waterflood (Injection Rate = 450 cc/hr,  $hw/ho = 1/3$ , Oil Viscosity = 34.3 mPa.s)

# Production History for Experimental Run 16

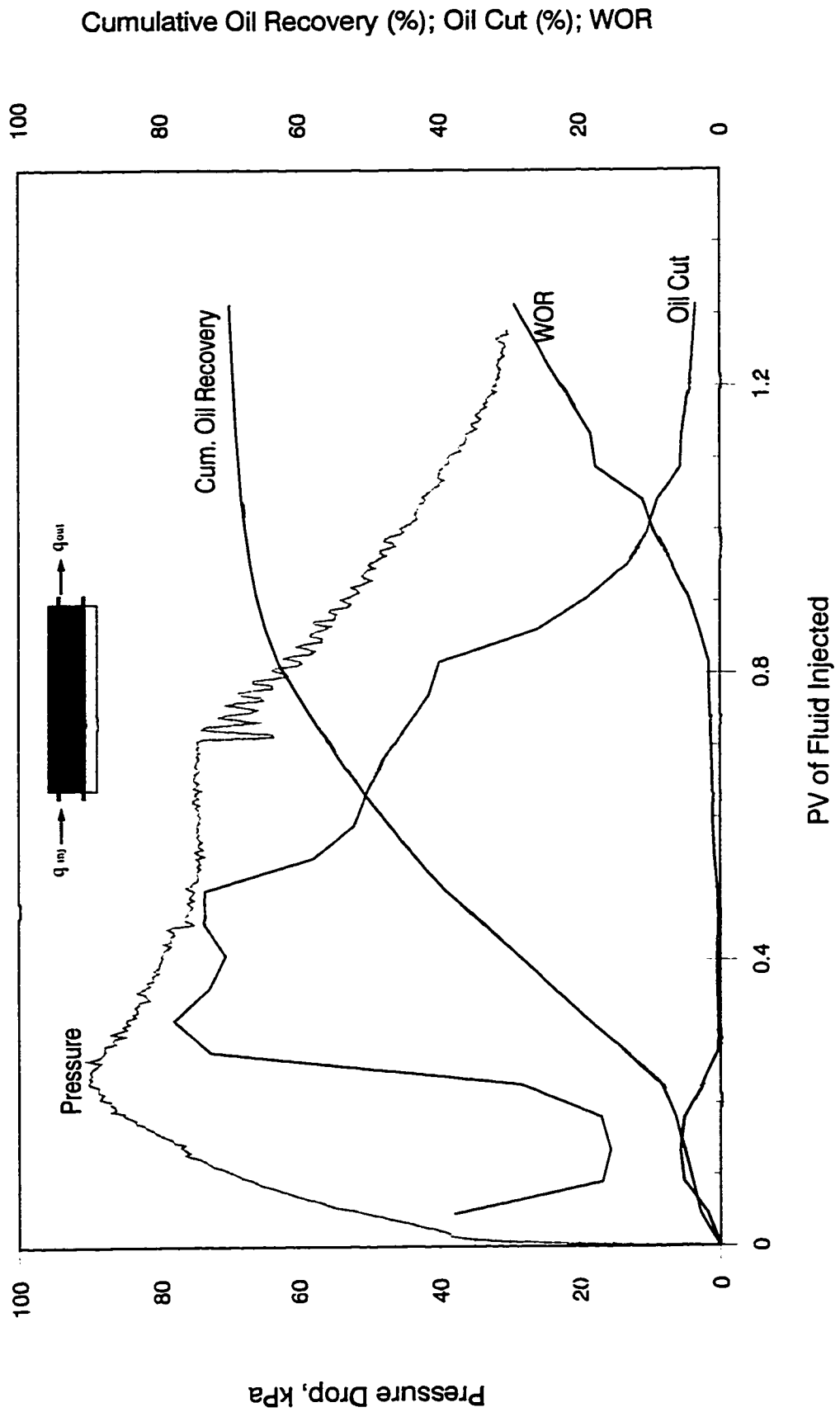


Figure F-16: Bottom-Water Pack Polymer Flood ( $q = 450$  cc/hr, Con. = 500 ppm,  $hw/ho = 1/3$ ,  $U_o = 34.3$  mPa.s)

# Production History for Experimental Run 17

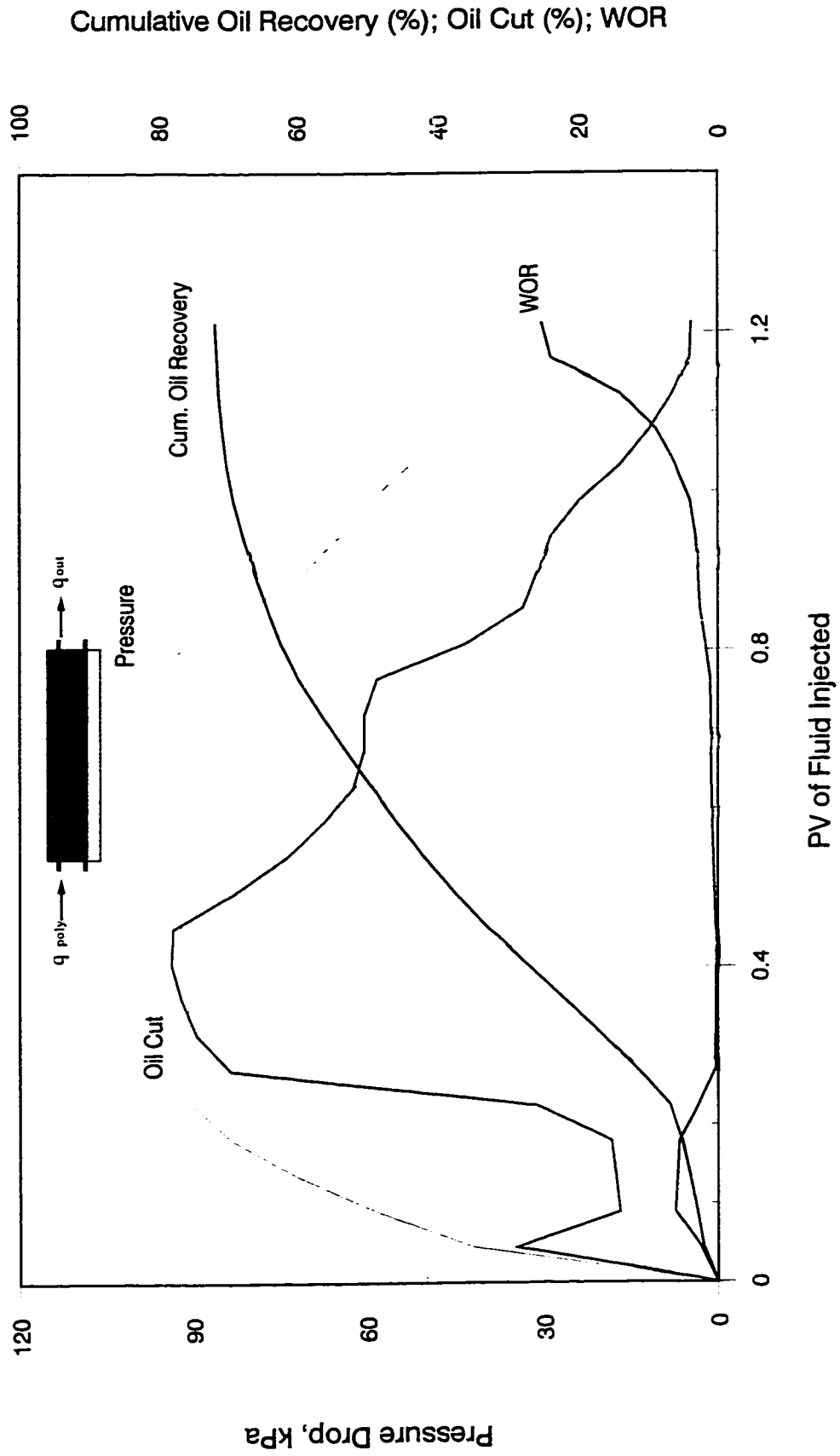


Figure F-17: Bottom-Water Pack Polymer Flood ( $q = 450$  cc/hr, Con. = 1000 ppm,  $hw/h_o = 1/3$ ,  $U_o = 34.3$  mPa.s)

# Production History for Experimental Run 18

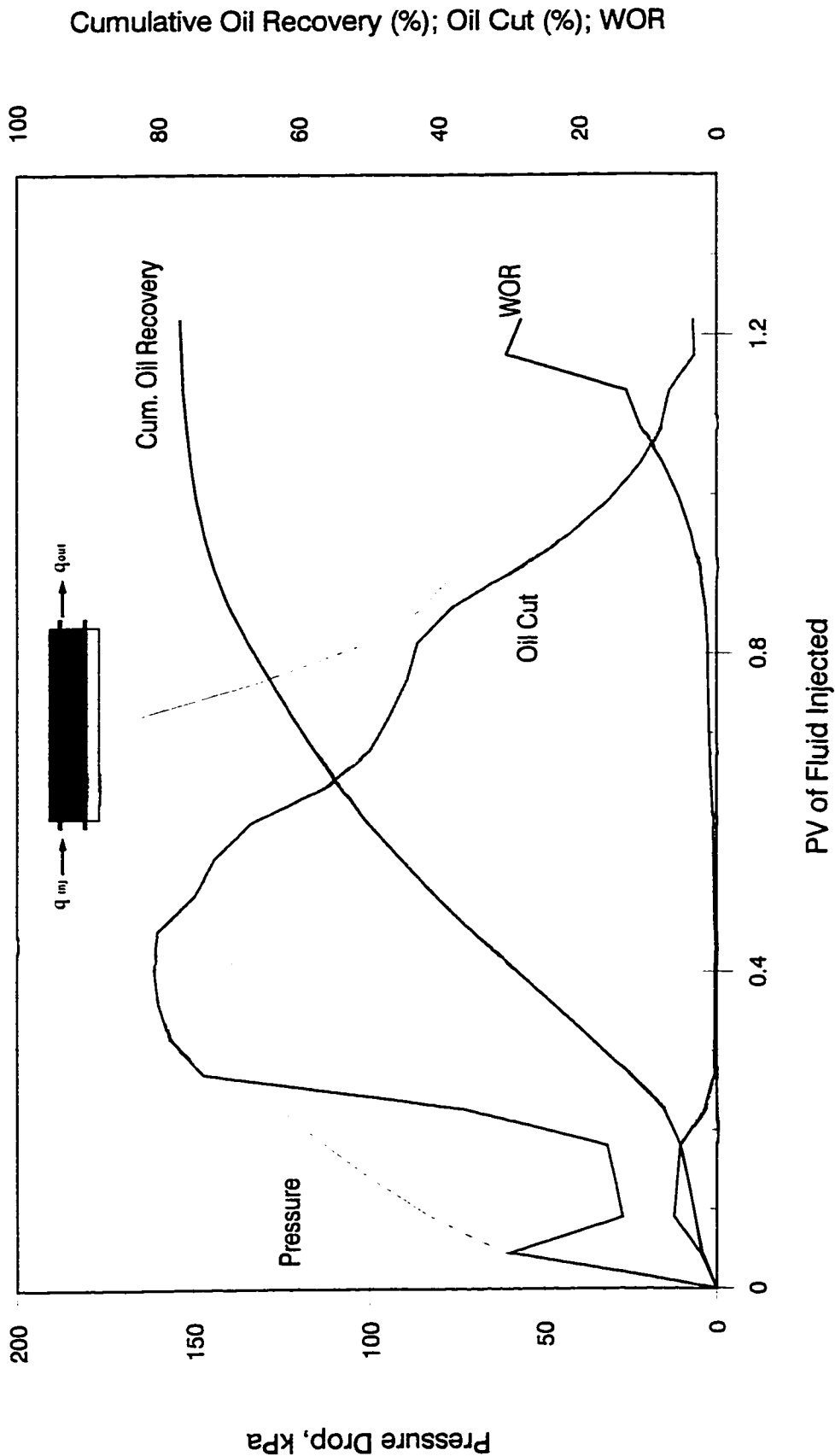


Figure F-18: Bottom-Water Pack Polymer Flood ( $q = 450\text{cc/hr}$ ,  $\text{Con.} = 1500\text{ ppm}$ ,  $h_w/h_o = 1/3$ ,  $U_o = 34.3\text{ mPa.s}$ )



# Production History for Experimental Run 19

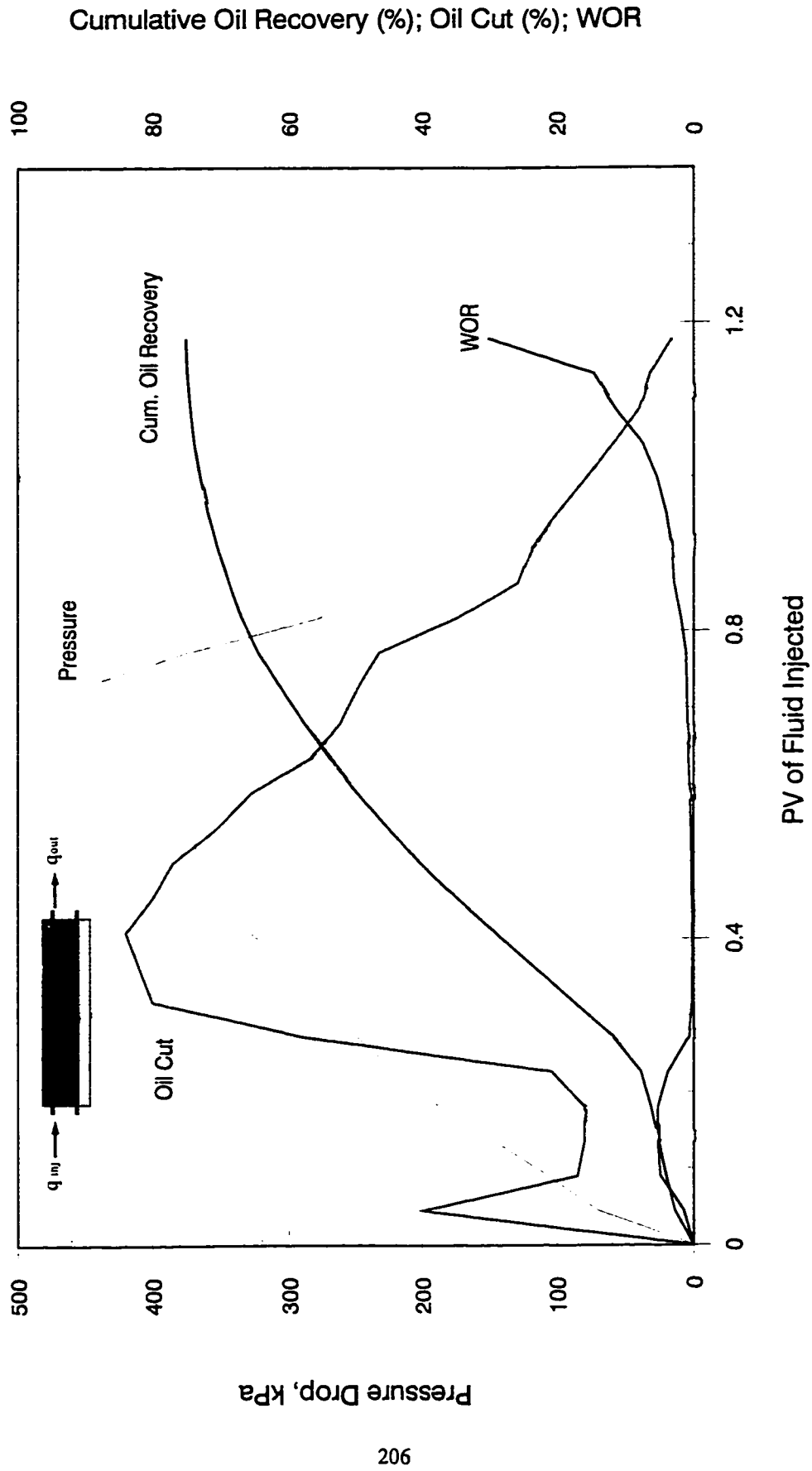


Figure F-19: Bottom-Water Pack Polymer Flood ( $q = 450$  cc/hr, Con. = 2000 ppm,  $hw/ho = 1/3$ ,  $U_o = 34.3$  mPa.s)

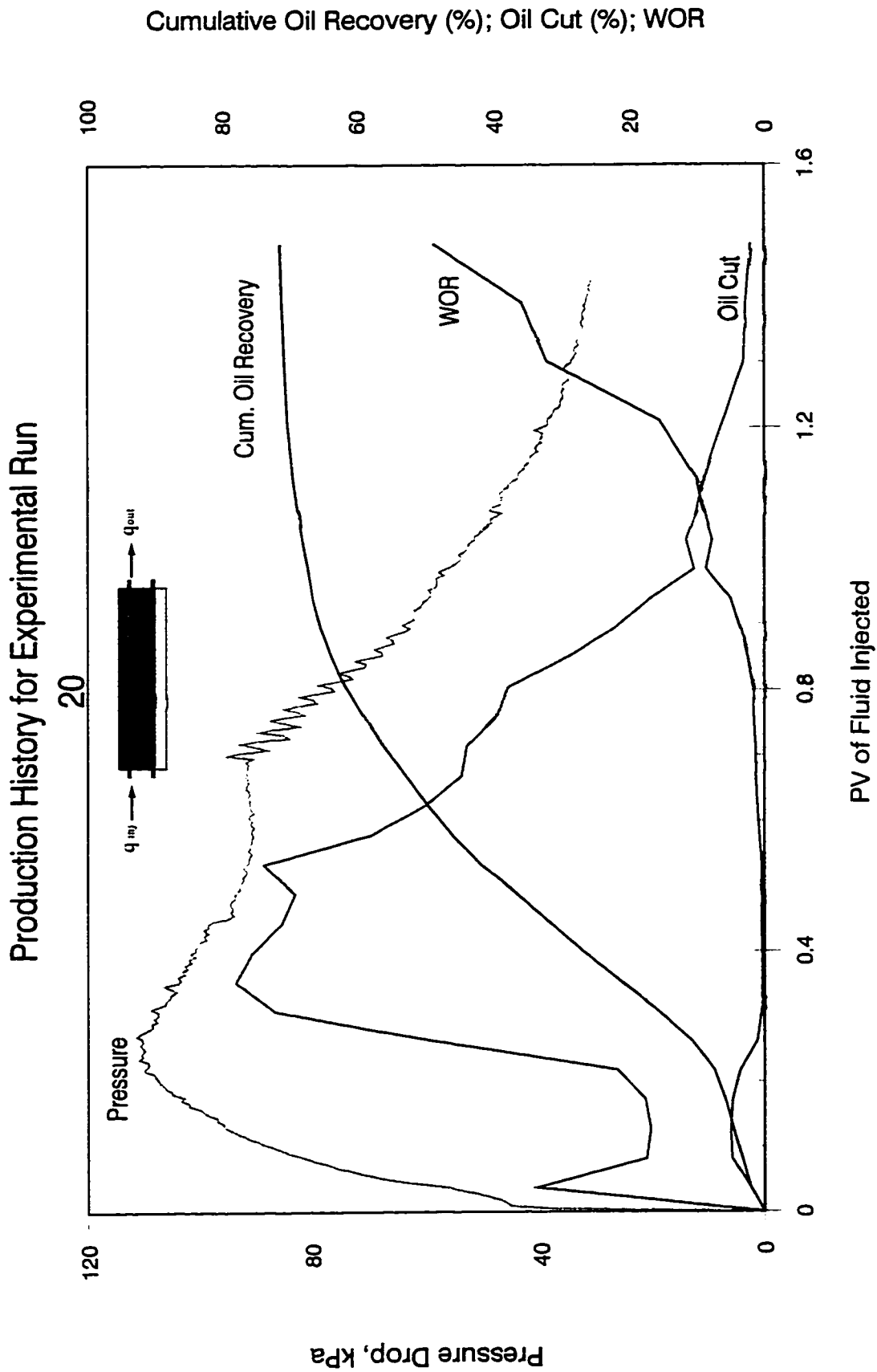


Figure F-20: Bottom-Water Pack Polymer Flood ( $q = 750$  cc/hr,  $Con. = 500$  ppm,  $hw/h_o = 1/3$ ,  $U_o = 34.3$  mPa.s)

# Production History for Experimental Run 21

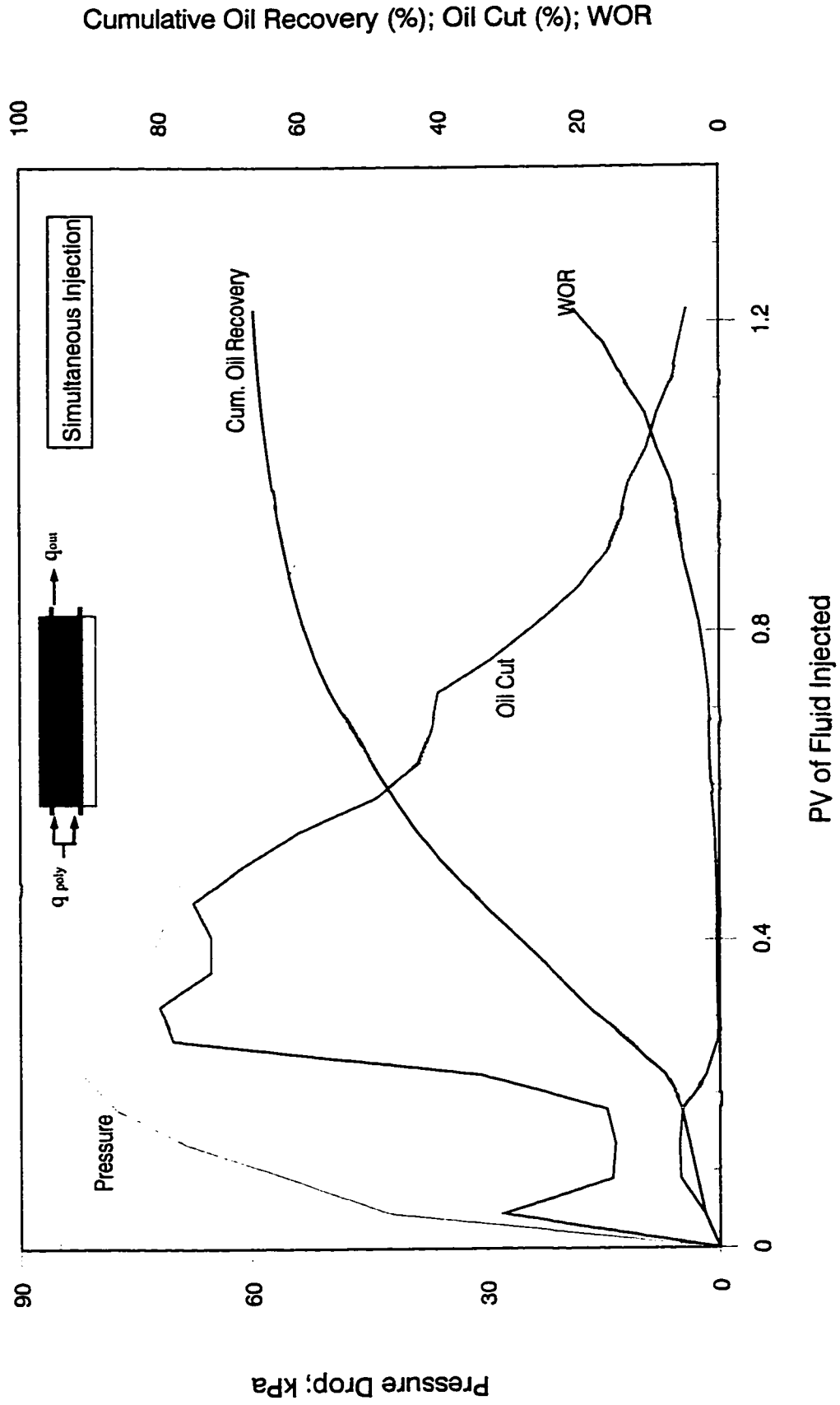


Figure F-21: Bottom-Water Pack Polymer Flood ( $q = 450$  cc/hr,  $Con. = 500$  ppm,  $hw/ho = 1/3$ ,  $U_o = 34.3$  mPa.s)

# Production History for Experimental Run 22

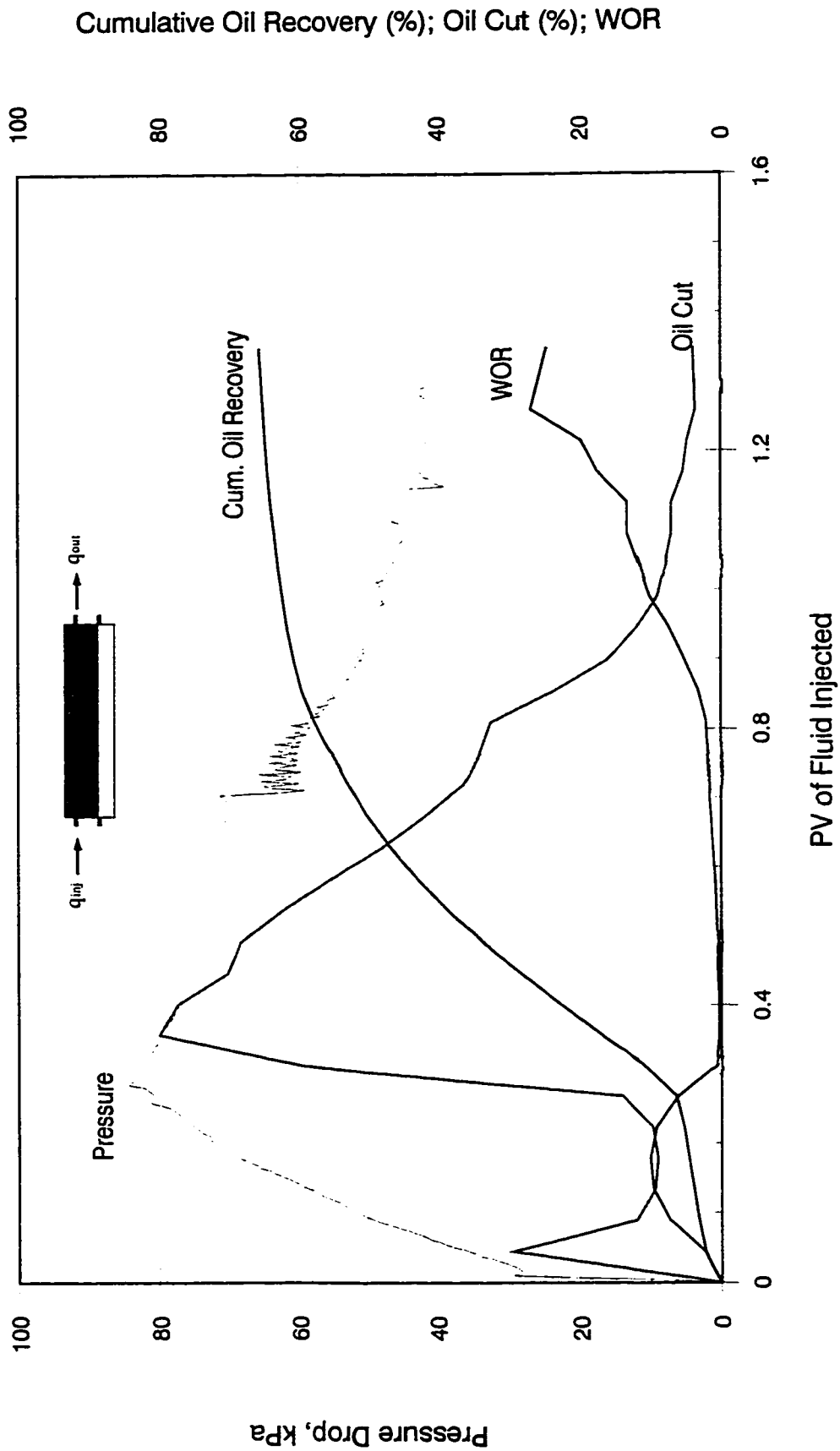


Figure F-22: Bottom-Water Pack Polymer Flood ( $q = 450$  cc/hr, Con. = 500 ppm,  $hw/h_o = 1/2$ ,  $U_o = 34.3$  mPa.s)

# Production History for Experimental Run 23

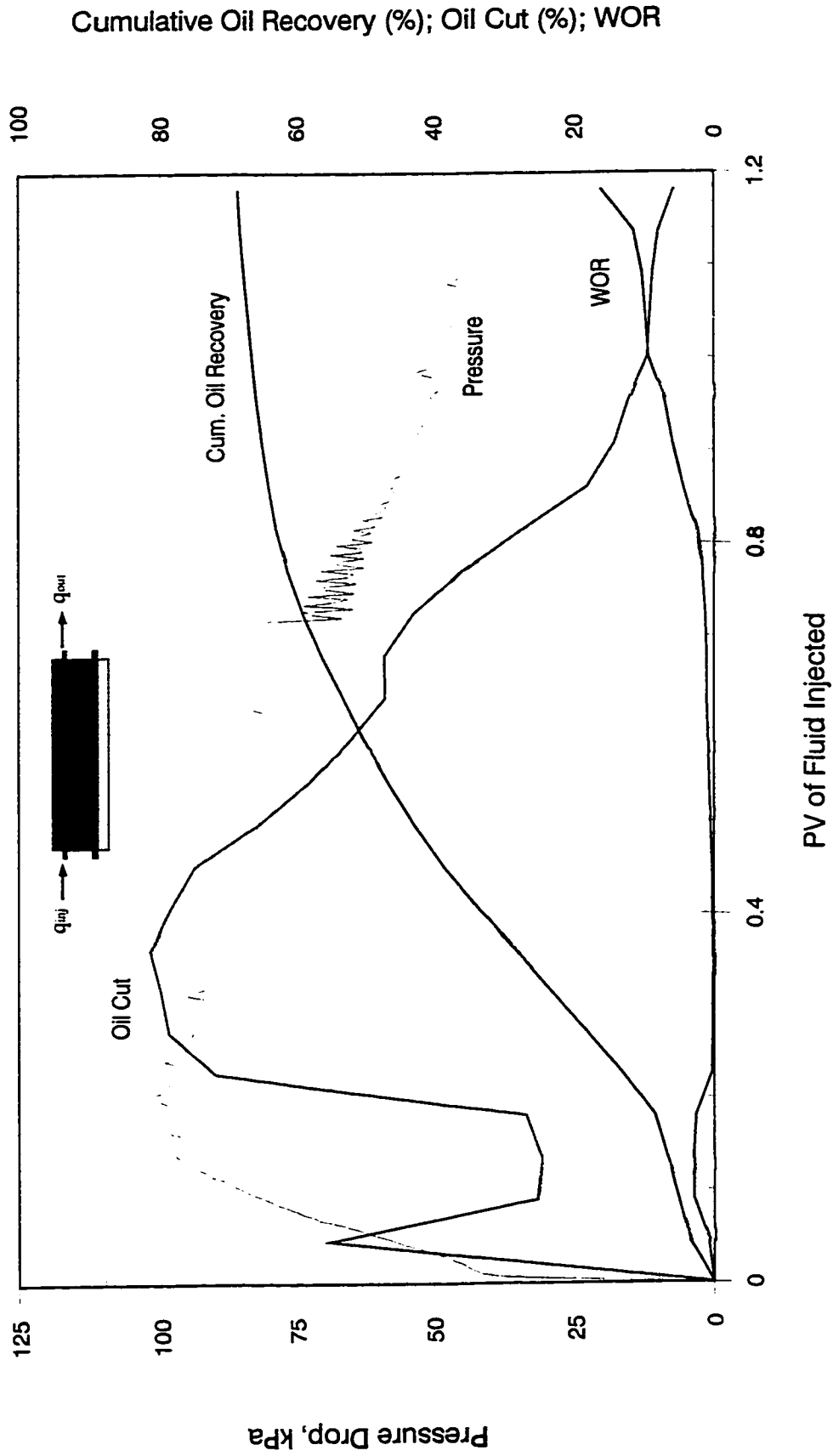


Figure F-23: Bottom-Water Pack Polymer Flood ( $q = 450$  cc/hr, Con. = 500 ppm,  $hw/ho = 1/4$ ,  $U_o = 34.3$  mPa.s)

# Production History for Experimental Run 24

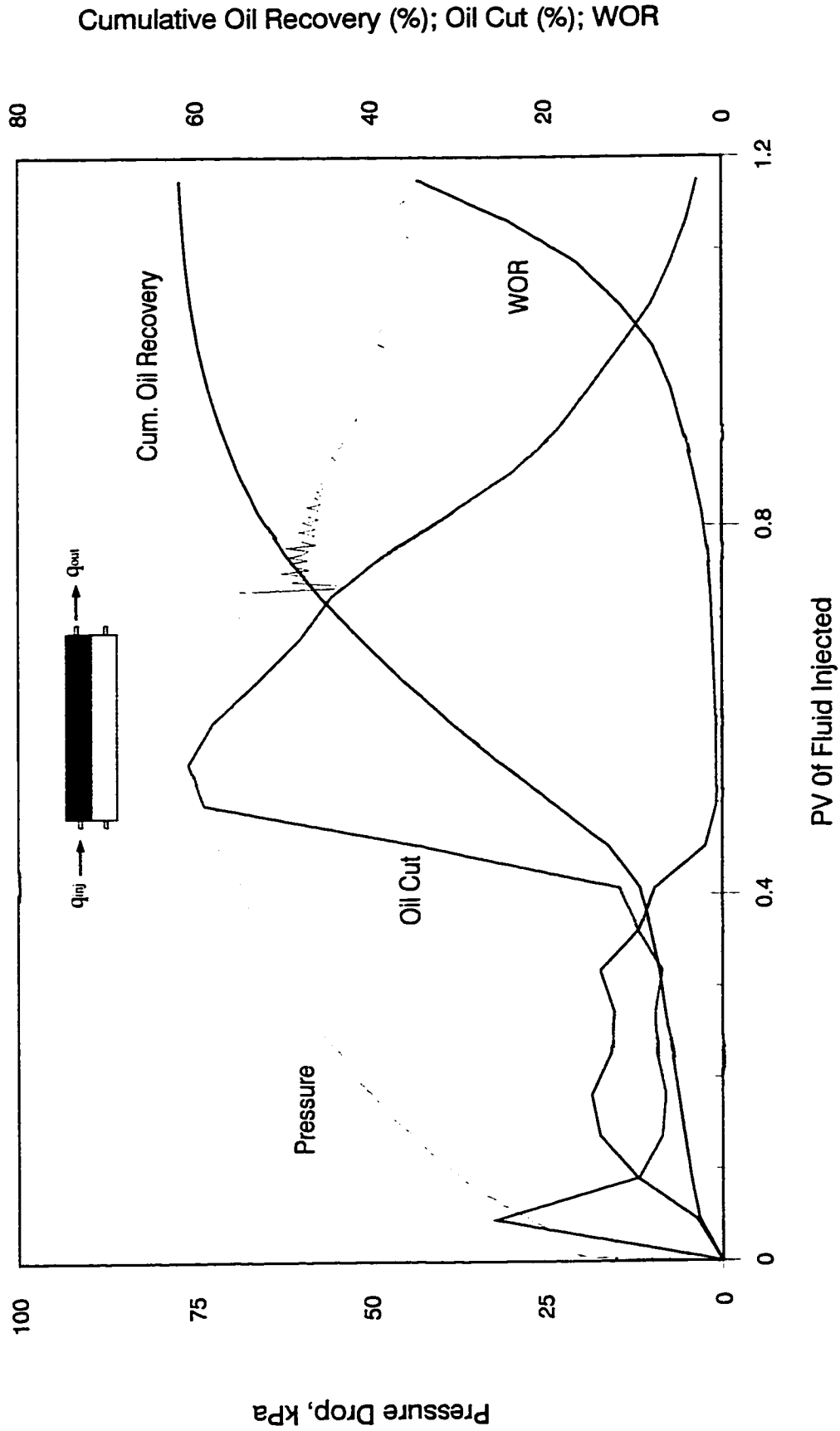


Figure F-24: Bottom-Water Pack Polymer Flood ( $q = 450$  cc/hr, Con. = 500 ppm,  $hw/ho = 1/1$ ,  $U_o = 34.3$  mPa.s)

# Production History for Experimental Run 25

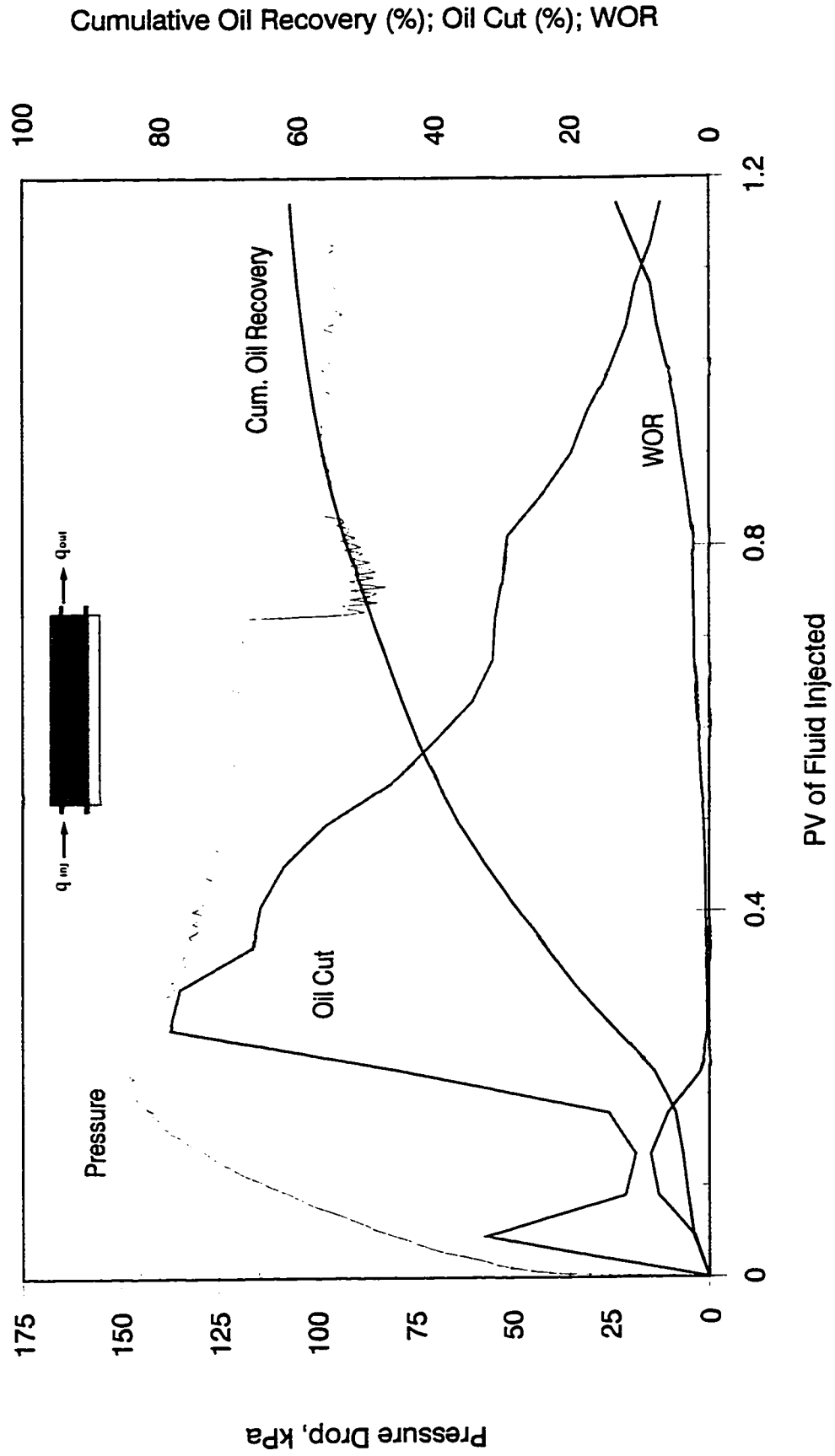


Figure F-25: Bottom-Water Pack Polymer Flood ( $q = 450$  cc/hr, Con. = 500 ppm,  $hw/ho = 1/3$ ,  $U_o = 68.0$  mPa.s)

# Production History for Experimental Run 26

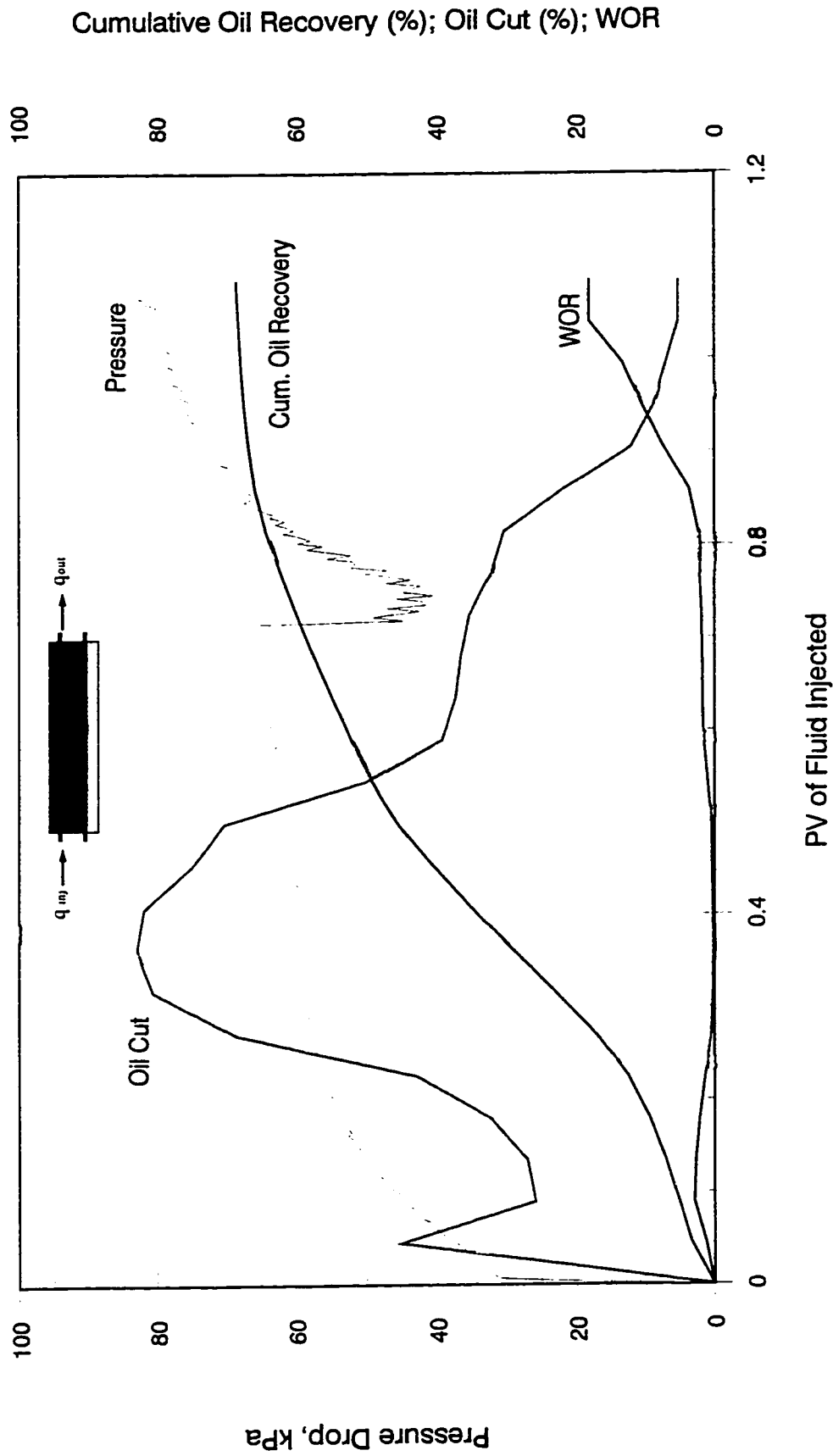


Figure F-26: Bottom-Water Pack Polymer Flood ( $q = 450$  cc/hr, Con. = 500 ppm,  $hw/ho = 1/3$ ,  $U_o = 11.0$  mPa.s)



# Production History for Experimental Run 27

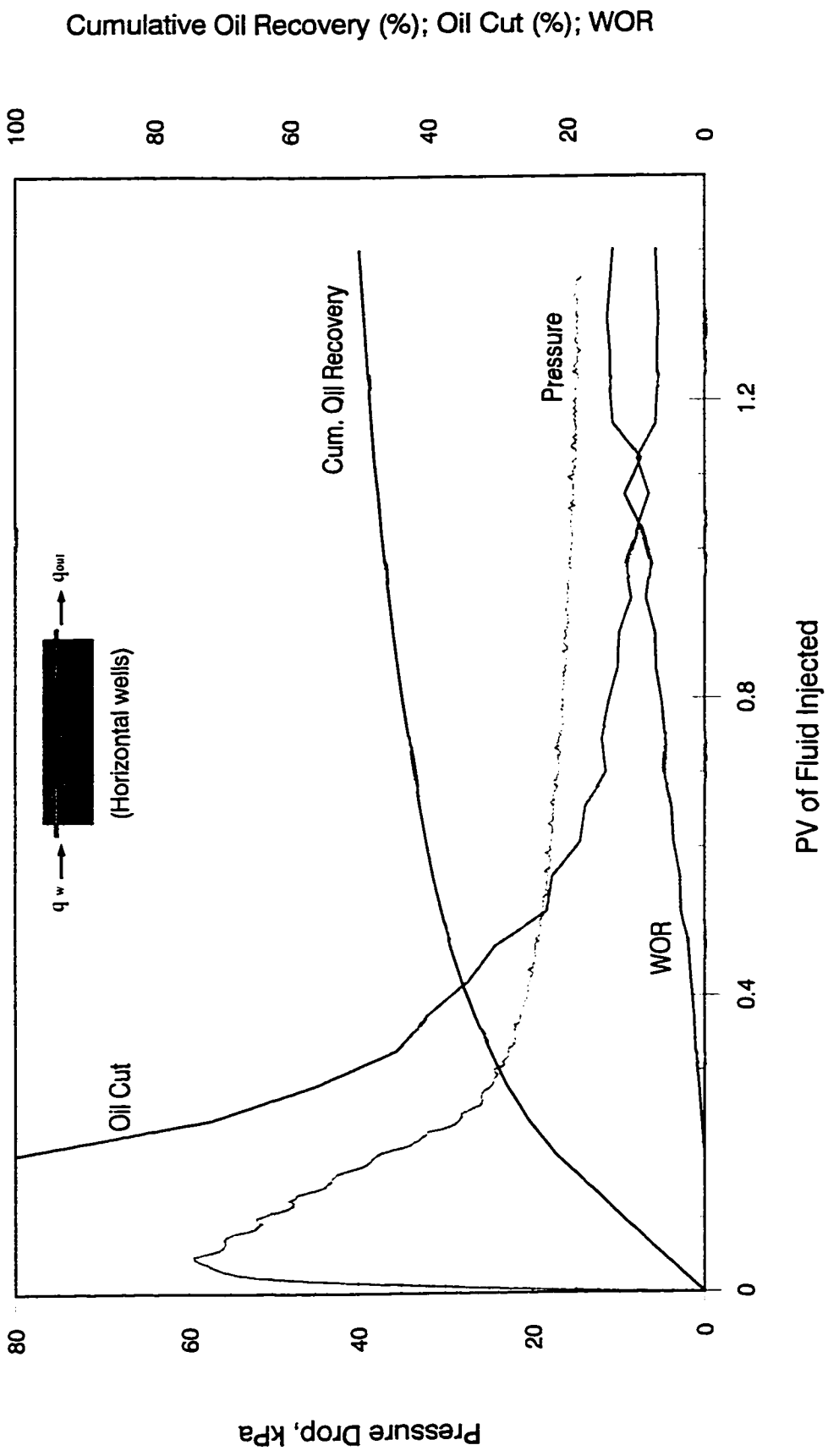


Figure F-27: Homogeneous Pack Waterflood ( Injection Rate = 450 cc/hr, Oil Viscosity = 34.3 mPa.s )

# Production History for Experimental Run 28

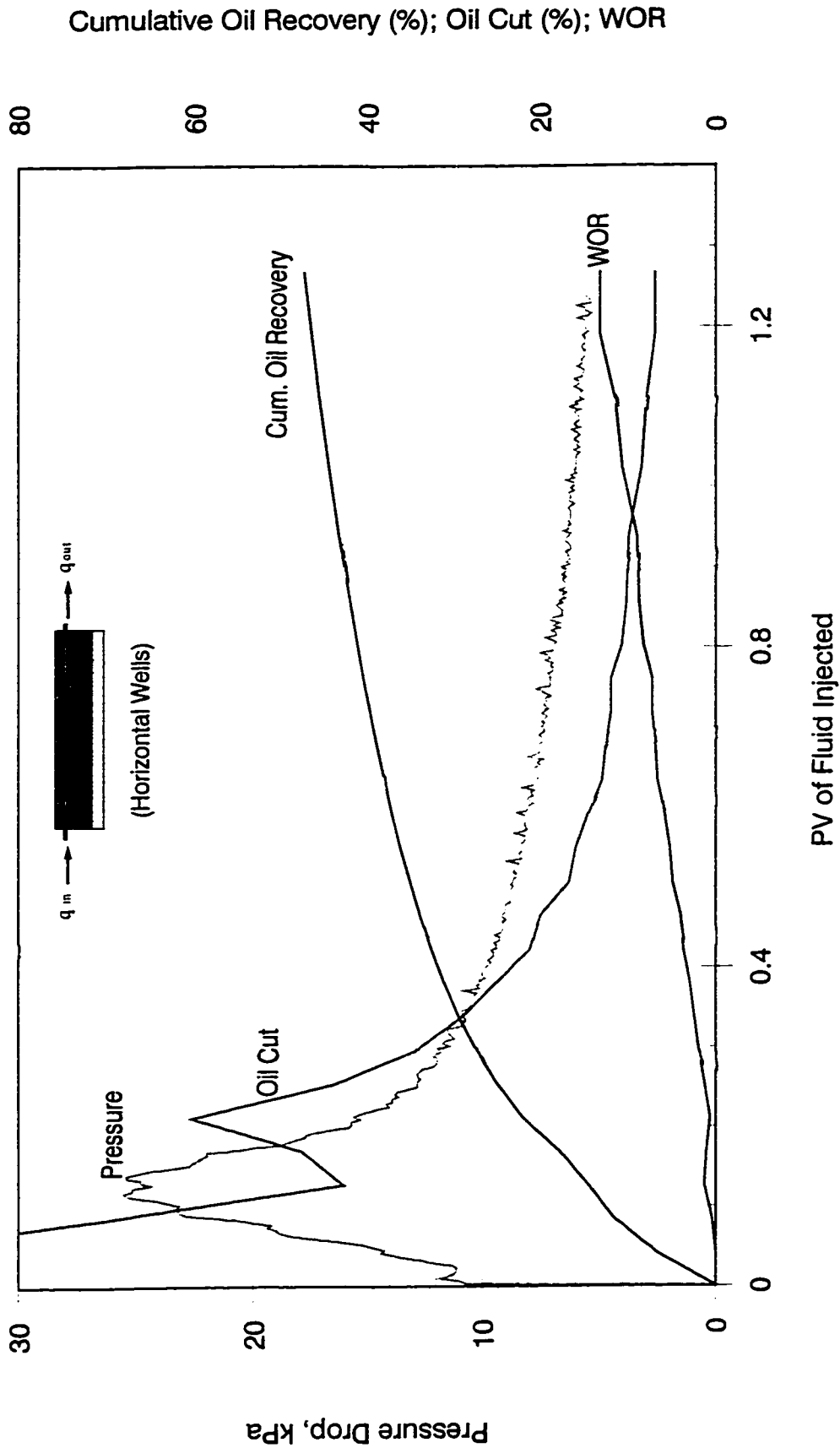


Figure F-28: Bottom-Water Pack Waterflood (  $q = 450$  cc/hr,  $hw/ho = 1/3$ , Oil Viscosity =  $34.3$  mPa.s )

# Production History for Experimental Run 29

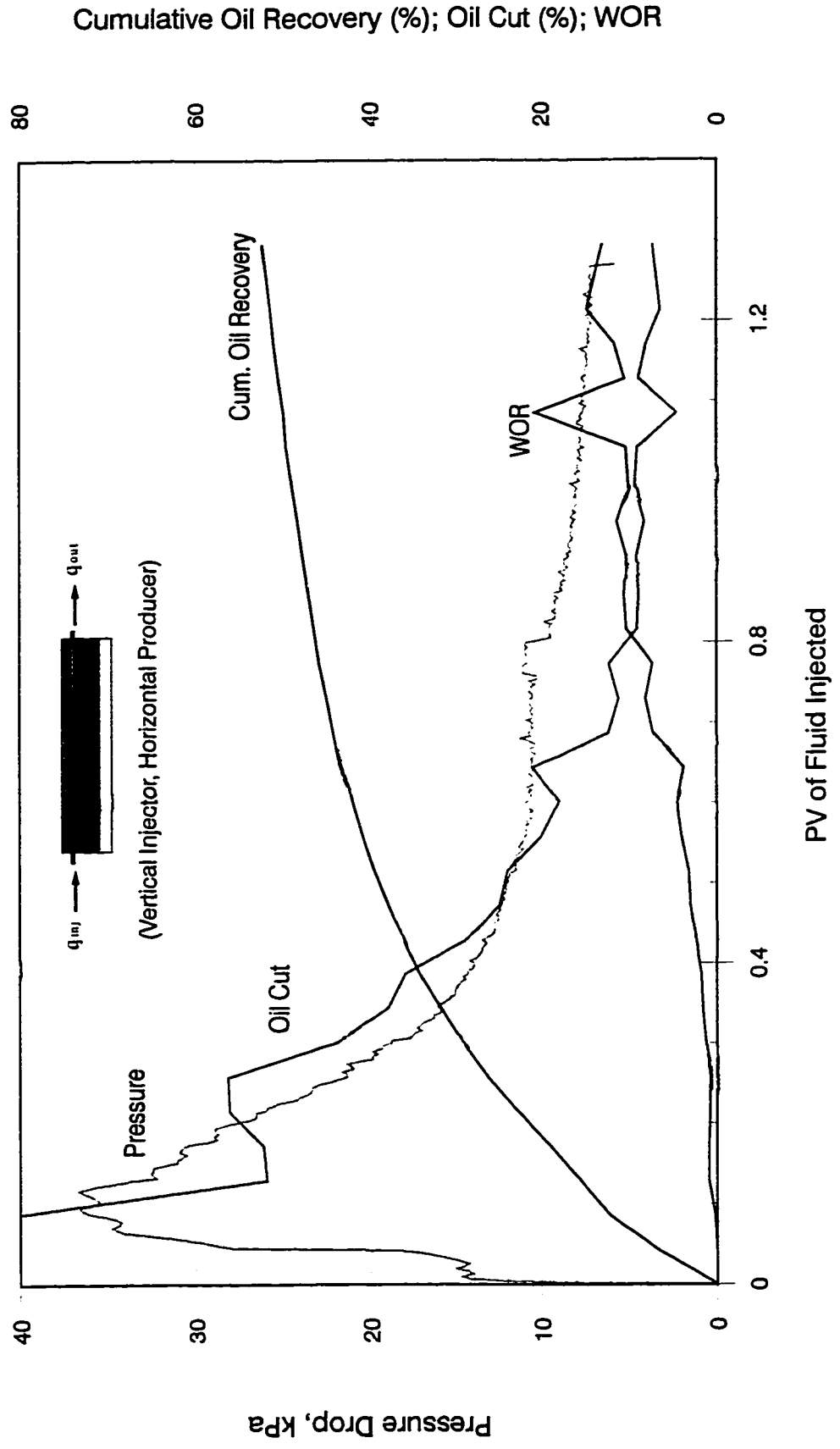


Figure F-29: Bottom-Water Pack Waterflood (  $q = 450$  cc/hr,  $hw/ho = 1/3$ , Oil Viscosity =  $34.3$  mPa.s )

# Production History for Simulation Run 30

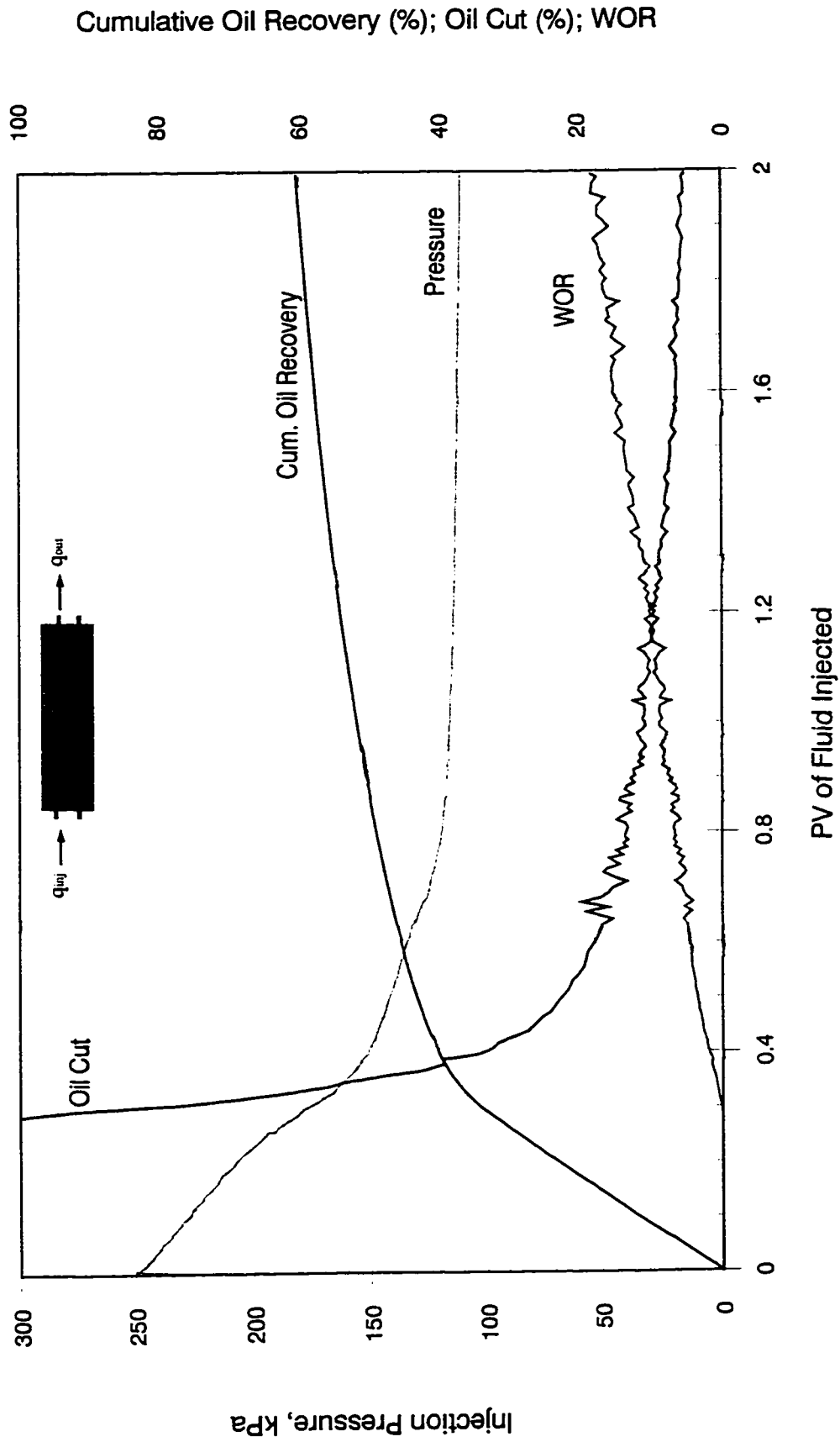


Figure F-30: Homogeneous Pack Waterflood ( Injection Rate = 450 cc/hr, Oil Viscosity = 34.3 mPa.s )

# Production History for Simulation Run 31

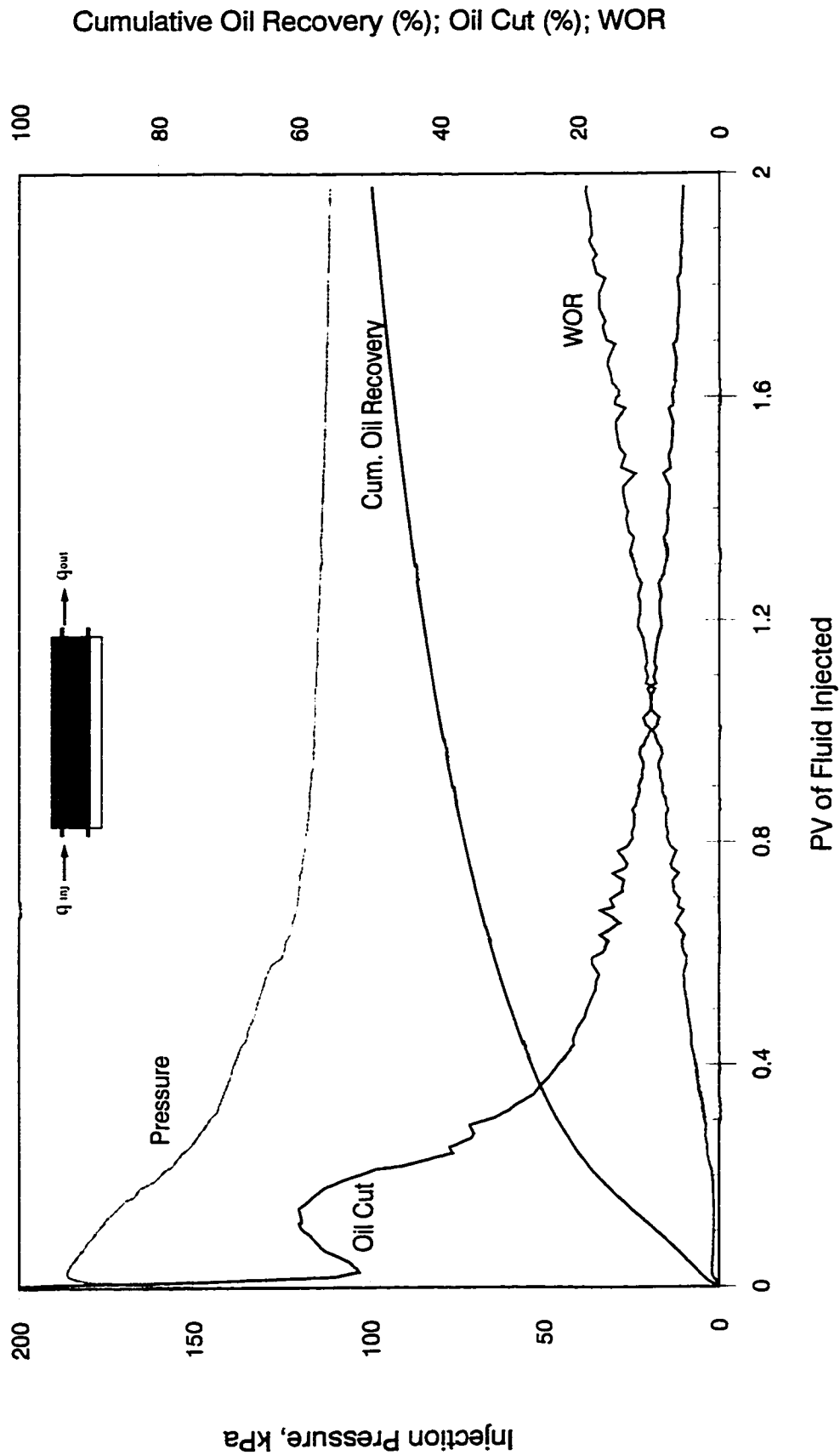


Figure F-31: Bottom-Water Pack Waterflood (  $q = 450$  cc/hr,  $h_w/h_o = 1/3$ , Oil Viscosity =  $34.3$  mPa.s )

# Production History for Simulation Run 32

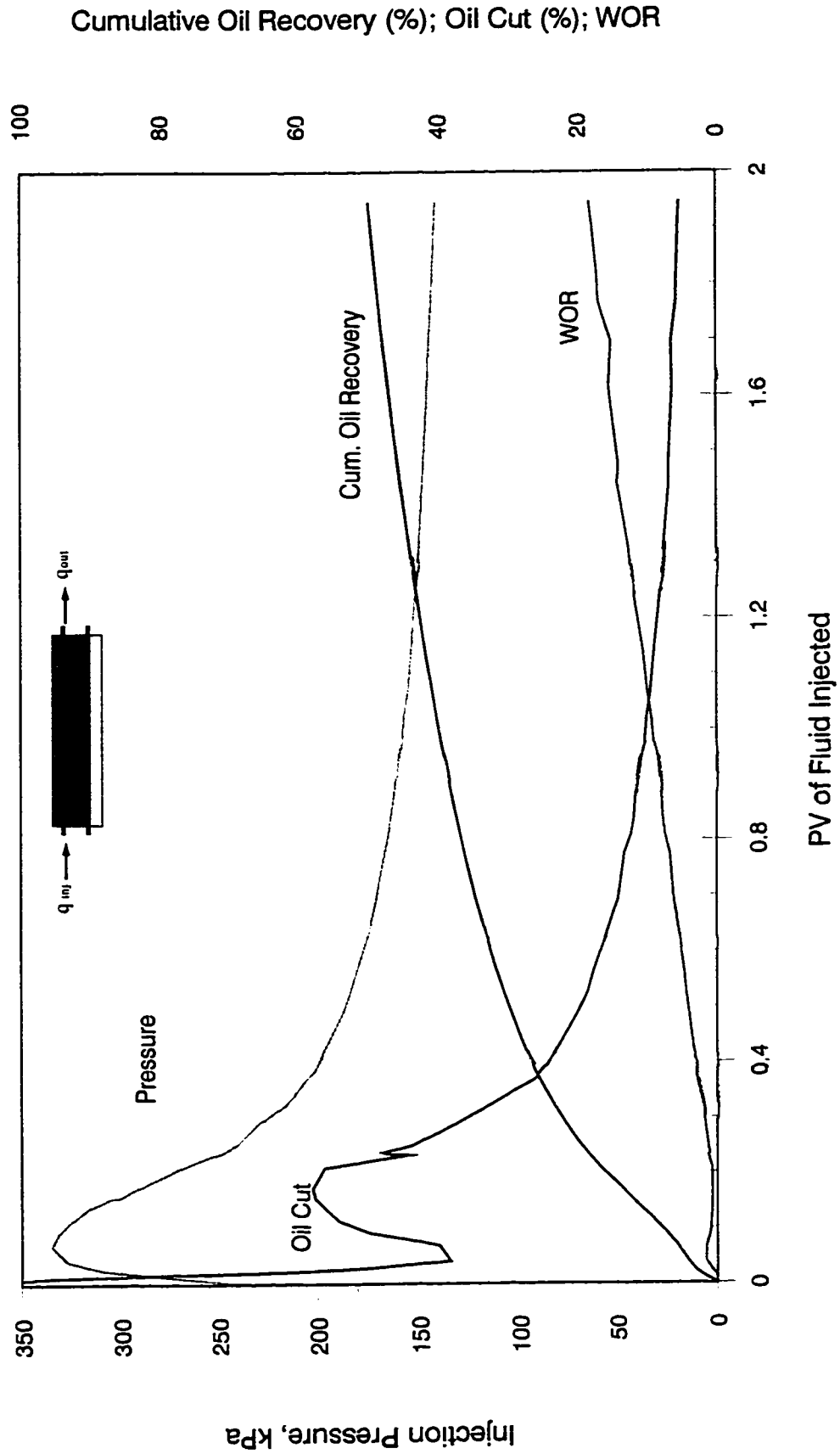


Figure F-32: Bottom-Water Pack Waterflood (  $q = 1200$  cc/hr,  $hw/ho = 1/3$ , Oil Viscosity =  $34.3$  mPa.s )

### Production History for Simulation Run 33

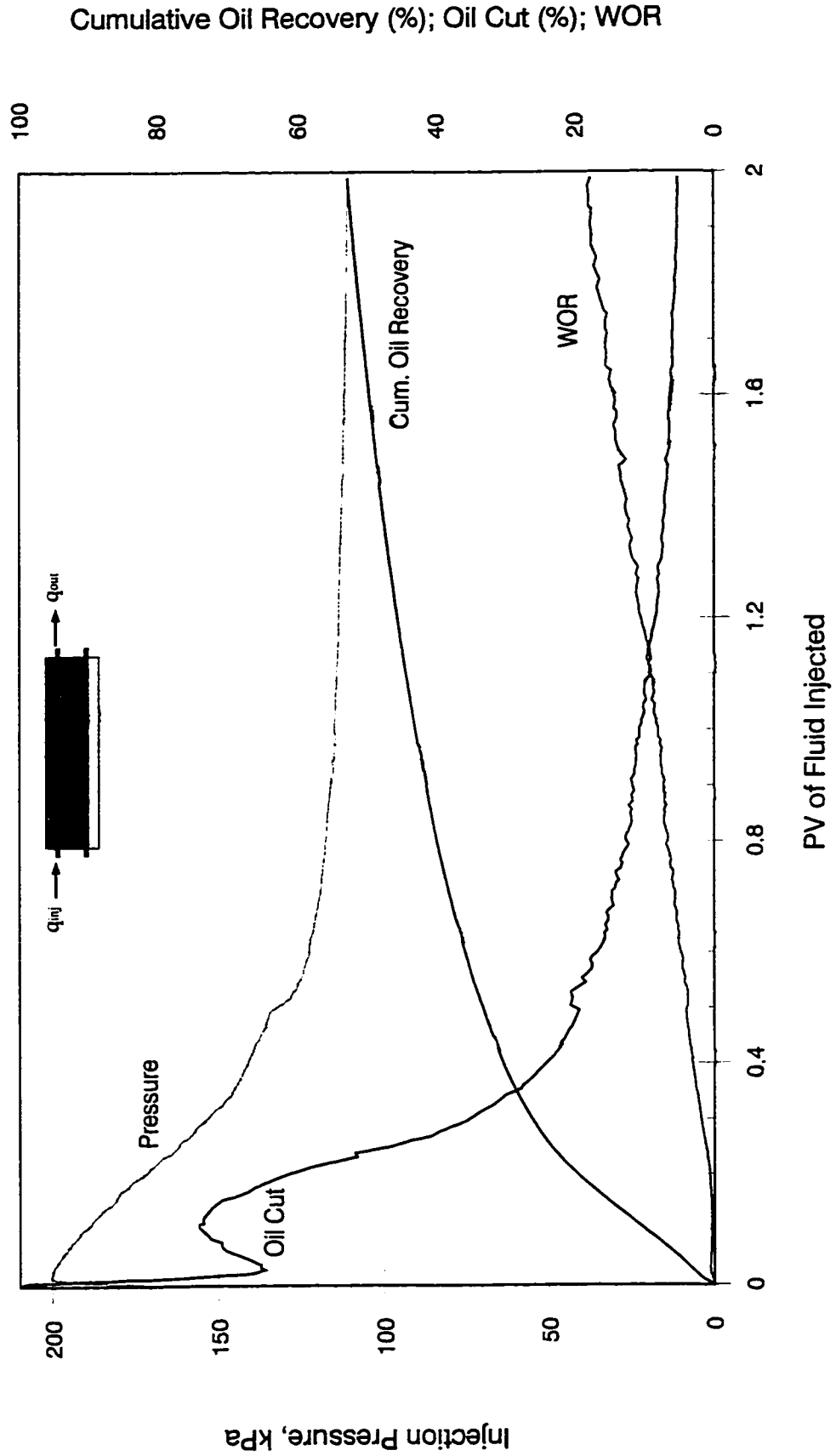
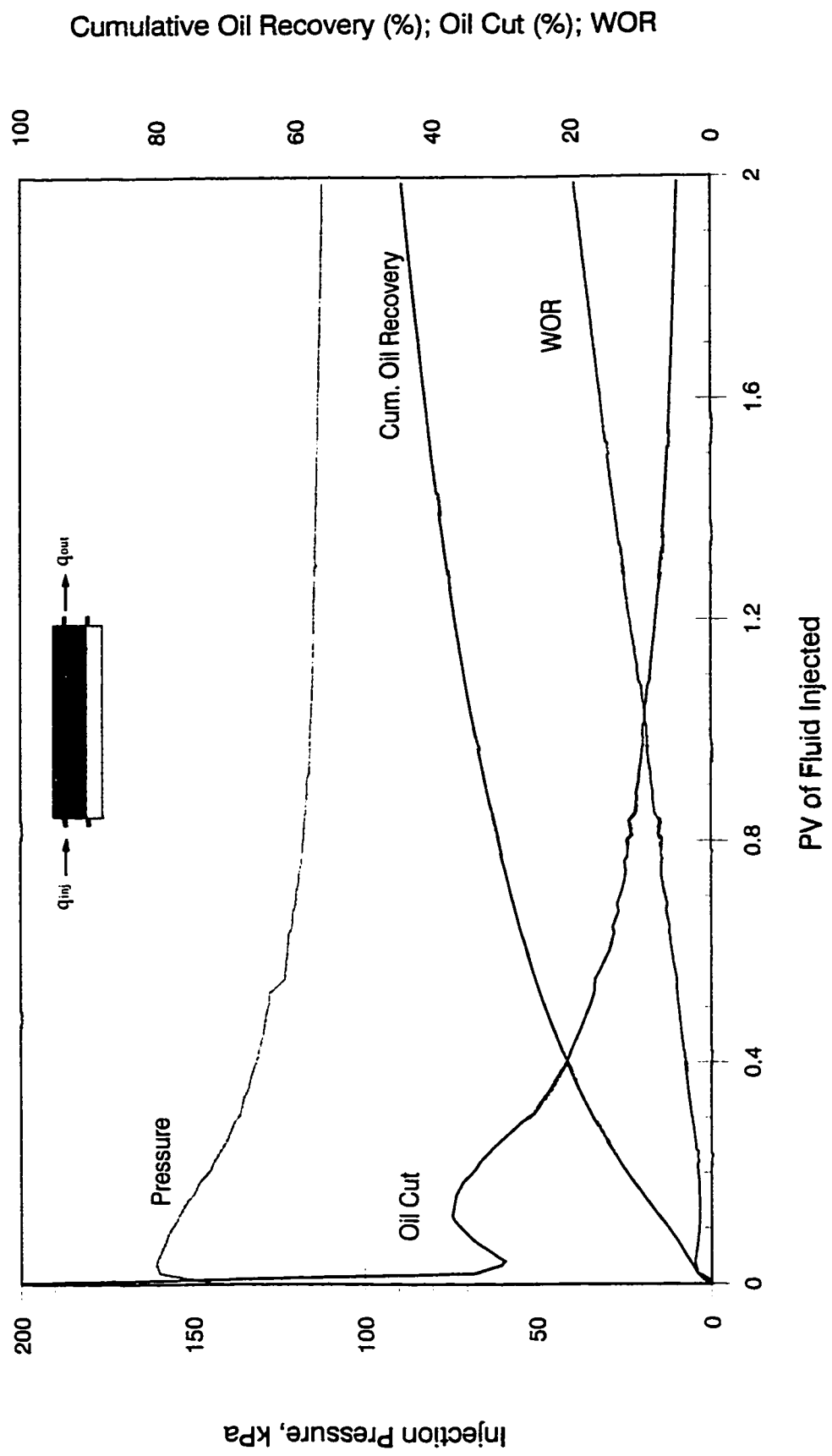


Figure F-33: Bottom-Water Pack Waterflood (  $q = 450$  cc/hr,  $hw/ho = 1/4$ , Oil Viscosity =  $34.3$  mPa.s )

# Production History for Simulation Run 34



Cumulative Oil Recovery (%); Oil Cut (%); WOR

Figure F-34: Bottom-Water Pack Waterflood (  $q = 450$  cc/hr,  $hw/ho = 1/2$ , Oil Viscosity =  $34.3$  mPa.s )



# Production History for Simulation Run 35

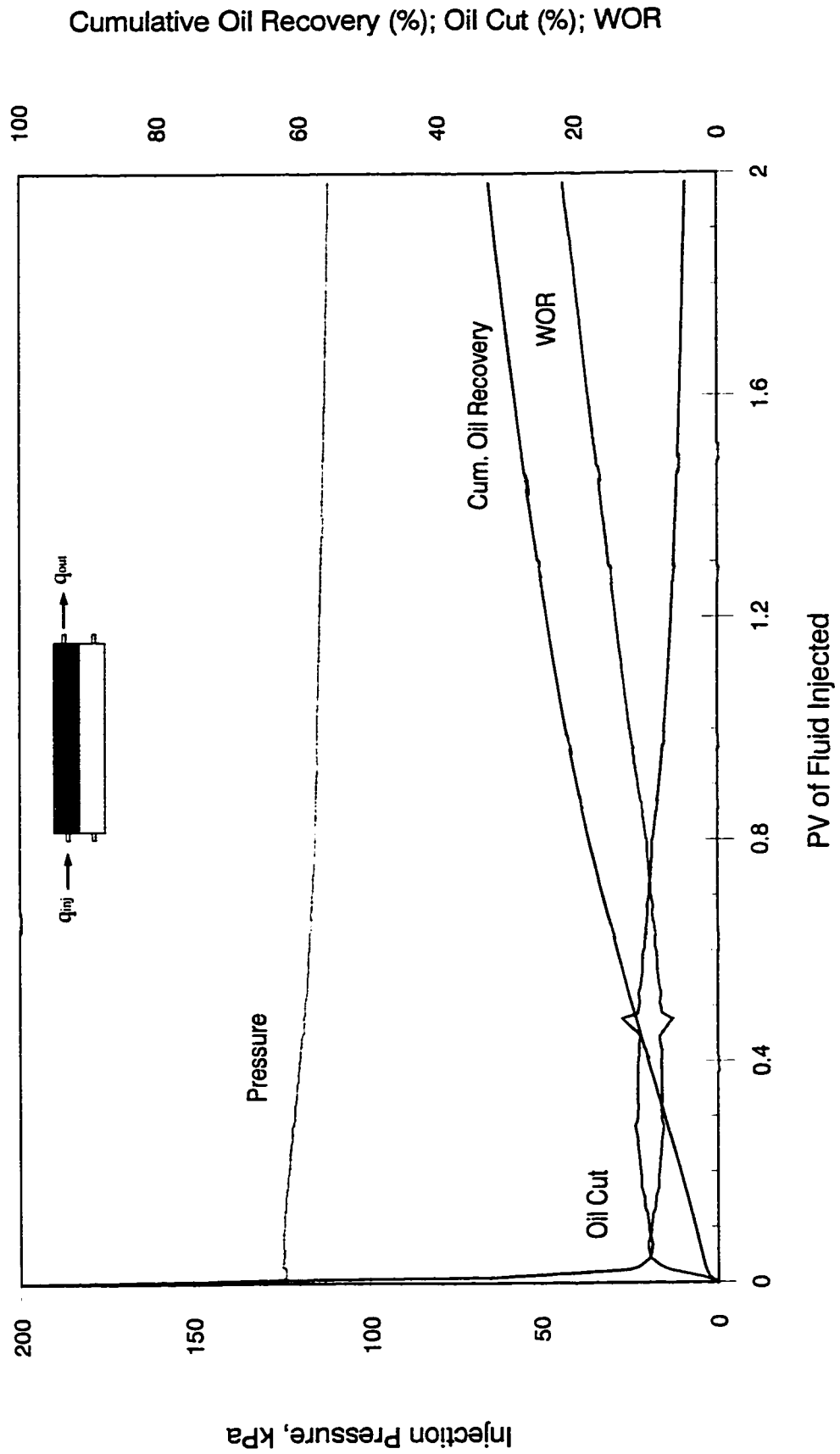


Figure F-35: Bottom-Water Pack Waterflood (  $q = 450$  cc/hr,  $hw/ho = 1/1$ , Oil Viscosity =  $34.3$  mPa.s )

# Production History for Simulation Run 36

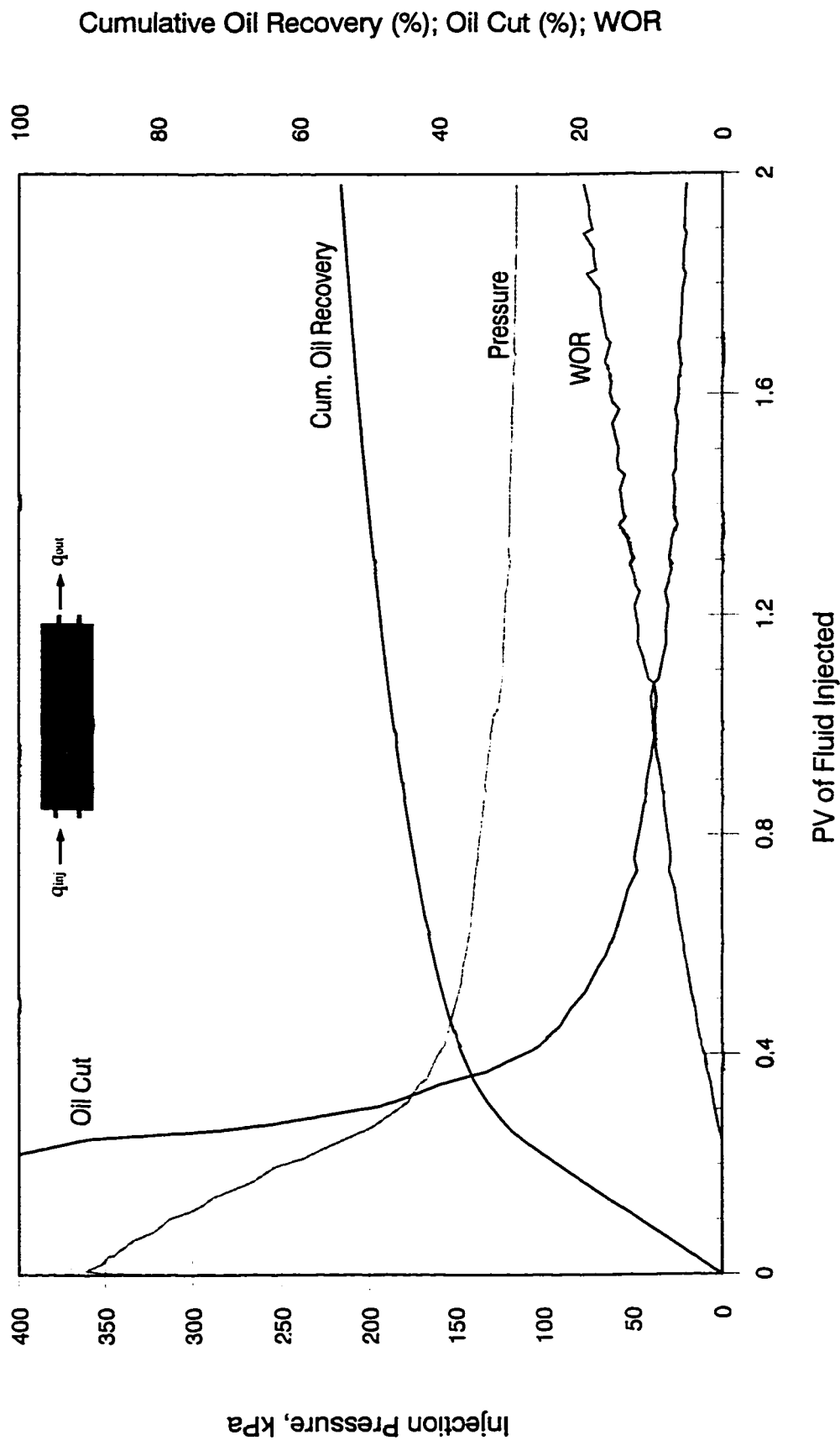


Figure F-36: Homogeneous Pack Waterflood ( Injection Rate = 450 cc/hr, Oil Viscosity = 68.0 mPa.s )

# Production History for Simulation Run 37

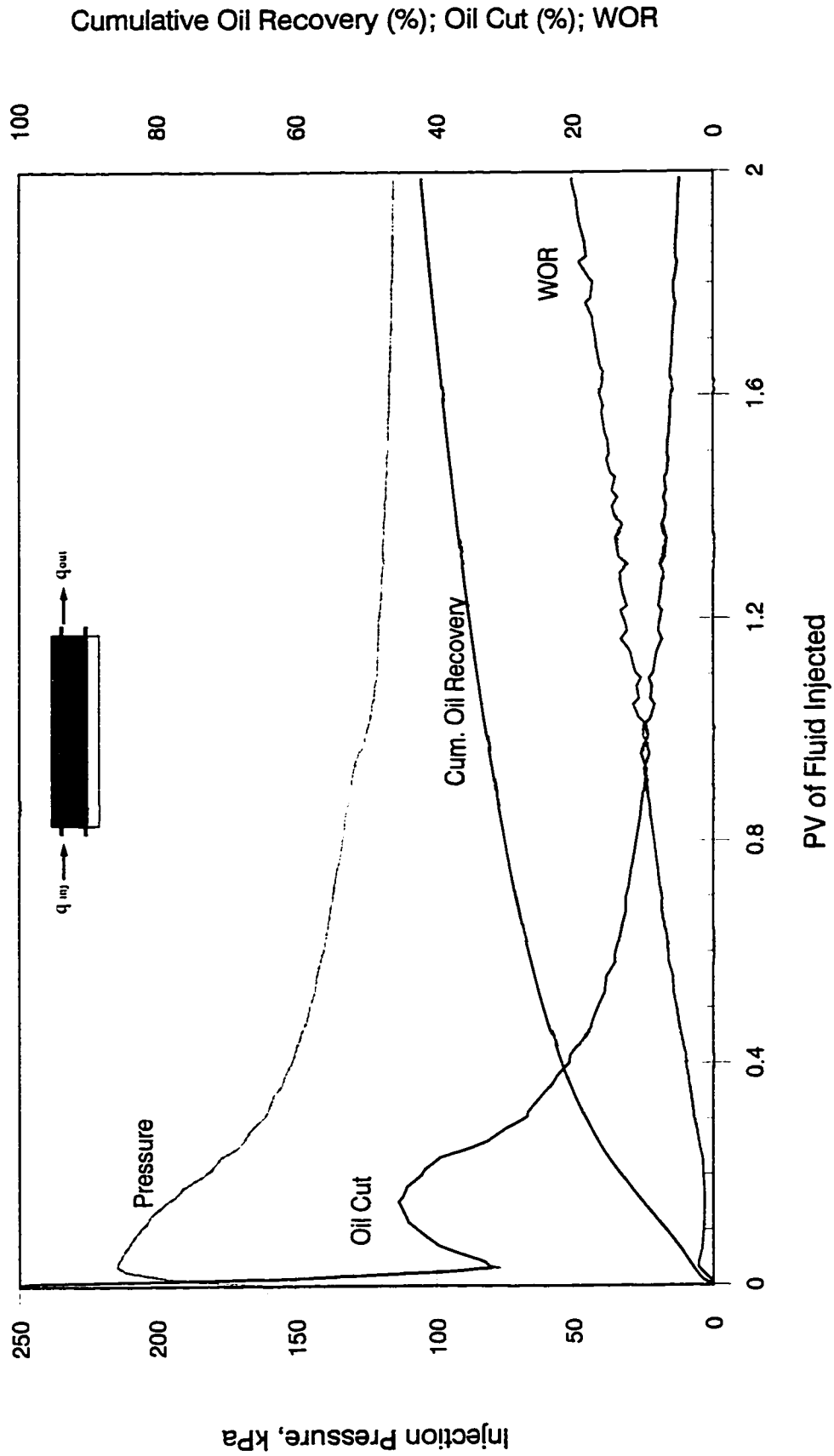


Figure F-37: Bottom-Water Pack Waterflood (  $q = 450$  cc/hr,  $hw/ho = 1/3$ , Oil Viscosity =  $68.0$  mPa.s )

### Production History for Simulation Run 38

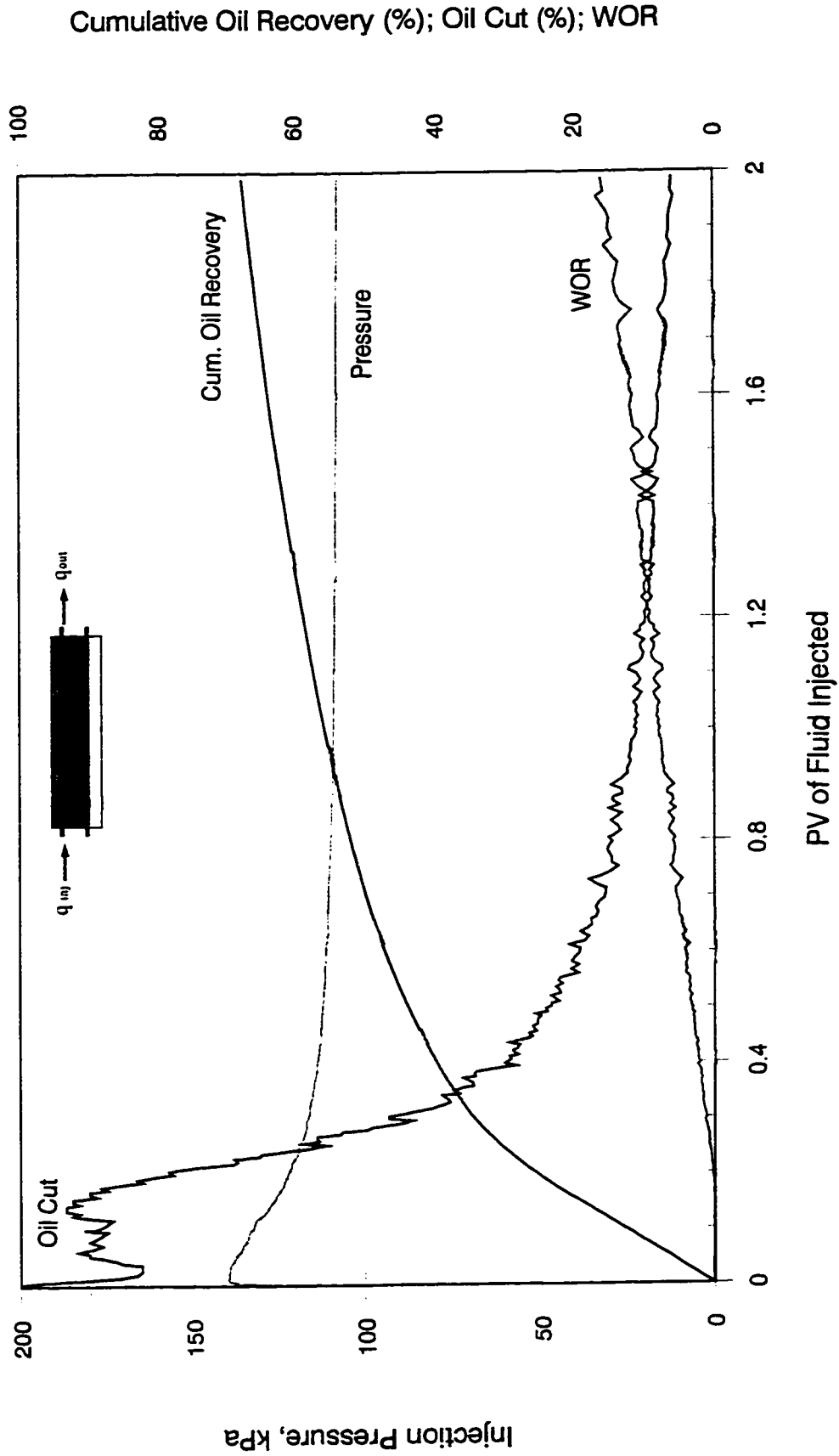


Figure F-38: Bottom-Water Pack Waterflood (  $q = 450$  cc/hr,  $h_w/h_o = 1/3$ , Oil Viscosity =  $11.0$  mPa.s )

# Production History for Simulation Run 39

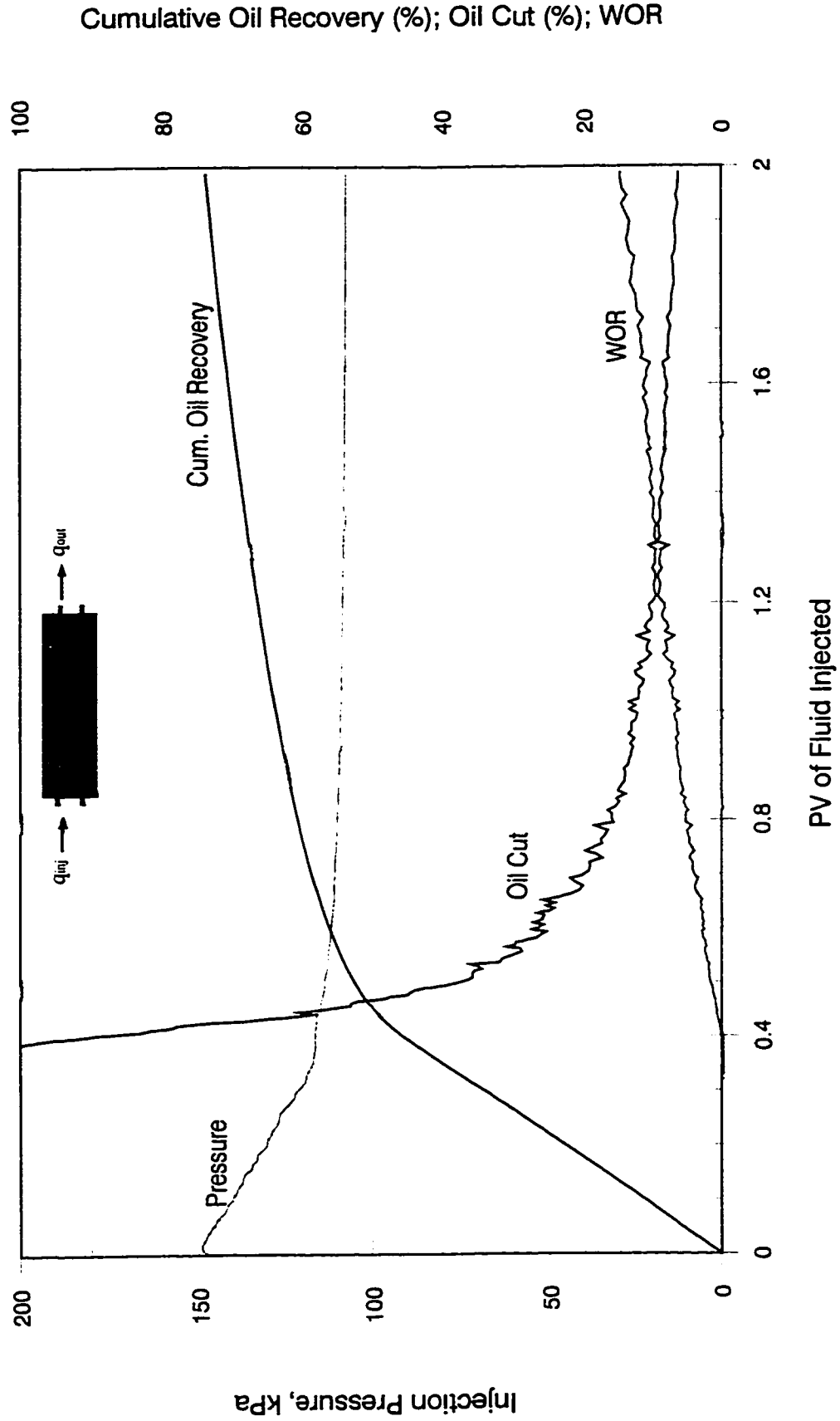


Figure F-39: Homogeneous Pack Waterflood ( Injection Rate = 450 cc/hr, Oil Viscosity = 11.0 mPa.s )

# Production History for Simulation Run 40

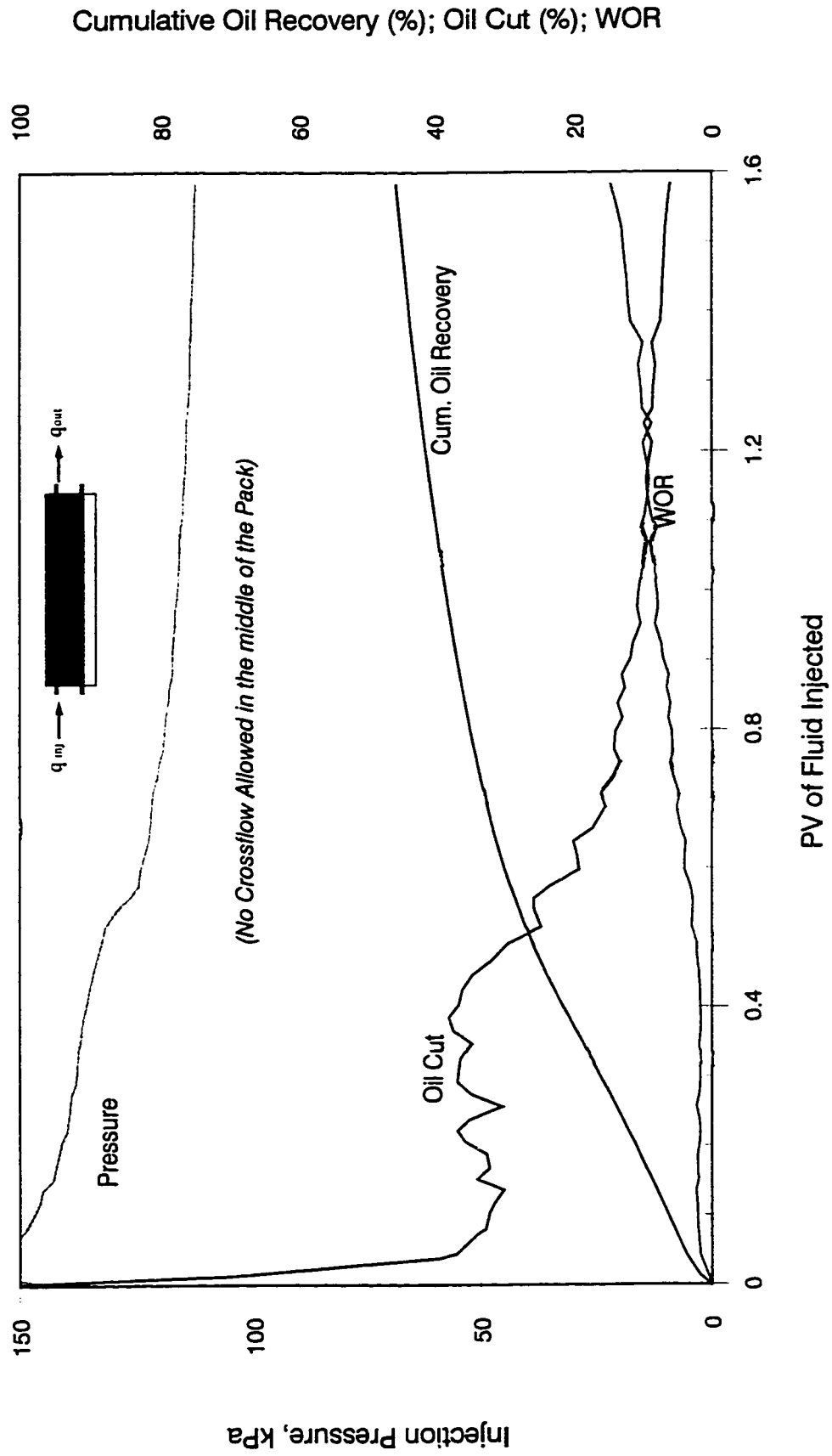


Figure F-40: Bottom-Water Pack Waterflood (  $q = 450$  cc/hr,  $h_w/h_o = 1/3$ , Oil Viscosity =  $34.3$  mPa.s )

# Production History for Simulation Run 41

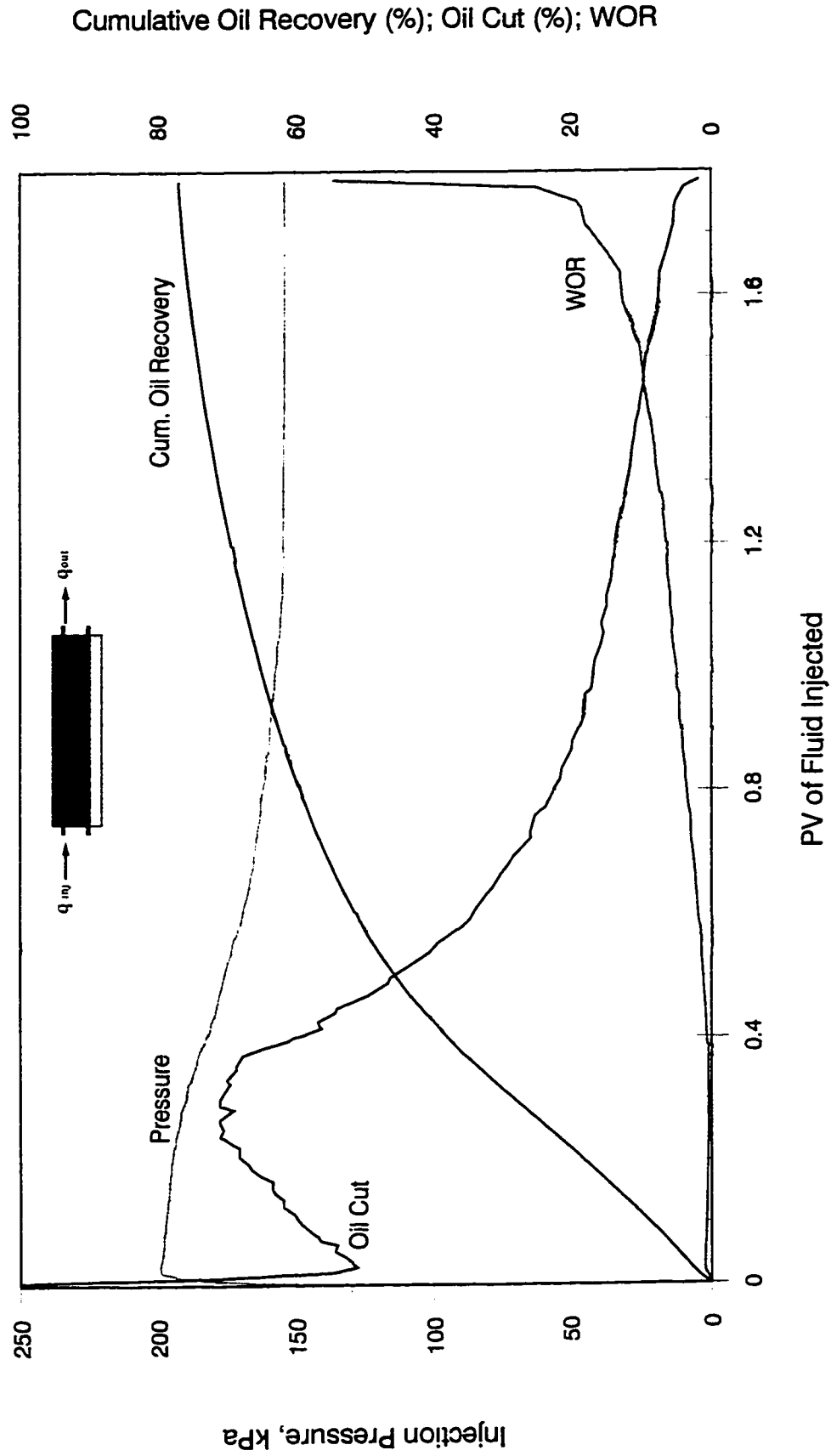


Figure F-41: Bottom-Water Pack Polymer Flood ( $q = 450$  cc/hr, Con. = 500 ppm,  $hw/ho = 1/3$ ,  $U_o = 34.3$  mPa.s)

# Production History for Simulation Run 42

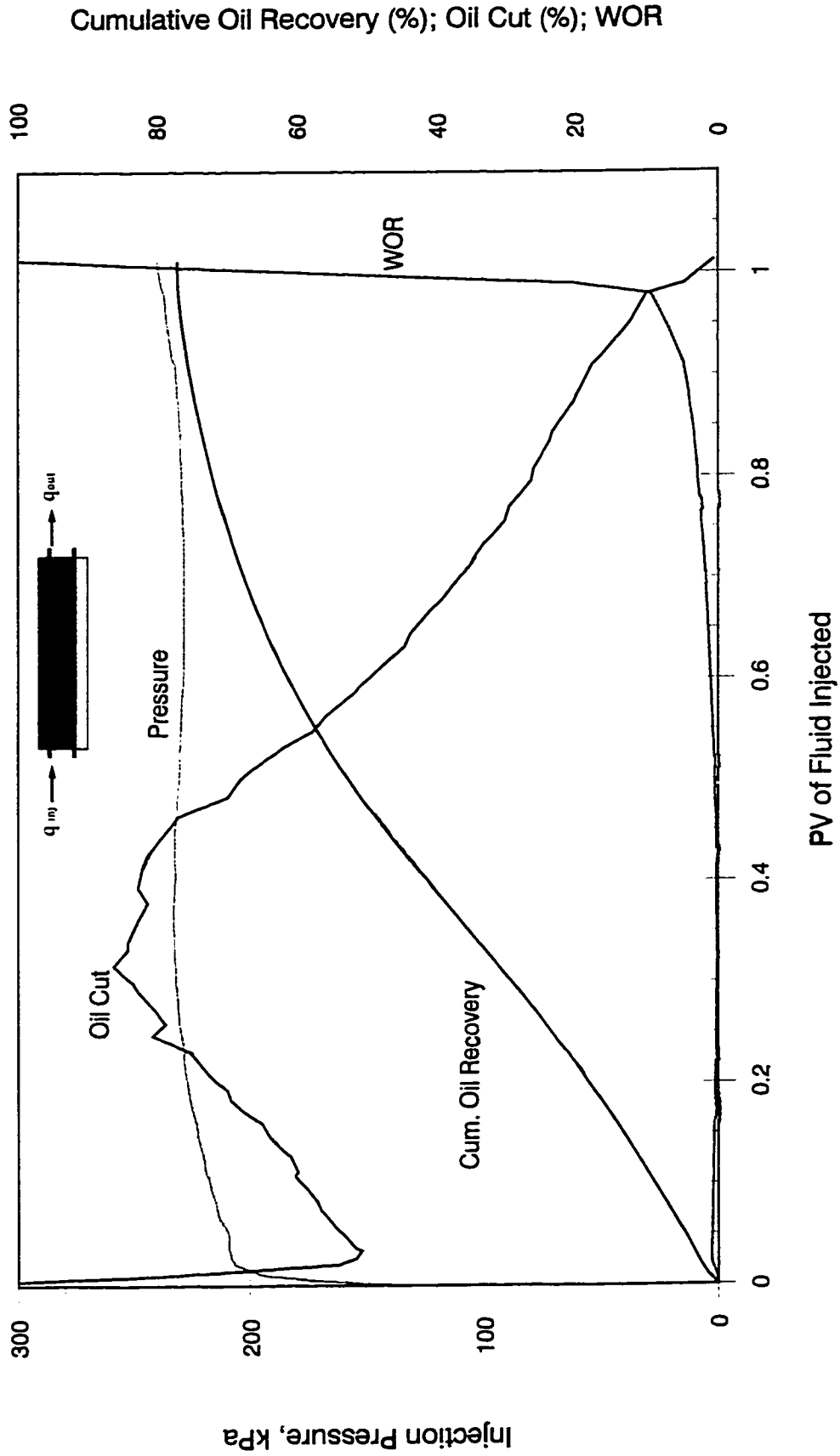


Figure F-42: Bottom-Water Pack Polymer Flood ( $q = 450$  cc/hr,  $Con. = 1000$  ppm,  $hw/ho = 1/3$ ,  $U_o = 34.3$  mPa.s)



# Production History for Simulation Run 43

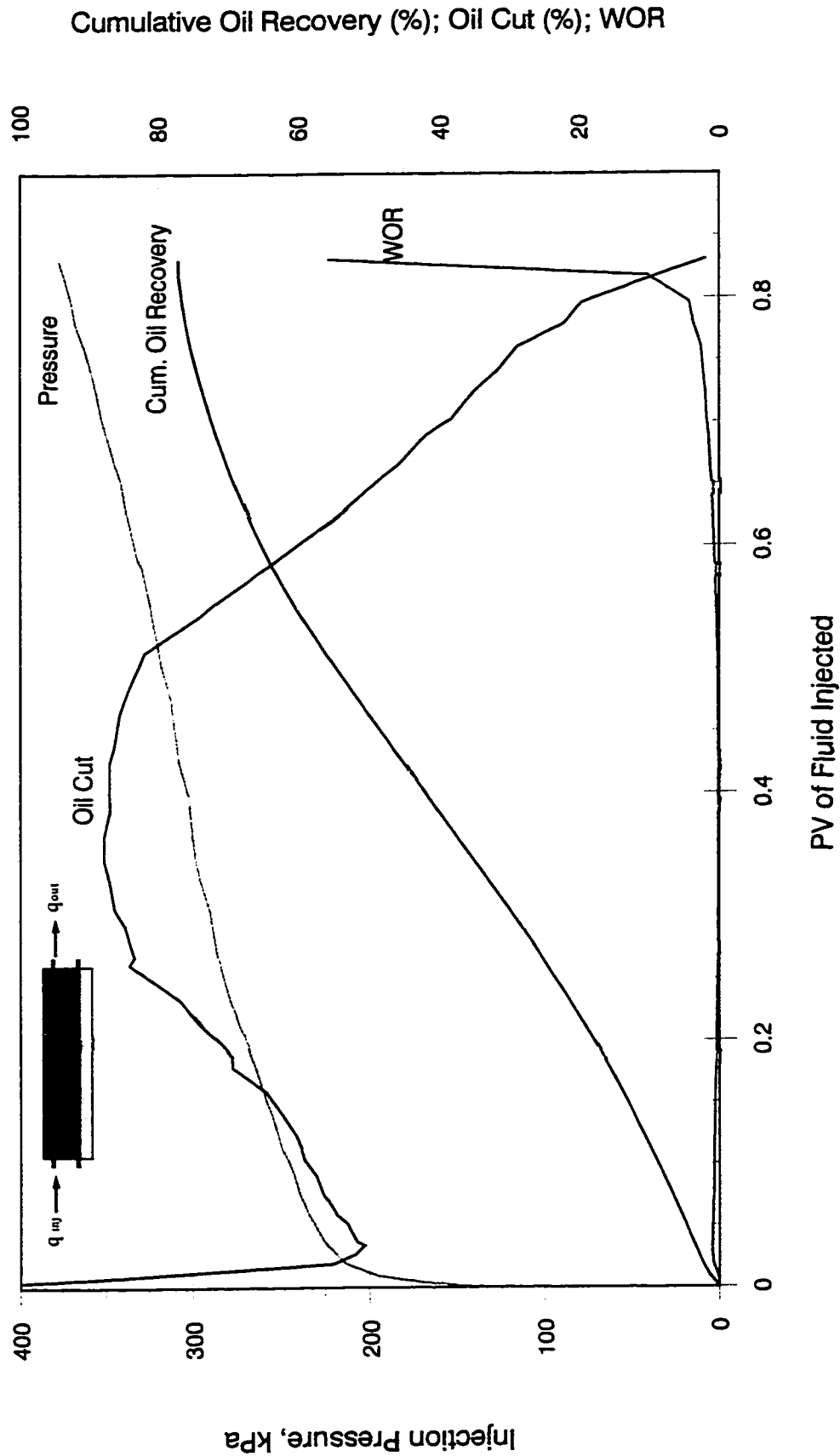


Figure F-43: Bottom-Water Pack Polymer Flood ( $q = 450$  cc/hr,  $Con. = 1500$  ppm,  $hw/ho = 1/3$ ,  $U_o = 34.3$  mPa.s)

# Production History for Simulation Run 44

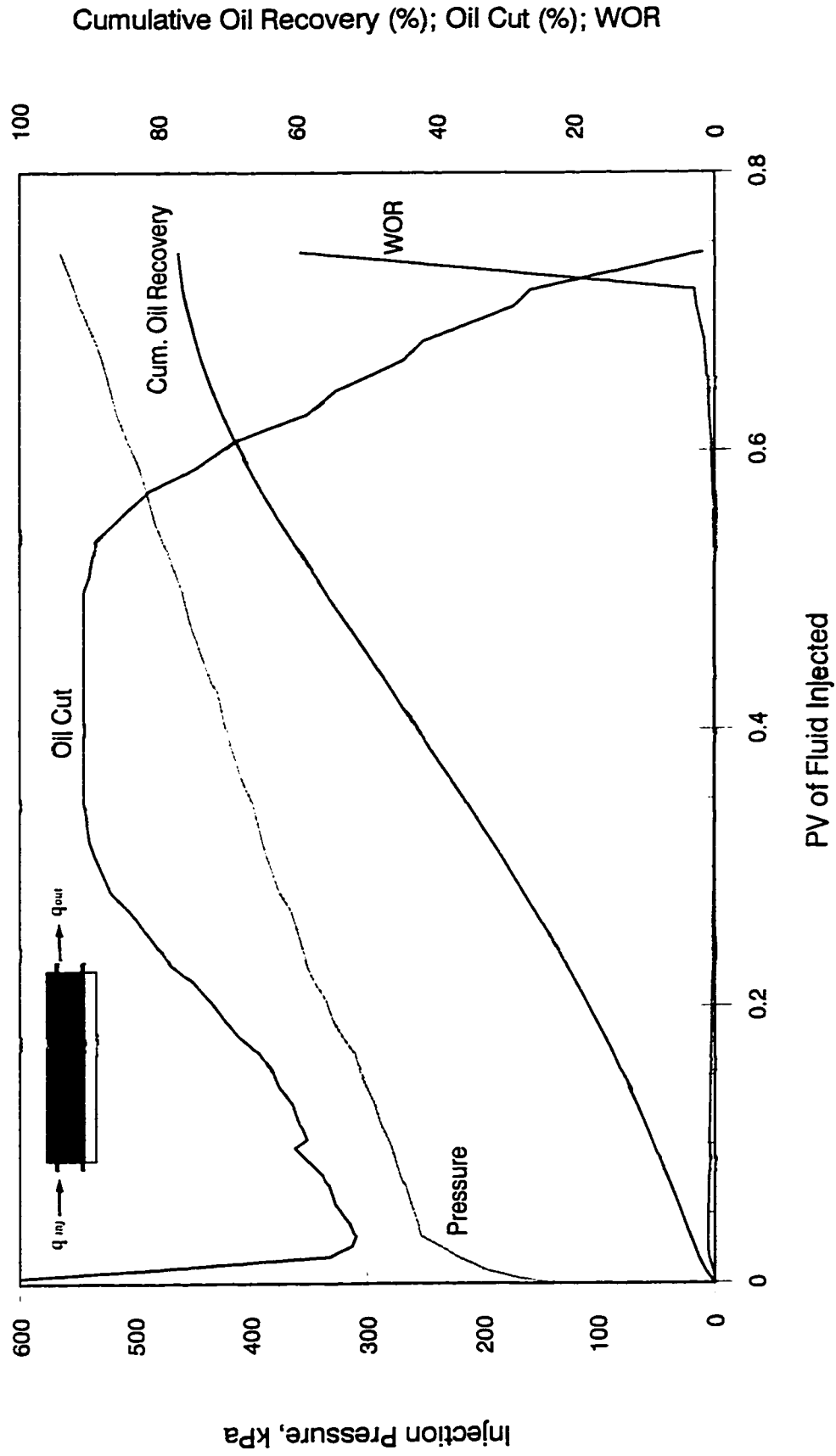


Figure F-44: Bottom-Water Pack Polymer Flood ( $q = 450$  cc/hr,  $Con. = 2000$  ppm,  $hw/ho = 1/3$ ,  $U_o = 34.3$  mPa.s)

# Production History for Simulation Run 45

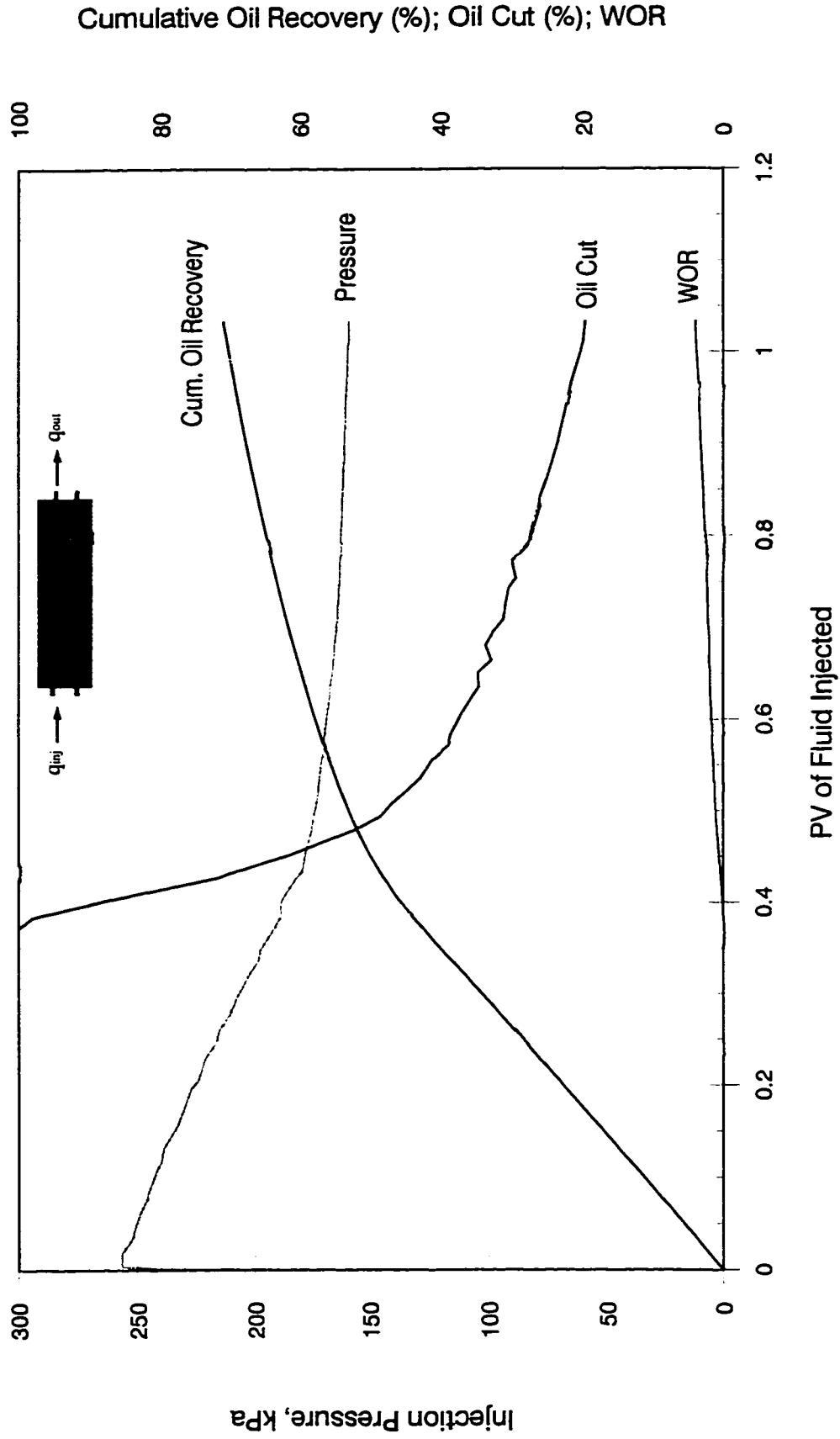


Figure F-45: Homogeneous Pack Polymer Flood (  $q = 450$  cc/hr, Con. = 500 ppm, Oil Vis. = 34.3 mPa.s )

# Production History for Simulation Run 46

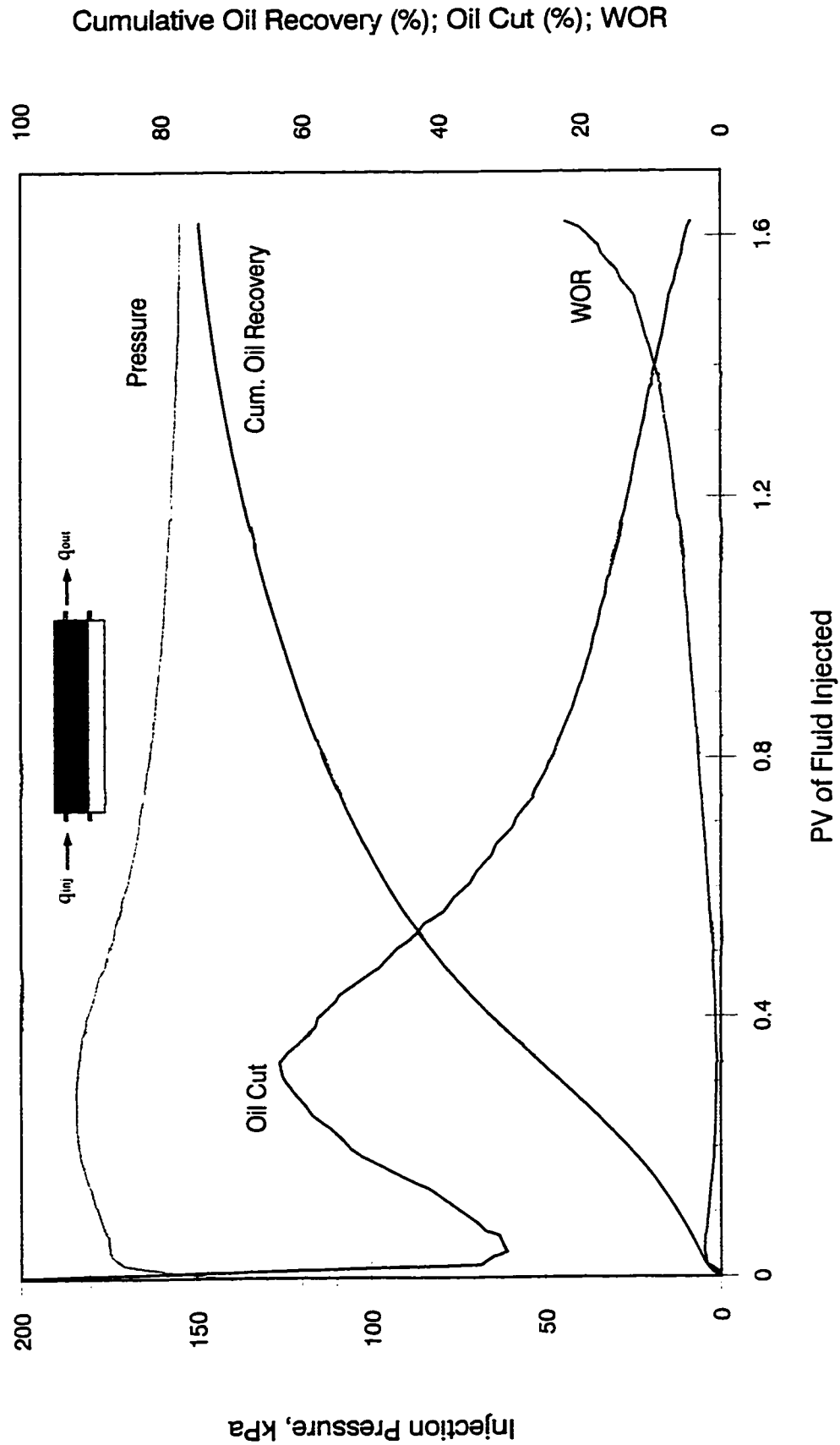


Figure F-46: Bottom-Water Pack Polymer Flood ( $q = 450$  cc/hr, Con. = 500 ppm,  $hw/ho = 1/2$ ,  $U_o = 34.3$  mPa.s)

# Production History for Simulation Run 47

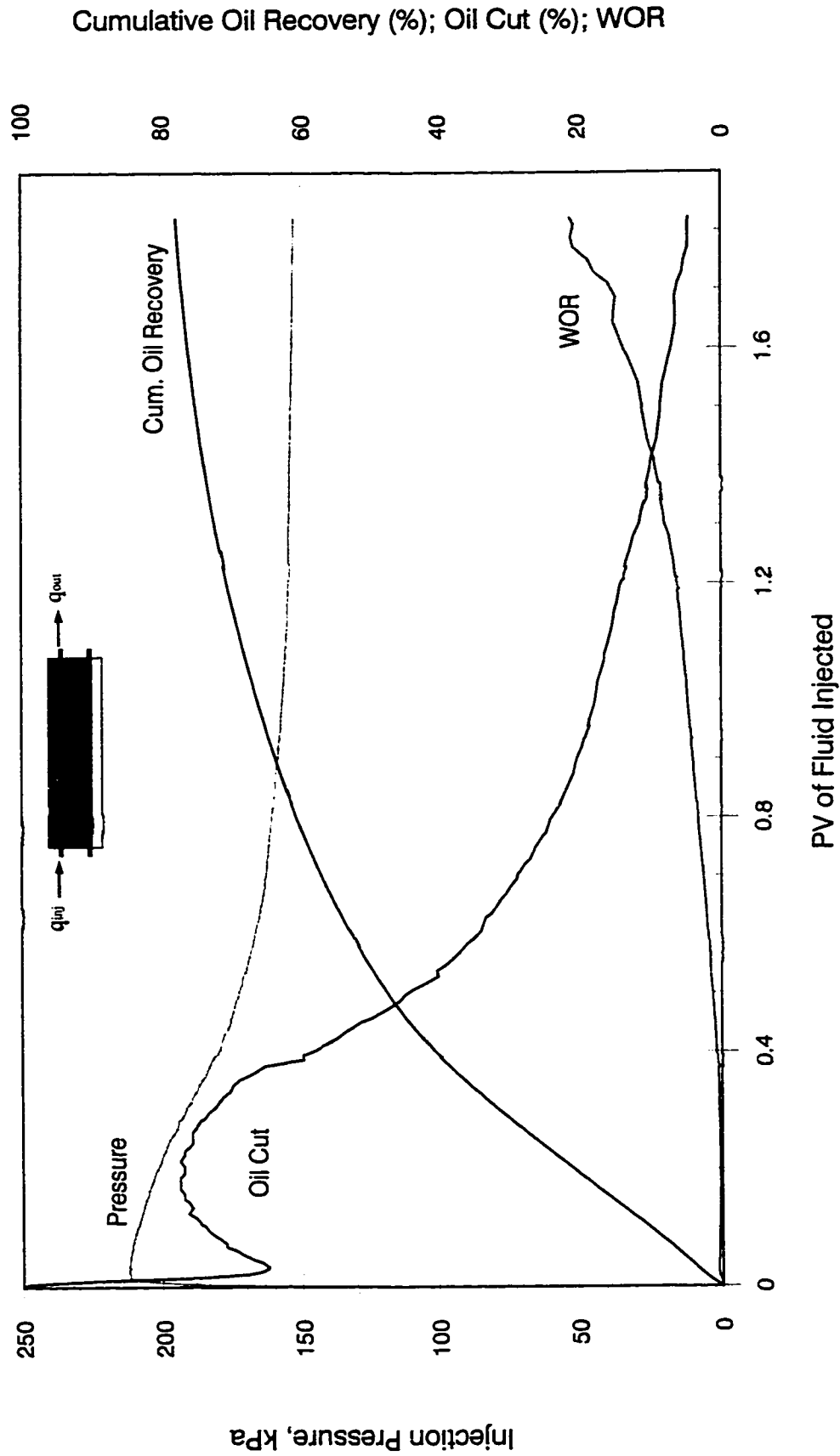


Figure F-47: Bottom-Water Pack Polymer Flood ( $q = 450$  cc/hr, Con. = 500 ppm,  $hw/ho = 1/4$ ,  $U_o = 34.3$  mPa.s)

# Production History for Simulation Run 48

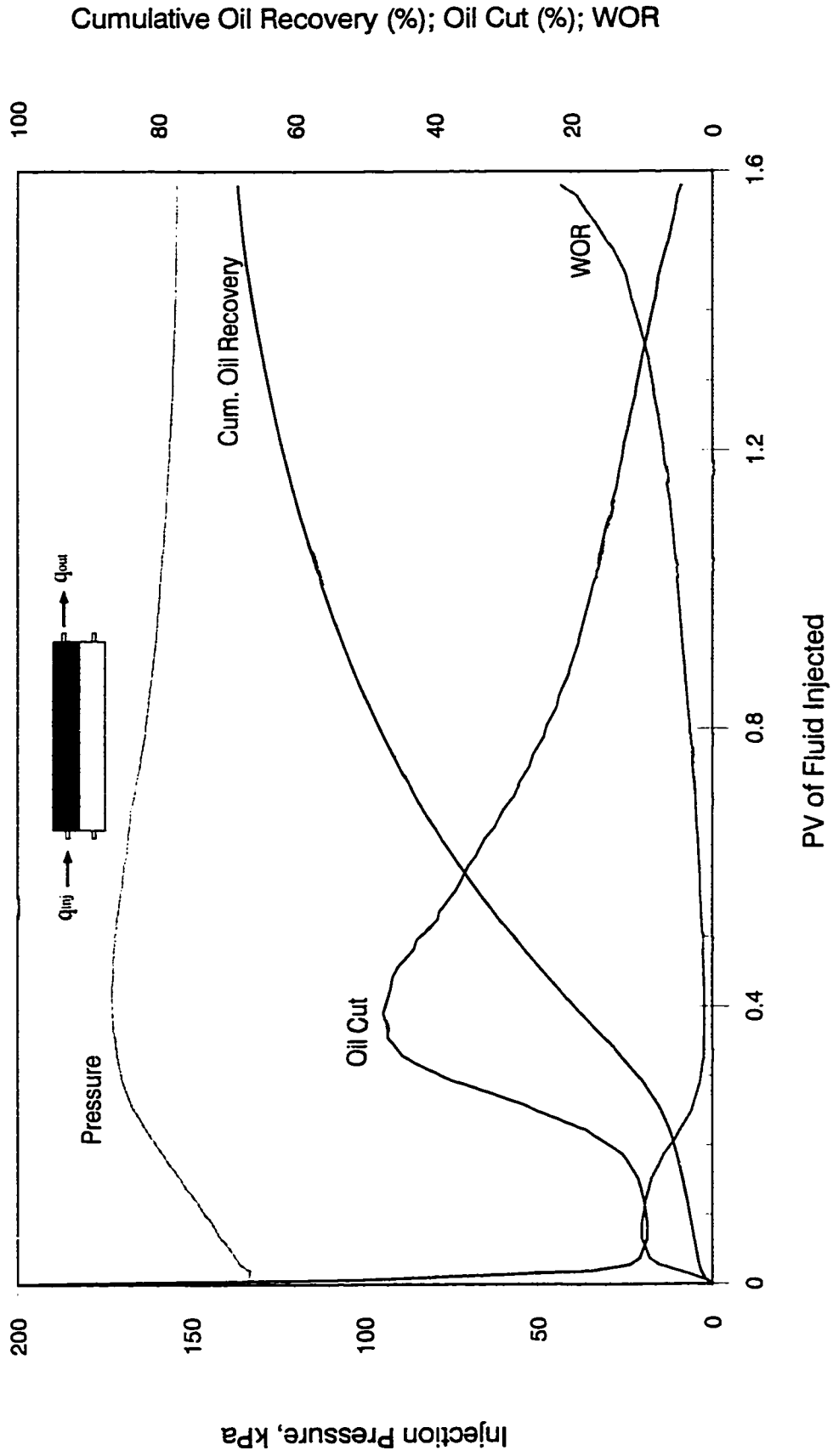


Figure F-48: Bottom-Water Pack Polymer Flood ( $q = 450$  cc/hr, Con. = 500 ppm,  $hw/ho = 1/1$ ,  $U_o = 34.3$  mPa.s)

# Production History for Simulation Run 49

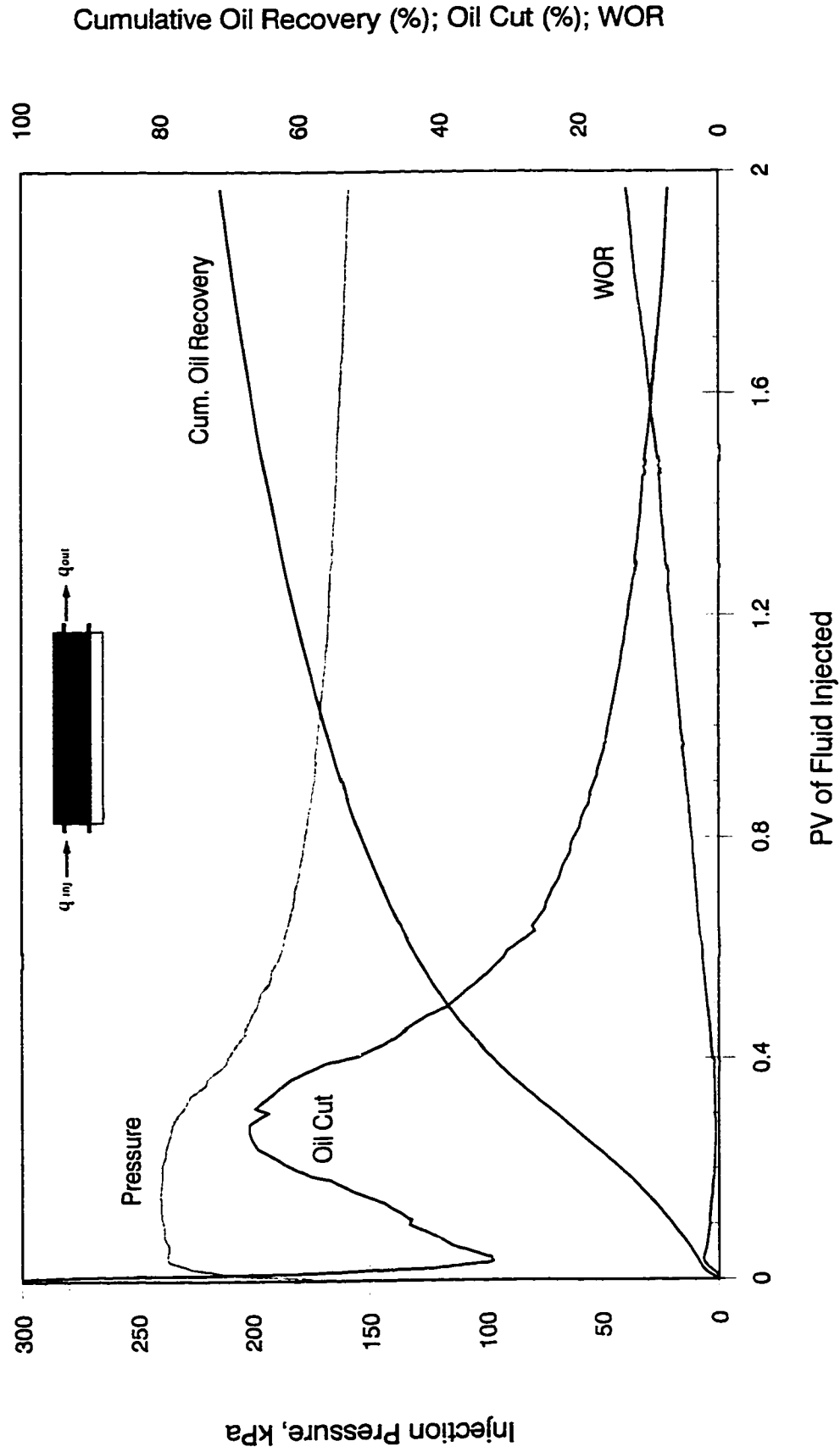


Figure F-49: Bottom-Water Pack Polymer Flood ( $q = 450$  cc/hr, Con. = 500 ppm,  $hw/ho = 1/3$ ,  $U_o = 68.0$  mPa.s)

# Production History for Simulation Run 50

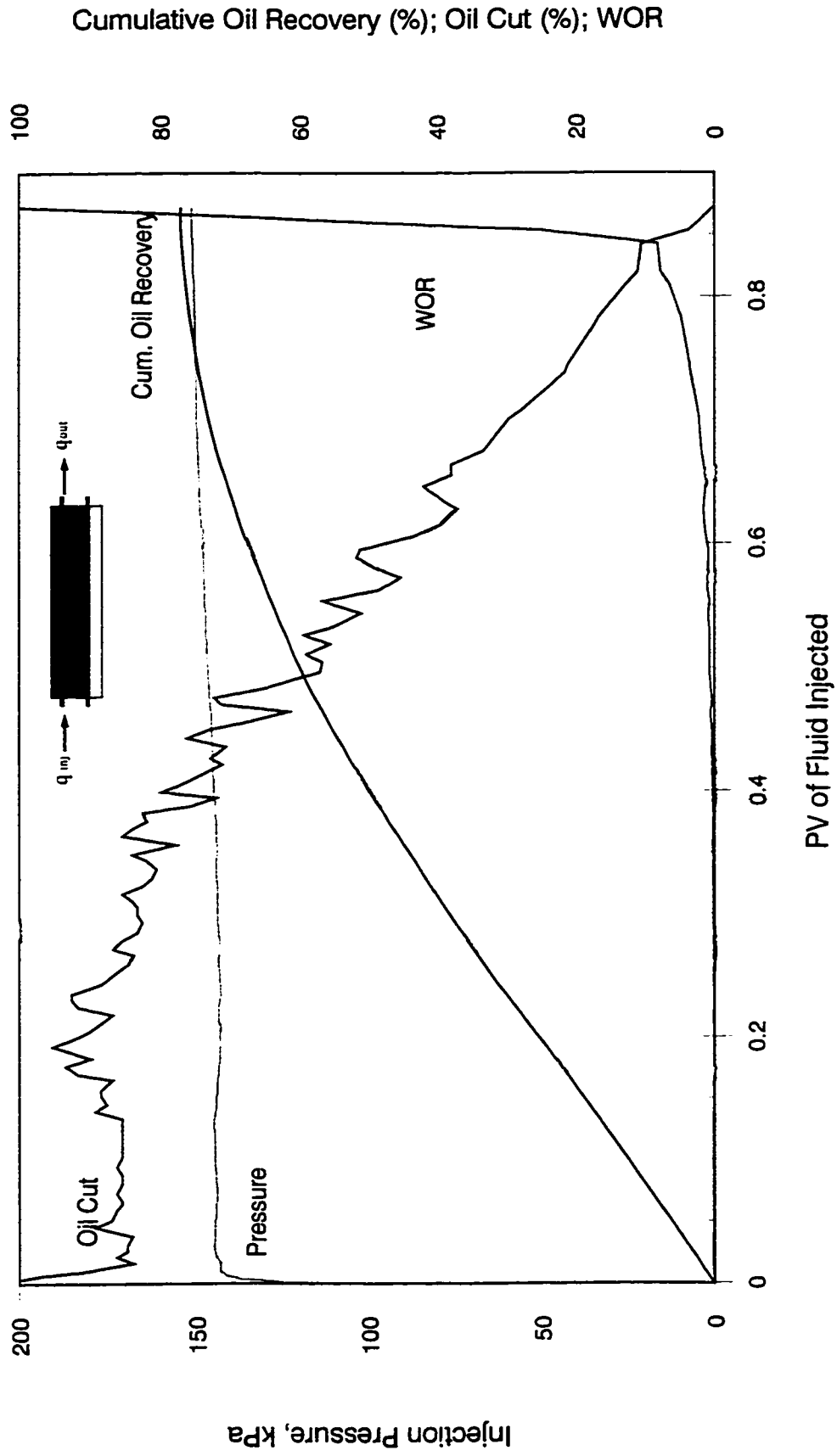


Figure F-50: Bottom-Water Pack Polymer Flood (  $q = 450$  cc/hr, Con. = 500 ppm,  $h_w/h_o = 1/3$ ,  $U_o = 11.0$  mPa.s )



# Production History for Simulation Run 51

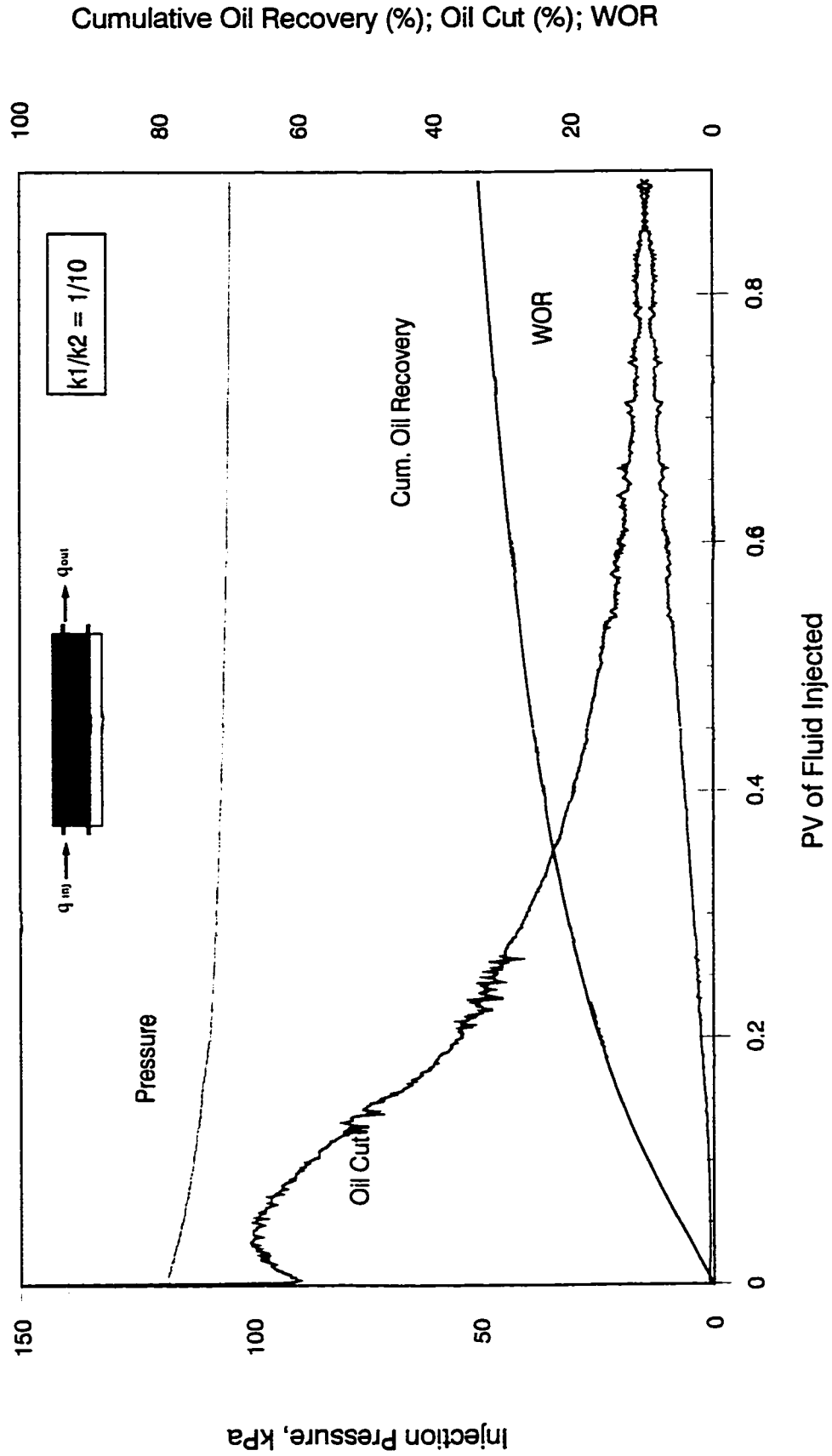


Figure F-51: Bottom-Water Pack Polymer Flood (  $q = 450$  cc/hr,  $hw/h_o = 1/3$ , Oil Viscosity =  $34.3$  mPa.s )

# Production History for Simulation Run 52

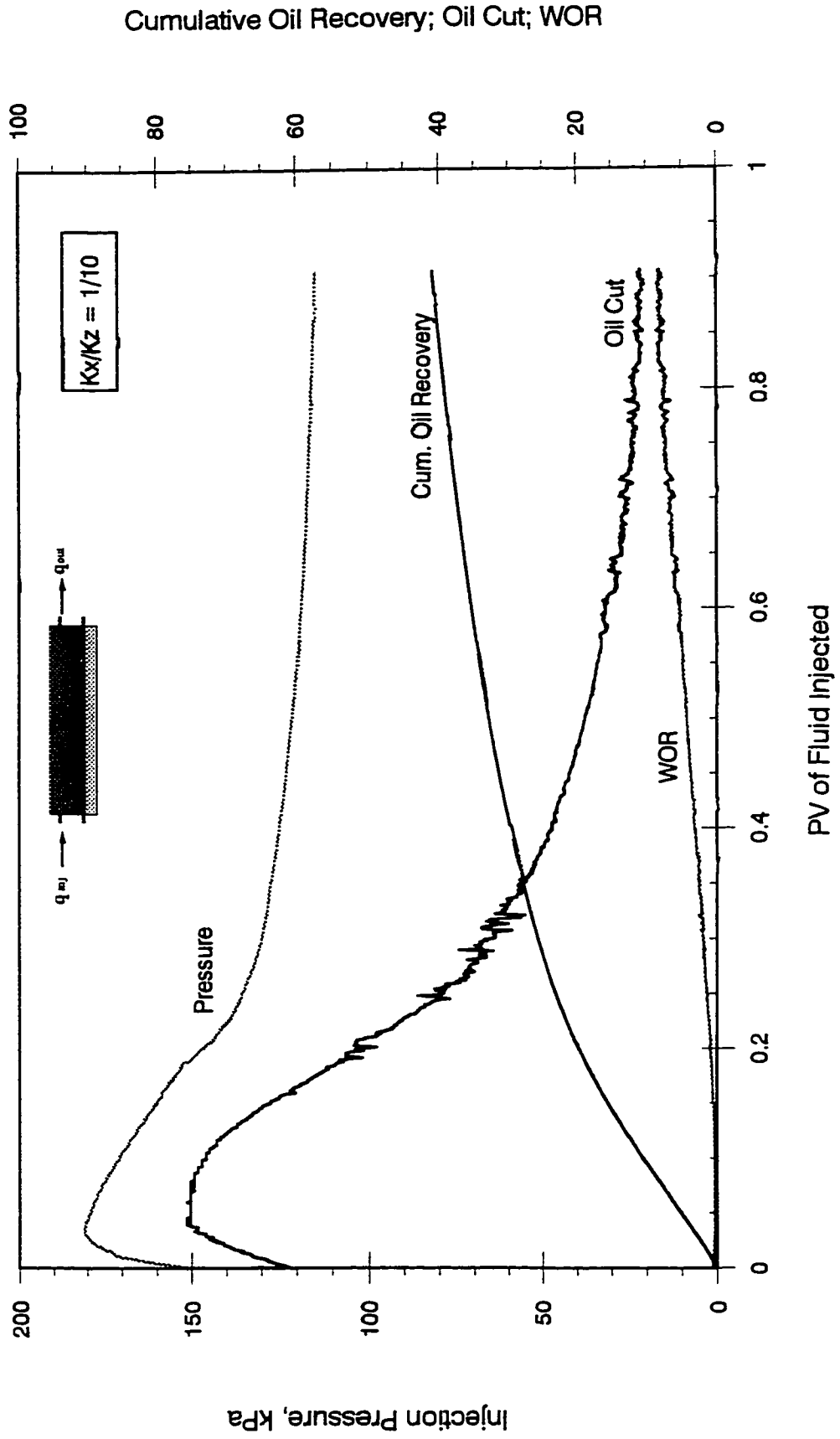


Figure F-52: Bottom-Water Pack Polymer Flood ( $q = 450$  cc/hr,  $hw/h_o = 1/3$ , Oil Viscosity =  $34.3$  mPa.s)

# Production History for Analytical Runs 53 Through 57

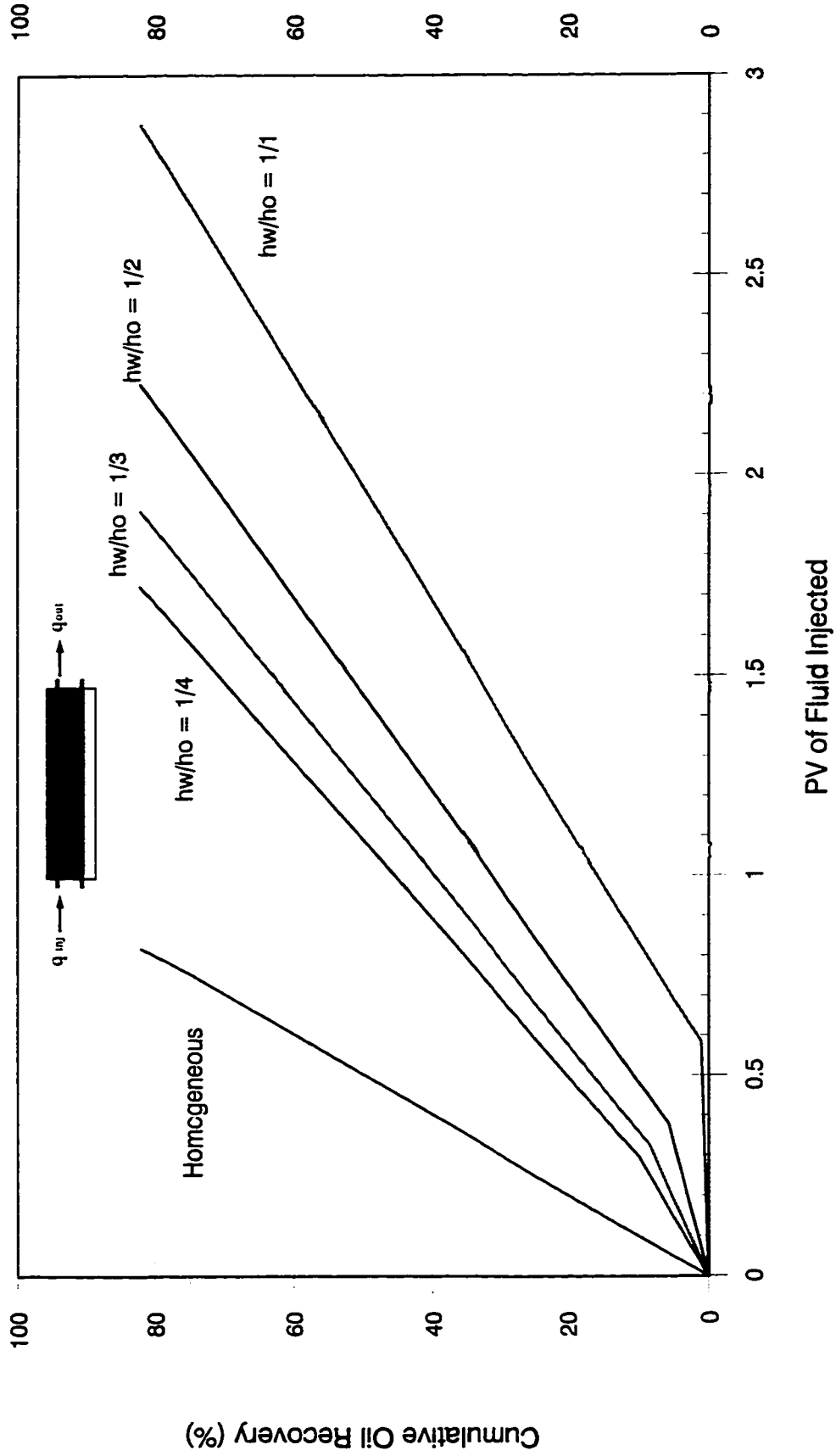


Figure F-53: Bottom-Water Pack Waterflood ( $k_1/k_2 = 1:1$ , Oil Viscosity = 34.3 mPa.s)

# Production History for Analytical Runs 58 and 59

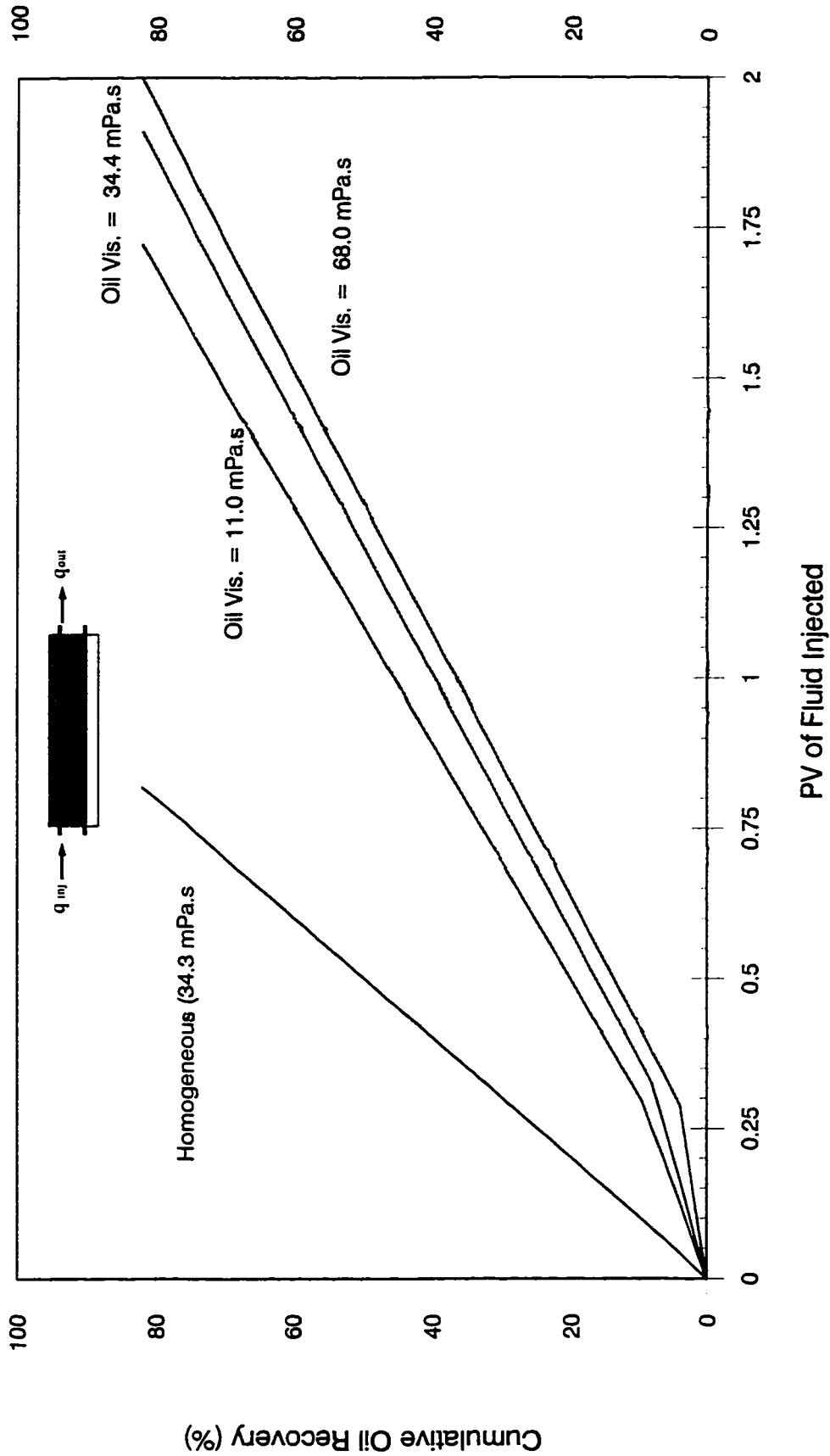


Figure F-54: Bottom-Water Pack Waterflood (  $k_1/k_2 = 1:1$ ,  $h_w/h_o = 1/3$  )

# Production History for Analytical Runs 60 Through 62

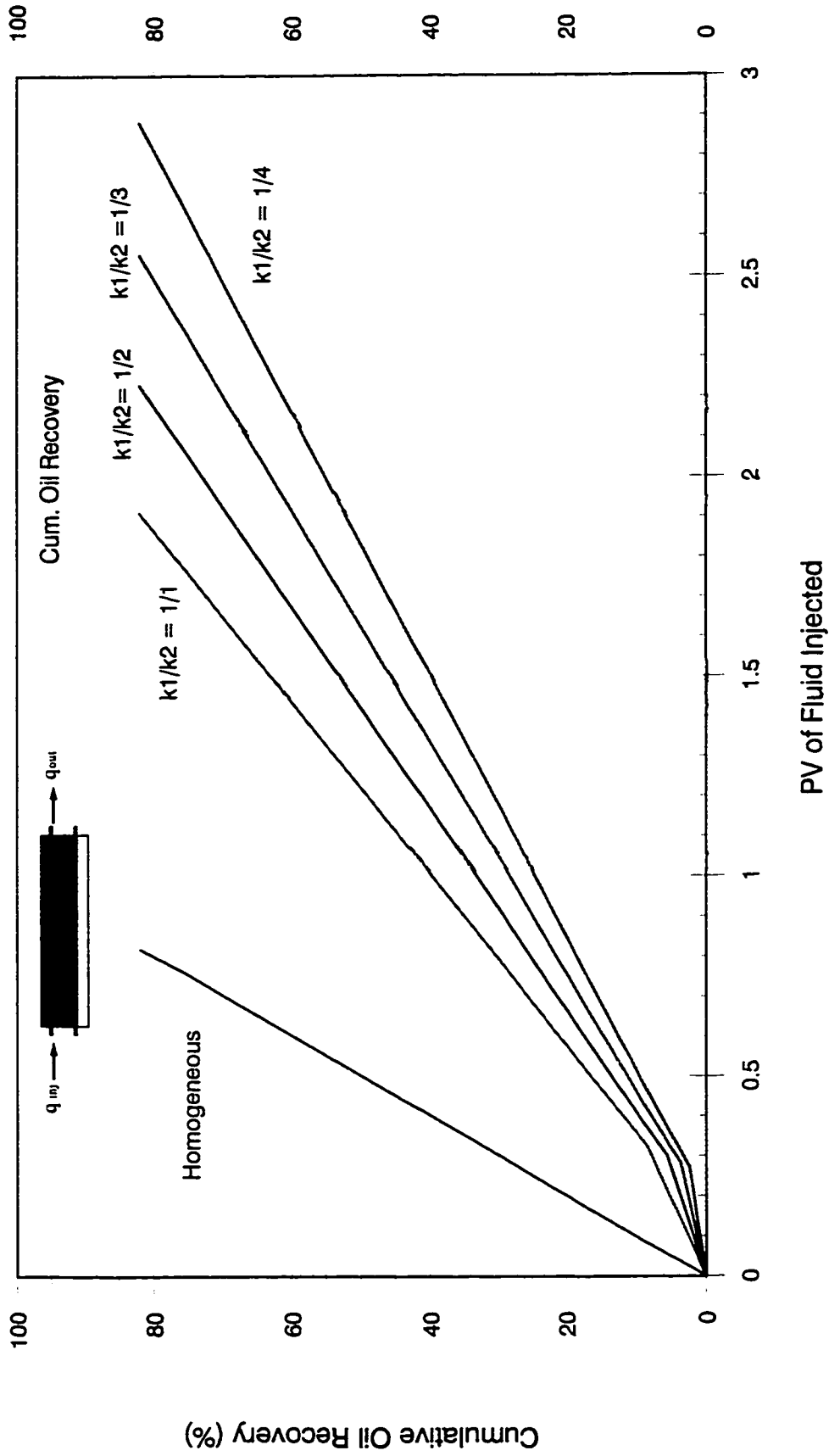
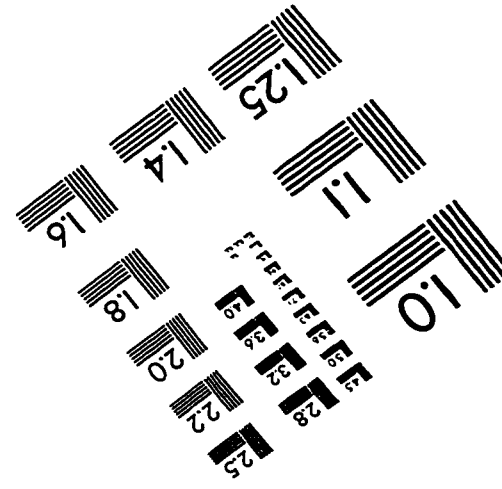
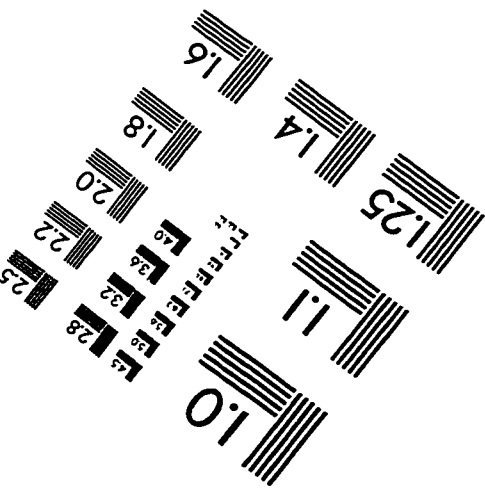
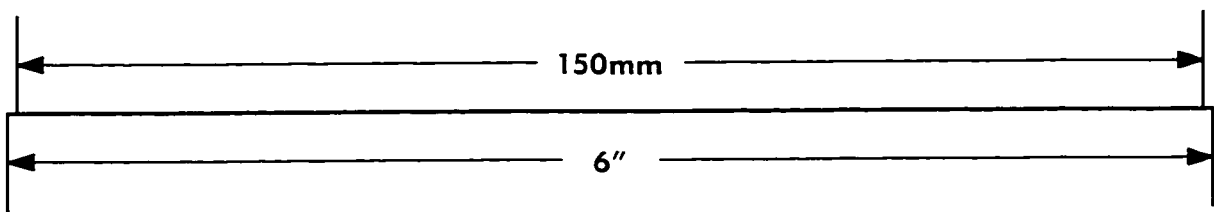
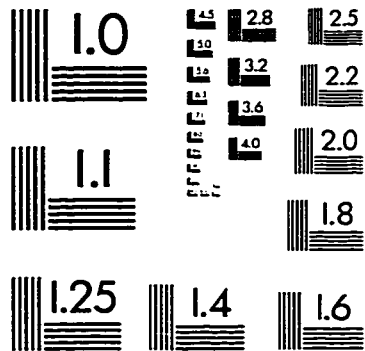
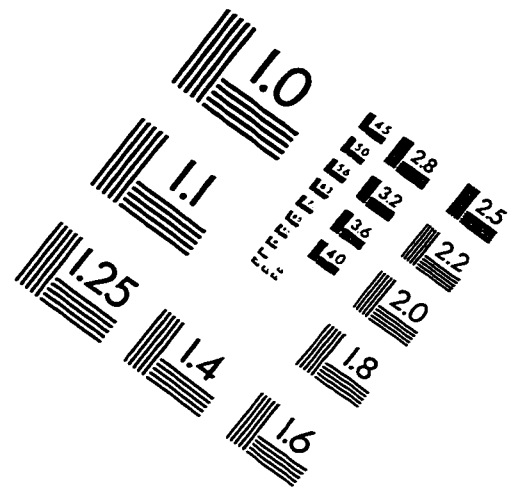
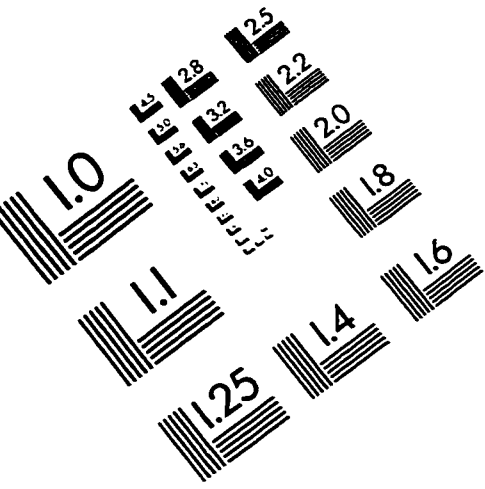


Figure F-55: Bottom-Water Pack Waterflood (  $h_w/h_o = 1/3$ , Oil Viscosity = 34.3 mPa.s )

# IMAGE EVALUATION TEST TARGET (QA-3)



**APPLIED IMAGE, Inc**  
 1653 East Main Street  
 Rochester, NY 14609 USA  
 Phone: 716/482-0300  
 Fax: 716/288-5989

© 1993, Applied Image, Inc., All Rights Reserved